frontiers | Research Topics

Integrated nutrients management: An approach for sustainable crop production and food security in changing climates, 2nd edition

Edited by
Amanullah, Gabrijel Ondrasek and
Abdel Rahman Mohmmad Said Al -Tawaha

Published in
Frontiers in Plant Science

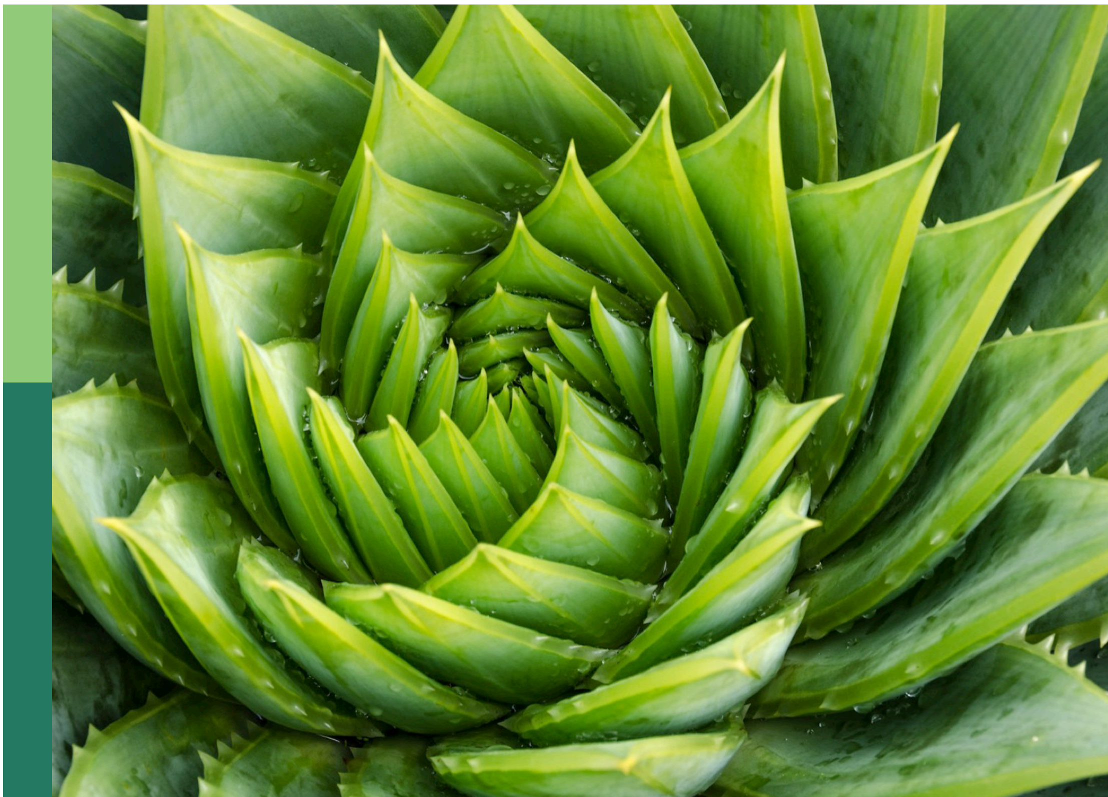

ISSN 1664-8714
ISBN 978-2-8325-5063-2
DOI 10.3389/978-2-8325-5063-2

About Frontiers

Frontiers is more than just an open access publisher of scholarly articles: it is a pioneering approach to the world of academia, radically improving the way scholarly research is managed. The grand vision of Frontiers is a world where all people have an equal opportunity to seek, share and generate knowledge. Frontiers provides immediate and permanent online open access to all its publications, but this alone is not enough to realize our grand goals.

Frontiers journal series

The Frontiers journal series is a multi-tier and interdisciplinary set of open-access, online journals, promising a paradigm shift from the current review, selection and dissemination processes in academic publishing. All Frontiers journals are driven by researchers for researchers; therefore, they constitute a service to the scholarly community. At the same time, the *Frontiers journal series* operates on a revolutionary invention, the tiered publishing system, initially addressing specific communities of scholars, and gradually climbing up to broader public understanding, thus serving the interests of the lay society, too.

Dedication to quality

Each Frontiers article is a landmark of the highest quality, thanks to genuinely collaborative interactions between authors and review editors, who include some of the world's best academicians. Research must be certified by peers before entering a stream of knowledge that may eventually reach the public - and shape society; therefore, Frontiers only applies the most rigorous and unbiased reviews. Frontiers revolutionizes research publishing by freely delivering the most outstanding research, evaluated with no bias from both the academic and social point of view. By applying the most advanced information technologies, Frontiers is catapulting scholarly publishing into a new generation.

What are Frontiers Research Topics?

Frontiers Research Topics are very popular trademarks of the *Frontiers journals series*: they are collections of at least ten articles, all centered on a particular subject. With their unique mix of varied contributions from Original Research to Review Articles, Frontiers Research Topics unify the most influential researchers, the latest key findings and historical advances in a hot research area.

Find out more on how to host your own Frontiers Research Topic or contribute to one as an author by contacting the Frontiers editorial office: frontiersin.org/about/contact

Integrated nutrients management: An approach for sustainable crop production and food security in changing climates, 2nd edition

Topic editors
Amanullah — University of Agriculture, Peshawar, Pakistan
Gabrijel Ondrasek — University of Zagreb, Croatia
Abdel Rahman Mohmmad Said Al -Tawaha — Al-Hussein Bin Talal University, Jordan

Citation
Amanullah., Ondrasek, G., Al –Tawaha, A. R. M. S., eds. (2024). *Integrated nutrients management: An approach for sustainable crop production and food security in changing climates, 2nd edition*. Lausanne: Frontiers Media SA.
doi: 10.3389/978-2-8325-5063-2

Publisher's note: This is a 2nd edition due to an article retraction.

Table of contents

frontiers | Frontiers in Plant Science

TYPE Editorial
PUBLISHED 09 October 2023
DOI 10.3389/fpls.2023.1288030

Check for updates

OPEN ACCESS

EDITED AND REVIEWED BY
Richard William Bell,
Murdoch University, Australia

*CORRESPONDENCE
Amanullah
amanullah@aup.edu.pk

RECEIVED 03 September 2023
ACCEPTED 15 September 2023
PUBLISHED 09 October 2023

CITATION
Amanullah, Ondrasek G and Al-Tawaha AR (2023) Editorial: Integrated nutrients management: an approach for sustainable crop production and food security in changing climates.
Front. Plant Sci. 14:1288030.
doi: 10.3389/fpls.2023.1288030

Editorial: Integrated nutrients management: an approach for sustainable crop production and food security in changing climates

Amanullah[1]*, Gabrijel Ondrasek[2] and Abdel Rahman Al-Tawaha[3]

[1]Department of Agronomy, Faculty of Crop Production Sciences, The University of Agriculture, Peshawar, Pakistan, [2]Faculty of Agriculture, The University of Zagreb, Zagreb, Croatia, [3]Department of Biological sciences, Al Hussein Bin Talal University Ma'an, Ma'an, Jordan

KEYWORDS

integrated nutrients management, chemical fertilizers, organic fertilizers, biofertilizers and nanofertilizers, yield and food security

Editorial on the Research Topic
Integrated nutrients management: an approach for sustainable crop production and food security in changing climates

Introduction

In an era of shifting climates and evolving agricultural paradigms, the need for sustainable approaches to crop production and food security has become paramount. This Research Topic, titled "Integrated Nutrients Management for Sustainable Crop Production and Food Security in Changing Climates," presents a collection of pioneering research that addresses the intricate relationship between INM, soil health, and global agricultural sustainability in the context of changing climates (Amanullah, 2017; Amanullah and Fahad, 2018). The issue has been meticulously curated under the editorial guidance of Amanullah, Gabrijel Ondrasek, and Abdel Rahman Al-Tawaha, with the aim of contributing to the advancement of agriculture in a changing world by emphasizing the critical role of INM in increasing crop productivity, reducing fertilizer costs, and solving food security challenges.

INM and soil health

Integrated Nutrient Management (INM) plays a pivotal role in enhancing soil health, particularly in the context of changing climates. INM's holistic approach involves the synergistic use of organic, chemical, and bio-fertilizers. By maintaining a balanced nutrient profile and fostering beneficial microbial communities in the soil, INM contributes to improved soil structure and fertility (FAO and ITPS, 2016). This is essential for adapting to climate variability, as healthier soils are better equipped to withstand extreme weather events and support sustained crop production (Krasilnikov et al., 2022).

INM and crop productivity

INM is intrinsically linked to increased crop productivity, a critical aspect of food security in a changing climate. By optimizing nutrient availability to crops, INM ensures that plants receive the essential elements they need for growth and development (Amanullah et al., 2019a; Amanullah et al., 2019b). The judicious use of organic matter, bio-fertilizers, and targeted nutrient applications enhances crop yield and resilience, ultimately leading to higher agricultural productivity. This boost in productivity is vital to meet the growing global demand for food while mitigating the impacts of climate change on crop production.

INM and costs of chemical fertilizers

One of the primary benefits of INM is its potential to reduce the reliance on expensive chemical fertilizers. With climate change exacerbating resource constraints and increasing fertilizer costs, the adoption of INM practices can be cost-effective for farmers (Amanullah et al., 2020; Amanullah et al., 2021). By incorporating organic materials and bio-fertilizers, INM allows for more efficient nutrient utilization, minimizing the need for excessive chemical inputs. This not only lowers production costs but also promotes sustainable agricultural practices, which are essential in a changing climate (Khan et al., 2022; Imran and Amanullah, 2023).

INM and food security

Food security is inextricably linked to INM, especially in the face of climate change-induced challenges. INM practices contribute to higher crop yields, ensuring a stable food supply (Khalid et al., 2022). By maintaining soil fertility, INM helps safeguard agricultural productivity against climate-related shocks, such as droughts and floods. Additionally, the sustainable nature of INM reduces the environmental impact of agriculture, preserving ecosystems and safeguarding the long-term availability of food resources (Nadia et al., 2023).

INM and climate change adaptation

As climate change alters temperature and precipitation patterns, INM emerges as a valuable tool for climate change adaptation in agriculture. INM practices help crops better withstand environmental stressors like heat and water scarcity by enhancing their resilience (Krasilnikov et al., 2022). Moreover, the reduced carbon footprint associated with INM aligns with global efforts to mitigate climate change. By sequestering carbon in soils and reducing greenhouse gas emissions from synthetic fertilizers, INM contributes to a more sustainable and climate-resilient agricultural system (FAO and ITPS, 2016).

These integrated approaches are essential for addressing the complex challenges posed by changing climates and ensuring a resilient and food-secure future.

Articles and insights

This Research Topic features 12 articles that collectively illuminate various dimensions of INM's impact on sustainable agriculture. The diverse research contributions delve into vital aspects of agricultural sustainability, exploring novel solutions that extend from nano-technological interventions to organic waste management.

Here are insights from all 12 articles published in the Research Topic on Integrated Nutrient Management (INM), along with their relevance to soil health, crop productivity, lower costs of chemical fertilizers, food security, and climate change, while also including information related to yield and food security:

Eco-friendly disease management

Khan et al. demonstrate the potential of eco-friendly IONPs synthesized from M. spicata in combatting late blight disease. This research offers an eco-conscious approach to disease control, reducing yield losses and contributing to food security. It also aligns with sustainable agriculture by minimizing chemical pesticide usage and preserving soil health.

Enhancing manure quality

Holatko et al. explore co-composting cattle manure with biochar and elemental sulfur. This strategy not only enhances soil microbiological characteristics but also improves manure quality. Better-quality manure means improved nutrient content for crops, higher yields, and reduced reliance on synthetic fertilizers, contributing to food security.

Transitioning to biological fertilizers

Abdo et al. advocate for shifting from chemical fertilizers to biological fertilizers and growth stimulants. Their research underscores the positive impact of these alternatives on crop yield and soil health, promoting higher productivity and food security while reducing environmental impact.

Alternative fertilization

Dombinov et al. investigate sugarcane bagasse ash (SCBA) as a potential fertilizer for soybeans. SCBA's nutrient-rich composition offers a sustainable alternative to traditional fertilizers, reducing costs, and ensuring a stable yield, contributing to food security.

Flooding stress tolerance

Yijun et al. explore strategies to enhance flooding stress tolerance in soybean. This research provides insights into mitigating climate-induced challenges, ensuring crop productivity, and safeguarding food security even in adverse environmental conditions.

Precision agriculture

Li et al. introduce unmanned aerial vehicle (UAV) multispectral imaging for efficient plant nutrient deficiency diagnosis. This technology enhances precision agriculture practices, optimizing nutrient management, and crop yield, ultimately supporting food security.

Phosphorus and manure integration

Jamal et al. emphasize the integrated use of phosphorus fertilizer and farmyard manure for improving wheat productivity. This approach can reduce reliance on synthetic phosphorus fertilizers, lower production costs, and ensure a stable wheat yield, contributing to food security.

Nanomaterials in agriculture

Hammerschmiedt et al. explore the effects of graphene oxide and elemental nano-sulfur on soil biological properties and lettuce plant biomass. This research showcases the potential of nanomaterials in sustainable agriculture, with implications for soil health, higher crop productivity, and food security.

Organic manure alternatives

Lee et al. highlight the value of Hanwoo manure as an organic alternative to chemical fertilizers. This research offers a sustainable pathway to maintaining soil fertility, increasing crop yield, and ensuring food security while reducing the environmental impact.

Tillage and mowing strategies

Du et al. uncover the impact of tillage methods and mowing time on Cyperus esculentus cultivation. This study provides insights into sustainable practices for specific crops, which are critical for climate-resilient agriculture, higher yields, and food security.

Improving soil microbial communities

Guo et al. focus on the transformative role of biochar from organic waste in enhancing soil fertility and citrus growth on acid red soil. Improved soil health and fertility contribute to increased crop yield and food security, while the use of organic waste aligns with sustainability.

Alleviating root rot

Tagele et al. investigate cow dung's potential as a soil amendment to alleviate ginseng root rot. By enhancing soil health and crop resilience, this research supports higher yields and food security in the face of changing climates.

These insights collectively underscore the multidimensional benefits of INM, ranging from improved soil health and higher crop productivity to reduced costs, enhanced food security, and resilience to climate change. Adopting INM practices is a crucial step towards achieving sustainable agriculture and ensuring a stable food supply in a changing world.

Conclusion and future prospects

This Research Topic underscores the pivotal role of INM in promoting sustainable agriculture, improving soil health, and ensuring global food security in the context of changing climates. The findings collectively support the notion that INM is a fundamental strategy to enhance soil fertility, health, and resilience, which is crucial in the face of climate variability. As research continues to evolve, precision agriculture technologies, genetic diversity preservation, and innovative practices promise to shape a future where sustainable agriculture is the cornerstone of food security, even amidst the challenges posed by changing climates.

Author contributions

A: Writing – original draft, Writing – review & editing. GO: Writing – review & editing. AA: Writing – review & editing.

Acknowledgments

We would like to extend our sincere gratitude to Frontier in Plant Science for entrusting us with the responsibility of guest editing the Research Topic titled “Integrated Nutrients Management for Sustainable Crop Production and Food Security: A Frontier in Changing Climates.” Our heartfelt thanks also go to the authors, reviewers, and contributors who have made this Research Topic a valuable and insightful resource.

Conflict of interest

The authors declare that the research was conducted in the absence of any commercial or financial relationships that could be construed as a potential conflict of interest.

Publisher's note

References

Amanullah. (2017). "Integrated use of organic carbon, plant nutrients and bio-fertilizers is key to improve field crops productivity under arid and semiarid climates," in *FAO (2017) Proceedings of the global symposium on soil organic carbon 2017* (Rome, Italy: Food and Agriculture Organization of the United Nations), 480–481.

Amanullah, and Fahad, S. (2018). "Integrated nutrient management in corn production: symbiosis for food security and grower's income in arid and semiarid climates," in *Corn - production and human health in changing climate*. Eds. Amanullah, and S. Fahad (London, UK: InTech), 03–12.

Amanullah, Inamullah, Alkahtani, J., Elshikh, M. S., Alwahibi, M. S., Muhammad, A., et al. (2020). Phosphorus and zinc fertilization improve productivity and profitability of rice cultivars under rice-wheat system. *Agronomy* 10, 1085. doi: 10.3390/agronomy10081085

Amanullah, Khan, A., Khalid, S., Shah, A., Parmar, B., Muhammad, A., et al. (2019a). Integrated management of phosphorus, organic sources, and beneficial microbes improve dry matter partitioning of maize. *Commun. Soil Sci. Plant Anal.* 50 (20), 2544–2569. doi: 10.1080/00103624.2019.1667378

Amanullah, Khalid, S., Imran, Ali Khan, H., Arif, M., Altawaha, A. R., et al. (2019b). "Organic matter management in cereals based system: symbiosis for improving crop productivity and soil health," in *Sustainable agriculture reviews-29*, vol. 29 . Eds. R. Lal and R. Francaviglia (Cham: Springer), 67–92.

Amanullah, Khalid, S., Muhammad, A., Yar, M., Elshikh, M. S., Akram, H. M., et al. (2021). Integrated use of biofertilizers with organic and inorganic phosphorus sources improve dry matter partitioning and yield of hybrid maize, Comm. *Soil Sci. Plant Anal.* 52 (21), 2732–2747. doi: 10.1080/00103624.2021.1956520

FAO and ITPS (2016). *Voluntary guidelines for sustainable soil management (VGSSM)* (Rome, Italy: Global Soil Partnership. FAO).

Imran and Amanullah,. (2023). Integration of peach (*Prunus persica* L) remnants in combination with beneficial microbes and phosphorus differ phosphorus use efficiency, agronomic efficiency and partial factor productivity in soybean vs. maize crops. *J. Plant Nutr.* 46 (8), 1745–1756. doi: 10.1080/01904167.2022.2099890

Khalid, S., Amanullah and Ahmed, I. (2022). Enhancing zinc biofortification of wheat through integration of zinc, compost, and zinc-solubilizing bacteria. *Agriculture* 12, 968. doi: 10.3390/agriculture12070968

Khan, I., Amanullah, Jamal, A., Mihoub, A., Farooq, O., Saeed, M. F., et al. (2022). Partial substitution of chemical fertilizers with organic supplements increased wheat productivity and profitability under limited and assured irrigation regimes. *Agriculture* 12, 1754. doi: 10.3390/agriculture12111754

Krasilnikov, P., Taboada, M. A., and Amanullah, (2022). Fertilizer use, soil health and agricultural sustainability. *Agriculture* 12, 462. doi: 10.3390/agriculture12040462

Nadia, Amanullah, Arif, M., and Muhammad, D. (2023). Improvement in wheat productivity with integrated management of beneficial microbes along with organic and inorganic phosphorus sources. *Agriculture* 13, 1118. doi: 10.3390/agriculture13061118

frontiers | Frontiers in Plant Science

TYPE Original Research
PUBLISHED 29 September 2022
DOI 10.3389/fpls.2022.1004879

Check for updates

Co-composting of cattle manure with biochar and elemental sulphur and its effects on manure quality, plant biomass and microbiological characteristics of post-harvest soil

Jiri Holatko[1,2], Tereza Hammerschmiedt[1], Antonin Kintl[1,3], Adnan Mustafa[1,4,5*], Muhammad Naveed[6], Tivadar Baltazar[1], Oldrich Latal[1,2], Petr Skarpa[1], Pavel Ryant[1] and Martin Brtnicky[1,4*]

[1]Department of Agrochemistry, Soil Science, Microbiology and Plant Nutrition, Faculty of AgriSciences, Mendel University in Brno, Brno, Czechia, [2]Agrovyzkum Rapotin, Ltd., Rapotin, Czechia, [3]Agricultural Research, Ltd., Troubsko, Czechia, [4]Institute of Chemistry and Technology of Environmental Protection, Faculty of Chemistry, Brno University of Technology, Brno, Czechia, [5]Institute for Environmental Studies, Faculty of Science, Charles University in Prague, Praha, Czechia, [6]Institute of Soil and Environmental Science, University of Agriculture Faisalabad, Faisalabad, Pakistan

OPEN ACCESS

EDITED BY
Khan Amanullah,
University of Agriculture, Peshawar, Pakistan

REVIEWED BY
Heba Elbasiouny,
Al-Azhar University, Egypt
Lal Singh,
National Environmental Engineering Research Institute (CSIR), India

*CORRESPONDENCE
Adnan Mustafa
adnanmustafa780@gmail.com
Martin Brtnicky
martin.brtnicky@seznam.cz

SPECIALTY SECTION
This article was submitted to Plant Nutrition, a section of the journal Frontiers in Plant Science

RECEIVED 27 July 2022
ACCEPTED 08 September 2022
PUBLISHED 29 September 2022

CITATION
Holatko J, Hammerschmiedt T, Kintl A, Mustafa A, Naveed M, Baltazar T, Latal O, Skarpa P, Ryant P and Brtnicky M (2022) Co-composting of cattle manure with biochar and elemental sulphur and its effects on manure quality, plant biomass and microbiological characteristics of post-harvest soil. *Front. Plant Sci.* 13:1004879.
doi: 10.3389/fpls.2022.1004879

Improvement of manure by co-composting with other materials is beneficial to the quality of the amended soil. Therefore, the manure was supplied with either biochar, elemental sulphur or both prior to fermentation in 50 L barrels for a period of eight weeks. The manure products were subsequently analyzed and used as fertilizers in a short-term pot experiment with barley fodder (*Hordeum vulgare* L.). The experiment was carried out under controlled conditions in a growth chamber for 12 weeks. The sulphur-enriched manure showed the lowest manure pH and highest ammonium content. The co-fermentation of biochar and sulphur led to the highest sulphur content and an abundance of ammonium-oxidizing bacteria in manure. The biochar+sulphur-enriched manure led to the highest dry aboveground plant biomass in the amended soil, whose value was 98% higher compared to the unamended control, 38% higher compared to the variant with biochar-enriched manure and 23% higher compared to the manure-amended variant. Amendment of the sulphur-enriched manure types led to the highest enzyme activities and soil respirations (basal, substrate-induced). This innovative approach to improve the quality of organic fertilizers utilizes treated agricultural waste (biochar) and a biotechnological residual product (elementary sulphur from biogas desulphurization) and hence contributes to the circular economy.

KEYWORDS

manure enrichment, soil nutrients, organic matter, soil amendments, fertilizers, modified biochar

1 Introduction

Widely observed soil degradation is currently one of the main global concerns. It is caused by a combination of natural and anthropogenic detrimental processes, such as pollution, deforestation and consequences of poor land management and unsustainable agricultural practices: wind and water erosion, physicochemical changes as compaction, salinization, acidification, loss of soil organic matter (SOM) and nutrients (Virto et al., 2014; Tetteh, 2015; EC, European Commission, 2021). Additionally, agriculture intensification, driven by a necessity to meet human needs, has resulted in serious threats of soil pollution, environmental degradation and climate change (Lal, 2020).

The loss of SOM is closely related to the decline in soil fertility and the biological function of soils (Lal, 2009). Application of organic fertilizers in this regard can restore and preserve the sustainable SOM content in soil (Liu et al., 2011). Farmyard manure is the most common type of organic fertilizer. It plays a significant role in maintaining high quality healthy arable soils and sustainable agriculture (Kirchmann and Thorvaldsson, 2000). According to the recent literature, manure application to agricultural soil has a positive effect on the build-up of SOM and thus improves the soil structure as well as the intrinsic fertility of the soils (Mustafa et al., 2020; Mustafa et al., 2021). In addition, manure application may significantly increase the soil water storage and crop yield and has a positive effect on soil microbial activity (Wang et al., 2016; Hoover et al., 2019; Ashraf et al., 2021). It represents a good source of nutrients, especially carbon (C), nitrogen (N), phosphorus (P) and minerals, for both plants and soil organisms, including microbes (Qaswar et al., 2019). However, the properties of manure are variable and depend mainly on the type of livestock, bedding material and the conditions of fermentation, which can be modified to achieve the intended quality of product (Naveed et al., 2021).

Therefore, amendment of soil with manure as the primary source of organic matter, enriched with biochar and elemental sulphur (S), has brought promising results in previous studies. Fermentation of biochar-enriched manure mitigated emissions of greenhouse gases (Rogovska et al., 2011; Maurer et al., 2017), ammonia (Janczak et al., 2017), prevented nutrient losses (Hagemann et al., 2018). Biochar addition modified the thermodynamics and heat generation in the fermentation process (Czekała et al., 2016) and changed the content and functional diversity of microorganisms (He et al., 2018), as well as microbial mineralization (Jindo et al., 2012) in manure.

Moreover, the effect of S on manure composting is the subject of several studies in the recent literature. Sulphur is not only a useful nutrient for microorganisms and plants (Skwierawska et al., 2016; Bouranis et al., 2019), but also serves as soil conditioner improving the physicochemical properties of soil (Skwierawska et al., 2008; Abou Hussien et al., 2020). It has also been shown to increase crop yields (Soltanaeva et al., 2018). The S deficiency in Europe's agricultural soils is linked to a significant decline in sulphur dioxide (SO_2) emissions, which have been reduced by 70–80% over the last 30 years (Hoesly et al., 2018). For example, the available results of soil analyses carried out in the Czech Republic show that 85% of samples have low S content (Kulhánek et al., 2018). The effect of elemental S (upon the combined treatments with manure or biochar) on manure quality, soil properties and plant growth has been reported in only a few studies, e.g. (Mahimairaja et al., 1994b; de la Fuente et al., 2007; Godlewska, 2018b), and thus has left room for further studies. Moreover, the amendment of co-composted manure with elemental S may significantly alter soil enzyme activity (Malik et al., 2021), with a putative benefit of increased rate of nutrient transformation *via* enhancement of microbial activity and abundance by combination of external organic matter and elemental S amendment (Hammerschmiedt et al., 2021; Malik et al., 2021). Biochar addition to soil was also referred to affect activity of nutrient-transforming enzymes in soil not only negatively (Li et al., 2018; Song et al., 2019), but also positively (Azeem et al., 2019; Zhang et al., 2021). The novelty of this research lies in the pre-maturation enrichment of manure with elemental S, which is assumed to be promoted during the manure fermentation to the accelerated transformation into plant-available form and modulated in this process by a presence of biochar.

The objectives of this study were to evaluate (I) the impact of manure enrichment (prior to fermentation) with biochar, elemental S and a combination of both on the fertilizing properties of produced manure types, (II) the effect of soil amendment with these various manure types on the chemical and biological properties (i.e. activity of nutrient-transforming soil enzymes), and biomass of a test crop, barley fodder (*Hordeum vulgare* L.). It was hypothesized that the acidifying effect of elemental S would counteract the alkalizing effect of biochar in the case of their co-fermentation in manure, and that it could modify the biological properties of manure *via* S oxidation-promoted nutrient mineralization, accompanied by reduced ammonia emission.

2 Materials and methods

2.1 Collection, preparation, and analysis of modified manure

Animal manure was collected from a cattle-breeding farm of Research Institute for Cattle Breeding Ltd., located in the village of Rapotin, Czech Republic, Central Europe (49°58'46.4" N, 17° 0'26,6" E). Experimental matured manure was prepared in the 50 L sealable containers (three containers per variant), filled with 10 kg of collected manure, which was (optionally) mixed with biochar and elemental S to create four experimental variants: [M] manure, [M+B] manure + biochar (40 $g{\cdot}kg^{-1}$), [M+S] manure + elemental S (1.4 $g{\cdot}kg^{-1}$), [M+B+S] manure + biochar (40 $g{\cdot}kg^{-1}$) + elemental S (1.4 $g{\cdot}kg^{-1}$). Each variant was prepared in three replicates. Used biochar was produced from agricultural waste at 600°C (Sonnenerde GmbH, Riedlingsdorf, Austria), and its properties were according the analyses of manufacturer as follows: elements (in $g{\cdot}kg^{-1}$) - C 866, N 3.0, O 10.0, H 14.2; $Ash_{550°C}$ 11.7%, salts 0.42%, pH ($CaCl_2$) 8.5. Elemental S was a waste product obtained during desulphurization of biogas at sugar factory biogas plant in THIOPAQ scrubber (Paques, Netherlands).

The activation process ran for eight weeks at a laboratory-controlled temperature (20 ± 2°C) at stable air humidity (measured weekly). At the end of the process, a mixed sample from each variant was taken and analyzed. Manure pH in $CaCl_2$ was determined according to (ISO 10390:2005); total Kjeldahl nitrogen (TKN) was determined according to (ISO 11261:1995); and ammonium nitrogen ($N\text{-}NH_4$) was measured according to (ISO 15476:2009). The available P was determined according to (Egnér et al., 1960); dry matter (DM) was measured gravimetrically (Hoskins et al., 2003); and organic C (C_{org}) was measured according to (EN 15936:2012). Total S was determined according to (EN 15749:2009), ammonium-oxidizing bacteria (AOB) according to (Rotthauwe et al., 1997), denitrifying microorganisms (*nirS*) according to (Kandeler et al., 2006) and S-reducing microorganisms (*dsr*) according to (Ben-Dov et al., 2007).

2.2 Pot experiment

All four produced manure types were used as soil amendments in pot experiments with barley fodder (*Hordeum vulgare* L.) as a test crop. All experimental pots (volume 5 L) were filled with soil substrate: fine quartz sand (0.1–1.0 mm) mixed with sieved (2.0 mm) topsoil (0–15 cm) from the rural area near the town of Troubsko, Czech Republic - 49°10'28"N 16°29'32"E in ratio 1:1, w/w. The soil was a silty clay loam (according to USDA Textural Triangle), Haplic Luvisol [according to WRB soil classification (FAO, Food and Agriculture Organization of the United Nations, 2014)], and its properties were as follows: soil macronutrients ($g{\cdot}kg^{-1}$) - total C 14.00, total N 1.60 - available nutrients ($mg{\cdot}kg^{-1}$) - P 97, S 100, Ca 3259, Mg 236, K 231; mineral N forms ($mg{\cdot}kg^{-1}$) – N_{min} 62.84, $N\text{-}NO_3$ 56.80, $N\text{-}NH_4$ 6.04; pH ($CaCl_2$) 7.3.

The four pot experimental variants were made by thoroughly mixing a soil:sand blend (5 kg) with the particular manure type in amounts of 200 g per pot (the manure amount being equal to 50 $t{\cdot}ha^{-1}$). An unamended control contained only 5 kg of soil:sand blend. The treatments included (1) control, (2) manure (M), (3) manure + biochar (M+B), (4) manure + elemental S (M+S), (5) manure + biochar + elemental S (M+B +S). Each variant was prepared in five replicates. Each pot was sown with 16 barley seeds 2 cm under the soil surface and was watered with distilled water to achieve 65% water-holding capacity (WHC). This moisture level was maintained throughout the entire experiment. All pots were placed randomly into a growth chamber (CLF Plant Climatics GmbH, Germany). Controlled conditions were set as follows: 12-hours photoperiod, light intensity 20 000 lx, temperature (day/night) 20/12°C, relative air humidity (day/night) 45%/70%. After 14 days, the number of plants was reduced to 12 in each pot. Moreover, the pots were randomly rotated every other day to ensure the homogeneity of the conditions for the treatments.

2.3 Plant biomass measurements

The barley plants were grown for 12 weeks. After that, the shoots were cut at the ground level, washed with distilled water (Iocoli et al., 2019), and dried at 60°C until a constant weight was obtained. The dry aboveground biomass (AGB) was determined gravimetrically using the analytical scales.

2.4 Post-harvest soil characterization and statistical analysis

The soil samples were taken after the harvesting of AGB of barley. The homogenization of the samples was done by sieving through a 2 mm mesh. The samples for the enzyme activity assays (ISO 20130:2018) – β-glucosidase (GLU), arylsulfatase (ARS), phosphatase (Phos), N-acetyl-β-D-glucosaminidase (NAG) and urease (Ure) – were freeze-dried. The samples stored at 4°C were used for determination of dehydrogenase activity (DHA), soil basal (BR) and substrate induced respirations (Campbell et al., 2003): D-glucose (Glc-SIR), D-trehalose (Tre-SIR), citric acid (Cit-SIR), N-acetyl-β-D-glucosamine (NAG-SIR), L-alanine (Ala-SIR), L-lysine (Lys-SIR) and L-arginine (Arg-SIR). The total soil carbon (TC) and nitrogen (TN) content (ISO 10694:1995, ISO 13878:1998) were analyzed using air-dried samples.

DHA was measured by 2,3,5-triphenyltetrazolium chloride (TTC)-based method. The *p*-nitrophenol (PNP)-derivatives of the specific soil substrates were used for Vis spectrophotometric measurement (Infinite M Nano, Tecan Trading AG, Switzerland) at Λ = 405 nm (β-glucosidase, arylsulfatase, phosphatase, and N-acetyl-β-D-glucosaminidase). Urease activity was determined as an amount of ammonium produced from the substrate urea, detected Vis spectrophotometrically by the reagent cyanurate (Λ = 650 nm). Other soil properties were determined by the standard methods and the data obtained was statistically analyzed as listed in (Table 1).

The Shapiro–Wilk and the Levene tests (at $p \leq 0.05$) were performed for the verification of normality and homogeneity of variances. Principal component analysis (PCA), and one-way analysis of variance (ANOVA) type I (sequential) sum of squares at 5% significance level were used for characterization of relationship between the treatments and selected soil properties. Tukey's HSD (honestly significant difference) test was used for detection the statistically significant difference among factor level means, and "treatment contrast" was calculated as factor level means for each treatment. The results were also graphically presented with Rohlf biplot for standardized PCA. Pearson correlation analysis was performed for measuring the linear dependence between soil properties. Pearson correlation coefficient was interpreted as follows: $0.0 < r < 0.3$ (negligible correlation), $0.3 < r < 0.5$ (low correlation), $0.5 < r < 0.7$ (moderate correlation), $0.7 < r < 0.9$ (high correlation), and $0.9 < r < 1.0$ (very high correlation).

3 Results

3.1 Effect of added amendments on pH and nitrogen forms in manure

It was observed that both M+S and M+B+S exerted significantly lower pH values (6.85 ± 0.01 and 7.21 ± 0.01, respectively) compared to the M and M+B (9.04 ± 0.01 and 9.05 ± 0.01, respectively) – (Figure 1A). The S enrichment of the M+S variant caused a significantly lower TKN (by 4.8%) value but a significantly higher $N\text{-}NH_4$ (by 83.1% as compared to the M) – (Figures 1B, C). The M+S manure did not differ in both TKN and $N\text{-}NH_4$ content from the M+S+B manure, whereas this variant showed significantly decreased total TKN (by 7.2%) and increased $N\text{-}NH_4$ (by 161%) content compared to the M+B.

3.2 Effect of added amendments on manure – derived phosphorus and organic carbon

In both S-enriched variants (M+S and M+B+S), the available P was decreased compared to the M (by 39% and 32%, respectively) – (Figure 1D). The M+B variant showed significantly lower C_{org} compared to the M (by 3.7%) and M+B+S. A similar decrease in the C_{org} content was detected in the M+S variant (by 5.5% compared to M) – (Figure 1E).

3.3 Effect of added materials on sulphur content in manure

A significantly decreased total S value for the M+B manure (by 62% compared to the M) was received, whereas the M+B+S

TABLE 1 Determined soil properties, methods used for measurement and statistics, relevant references.

Property	Method	Unit	Reference
Total soil carbon	Dry combustion using, LECO TruSpec analyzer (MI USA)	$mg{\cdot}g^{-1}$	(ISO 10694:1995)
Total soil nitrogen			(ISO 13878:1998)
Dehydrogenase activity	Triphenyl tetrazolium chloride (TTC)-based method	$\mu g\ TPF{\cdot}g^{-1}{\cdot}h^{-1}$	(Doi and Ranamukhaarachchi, 2009)
Soil enzyme activities (GLU, ARS, Phos, NAG, Urea)	Microplate incubation, Vis spectrophotometry	$\mu mol\ PNP{\cdot}g^{-1}{\cdot}h^{-1}$, $\mu mol\ NH_3{\cdot}g^{-1}{\cdot}h^{-1}$	(ISO 20130:2018)
Basal soil respiration	MicroResp® device	$\mu g\ CO_2{\cdot}g^{-1}{\cdot}h^{-1}$	(Campbell et al., 2003)
Substrate induced soil respiration	MicroResp® device + inducers (sugars, amino acids)		
Processing	**Method**	**Tool**	**Reference**
Statistical analysis	Multivariate analysis of variance (MANOVA), one-way analysis of variance (ANOVA) with Tukey's *post-hoc* test, principal component analysis (PCA), Pearson's correlation analysis	Program R version 3.6.1.	(Holatko et al., 2020)

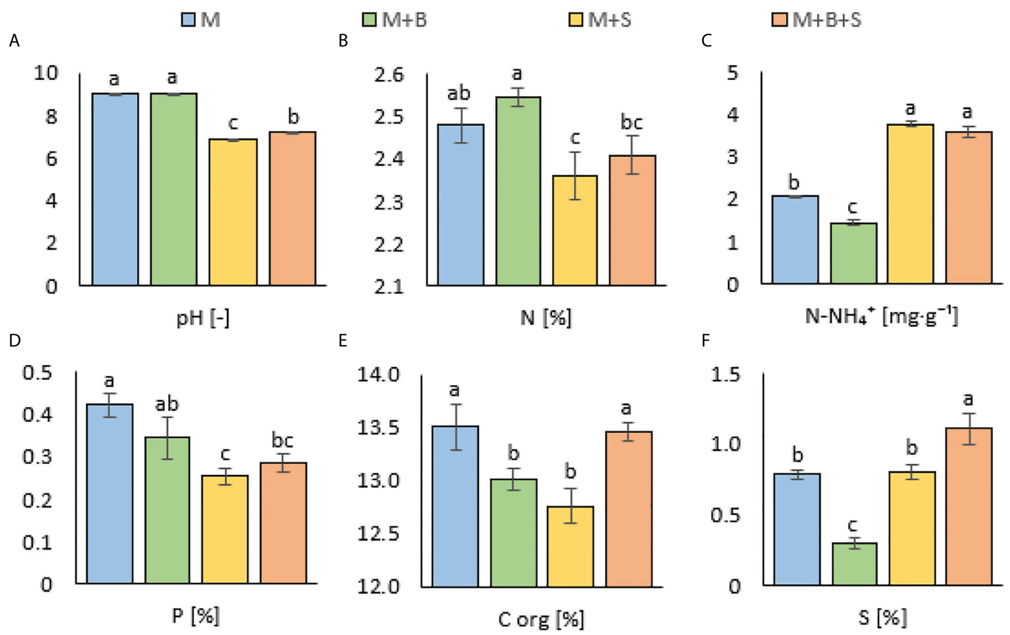

FIGURE 1
Properties of the maturated manures enriched with additives (biochar and S). **(A)** pH, **(B)** total Kjeldahl nitrogen, **(C)** ammonium nitrogen, **(D)** available phosphorus, **(E)** organic carbon, **(F)** total sulphur. Different letters indicate differences at level of significance $p \leq 0.05$.

variant was significantly the highest (41% higher than M) – (Figure 1F). The total S in manure was significantly related to the microbiological traits of *dsr* ($p \leq 0.05$, $r = 0.51$), and (at $p \leq 0.00$) AOB ($r = 0.76$), *nirS* ($r = -0.82$), and to the N-NH_4 nitrogen ($r = 0.76$) (Figure 2). These relationships are apparent also from the PCA biplot (Figure 3).

3.4 Effect of added amendments on microbial abundance in manure

Significantly increased *dsr* (determinant of the S-reducing microorganisms) was found the in the M+S and M+B+S variants (supplied with S) compared to the M and M+B (non-supplied with S): the values were ~10-fold and ~7.7-fold higher (than M), respectively (Figure 4A). The addition of S to the unmatured manure was crucial for the abundance of N-transforming microbiota: *dsr* correlated positively ($p \leq 0.001$) with AOB ($r = 0.82$) and N-NH_4 ($r = 0.93$), whereas *nirS* correlated negatively ($p \leq 0.001$) with N-NH_4 ($r = -0.81$), S ($r = -0.82$), AOB ($r = -0.64$) and *dsr* ($r = -0.56$) (Figure 2).

The AOB was significantly increased in the M+S and M+B+S variants (by 102% and 169%) compared to the M and M+B; the significantly highest AOB value was detected in the M+B+S manure (Figure 4B). The significantly lowest nirS value was revealed in the M+B+S variant (20.5% lower than M) and the significantly highest in the M+B variant (27.4% higher than M) (Figure 4C)

3.5 Effect of manure types on soil fertility and plant biomass yield

All manure-amended variants (M, M+B, M+S, M+B+S) showed a significant increase (by 62%, 43%, 86%, 98%, respectively) of AGB compared to the AGB of the control (Figure 5A). Further, the AGB value of the variant M+B+S was significantly higher than the AGB of M+B. The positive significant correlation ($p \leq 0.001$, $r = 0.69$) that was found for AGB and TC, BR, Ure, corroborated the relation between plant biomass and soil nutrient availability. These values were significantly increased in M+B+S soil compared to the control soil (Ure) as well as compared to both the control and M variant (TC, BR).

The TC and TN content in the amended soil variants (M, M+B, M+S, and M+B+S) was significantly higher compared to the control: by 9%, 17%, 16%, 18% (TC) and by 13%, 18%, 17%, 19% (TN) (Figures 5B, C). TN values were similar among all these manure-supplied variants, whereas the TC was significantly lower in the M variant compared to the M+B, M+S and M+B+S. The variants did not differ significantly in C:N ratio (Figure 5D).

3.6 Effect of manure types on soil microbial activity

Significantly increased DHA was reached in all manure-amended variants (M, M+B, M+S, M+B+S) compared to the

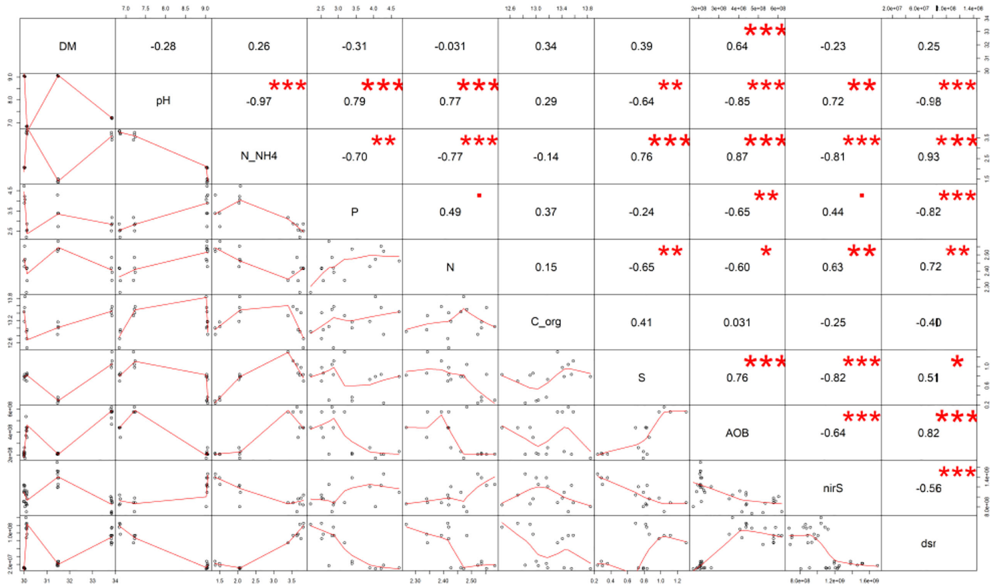

FIGURE 2
The Pearson's correlation matrix of the maturated manure properties. Explanation: Significance at · $p \leq 0.10$; *$p \leq 0.05$; **$p \leq 0.01$; ***$p \leq 0.001$.

control: the values were higher by 35%, 53%, 67%, 50% (Figure 5E). Furthermore, the significantly higher DHA value was obtained in the M+S variant compared to the M variant. It assumed a general effect of M+S amendment on the microbial soil activity because DHA correlated significantly ($p \leq 0.001$) positively with Ure ($r = 0.79$), BR ($r = 0.54$) and GLU ($r = 0.53$). The values of ARS in the soil variants amended with S-enriched manures (M+S, M+B+S) were not significantly higher than in the control soil (Figure 5F), whereas the variants M and M+B showed significantly lower ARS values (by 29% and 12%, respectively). Nevertheless, the amendment of S-enriched manures to soil resulted in a demonstrated significant increase (in M+S and M+B+S, compared to the control) of Ure (by 64% and 55%, Figure 5G), Phos (by 28% and 42%, Figure 5H), NAG

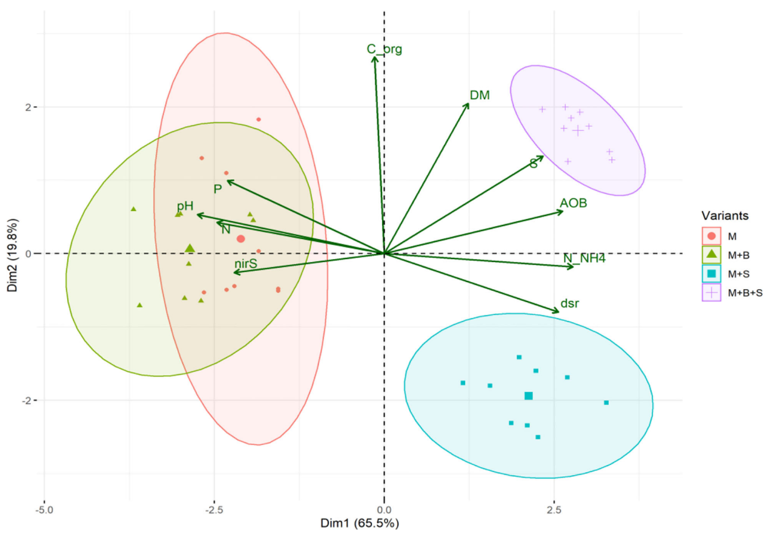

FIGURE 3
The PCA biplot of the maturated manure properties.

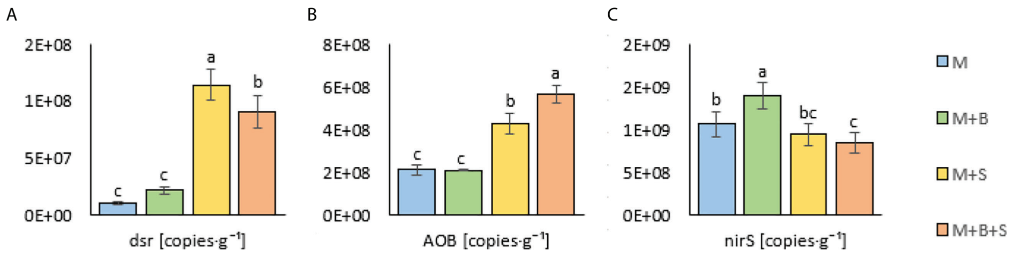

FIGURE 4
Microbial properties of the maturated manures enriched with additives (biochar and S). **(A)** sulphur-reducing, **(B)** ammonia-oxidizing, and **(C)** denitrifying microorganisms in the maturated manures enriched with additives. Different letters indicate differences at level of significance $p \leq 0.05$.

(by 37% and 11%, Figure 5I) and GLU (by 21% and 16%, Figure 5J) activities. The values in M+S were significantly higher for Ure, NAG and GLU compared to the M and M+B values. The Phos was highest in M+B+S.

Compared to the control, BR was significantly increased in variants amended with all types of manure. Moreover, the received BR values were significantly higher in the S-enriched manure-treated variants (M+S and M+B+S, by 54% and 51% compared to control) than in the non-enriched manure variant M (by 24% higher than control) – (Figure 5K).

Results similar to the BR determination were obtained for substrate induced respirations, Glc-SIR, Tre-SIR, Lys-SIR; the control soil exerted significantly lower respiration values compared to the amended soil variants, and these showed significantly higher values due to the addition of enriched manures (M+B, M+S, M+MB+S) than after the addition of the control sole manure M (Figures 5L-N). On the contrary, the Ala-SIR (Figure 5O) and Arg-SIR (Figure 5P) showed in variants M+B and M+B+S no difference to the M variant, whereas the Ala-SIR in M+S was lower compared to the M variant. NAG-SIR was significantly decreased in non-biochar-amended variants (M and M+S) compared to the biochar-treated variants (M+B and M+B+S) (Figure 5Q).

4 Discussion

4.1 Effect of added amendments on pH and nitrogen forms in manure

The lower pH of the M+S and M+B+S variants (compared to the M and M+B) was ascribed to the acidifying potential of the elemental S addition, which was already reported (de la Fuente et al., 2007). Such biological oxidation of elemental S added to the alkaline mixed manure was referred to by (Costello et al., 2019). On the contrary, biochar in the manure M+B caused no pH change compared to the unamended manure (M), probably due to a negligible difference in the pH of the blended materials (manure and biochar). A significantly higher pH in M+B+S compared to the M+S variant was presumably caused by the neutralizing effect of added biochar, due to the sorption of S on its surface, such as reported by (Xu et al., 2014). These findings corroborated our hypotheses. The pH effect on other manure properties was ascribed from pH-significant ($p \leq 0.001$) correlations: positive with TKN ($r = 0.77$), P ($r = 0.79$), *nirS* ($r = 0.72$), and negative with N-NH_4 ($r = -0.97$), AOB ($r = -0.85$), *dsr* ($r = -0.98$) – these relations are also apparent from the PCA biplot.

Whereas the M+S variant showed significantly decreased TKN but significantly increased ammonium nitrogen compared to the unenriched manure; the M+S+B manure exerted significantly increased N-NH_4 content and decreased TKN compared to the M+B. The S-enriched variants (M+S, M+B+S) showed higher ammonium content than non-S-enriched ones, putatively due to increased acidity, which was coupled with the microbial production of H_2SO_4. Sulphuric acid may promote activity of proteolytic bacteria, neutralize and protonate NH_3 and, thus, mitigate its release from the manure. This mechanism is in line with the findings of (Mahimairaja et al., 1994b). Moreover, nitrification activity has a pH optimum for oxygen uptake between 7.0 and 7.4. Despite the presumed reduction in N loss *via* volatilization with S-treatment of the manure, higher TKN content in M and M+B (as compared to M+S and M+B+S) was observed. Concurrent with the previously reported benefit of acid manure to nitrification, an acidic pH increased the formation of bicarbonate during the hydrolysis of uric acid and urea (Vlek and Stumpe, 1978). Bicarbonate in manure may (opposite to the effect of sulphuric acid) cause higher losses of NH_3. The reduction in nitrogen losses due to its immobilization during co-composting with carbonaceous biochar-derived materials, referred to by (Wang et al., 2018; Nguyen et al., 2022), could also be involved.

4.2 Effect of added amendments on manure – derived phosphorus and organic carbon

The availability of P in the manure variants seemed to be pH-dependent and significantly related to the S reduction ($r = -0.82$,

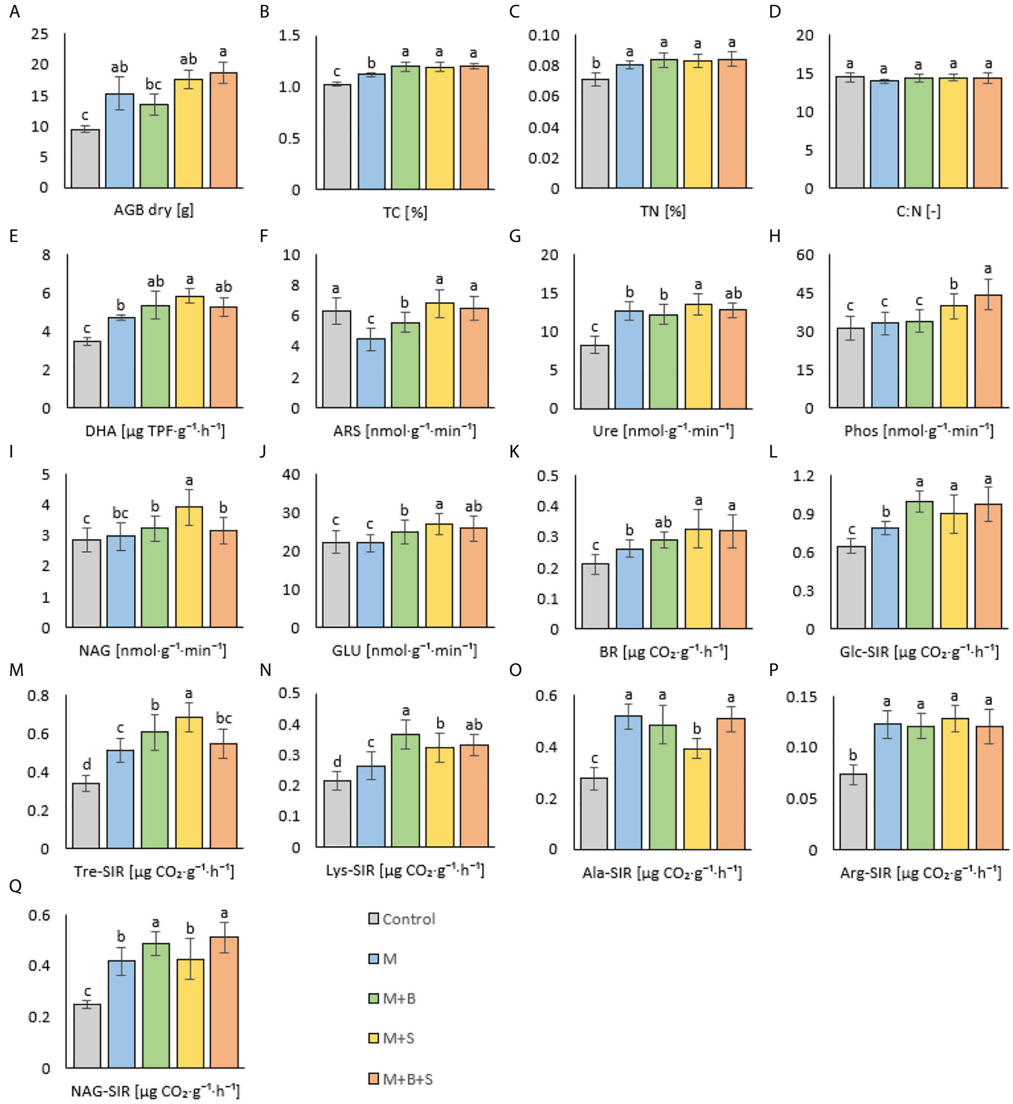

FIGURE 5
Dry plant above ground biomass and soil properties of variants amended with various manure types. **(A)** dry above ground biomass, **(B)** total carbon, **(C)** total nitrogen, **(D)** C:N ratio, **(E)** dehydrogenase activity, **(F)** arylsulfatase act., **(G)** urease act., **(H)** phosphatase act., **(I)** N-acetyl-β-D-glucosaminidase act., **(J)** β-glucosidase act., **(K)** basal respiration, **(L)** D-glucose-induced resp., **(M)** D-trehalose-induced resp., **(N)** L-lysine-induced resp., **(O)** L-alanine-induced resp., **(P)** L-arginine-induced resp., **(Q)** N-acetyl-β-D-glucosamine-induced resp. Different letters indicate differences at level of significance $p \le 0.05$.

$p \le 0.001$) and ammonium content ($r = -0.70$, $p \le 0.01$). Both M +S and M+B+S exerted the available P content lower than the manure M. These results may be explained by the acidifying effect of either sulphuric acid (H_2SO_4) or hydrogen sulphide (H_2S) and increased access of protons from acidified ammonium (NH_4^+), all of which factors favored the precipitation of P. Previous studies (Mahimairaja et al., 1994a; Penn and Camberato, 2019) referred to these mechanisms, which make phosphates less soluble at a low pH. The single-enriched variants (M+B, M+S) showed significantly lower C_{org} compared to the M and M+B+S. The TC content was close to the TN content. The access of biochar carbon putatively affected the C_{org} content in the variants M+B (and also M+B+S), which showed highest decomposition and C mineralization level. The highest composting rate could lead to increased C volatilization in the form of CO_2 (or CH_4) (Jiang et al., 2011). However, no excessive C_{org} source was added to the unmatured manure of this variant. Elemental S was presumed to increase microbial abundance and stimulate the microbial decomposing activity (Roig et al., 2004). Moreover, elemental S may enhance the formation of sulphuric acid, as was described by de la Fuente et al. (2007). The authors of the study revealed that sulphuric acid combined with carbonate materials leads to the production of sulphates and the removal of carbonates (in the form of CO_2). A significantly higher microbial activity in the M+B+S variant was presumed too and related to the evidence of increased aeration, which may cause desiccation similar as reported severe drying in the compost (Sundberg, 2005).

4.3 Effect of added materials on sulphur content in manure

The M+B manure contained a significantly less total S compared to the unenriched manure, whereas the total S value of the M+B+S variant was significantly the highest. The M+B manure was supplied with the biochar, i.e. the material with significantly lower S content compared to the unmatured manure, whereas the M+B+S was enriched by the excessive dose of elemental S together with biochar. The pyrolyzed matter has the potential to adsorb and stabilize any form of S transformation (Zhang et al., 2016; Lin et al., 2021) and mitigate its putative volatilization, e.g. in the form of H_2S. Under insufficient aerobic conditions, one can expect a partial reduction of elemental S to H_2S and its release into the environment.

4.4 Effect of added amendments on microbial abundance in manure

The co-fermentation of elemental sulphur and manure significantly modified biological properties; it led to the increased biomass of ammonia oxidizers and sulphur reducers. The addition of elemental S to the unmatured manure was crucial also for the abundance of microbiota. The significantly highest *dsr* value in the M+S was attributed to the absence of the putative biochar-mediated adsorption (as assumed for M+B+S) of elemental S, as described by Turk et al. (1992), which may function as a hindrance to the S reduction to H_2S (Lovley and Phillips, 1994).

The abundance of ammonium oxidizers was significantly increased in the M+S and M+B+S variants compared to the unenriched manure and M+B; the highest AOB biomass was found in the M+B+S manure (Figure 2B). The obtained results may be explained by the increased availability of the substrate for the AOB-mediated oxidation (acidified ammonium NH_4^+) in the respective S-supplied manures, which the finding agreed with the previous observations (Gu et al., 2011; Soaud et al., 2011). The higher abundance of AOB in M+B+S was presumably due to a higher C_{org} and to general biochar-stimulated microbial growth.

The results of *nirS* determination (an indicator of denitrifying microflora in manure) were contrary to the AOB values: the lowest value in the M+B+S variant (significantly decreased compared to the control manure) and significantly the highest value in the M+B variant. Denitrification is the biochar-mediated and stimulated process that may occur simultaneously with nitrification (Cayuela et al., 2013). However, a low pH strongly interferes with the nitrate oxidation (Brenzinger et al., 2015), which present a considerable reason for the lower abundance of denitrifying microorganisms in the S-supplied variants.

4.5 Effect of manure types on soil fertility and plant biomass yield

The dry ABG was the key property for the evaluation of the agriculture benefit of the co-composted manure. Compared to the control, amendment of any type of manure to soil led to the significantly higher AGB. The highest AGB value was found in the M+B+S variant. The best fertilizing properties of M+B+S from all four used amendments were ascribed from the significantly highest content of dry biomass and total S in the respective manure. AGB correlated significantly ($p \leq 0.01$) positively also with DHA ($r = 0.66$) and Ala-SIR ($r = 0.62$). The study by Yu et al. (2017) referred to a positive correlation between crop yield and soil N-NH_4, the available P and K and microbial diversity or microbial abundance preservation. A beneficial increase of corn plant biomass in the soil amended with S-enriched biochar, which occurred due to the enhanced plant uptake of S (Zhang et al., 2016), corroborated the results with M+B+S manure.

All manure-amended variants increased the soil TC and TN content compared to the control. The TN values among all manure-amended variants were comparable. Albeit the non-enriched M manure was markedly C_{org}-abundant; the soil M variant showed a significantly decreased TC compared to the M+B, M+S, M+B+S. However, both M+B+S and M+S manures showed higher ammonium nitrogen content and nitrification potential (AOB marker) compared to the M variant, and this indicated their higher N mineralization rate. Thus, enhanced C sequestration was presumably achieved due to application of manure with increased N conversion. The C:N ratio did not differ significantly between all variants. Both TC and TN correlated significantly ($p \leq 0.001$) positively with DHA ($r = 0.82$ and 0.66, respectively), Ure ($r = 0.77$ and 0.66, respectively) and substrate-induced respirations, e.g. Tre-SIR ($r = 0.64$ and 0.55, respectively), NAG-SIR ($r = 0.68$ and 0.57, respectively), Lys-SIR ($r = 0.67$ and 0.54, respectively) and Arg-SIR ($r = 0.76$ and 0.66, respectively). These relations proved that the amendment of enriched manures (M+S, M+B+S, eventually M+B) enhanced microbial activity and mineralization due to the derived higher nutrient content and availability (Holatko et al., 2022).

4.6 Effect of manure types on soil microbial activity

The manures applied to the pot experiment with barley (*Hordeum vulgare* L.) led to differences in soil properties compared to the control unamended soil, and between the variants amended with unenriched manure and the enriched manures. All manure variants, applied to the soil, significantly enhanced DHA activity compared to the control (Figure 3E). The increase in DHA due to the combined effect of manure and biochar was already reported (Brtnicky et al., 2019; Yilmaz and Ergun, 2019). Furthermore, a significantly higher DHA value was obtained in the M+S variant compared to the M variant because the S-enriched manure exerted properties (lowest pH, highest N-NH_4 and S-reducing microflora among the manures) that most enhanced the decomposing microbial activity in the amended soil. The higher access of S in the soil was reported to correlate with higher DHA (Katkar et al., 2011; Lemanowicz et al., 2020).

The elemental S amendment to manures (M+S, M+B+S) did not significantly change the soil ARS compared to the control, and the variants M and M+B showed even significantly lower ARS values. Our presumption of elemental S-stimulated enhancement of soil organic S mineralization (catalyzed by ARS), ascribed from (Castellano and Dick, 1991), was denied. On the contrary, the results imply the retarded S mineralization in the M and M+B soil variants due to the putatively higher portion of added mineral and readily available S, which might be caused by efficient ARS-mediated mineralization during the manure (M, M+B) fermentation. A similar significant biochar-derived increase in ARS was referred to in the soil environment (Khadem et al., 2019).

Significantly increased Ure, Phos, NAG and GLU activities were observed in the variants M+S and M+B+S, compared to the control. The M+S variants also induced the Ure, NAG and GLU values compared to the M and M+B enzyme values. The Phos was the highest in M+B+S. Previously, elemental S amendment was referred to increase soil ARS, Phos and Ure (Godlewska, 2018a). A significant ($p \leq 0.001$) positive correlation of Phos with Tre-SIR and Arg-SR ($r = 0.66$ and 0.59, respectively) and with dry AGB ($r = 0.69$) was found. NAG also correlated with AGB ($r = 0.53$; $p \leq 0.05$). These relations implied that S-amendment mediated enhanced organic matter decomposition led to higher transformation and anticipated increased nutrient uptake for higher plant biomass yield. A similar benefit of combined use of biochar and poultry manure was referred to by Lu et al. (2015) to enhance microbial growth and enzyme activities (e.g. Ure). However, the significant beneficial synergic effect of elemental S and manure on the soil enzyme activities was novel and not yet mentioned in the literature. The enzyme activity dependence on SOM decomposition and their positive relation is known (Wutzler et al., 2017) and was shown in the PCA biplot (Figure 6).

S-enriched manure-treated variants (M+S and M+B+S) exerted higher basal respiration compared to both the control and the non-enriched manure variant M (Figure 3K). It verified our presumption of a significantly stimulating effect of S (co-composed with manure) on the enhancement of soil microbial abundance and activity. Enhanced microbial BR implied the intensified mineralization and putatively increased availability of

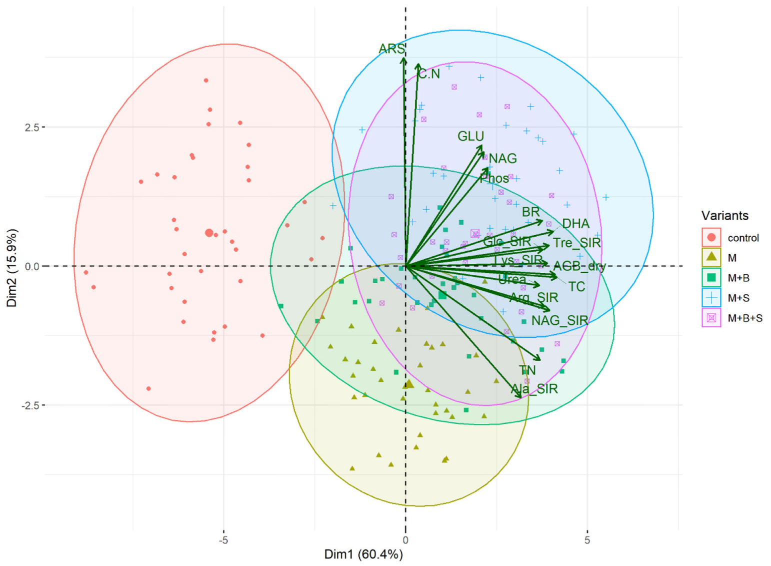

FIGURE 6
The PCA biplot of the soil properties.

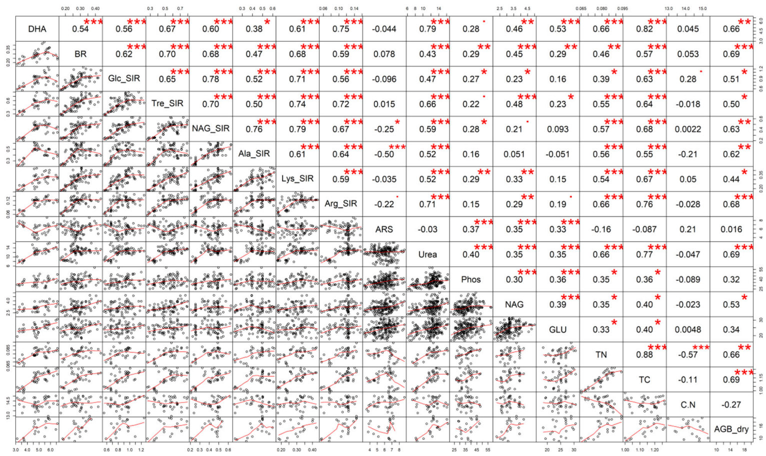

FIGURE 7
The Pearson's correlation matrix of the soil properties. Explanation: Significance at · $p \leq 0.10$; *$p \leq 0.05$; **$p \leq 0.01$; ***$p \leq 0.001$.

nutrients for plants, which lead to higher plant biomass yield, TC and TN, as shown on the positive significant ($p \leq 0.001$) correlation of BR and AGB ($r = 0.69$), TC ($r = 0.57$), and TN ($r = 0.46$, $p \leq 0.01$) (Figure 7).

The results of all types of substrates-induced respirations seemed to be close to the results of BR, as shown by the significant ($p \leq 0.001$-0.05) moderate to high correlation (r up to 0.79). Nevertheless, it was ascribed that manure enriched with biochar tended to stimulate more respiration inducible by N-rich substrates, whereas the application of S-enriched manure promoted higher respiration inducibility by the (non-nitrous) sugars. These differences implied a variable impact of used types of manure on functional soil diversity with the final consequence in the changes in the nutrient and other soil properties that affected the plant growth and biomass yield.

5 Conclusions

The sulphur-enriched manure showed the most lowered manure pH at the concurrent highest ammonium content. When manure, biochar and sulphur were co-fermented, the highest sulphur content and abundance of ammonium-oxidizing bacteria was observed. When added to soil, this biochar+sulphur-enriched manure promoted the highest dry aboveground plant biomass, the value was 98% higher compared to the unamended control, 38% higher compared to the amendment of biochar-enriched manure and 23% higher compared to the manure-amended variant. Sulphur-enriched manure types enhanced the most enzyme activities and soil respirations (basal, substrate-induced). Based on the results obtained, it was concluded that the co-fermentation of biological manures with bio-based materials, such as biochar and sulphur resulting as a by-product of biogas, is an attractive approach, not only to improve the enriched manure product but also to enhance soil fertility, health and crop productivity. This improvement of organic fertilizers may contribute to the circular economy and it will be further investigated by up-scaling on the field level.

Data availability statement

The original contributions presented in the study are included in the article/supplementary material. Further inquiries can be directed to the corresponding authors.

Author contributions

Conceptualization, MB and TH; methodology, TH, AK, and OL; software, TB; validation, TB, PS, PR, and JH; formal analysis, TH; investigation, AM; resources, JH and OL; data curation, TH, OL, and AK; writing - original draft preparation, JH, TH, AM, and PS; writing - review and editing, TH, AK, AM, MN, PS, PR, and MB; visualization, TB and AM; supervision, MB, TH, and MN; project administration, MB and AK.; funding acquisition, JH, AK, and MB. All authors have read and agreed to the published version of the manuscript.

Funding

The work was supported by the project of Technology Agency of the Czech Republic number TH04030142, by the Ministry of Agriculture of the Czech Republic, institutional support MZE-RO1218 and MZE-RO1722 and by Ministry of Education, Youth and Sports of the Czech Republic, grant number FCH-S-22-8001.

Conflict of interest

The authors JH, OL and AK are employed by Agrovyzkum Rapotin, Ltd., Vyzkumniku 267, 788 13 Rapotin, Czech Republic and Agricultural Research, Ltd., Troubsko, Czech Republic.

The remaining authors declare that the research was conducted in the absence of any commercial or financial relationships that could be construed as a potential conflict of interest.

Publisher's note

All claims expressed in this article are solely those of the authors and do not necessarily represent those of their affiliated organizations, or those of the publisher, the editors and the reviewers. Any product that may be evaluated in this article, or claim that may be made by its manufacturer, is not guaranteed or endorsed by the publisher.

References

Abou Hussien, E., Nada, W., and Elgezery, M. (2020). Influence of sulphur compost application on some chemical properties of calcareous soil and consequent responses of *Hordeum vulgare* l. plants. *Egyptian. J. Soil Sci.* 60 (1), 67–82. doi: 10.21608/ejss.2019.18503.1318

Ashraf, M. N., Jusheng, G., Lei, W., Mustafa, A., Waqas, A., Aziz, T., et al. (2021). Soil microbial biomass and extracellular enzyme–mediated mineralization potentials of carbon and nitrogen under long-term fertilization (> 30 years) in a rice–rice cropping system. *J. Soils. Sediments.* 21 (12), 3789–3800. doi: 10.1007/s11368-021-03048-0

Azeem, M., Hayat, R., Hussain, Q., Tahir, M. I., Imran, M., Abbass, Z., et al. (2019). Effects of biochar and NPK on soil microbial biomass and enzyme activity during 2 years of application in the arid region. *Arab. J. Geosci.* 12, 13. doi: 10.1007/s12517-019-4482-1

Ben-Dov, E., Brenner, A., and Kushmaro, A. (2007). Quantification of sulfate-reducing bacteria in industrial wastewater, by real-time polymerase chain reaction (PCR) using *dsrA* and *apsA* genes. *Microbial. Ecol.* 54 (3), 439–451. doi: 10.1007/s00248-007-9233-2

Bouranis, D. L., Venieraki, A., Chorianopoulou, S. N., and Katinakis, P. (2019). Impact of elemental sulfur on the rhizospheric bacteria of durum wheat crop cultivated on a calcareous soil. *Plants* 8 (10), 379. doi: 10.3390/plants8100379

Brenzinger, K., Dörsch, P., and Braker, G. (2015). pH-driven shifts in overall and transcriptionally active denitrifiers control gaseous product stoichiometry in growth experiments with extracted bacteria from soil. *Front. Microbiol.* 6, 961. doi: 10.3389/fmicb.2015.00961

Brtnicky, M., Dokulilova, T., Holatko, J., Pecina, V., Kintl, A., Latal, O., et al. (2019). Long-term effects of biochar-based organic amendments on soil microbial parameters. *Agronomy* 9 (11), 747. doi: 10.3390/agronomy9110747

Campbell, C. D., Chapman, S. J., Cameron, C. M., Davidson, M. S., and Potts, J. M. (2003). A rapid microtiter plate method to measure carbon dioxide evolved from carbon substrate amendments so as to determine the physiological profiles of soil microbial communities by using whole soil. *Appl. Environ. Microbiol.* 69 (6), 3593–3599. doi: 10.1128/AEM.69.6.3593-3599.2003

Castellano, S. D., and Dick, R. P. (1991). Cropping and sulfur fertilization influence on sulfur transformations in soil. *Soil Sci. Soc. America J.* 55 (1), 114–121. doi: 10.2136/sssaj1991.03615995005500010020x

Cayuela, M. L., Sánchez-Monedero, M. A., Roig, A., Hanley, K., Enders, A., and Lehmann, J. (2013). Biochar and denitrification in soils: When, how much and why does biochar reduce N_2O emissions? *Sci. Rep.* 3 (1), 1–7. doi: 10.1038/srep01732

Costello, R. C., Sullivan, D. M., Bryla, D. R., Strik, B. C., and Owen, J. S. (2019). Compost feedstock and compost acidification affect growth and mineral nutrition in northern highbush blueberry. *HortScience* 54 (6), 1067–1076. doi: 10.21273/HORTSCI13599-18

Czekała, W., Malińska, K., Cáceres, R., Janczak, D., Dach, J., and Lewicki, A. (2016). Co-Composting of poultry manure mixtures amended with biochar – the effect of biochar on temperature and c-CO_2 emission. *Bioresour. Technol.* 200, 921–927. doi: 10.1016/j.biortech.2015.11.019

de la Fuente, R. G., Carrión, C., Botella, S., Fornes, F., Noguera, V., and Abad, M. (2007). Biological oxidation of elemental sulphur added to three composts from different feedstocks to reduce their pH for horticultural purposes. *Bioresour. Technol.* 98 (18), 3561–3569. doi: 10.1016/j.biortech.2006.11.008

Doi, R., and Ranamukhaarachchi, S. L. (2009). Soil dehydrogenase in a land degradation-rehabilitation gradient: Observations from a savanna site with a wet/dry seasonal cycle. *Rev. Biol. Trop.* 57, 223–234.

EC, European Commission (2021). Soil and Land. EU Soil Strategy for 2030 Reaping the benefits of healthy soils for people, food, nature and climate. Document 52021DC0699. Brussels, 1–26.

Egnér, H. A., Riehm, H., and Domingo, W. R. (1960). Untersuchungen über die chemische bodenanalyse als grundlage für die beurteilung des nährstoffzustandes der böden. II. chemische extraktionsmethoden zur phosphor-und kaliumbestimmung. *Kungliga. Lantbrukshögskolans. Annaler.* 26, 199–215.

FAO, Food and Agriculture Organization of the United Nations (2014). *World reference base for soil resources*. (Rome, Italy: Food and Agriculture Organization of the United Nations).

Godlewska, A. (2018a). Assessment of the effect of NPK fertilisation and elemental sulphur on soil enzyme activity. *Fresenius. Environ. Bull.* 27 (1), 180–186.

Godlewska, A. (2018b). Sulphur content in test plants and arylsulfatase activity in soil after application of waste materials. *Appl. Ecol. Environ. Res.* 16 (1), 145–152. doi: 10.15666/aeer/1601_145152

Gu, W., Zhang, F., Xu, P., Tang, S., Xie, K., Huang, X., et al. (2011). Effects of sulphur and *Thiobacillus thioparus* on cow manure aerobic composting. *Bioresour. Technol.* 102 (11), 6529–6535. doi: 10.1016/j.biortech.2011.03.049

Hagemann, N., Subdiaga, E., Orsetti, S., de la Rosa, J. M., Knicker, H., Schmidt, H. P., et al. (2018). Effect of biochar amendment on compost organic matter composition following aerobic composting of manure. *Sci. Total. Environ.* 613, 20–29. doi: 10.1016/j.scitotenv.2017.08.161

Hammerschmiedt, T., Holatko, J., Sudoma, M., Kintl, A., Vopravil, J., Ryant, P., et al. (2021). Biochar and sulphur enriched digestate: Utilization of agriculture associated waste products for improved soil carbon and nitrogen content, microbial activity, and plant growth. *Agronomy* 11 (10), 2041. doi: 10.3390/agronomy11102041

He, X., Yin, H., Sun, X., Han, L., and Huang, G. (2018). Effect of different particle-size biochar on methane emissions during pig manure/wheat straw aerobic composting: Insights into pore characterization and microbial mechanisms. *Bioresour. Technol.* 268, 633–637. doi: 10.1016/j.biortech.2018.08.047

Hoesly, R. M., Smith, S. J., Feng, L., Klimont, Z., Janssens-Maenhout, G., Pitkanen, T., et al. (2018). Historical, (1750–2014) anthropogenic emissions of reactive gases and aerosols from the community emissions data system (CEDS). *Geosci. Model. Dev.* 11 (1), 369–408. doi: 10.5194/gmd-11-369-2018

Holatko, J., Hammerschmiedt, T., Datta, R., Baltazar, T., Kintl, A., Latal, O., et al. (2020). Humic acid mitigates the negative effects of high rates of biochar application on microbial activity. *Sustainability* 12 (22), 9524. doi: 10.3390/su12229524

Holatko, J., Hammerschmiedt, T., Mustafa, A., Kintl, A., Radziemska, M., Baltazar, T., et al. (2022). Carbon-enriched organic amendments differently affect the soil chemical, biological properties and plant biomass in a cultivation time-dependent manner. *Chem. Biol. Technol. Agric.* 9, 52. doi: 10.1186/s40538-022-00319-x

Hoover, N. L., Law, J. Y., Long, L. A., Kanwar, R. S., and Soupir, M. L. (2019). Long-term impact of poultry manure on crop yield, soil and water quality, and crop revenue. *J. Environ. Manage.* 252, 109582. doi: 10.1016/j.jenvman.2019.109582

Hoskins, B., Wolf, A., and Wolf, N. (2003). "Dry matter analysis," in *Recommended methods of manure analysis*. Eds. J. Peters, S. Combs, B. Hoskins, J. Jarman, J. Kovar, M. Watson, A. Wolf and N. Wolf (Madison, WI, USA: Univ. of Wisconsin Cooperative Extension Publishing), 14–17.

Iocoli, G. A., Zabaloy, M. C., Pasdevicelli, G., and Gómez, M. A. (2019). Use of biogas digestates obtained by anaerobic digestion and co-digestion as fertilizers: Characterization, soil biological activity and growth dynamic of *Lactuca sativa* l. *Sci. Total. Environ.* 647, 11–19. doi: 10.1016/j.scitotenv.2018.07.444

Janczak, D., Malińska, K., Czekała, W., Cáceres, R., Lewicki, A., and Dach, J. (2017). Biochar to reduce ammonia emissions in gaseous and liquid phase during composting of poultry manure with wheat straw. *Waste. Manage.* 66, 36–45. doi: 10.1016/j.wasman.2017.04.033

Jiang, T., Schuchardt, F., Li, G., Guo, R., and Zhao, Y. (2011). Effect of C/N ratio, aeration rate and moisture content on ammonia and greenhouse gas emission during the composting. *J. Environ. Sci. (China)* 23, 1754–1760.

Jindo, K., Suto, K., Matsumoto, K., García, C., Sonoki, T., and Sanchez-Monedero, M. A. (2012). Chemical and biochemical characterisation of biochar-blended composts prepared from poultry manure. *Bioresour. Technol.* 110, 396–404. doi: 10.1016/j.biortech.2012.01.120

Kandeler, E., Deiglmayr, K., Tscherko, D., Bru, D., and Philippot, L. (2006). Abundance of *narG, nirS, nirK*, and *nosZ* genes of denitrifying bacteria during primary successions of a glacier foreland. *Appl. Environ. Microbiol.* 72 (9), 5957–5962. doi: 10.1128/AEM.00439-06

Katkar, R. N., Sonune, B. A., and Kadu, P. R. (2011). Long-term effect of fertilization on soil chemical and biological characteristics and productivity under sorghum (*Sorghum bicolor*)-wheat (*Triticum aestivum*) system in vertisol. *Indian J. Agric. Sci.* 81 (8), 734.

Khadem, A., Besharati, H., and Khalaj, M. A. (2019). Biochar application changed arylsulfatase activity, kinetic and thermodynamic aspects. *Eur. J. Soil Biol.* 95, 103134. doi: 10.1016/j.ejsobi.2019.103134

Kirchmann, H., and Thorvaldsson, G. (2000). Challenging targets for future agriculture. *Eur. J. Agron.* 12 (3-4), 145–161. doi: 10.1016/S1161-0301(99)00053-2

Kulhánek, M., Černý, J., Balík, J., Sedlář, O., and Suran, P. (2018). Potential of Mehlich 3 method for extracting plant available sulfur in the Czech agricultural soils. *Plant Soil Environ.* 64, 455–462. doi: 10.17221/372/2018-PSE

Lal, R. (2009). Challenges and opportunities in soil organic matter research. *Eur. J. Soil Sci.* 60, 158–169. doi: 10.1111/j.1365-2389.2008.01114.x

Lal, R. (2020). Managing soils for resolving the conflict between agriculture and nature: The hard talk. *Eur. J. Soil Sci.* 71, 1–9. doi: 10.1111/ejss.12857

Lemanowicz, J., Brzezińska, M., Siwik-Ziomek, A., and Koper, J. (2020). Activity of selected enzymes and phosphorus content in soils of former sulphur mines. *Sci. Total. Environ.* 708, 134545. doi: 10.1016/j.scitotenv.2019.134545

Li, Y. F., Hu, S. D., Chen, J. H., Müller, K., Li, Y. C., Fu, W. J., et al. (2018). Effects of biochar application in forest ecosystems on soil properties and greenhouse gas emissions: a review. *J. Soil. Sediment.* 18, 546–563. doi: 10.1007/s11368-017-1906-y

Lin, J. C., Cheng, A. C., Shiu, Y. L., Wong, Y. C., Yeh, S. P., Simangunsong, T., et al. (2021). Using the biochar produced from spend mushroom substrate to improve the environmental condition of aquaculture pond. *Aquac. Res.* 52, 3532–3539. doi: 10.1111/are.15194

Liu, X., Herbert, S. J., Hashemi, A. M., Zhang, X., and Ding, G. (2011). Effects of agricultural management on soil organic matter and carbon transformation - A review. *Plant. Soil Environ.* 52, 531–543. doi: 10.17221/3544-PSE

Lovley, D. R., and Phillips, E. J. (1994). Novel processes for anaerobic sulfate production from elemental sulfur by sulfate-reducing bacteria. *Appl. Environ. Microbiol.* 60 (7), 2394–2399. doi: 10.1128/aem.60.7.2394-2399.1994

Lu, H., Lashari, M. S., Liu, X., Ji, H., Li, L., Zheng, J., et al. (2015). Changes in soil microbial community structure and enzyme activity with amendment of biochar-manure compost and pyroligneous solution in a saline soil from central China. *Eur. J. Soil Biol.* 70, 67–76. doi: 10.1016/j.ejsobi.2015.07.005

Mahimairaja, S., Bolan, N. S., and Hedley, M. J. (1994a). Dissolution of phosphate rock during the composting of poultry manure: An incubation experiment. *Fertilizer. Res.* 40 (2), 93–104.

Mahimairaja, S., Bolan, N. S., Hedley, M. J., and Macgregor, A. N. (1994b). Losses and transformation of nitrogen during composting of poultry manure with different amendments: An incubation experiment. *Bioresour. Technol.* 47 (3), 265–273. doi: 10.1016/0960-8524(94)90190-2

Malik, K. M., Khan, K. S., Billah, M., Akhtar, M. S., Rukh, S., Alam, S., et al. (2021). Organic amendments and elemental sulfur stimulate microbial biomass and sulfur oxidation in alkaline subtropical soils. *Agronomy-Basel* 11 (12), 2514. doi: 10.3390/agronomy11122514

Maurer, D. L., Koziel, J. A., Kalus, K., Andersen, D. S., and Opalinski, S. (2017). Pilot-scale testing of non-activated biochar for swine manure treatment and mitigation of ammonia, hydrogen sulfide, odorous volatile organic compounds (VOCs), and greenhouse gas emissions. *Sustainability* 6), 929. doi: 10.3390/su9060929

Mustafa, A., Hu, X., Abrar, M. M., Shah, S. A., Nan, S., Saeed, Q., et al. (2021). Long-term fertilization enhanced carbon mineralization and maize biomass through physical protection of organic carbon in fractions under continuous maize cropping. *Appl. Soil Ecol.* 165, 103971. doi: 10.1016/j.apsoil.2021.103971

Mustafa, A., Minggang, X., Shah, S. A., Abrar, M. M., Nan, S., Baoren, W., et al. (2020). Soil aggregation and soil aggregate stability regulate organic carbon and nitrogen storage in a red soil of southern China. *J. Environ. Manage.* 270, 110894. doi: 10.1016/j.jenvman.2020.110894

Naveed, M., Ditta, A., Ahmad, M., Mustafa, A., Ahmad, Z., Conde-Cid, M., et al. (2021). Processed animal manure improves morpho-physiological and biochemical characteristics of *Brassica napus* l. under nickel and salinity stress. *Environ. Sci. pollut. Res.* 28 (33), 45629–45645. doi: 10.1007/s11356-021-14004-3

Nguyen, M. K., Lin, C., Hoang, H. G., Sanderson, P., Dang, B. T., Bui, X. T., et al. (2022). Evaluate the role of biochar during the organic waste composting process: A critical review. *Chemosphere* 299, 134488. doi: 10.1016/j.chemosphere.2022.134488

Penn, C. J., and Camberato, J. J. (2019). A critical review on soil chemical processes that control how soil pH affects phosphorus availability to plants. *Agriculture* 9 (6), 120. doi: 10.3390/agriculture9060120

Qaswar, M., Ahmed, W., Jing, H., Hongzhu, F., Xiaojun, S., Xianjun, J., et al. (2019). Soil carbon (C), nitrogen (N) and phosphorus (P) stoichiometry drives phosphorus lability in paddy soil under long-term fertilization: A fractionation and path analysis study. *PloS One* 14 (6), 0218195. doi: 10.1371/journal.pone.0218195

Rogovska, N., Laird, D., Cruse, R., Fleming, P., Parkin, T., and Meek, D. (2011). Impact of biochar on manure carbon stabilization and greenhouse gas emissions. *Soil Sci. Soc. Am. J.* 75, 871–879.

Roig, A., Cayuela, M. L., and Sánchez-Monedero, M. A. (2004). The use of elemental sulphur as organic alternative to control pH during composting of olive mill wastes. *Chemosphere* 57 (9), 1099–1105. doi: 10.1016/j.chemosphere.2004.08.024

Rotthauwe, J. H., Witzel, K. P., and Liesack, W. (1997). The ammonia monooxygenase structural gene *amoA* as a functional marker: Molecular fine-scale analysis of natural ammonia-oxidizing populations. *Appl. Environ. Microbiol.* 63 (12), 4704–4712. doi: 10.1128/aem.63.12.4704-4712.1997

Skwierawska, M., Benedycka, Z., Jankowski, K., and Skwierawski, A. (2016). Sulphur as a fertiliser component determining crop yield and quality. *J. Elementol.* 21 (2), 209–223. doi: 10.5601/jelem.2015.20.3.992

Skwierawska, M., Zawartka, L., and Zawadzki, B. (2008). The effect of different rates and forms of sulphur applied on changes of soil agrochemical properties. *Plant Soil Environ.* 54 (4), 171–177. doi: 10.17221/391-PSE

Soaud, A. A., Saleh, M. E., El-Tarabily, K. A., Sofian-Azirun, M., and Rahman, M. M. (2011). Effect of elemental sulfur application on ammonia volatilization from surface applied urea fertilizer to calcareous sandy soils. *Aust. J. Crop Sci.* 5 (5), 611–619.

Soltanaeva, A., Suleimenov, B., Saparov, G., and Vassilina, T. (2018). Effect of sulfur-containing fertilizers on the chemical properties of soil and winter wheat yield. *Bulgarian. J. Agric. Sci.* 24 (4), 586–591.

Song, Y. Z., Li, Y. F., Cai, Y. J., Fu, S. L., Luo, Y., Wang, H. L., et al. (2019). Biochar decreases soil N2O emissions in moso bamboo plantations through decreasing labile n concentrations, n-cycling enzyme activities and nitrification/denitrification rates. *Geoderma* 348, 135–145. doi: 10.1016/j.geoderma.2019.04.025

Sundberg, C. (2005). Improving compost process efficiency by controlling aeration, temperature and pH. Uppsala, Sveriges lantbruksuniv. *Acta Universitatis Agriculturae Sueciae* 103, 1652–6880.

Tetteh, R. N. (2015). Chemical soil degradation as a result of contamination: A review. *J. Soil Sci. Environ. Manage.* 6 (11), 301–308. doi: 10.5897/JSSEM15.0499

Turk, A., Sakalis, E., Rago, O., and Karamitsos, H. (1992). Activated carbon systems for removal of light gasesa. *Ann. N. Y. Acad. Sci.* 661 (1), 221–228. doi: 10.1111/j.1749-6632.1992.tb26043.x

Virto, I., Imaz, M. J., Fernández-Ugalde, O., Gartzia-Bengoetxea, N., Enrique, A., and Bescansa, P. (2014). Soil degradation and soil quality in Western Europe: Current situation and future perspectives. *Sustainability* 7 (1), 313–365. doi: 10.3390/su7010313

Vlek, P. L., and Stumpe, J. M. (1978). Effects of solution chemistry and environmental conditions on ammonia volatilization losses from aqueous systems. *Soil Sci. Soc. America J.* 42 (3), 416–421. doi: 10.2136/sssaj1978.03615995004200030008x

Wang, Q., Awasthi, M. K., Ren, X., Zhao, J., Li, R., Wang, Z., et al. (2018). Combining biochar, zeolite and wood vinegar for composting of pig manure: The effect on greenhouse gas emission and nitrogen conservation. *Waste. Manage.* 74, 221–230. doi: 10.1016/j.wasman.2018.01.015

Wang, X., Jia, Z., Liang, L., Yang, B., Ding, R., Nie, J., et al. (2016). Impacts of manure application on soil environment, rainfall use efficiency and crop biomass under dryland farming. *Sci. Rep.* 6 (1), 1–8. doi: 10.1038/srep20994

Wutzler, T., Zaehle, S., Schrumpf, M., Ahrens, B., and Reichstein, M. (2017). Adaptation of microbial resource allocation affects modelled long term soil organic matter and nutrient cycling. *Soil Biol. Biochem.* 115, 322–336. doi: 10.1016/j.soilbio.2017.08.031

Xu, X., Cao, X., Zhao, L., and Sun, T. (2014). Comparison of sewage sludge-and pig manure-derived biochars for hydrogen sulfide removal. *Chemosphere* 111, 296–303. doi: 10.1016/j.chemosphere.2014.04.014

Yilmaz, I. F., and Ergun, Y. A. (2019). Impact of biochar and animal manure on some biological and chemical properties of soil. *Appl. Ecol. Environ. Res.* 17 (4), 8865–8876. doi: 10.15666/aeer/1704_88658876

Yu, L., Lu, X., He, Y., Brookes, B. C., Liao, H., and Xu, J. M. (2017). Combined biochar and nitrogen fertilizer reduces soil acidity and promotes nutrient use efficiency by soybean crop. *J. Soils Sediments* 17, 599–610.

Zhang, H., Voroney, R. P., Price, G. W., and White, A. J. (2016). Sulfur-enriched biochar as a potential soil amendment and fertiliser. *Soil Res.* 55 (1), 93–99. doi: 10.1071/sr15256

Zhang, H., Wang, S., Zhang, J., Tian, C., and Luo, S. (2021). Biochar application enhances microbial interactions in mega-aggregates of farmland black soil. *Soil Tillage. Res.* 213, 105145. doi: 10.1016/j.still.2021.105145

frontiers | Frontiers in Plant Science

TYPE Original Research
PUBLISHED 20 October 2022
DOI 10.3389/fpls.2022.1001740

Check for updates

OPEN ACCESS

EDITED BY
Amanullah,
University of Agriculture,
Peshawar, Pakistan

REVIEWED BY
Dali Song,
Chinese Academy of Agricultural Sciences (CAAS), China
Md. Mizanur Rahman,
Islamic University, Bangladesh

*CORRESPONDENCE
Muhammad Musa Khan
drmusakhan@outlook.com
Qianhua Ji
qhgee@163.com

†Lead contact

SPECIALTY SECTION
This article was submitted to Plant Nutrition, a section of the journal Frontiers in Plant Science

RECEIVED 24 July 2022
ACCEPTED 23 September 2022
PUBLISHED 20 October 2022

CITATION
Guo YJ, Qiu BL, Khan Z, Jiang H, Ji QH, Fan QZ and Khan MM (2022) The potential for biochar application in "Shatangju" (*Citrus reticulate* cv.) orchard on acid red soil: biochar prepared from its organic waste in an orchard.
Front. Plant Sci. 13:1001740.
doi: 10.3389/fpls.2022.1001740

The potential for biochar application in "Shatangju" (*Citrus reticulate* cv.) orchard on acid red soil: Biochar prepared from its organic waste in an orchard

Yanjun Guo[1], Baoli Qiu[2], Zaid Khan[3], Hui Jiang[1], Qianhua Ji[1]*, Qizhou Fan[4] and Muhammad Musa Khan[5]*†

[1]Fruit Tree Research Institute/Life Sciences College of Zhaoqing University, Zhaoqing, China, [2]Chongqing Key Laboratory of Vector Insects, College of Life Sciences, Chongqing Normal University, Chongqing, China, [3]College of Natural Resources and Environment, South China Agricultural University, Guangzhou, China, [4]Engineering College of Huazhong Agricultural University, Wuhan, China, [5]Hainan Institute of Zhejiang University, Sanya, China

Carbonization of agricultural and forestry wastes is the main use of biochar application in agriculture. In this study, the effects of biochar on the physical and chemical properties of soil and diversity in rhizosphere microorganisms, leaf nutrients and fruit quality of acid red soil in "Shatangju" (*Citrus reticulate* cv.) orchard were studied using organic wastes and small-scale carbonization furnaces from orchards were used to produce biochar. The results showed that the finished rate of biochar produced from the organic wastes in the orchard was approximately 37%, and the carbon content of the finished product was as high as 80%. The results suggested that the biochar produced in the orchard could meet the annual consumption of the orchard. Applying biochar can improve the physical and chemical properties of acid soil in the "Shatangju" orchard by enhancing the availability of various mineral nutrients such as nitrogen, phosphorus, potassium, calcium, magnesium and boron. The species and quantity of root and rhizosphere microbial communities (fungi, bacteria and archaea) increased, and the dominant bacterial group changed, manifested in the increase in microbial diversity. Biochar directly affected the soil pH value and increased the soil organic carbon content, which may be the main reason for the change in microbial diversity in the soil and rhizosphere of "Shatangju" in the orchard and pot tests. The fruit quality of each treatment group with biochar was also better than that of the control group and improved fruit coloring. In the pure soil test, whether or not chemical fertilizer was applied, 3% biochar amendments can provide a suitable pH value for "Shatangju" growth and are relatively stable. Regardless of whether or not fertilizer was applied, 1.5%-3% biochar improved the soil in the pot test. In the field, the biochar at a rate of 2.4 kg/plant to 3.6 kg/plant, respectively, was the best in improving soil physical and chemical properties, foliar nutrition and fruit quality. Therefore, the amount of biochar added in the open environment (if the garden) can be slightly adjusted according to the results of the closed environment test (pure soil test and pot test). In this experiment, we explored the self-recycling of organic carbon, mainly through the preparation of a simple small-scale biochar furnace suitable for the use by orchards, and selected the appropriate amount of biochar to improve the physical and chemical conditions of "Shatangju" orchard soil and increase fruit quality.

KEYWORDS

biochar, *Citrus reticulate*, acid red soil, organic carbon cycle, soil microbiota, nitrogen content, fruit quality

1 Introduction

Agricultural practices improve soil quality and increase soil nutrient supply capacity, which has been emphasized in many fields across basic and applied sciences (Puget and Lal, 2005; Du et al., 2013; Iqbal et al., 2022). Fertilizers are important agricultural inputs that play an irreplaceable role in agricultural development. Excessive chemical fertilizer application is a common and serious problem in China as farmers are concerned about increased food demand, low soil fertility, and a high multiple cropping index (Tian et al., 2016). Excessive chemical fertilizer application reduces soil quality, acidification, and nonpoint source pollution (Xia et al., 2020). Thus, controlling chemical fertilizer application while ensuring high and stable yield is a key area of agricultural research. Limited use of organic nutrient resources and application of organic materials to replace some chemical fertilizers have been shown to effectively reduce the amount of chemical fertilizer needed, increase soil productivity, ensure crop yield, and improve local ecological functions (Liu et al., 2022).

Carbonization of agricultural and forestry wastes is the focus of biochar application in agriculture (Pawlak-Kruczek et al., 2020). Biochar is a carbon (C) rich thermally decomposed organic material produced through the pyrolysis process from the feedstock at high temperatures (300°C-700°C) under a limited supply of oxygen (Zhang et al., 2013b). The feedstock may include crop residues, tree bark, wood materials, chicken litter, sewage sludge or dairy manure (Oshunsanya and Aliku, 2016). It is important to mention that biochar differs from charcoal and carbon-based materials. It has distinctive biological, chemical and physical properties (Oni et al., 2019). Its porous structure, high surface area, and low degradation rate played an important role in soil nutrient retention (Khan et al., 2021b). The high pH, electric conductivity (EC), cation exchange capacity (CEC), high carbon contents and abundance surface functional groups are important for environmental pollutant complexation, e.g., heavy metals (Ahmad et al., 2014; Bashir et al., 2018). Incorporating biochar in the soil can prominently increase soil aeration, porosity, water holding capacity and nutrients, which improve soil fertility, plant growth and carbon sequestration in soil. The high pH of biochar is due to its high alkalinity and CEC, which can enhance soil efficiency (Ahmad et al., 2014).

Soil microorganisms play an imperative role in the nutrient cycle of soil, including the organic matter composition and soil aggregate arrangement (Oleszczuk et al., 2014). Soil microorganisms affect soil fertility and ecosystems (Tardy et al., 2015). Numerous studies have recorded an enhancement in soil microorganisms and biomass by adding biochar to soil (Bruun et al., 2014; Yu et al., 2019). Meng et al. (2019) documented that biochar derived from wheat straw incorporation into soil significantly increased the community abundance and diversity of plant beneficial bacterial and fungal taxa and the variety of plant wheat seedling rhizospheres. Additionally, Ahmad et al. (2016) described that the microbiota in the applied soil was significantly diverse, e.g., Pseudomonas, a major rhizosphere-encouraging bacteria, was markedly improved by the biochar applied treatments. Biochar may likewise enhance the abundance of ammonia-oxidizing bacteria and archaea and reduce (Proteobacteria, Firmicutes) the overall abundance of oligotrophic and copiotrophic taxa separately (Meng et al., 2019). On the other hand, biochar application was also reported to reduce abundance of microbial communities of Proteobacteria, Acidobacteria, Firmicutes, and Bacteroidetes (Wu et al., 2016).

"Shatangju" is China's main citrus variety and a famous distinct local variety (Wang et al., 2012b). It is characterized by easy peeling, no core, slagging and high sweetness (Li et al., 2012; Li et al., 2019). Recently, it has been mainly grown in Guangdong Province and Guangxi Province, belonging to the citrus industrial belt in the Xijiang River Basin of China. The "Shatangju" orchard covers an area of 6 million mu (Chaisiri et al., 2021). The soil in the main planting area of "Shatangju" is the acidic red soil. Fruit farmers generally use lime to improve the soil acidity with lime. However, a large amount of long-term application of lime will cause soil hardening, damage beneficial soil microorganisms, reduce soil organic carbon, and easily cause the imbalance of soil calcium, potassium, magnesium and other elements, and the soil is prone to acid reversion (Zhang et al., 2013c).

In China, relevant research on biochar was conducted, and there are many fields of application, but there are few examples related to production of “Shatangju.” This study was designed to evaluate the effect of biochar prepared from “Shatangju” orchard waste on improving the properties of acid red soil and affecting the yield and quality of “Shatangju.” The effect of “Shatangju” plant waste biochar on the soil physical and chemical properties of soil was explored in this study. The composition of soil and root microbial communities under different biochar amendments was also examined. At the same time, the effect of biochar on fruit quality was evaluated. The results of this study will provide information about self-made biochar under field conditions for improving “Shatangju” production.

2 Materials and methods

2.1 Plant material

The experiments were conducted in 2020 and 2021. The “Shatangju” plants (2 years old) plants were grown in root-pruning bags with a diameter of 60 cm and height of 40 cm filled with acid red soil and were used for pot experimentation; ten-year-old “Shatangju” plants were used as the experimental trees in the orchard, with row spacing of 2.5 m × 2.5 m. The acid red soil bearing the following physiochemical was used as potting soil: pH 4.43, OMC (Organic matter content) 15.17 g/kg, A-N (available nitrogen) 72.57 mg/kg, A-P (available phosphorus) 15.23 mg/kg, A-K (available potassium) 369.93 mg/kg, E-Ca (exchangeable calcium)1.82 g/kg, E-Mg (exchangeable magnesium) 0.15 g/kg, A-Zn (available zinc) 18.79 mg/kg, A-B (available boron)1.17 mg/kg, A-Cu (available copper) 0.54 mg/kg and E-Mn (exchangeable manganese) 18.57 g/kg. Orchard soil: moisture content 19.9%, field capacity 30%, bulk density1.22 g/cm, porosity 3.65%, pH4.82, OMC 21.48 g/kg, CEC 8.04 cmol/kg, A-N 110.52 mg/kg, A-P 22.71 mg/kg, A-K 153 mg/kg, E-Ca 889.45mg/kg, E-Mg 49.9 g/kg, A-Zn 3.88 mg/kg, and A-B0.86 mg/kg.

2.2 Test method

2.2.1 Preparation and index determination of biochar

Biochar was prepared from pruned citrus branches and interrow grass in the citrus orchard using a Shizishan brand carbonization furnace provided by the School of Engineering, Huazhong Agricultural University, Patent # ZL 201310290114.X. The branches were cut into 10-cm and 20-cm pieces after pyrolysis at 500°C-550°C under anoxic conditions. Biochar was screened through a 20-mesh sieve and used in the pot and field experiments. Plant ash was prepared with the same materials as the control. The samples’ yield rate, moisture content, ash content, and carbon content of the samples were measured (Brahmakshatriya and Donker, 1971; Wang et al., 2009). The experiment was repeated three times every year.

The effect of biochar on the pH value of red soil was determined by pouring 2 kg of acid red soil into each flower pot. Biochar was applied to the flowerpot according to 0%, 1%, 2%, 3%, 4%, 5% and 6% of the soil weight. NPK 1% (15-15-15) compound fertilizer was prepared and applied in a flowerpot containing biochar. The soil pH value was measured continuously throughout the soil incubation period. The experiment was repeated three times every year.

2.2.2 Biochar amendments on citrus in pot tests

The 25 kg crushed and air-dried red soil was spiked with biochar and placed in 35 L root-pruning bags. One “Shatangju” was planted in a bag in rain-shelter cultivation conditions. The percentages of biochar amendments to the dry weight of red soil were 0, 1.5%, 3%, 4.5%, and 6%. The base fertilizer was modified Hoagland-Amon nutrient solution [KH_2PO_4, KNO_3, $Ca (NO_3)_2$, and $MgSO_4.7H_2O$ were 136, 505, 1180, and 492 mg/kg, respectively; H_3BO_3, $MnCl.4H_2O$, $ZnSO_4.7H_2O$, $CuSO_4.5H_2O$, Na_2MoO_4 and EDTA-Fe were 2.86, 1.81, 0.22, 0.08, 0.09 and 48.5 mg/kg, respectively]. The experiment was repeated three times every year.

Including the control, ten treatments were established: 1.5% biochar (1.5% C), 3% biochar (3% C), 4.5% biochar (4.5% C), 6% biochar (6% C), base fertilizer (BF), base fertilizer + 1.5% biochar (BF+1.5% C), base fertilizer + 3% biochar (BF+3% C), base fertilizer + 4.5% biochar (BF+4.5% C) and base fertilizer + 6% biochar (BF+6% C). The soil and plant indices were measured at the time of planting and 9 months post-cultivation. In the control group, only the dressing furrow was dug, and the soil was backfilled. The experiment was repeated three times every year.

2.2.3 Biochar amendments on “Shatangju” in the orchard

Six treatments, including 0 kg biochar/plant (control), 1.2 kg biochar/plant (C-1.2 kg), 2.4 kg biochar/plant (C-2.4 kg), 3.6 kg biochar/plant (C-3.6 kg), 4.8 kg biochar/plant (C-4.8 kg) and 6 kg biochar/plant (C-6 kg), were established. The location of biochar application was at the drip line of the tree crown. One 80 cm long, 30 cm wide, and 30 cm deep dressing furrow was dug from the north and the south and the biochar and soil were mixed evenly before the application.

2.3 Sample collection and determination method

2.3.1 Soil and root samples

In the pot experiments, 0-20 cm topsoil at 5-10 cm away from the plant trunk was collected. In the orchard experiment, two biochar amendment sites were randomly selected, and the soil 0-30 cm deep from the soil layer was evenly collected. The quartering method was used diagonally, choosing 0.5 kg soil samples to determine the soil pH value and available nutrients. The roots and rhizosphere soil were frozen at -80°C, and the microbial community diversity of the soil, rhizosphere soil, and roots was measured.

The drying method was used for soil moisture content measurement, the Wilcox method for field capacity, and the ring-cutting method for bulk density (Khan et al., 2022). The pH value was determined by potentiometry (soil water ratio was 1:2.5), and soil organic matter was analyzed by oxidation by a saturated potassium dichromate solution with oil bath heating. The EDTA ammonium acetate exchange was used to determine the CEC. Available nitrogen was determined by the alkaline hydrolysis diffusion method, available phosphorus was determined by ammonium fluoride-hydrochloric acid by using extraction molybdenum antimony resistance colorimetric method, available potassium was determined by neutral ammonium acetate extraction-flame photometry, exchangeable calcium and magnesium were extracted by ammonium acetate and determined usnig atomic absorption spectrometry, available zinc was determined by DTPA extraction-atomic absorption spectrometry, and available boron was determined by boiling water extraction curcumin colorimetric (Mikula et al., 2020). The standard soil sample was GBW07417a (ASA-6a) from paddy soil in Guangdong Province.

The detection of microbial community diversity in the roots, rhizosphere, and soil was as follows. Genomic DNA was extracted for PCR amplification, and specific primers with barcodes were designed according to the designated sequencing region. Library construction and Illumina PE250 sequencing, OTU cluster analysis, and species taxonomy analysis were conducted to determine microbial community diversity, relative abundance and the community structure component diagram.

2.3.2 Leaf samples

From the tree canopy, the second to fourth intact and healthy leaves were collected from the top of underyearling vegetative spring shoots from all four directions. Three leaves were collected from each direction, which was repeated twice for each direction. Leaves were mixed in a plastic bag, and 24 leaves were chosen and brought back to the laboratory to determine nutrient content.

Total nitrogen was determined by the H_2SO_4-H_2O_2 Kjeldahl digestion method. Total potassium was determined by H_2SO_4-H_2O_2 Kjeldahl digestion and the molybdenum antimony resistance colorimetric method, total potassium was determined by H_2SO_4-H_2O_2 Kjeldahl digestion and flame photometry (Khan et al., 2022), and total calcium, magnesium, and zinc were determined by dry ashing-dilute hydrochloric acid dissolution atomic absorption spectrometry. Total boron was determined by dry ashing-dilute hydrochloric acid dissolution curcumin colorimetry (Bao, 2005).

2.3.3 Fruit samples

At the stage of maturation and harvesting, twelve fruits were randomly selected from each tree from all four directions around the upper part of the crown, and the single fruit weight and quality were determined.

The fruit uniformity was determined by the proportion of medium fruit (diameter of 36.5-42 mm) (Wang et al., 2012b). The color difference de, brightness L, redness a, and yellowness b of the peel were determined by a Minolta CR-300 automatic colorimeter. The fruit shape index was the ratio of longitudinal diameter to transverse diameter. The peel thickness was measured with a Vernier caliper according to the cross-section of the equatorial line. The solid soluble content was measured using the RA-250 WE digital sugar meter (KEM company, Japan). The titratable acid content was measured using the NaOH neutralization titration method (GB/T 12456-2008). Reducing sugar and total sugar were determined by 3,5-dinitrosalicylic acid colorimetry (Li, 2000). Vitamin C content was determined by the 2,6-dichlorophenol indophenol (DCPIP) titration method (GB/T 5009.86-2016).

2.4 Data analysis

The data were sorted out in Excel 2007. The differences between each treatment and the control were analyzed by t test; Duncan's multiple comparison method was used to analyze the significance of the differences among the treatments at $P<0.05$. The analysis was conducted with six replications (3 replications per year) The graphs of different experiments were made using Graphpad Prism 5. The test data were analyzed by SPSS (25) for Windows software.

3 Results

3.1 Optimization of biochar preparation conditions and comparative analysis

During the process of biochar preparation (Figure 1), the heating rate was affected by the type and length of the materials. The heating rate of grass was much higher than that of the "Shatangju" branches. The shorter the length the "Shatangju" branch was, the faster the heating rate was. After heating for 1 hour, the two began to show significant differences. The biochar

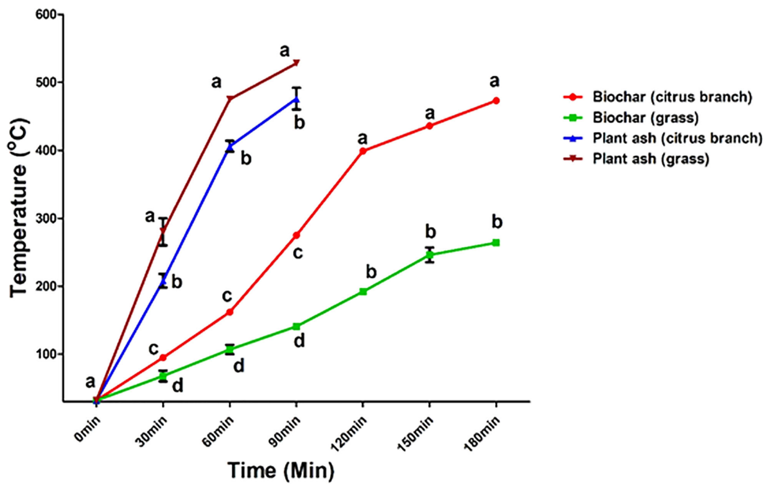

FIGURE 1
Response of time and temperature to various types of citrus branch and grass during biochar preparation. Lowercase letters show the difference among different temperatures at a specific time at *P*<0.05. Lowercase letters on a specific time have no significant difference. Error bars represent the standard deviation of the mean.

yield of grass was slightly higher than that of the "Shatangju" branches, and the biochar yield of the10-cm raw material was higher than that of the 20-cm raw material, but the difference did not reach a significant level. The carbon content in biochar from Citrus branches was significantly higher than that in biochar from grass (Table 1). Different proportions of biochar amendments could increase the pH value of acid red soil, and with increasing time, the pH value increased and remained relatively stable later (Table 2). When chemical fertilizer was applied to the red soil with biochar amendments (Table 3), the pH value of the soil in the sample groups with 3%, 4%, 5% and 6% biochar showed a decreasing trend. The pH value of red soil decreased slightly, but the change was not obvious in the sample groups with 1% and 2% biochar. With continuous fertilizer application, the pH value of the soil was maintained at approximately 5.5 in the sample group with 3% biochar, and the fluctuation range of pH value was smaller than that of the sample group with 4%, 5% and 6% biochar. Therefore, the pH of acid red soil with 3% biochar was improved and remained stable for a long time. This pH value (5.5) was close to that suitable for citrus growth.

3.2 Effects of different biochar amendments on potted "Shatangju"

3.2.1 Effects of different biochar amendments on the nutritional contents of leaves of potted "Shatangju"

Before planting, the nutrient contents of leaves were determined as follows: total nitrogen 20.42 g/kg, total phosphorus 2.46 g/kg, total potassium 14.39 g/kg, calcium 9.76 g/kg, magnesium 2.55 g/kg, zinc 26.8 mg/kg, and manganese 63.3 mg/kg. After nine months of cultivation (Table 4), the contents of calcium and zinc were significantly increased, the contents of phosphorus, potassium and manganese were

TABLE 1 Characteristics of biochar prepared by different materials.

Raw material	Yield (%)	Moisture (%)	Ash (%)	Carbon (%)
Biochar (citrus branch)	37.00±2.45 a	5.30±0.10 a	13.0±2.0 c	81.7±0.2 a
Biochar (grass)	39.00±1.50 a	5.07±0.07 a	20.3±0.3 c	74.7±0.7 b
Plant ash (citrus branch)	33.10±0.10 b	4.50±0.15 b	85.0±3.0 a	09.7±0.6 d
Plant ash (grass)	41.70±1.70 a	1.40±0.00 c	75.0±1.0 b	15.0±0.5 c

The lowercase letters behind the values of the same indicator in each column are different, indicating a significant difference between them at P<0.05. Similar letters indicate no significant difference.

TABLE 2 Effect of different incubation periods on the pH of different concentrations of biochar.

	Biochar concentration						
Days of incubation	Control(Mean ±SE)	1%(Mean ±SE)	2%(Mean ±SE)	3%(Mean ±SE)	4%(Mean ±SE)	5%(Mean ±SE)	6%(Mean ±SE)
0d	4.65±0.00eA	5.13±0.19dA	5.44±0.04cE	5.87±0.02bE	5.86±0.04bE	6.26±0.01aC	6.30±0.00aD
3d	4.51±0.01fC	5.15±0.01eA	5.48±0.04dDE	5.78±0.00cG	6.09±0.09bD	6.23±0.01bC	6.45±0.05aC
10d	4.60±0.00gA	5.2±0.00fA	5.56±0.00eD	6.27±0.01dC	6.09±0.01cD	6.79±0.09bB	7.15±0.00aA
17d	4.52±0.03gBC	5.21±0.01fA	5.65±0.00eC	6.22±0.02dD	6.33±0.03cBC	6.70±0.00bB	6.94±0.05aB
24d	4.58±0.00eAB	5.37±0.03dA	5.91±0.01cA	6.68±0.01bA	6.69±0.01bA	7.16±0.01aA	7.16±0.01aA
31d	4.53±0.01eBC	5.33±0.03dA	5.92±0.02cA	6.33±0.02bB	6.29±0.06bC	6.99±0.10aA	7.11±0.00aA
38d	4.50±0.03gC	5.21±0.02fA	5.82±0.02eB	6.15±0.00dE	6.47±0.02cB	6.76±0.06bB	7.16±0.01aA

The lowercase letters behind the values indicating statistical significance of the values in a row, while uppercase values indicating statistical significance of the values in a column at P<0.05. Similar letters indicate no significant difference.

TABLE 3 Effect of fertilization on the pH value of acid red soil with biochar amendments.

Amendment	Control	1%	2%	3%	4%	5%	6%
1d	3.94±0.01b	4.67±0.07b	5.14±0.00b	5.77±0.10a	6.27±0.02a	6.55±0.00a	6.87±0.02a
5d	4.22±0.02a	4.97±0.10a	5.39±0.09a	5.89±0.01a	5.96±0.02b	6.36±0.00b	6.58±0.01b
9d	4.24±0.04a	4.73±0.05ab	5.27±0.02a	5.75±0.07ab	5.87±0.02b	6.15±0.10c	6.32±0.00c
13d	4.25±0.05a	4.83±0.08a	5.14±0.06b	5.55±0.10bc	5.61±0.03c	5.89±0.01d	6.05±0.05d
17d	4.30±0.10a	4.81±0.09a	5.10±0.10b	5.39±0.10c	5.63±0.07c	5.79±0.05e	5.87±0.03e

The lowercase letters behind the values of the same indicator in each column are different, indicating a significant difference between them at P<0.05. Similar letters indicate no significant difference.

decreased, and the contents of nitrogen and magnesium were maintained at the original level. The contents of phosphorus, potassium and calcium increased with biochar amendments.

3.2.2 Effects of different biochar amendments on the soil of potted "Shatangju"

As shown in Table 3, the pH value of the soil increased after biochar amendments, and after adding base fertilizer, the increased range of pH values decreased. With the increase of 1.5% biochar, the pH value increased by approximately 0.26-0.47 units, and the OMC increased by 14-15 g/kg. Except for available manganese, the contents of all mineral elements showed an increasing trend. Among the treatments with biochar only, the change in alkali-hydrolyzed nitrogen was small, As shown in Table 5, after nine months of cultivation, the fluctuation range of the soil pH value was not large, and the pH value of each treatment with base fertilizer increased slightly, indicating that the stability of acidic soil improved by biochar was better. The biochar amendments promoted the utilization of organic matter and available boron, and the utilization rates of alkali-

TABLE 4 Changes in mineral nutrients in leaves of "Shatangju" after nine months of cultivation with different biochar amendments in pot tests.

Amendment	N (g/kg)	P (g/kg)	K (g/kg)	Ca (g/kg)	Mg (g/kg)	Zn (mg/kg)	Mn (mg/kg)
CK	22.82±0.07f	1.12±0.03e	09.18±0.01e	22.96±0.06g	2.48±0.08c	39.49±0.67c	35.65±0.67c
1.5%C	21.33±0.05h	1.62±0.01c	11.14±0.01c	25.55±0.04d	2.09±0.06d	39.00±0.80d	13.22±0.58e
3%C	22.07±0.08g	2.18±0.04a	10.47±0.02d	27.58±0.04c	2.88±0.07a	44.07±0.78b	11.33±0.30fg
4.5%C	21.08±0.04i	2.00±0.12b	11.56±0.02a	23.91±0.02f	2.06±0.03d	37.23±0.52d	10.47±0.38g
6%C	23.07±0.05e	2.01±0.04b	11.48±0.05a	27.98±0.03b	2.14±0.01d	37.14±0.04d	12.36±0.22ef
BF	27.81±0.08a	1.05±0.12e	08.63±0.03f	20.74±0.02h	2.84±0.05a	43.05±0.43b	59.50±0.40a
BF+1.5%C	24.05±0.10d	1.30±0.01d	09.14±0.01e	27.53±0.01c	2.5b±0.07c	40.56±0.19c	51.23±0.24b
BF+3%C	20.22±0.03j	1.60±0.08c	08.11±0.08g	25.44±0.08e	2.46±0.05c	37.72±0.27d	14.95±0.95d
BF+4.5%C	24.85±0.04c	1.55±0.03c	10.49±0.07d	28.12±0.07a	2.15±0.00d	40.76±0.22c	10.55±0.20g
BF+6%C	25.98±0.13b	1.56±0.05c	11.32±0.02b	24.92±0.02f	2.66±0.02b	75.08±0.46a	13.06±0.70e

The lowercase letters behind the values of the same indicator in each column are different, indicating a significant difference between them at P<0.05. Similar letters indicate no significant difference.

TABLE 5 Physicochemical properties of soil in different treatments when planted in pot tests.

Amendment	pH	OMC	A-N	A-P	A-K	E-Ca	E-Mg	A-Zn	A-B	A-Cu	E-Mn
CK	4.43 ±0.02e	15.17±0.12j	72.57±1.07g	15.23 ±0.73e	369.93 ±49.54bc	1.82 ±0.02g	0.15±0.01f	1.88±0.09f	1.17±0.10cd	0.54±0.04f	18.57±0.07e
1.5%C	5.57 ±0.02c	46.47 ±0.47f	74.43 ±3.63fg	36.84 ±0.66c	373.17 ±27.97bc	4.41 ±0.06e	0.38±0.03e	2.69±0.09c	1.28±0.03bc	0.99 ±0.05bcd	18.49±0.09e
3%C	5.57 ±0.03c	50.58 ±0.62e	76.53 ±2.73fg	35.37 ±0.37c	428.76 ±13.36ab	4.98 ±0.14d	0.45 ±0.03de	2.80±0.09c	1.41±0.01ab	0.89±0.02d	18.22±0.22e
4.5%C	5.94 ±0.03b	75.56 ±0.76b	78.63 ±2.73fg	53.06 ±0.84b	374.79 ±29.62bc	6.21 ±0.16c	0.46 ±0.06de	3.97±0.11b	1.07±0.02de	1.06±0.01ab	17.38±0.39f
6%C	6.35 ±0.03a	88.07 ±0.27a	81.43±1.00f	67.79 ±7.44a	465.46±23.86a	7.94 ±0.29b	0.56 ±0.06cd	4.74±0.01a	1.20 ±0.016bc	1.11±0.01a	22.57±0.07a
BF	3.92 ±0.07f	17.00 ±0.10i	156.57 ±3.58e	25.05 ±0.48d	267.39±31.49e	3.08 ±0.07f	0.75±0.03b	2.68± ±0.06c	0.98±0.07e	0.91±0.04d	20.13 ±0.11cd
BF+1.5%C	4.45 ±0.05e	31.93 ±0.70h	166.13 ±0.66d	30.46±0.99	299.23±8.92de	4.45 ±0.06e	0.67 ±0.09bc	2.11±0.01d	1.08±0.04de	1.03 ±0.02abc	18.5±0.09e
BF+3%C	4.91 ±0.03d	42.47 ±0.40g	173.83 ±1.41c	30.95±0.85	348.34±8.02cd	4.85 ±0.27e	0.62 ±0.05bc	2.39±0.04d	1.09±0.05de	0.90±0.05d	20.4±0.04c
BF+4.5%C	5.71 ±0.06c	58.40 ±0.27d	191.8±1.55b	56.99 ±1.00b	420.12±8.62bc	5.92 ±0.18c	0.64±0.02b	1.41±0.05g	1.17±0.06cd	0.93±0.03cd	19.78±0.03d
BF+6%C	5.88 ±0.10b	73.00 ±1.00c	206.03 ±2.51a	55.51 ±3.00b	416.88±6.08bc	8.02 ±0.02a	0.96±0.06a	2.24±0.04d	1.44±0.02a	0.62±0.02e	21.84±0.04b

BF: base fertilizer; OMC: Organic matter content; A: Available; E: Exchangeable; for OMC, exchangeable Ca, Mg and Mn, g/kg; for available N, P, K, Zn, B and Cu, mg/kg. The lower case letters behind the values of the same indicator in each column are different, indicating that there is a significant difference between them($P<0.05$).

hydrolyzable nitrogen, exchangeable calcium and available boron were all high in the treatments with base fertilizer.

3.2.3 Effects of different biochar amendments on soil and root microbial community diversity of potted "Shatangju"

After biochar amendments, the soil and rhizosphere microbial communities changed. The fungi were mainly from the phyla Ascomycota, Basidiomycota, Chytridiomycota, Mucoromycota and some unclassified groups. In the classification of genera, Alternaria, Cladophialophora, Ceratobasidium, Cladosporium, Exophiala, Fusarium, Humicola, Penicillium, Phialophora, Phoma, and Stepylotrichum were dominant. Fusarium and Ceratobasidium were the most dominant genera whether base fertilizer was added or not. Cladophialophora was the dominant genus in the roots of the control group, and Arthrographis was the dominant genus in the soil (Figures 2A, D).

The main bacteria were in the phyla of Cyanobacteria, Acidobacteria, Actinobacteria, Proteobacteria, Patescibacteria, Gemmatimonadetes, Chloroflex and Bacteroidetes. The dominant genera in roots in the control group were Acidothermus, Conexibaber, and Ktedonobacteraceae_uncultured. The dominant genera in the soil were Acidibacter and Dyella. Burkholderia-Caballeronia-Paraburkholderia, Chloroplast_norank, Gemmatimonas, Nocardioides, Nostocales_norank, Roseiflexaceae_uncultured and Subgroup 6_norank were the dominant genera of the soil and root systems after biochar amendments (Figures 2B, E).

The main archaea were in the phyla of Bacteroidetes, Cyanobacteria, Proteobacteria and Thaumarchaeota. The dominant genera in the control group were Group 1.1c_norank, Nitrososphaeraceae_norank, and Nitrosotaleaceae_norank. After biochar amendments, Niastella was the dominant genus in the roots and Mitochondria_norank, Flavisolibacter, Chloroplast_norank, and Chitinophagaceae_uncultured were the dominant genera in the soil. The results showed that biochar could significantly change the microbial diversity of "Shatangju" roots and soil around the rhizosphere (Figures 2C, F).

3.3 Effects of different biochar amendments on "Shatangju" in the orchard

3.3.1 Effects of different biochar amendments on the nutrient content of "Shatangju" leaves

The nutrient contents of leaves in the control group were as follows: total nitrogen 27.57 g/kg, total phosphorus 1.30 g/kg, total potassium 9.43 g/kg, calcium 26.14 g/kg, magnesium 2.80 g/kg, zinc 34.95 mg/kg, and boron 59.29 mg/kg. As shown in Table 6, after biochar amendments, the zinc content in leaves increased significantly, while the content of the other elements decreased.

3.3.2 Effects of different biochar amendments on soil physical and chemical properties in the orchard

As shown in Table 7, biochar can significantly reduce the soil bulk density and increase the soil water content, field capacity and

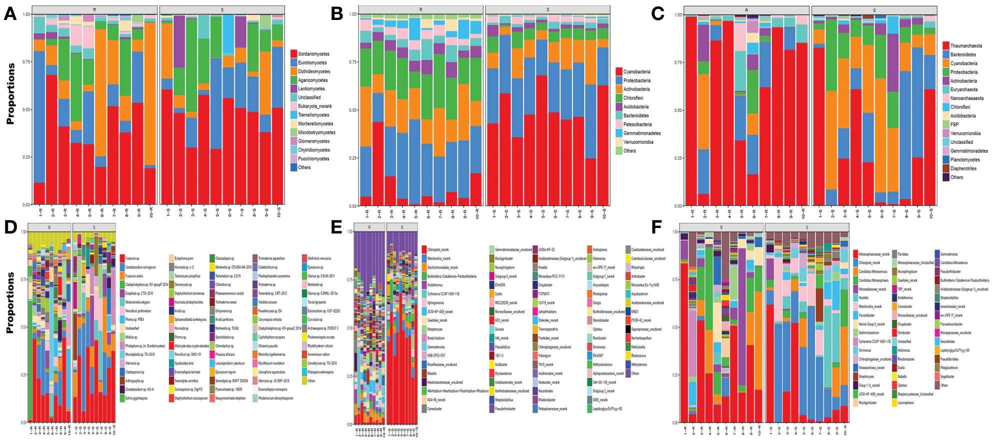

FIGURE 2
Soil and root microbial community composition of different biochar amendments in pot tests Notes: p-1 to p-10: CK, 1.5% C, 3% C, 4.5% C, 6% C, BF, BF+1.5% C, BF+3% C, BF+4.5% C and BF+6% C. S: soil; R: root. **(A–C)** representing the phylum and **(D–F)** representing the Genera. **(A, D)** showing the fungal, **(B, E)** showing bacterial and **(C, F)** showing the archaeal diversity. (clear pictures are provided in Supplementary Material A–F: Figures S1–6).

capillary porosity. With the increase in the amount of biochar amendments, the soil water content increased by 12.74%, 25.84%, 32.07%, 40.93% and 47.31%, the field water capacity increased by 17.28%, 28.10%, 39.15%, 53.93% and 67.08%, the capillary porosity increased by 8.75%, 11.42%, 14.10%, 19.56% and 23.61%, and the bulk density decreased by 7.55%, 13.21%, 18.22%, 22.56% and 26.12%. The results showed that biochar amendments could loosen the soil and improve the soil water retention property, so they could be used as an important measure to reduce the viscosity barrier of red soil. Biochar significantly increased the soil pH value and organic carbon content. Compared with that of the control, the soil organic matter in the treatment groups increased by 93.76%, 151.99%, 201.53%, 254.21% and 465.24%. This result indicated that biochar had obvious effects on improving soil acidification and fertilizer. The content of soil mineral elements in the biochar treatment groups was higher than that in the control group, and the changing trend was as follows: alkali hydrolyzable nitrogen and available phosphorus increased, and other elements increased first and then decreased. The inflection points of available potassium and boron were 2.4 kg/plant biochar, and the inflection points of exchangeable calcium, available magnesium and available zinc were 3.6 kg/plant biochar (Table 8).

3.3.3 Effects of different biochar amendments on soil and root microbial diversity in orchards

The fungi were mainly in the phyla of Ascomycota, Basidiomycota, Mucoromycota and unclassified. The dominant genera were Arthrographis, Fusarium, Humicola, Lophistoma, Melanconiella, Mortierella, Penicillium, Phoma and Trichoderma. Fusarium, Humicola, Mortierella, and Penicillium were the most dominant genera in the control,

TABLE 6 Changes in leaf nutrient contents with different amounts of biochar amendments in orchards.

Treatments	N	P	K	Ca	Mg	Zn	B
Control	27.57±0.12a	1.30±0.01a	9.43±0.03a	26.14±0.04ab	2.80±0.33a	34.95±0.10d	59.20±0.09b
C-1.2kg	27.49±0.09a	1.23±0.02ab	8.95±0.05a	25.07±0.07c	2.45±0.01a	73.81±0.16b	44.87±0.09e
C-2.4kg	25.86±0.05bc	1.14±0.01b	8.26±0.24b	23.08±0.08d	2.31±0.01b	74.08±0.08b	43.60±0.06f
C-3.6kg	25.84±0.09bc	1.18±0.01ab	7.42±0.37c	25.98±0.13b	2.57±0.07a	75.86±0.06a	48.69±0.05d
C-4.8kg	25.51±0.20c	1.20±0.10ab	8.00±0.11bc	25.21±0.10c	2.76±0.06a	74.12±0.02b	56.74±0.05c
C-6.0kg	26.25±0.25b	1.21±0.03ab	8.03±0.03bc	26.38±0.13a	2.65±0.04a	72.41±0.10c	61.83±0.09a

for N, P, K ,Ca and Mg, g/kg; for Zn and B, mg/kg. The lower case letters behind the values of the same indicator in each column are different, indicating that there is a significant difference between them($P<0.05$).

TABLE 7 Changes in soil physical properties with different biochar amendments in orchards.

Treatments	Moisture content (%)	Field capacity (%)	Bulk density(g.cm^{-1})	Porosity (%)
CK	19.90±0.90d	30.00±0.10f	1.22±0.02a	3.65±0.03d
C-1.2kg	22.44±0.32c	35.18±0.01e	1.13±0.06a	3.97±0.08c
C-2.4kg	25.04±0.52b	38.43±0.16d	1.06±0.01a	4.01±0.01bc
C-3.6kg	26.28±0.33b	41.75±0.39c	1.00±0.30a	4.16±0.05b
C-4.8kg	28.05±0.21a	46.18±0.09b	0.94±0.04a	4.36±0.03a
C-6.0kg	29.31±0.35a	50.13±0.02a	0.90±0.09a	4.51±0.04a

The lower case letters behind the values of the same indicator in each column are different, indicating that there is a significant difference between them(P<0.05).

and Arthrographis, Fusarium, Humicola, Mortierella and Penicillium were the most dominant genera in the root and rhizosphere soils. After different biochar amendments, the most dominant genera in root and rhizosphere soil changed into Arthrographis, Fusarium, Humicola, Lophistoma, Melanconiella, Mortierella, Penicillium, and Arthrographis in the root soil, and Fusarium, Humicola, Mortierella, Penicillium and Trechispora in the rhizosphere soil (Figures 3A, D).

The main bacteria phyla were Acidobacteria, Actinobacteria, Bacteroidetes, Chloroflexi, Cyanobacteria, Gemmatimonadetes and Proteobacteria; the dominant genera were Acidothermus, Burkholderia-Caballeronia-Paraburkholderia, Chloroplast_norank, Gemmatimonadaceae_uncultured, KF-JG30-C25_norank and Mitochondria_norank. Among them, the most dominant genera in the roots of the control group were Acidothermus, Bryobacter, Caldilineaceae_uncultured, Chitinophagaceae_uncultured, Chloroplast_norank and JG30-KF-AS9_norank. The dominant genera in rhizosphere soil were Acidothermus, Bryobacter, Chitinophagaceae_uncultured and KF-JG30-C25_norank. After biochar amendments, the most dominant genera in the roots were Acidothermus, Bryobacter, Burkholderia-Caballeronia-Paraburkholderia, Chloroplast_norank and Mitochondria_norank. The dominant genera in the rhizosphere soil were Acidothermus, Bryobacter, Burkholderia-Caballeronia-Paraburkholderia, Chitinophagaceae_uncultured, and KF-JG30-C25_norank (Figures 3B, E).

The main archaea were in the phyla of Bacteroidetes, Cyanobacteria, Euryarchaeota, Proteobacteria and Thaumarchaeota. Candidatus Nitrocosmicus, Candidatus Nitrososphaera, Candidatus Nitrosotalea, Candidatus Nitrosotenuis, Chitinophagaceae_uncultured, Chloroplast_norank, Group 1.1c_norank, Nitrososphaeraceae_norank, and Nitrosotaleaceae_norank were dominant genera. Candidatus Nitrocosmicus, FBP_norank and Flavitalea were the most dominant genera in the roots of the control group. Candidatus Nitrocosmicus was the most dominant genus in the rhizosphere soil. After different biochar amendments, the most dominant genera of roots were Candidatus Nitrososphaera, Candidatus Nitrocosmicus, Chloroplast_norank, Group 1.1c_norank, Marine Group II_norank, Nitrososphaeraceae_norank, and Nitrosotaleaceae_norank. In contrast, the most dominant genera in rhizosphere soil were Candidatus Nitrososphaera, Candidatus Nitrocosmicus, Group 1.1c_norank, Marine Group II_norank, Nitrososphaeraceae_norank, and Nitrosotaleaceae_norank (Figures 3C, F).

3.4 Effects of different biochar amendments on "Shatangju" fruit quality

After biochar amendments, the average fruit weight of "Shatangju" (37.44-40.44 g) did not change significantly, but the medium fruit proportion increased significantly. Compared with the control group, the number of medium fruits in each treatment group increased by 48.48%, 30.30%, 24.24%, 36.36% and 27.27%. Biochar amendments could reduce the peel thickness, and the peel thickness in groups with 3.6 kg/plant and 4.8 kg/plant biochar significantly decreased by 0.31 mm and

TABLE 8 Changes in soil chemical properties with different biochar amendments in orchards.

Treatments	pH	OMC	CEC	A-N	A-P	K	E-Ca	E-Mg	Zn	B
CK	4.80±0.02d	21.40±0.09f	08.04±0.04d	110.52±1.16e	22.71±0.10f	153.00±3.00c	889.45±9.21d	49.90±0.40f	3.88±0.04e	0.86±0.01c
C-1.2kg	6.54±0.03c	41.62±0.04e	09.85±0.04b	120.60±1.19d	39.81±0.06e	373.17±3.81b	1694.72±88.87c	94.40±0.40e	6.14±0.04b	1.00±0.10bc
C-2.4kg	6.86±0.12b	54.13±0.03d	10.08±0.03a	124.60±0.95c	47.09±0.04d	399.61±9.23a	2821.31±17.17a	135.56±0.56a	6.73±0.12a	1.00±0.00bc
C-3.6kg	7.13±0.08a	64.77±0.07c	09.37±0.04c	130.43±0.79b	53.65±0.08c	401.23±1.11a	2811.50±11.30a	131.64±0.54b	6.67±0.16a	1.46±0.03a
C-4.8kg	7.27±0.02a	76.08±0.08b	09.28±0.04c	132.53±0.91ab	55.73±0.05b	366.69±3.91b	2753.18±17.48ab	125.27±0.17c	5.68±0.14c	1.15±0.04b
C-6.0kg	7.31±0.01a	121.41±0.05a	09.32±0.02c	134.17±0.66a	58.61±0.01a	360.76±2.20b	2659.76±49.24b	114.10±0.21d	5.10±0.10d	0.96±0.05c

OMC, Organic matter content; CEC, cation exchange capacity; A, Available; E, Exchangeable; for exchangeable Ca, Mg and Mn, g/kg; for available N, P, K, Zn and B, mg/kg. The lower case letters behind the values of the same indicator in each column are different, indicating that there is a significant difference between them(P<0.05).

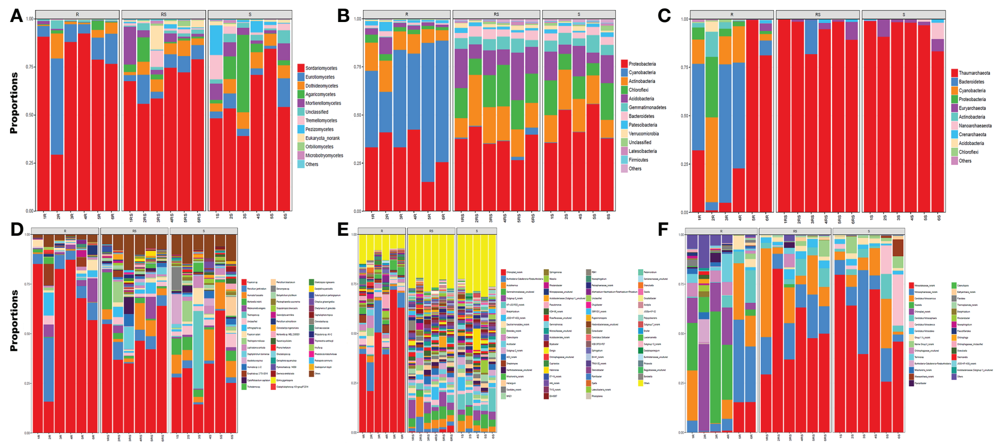

FIGURE 3
Soil and root microbial community composition of different biochar amendments in orchard Notes: p-1 to p-10: CK, 1.5% C, 3% C, 4.5% C, 6%C, BF, BF+1.5% C, BF+3% C, BF+4.5% C and BF+6% C. S: soil; R: root. **(A–C)** representing the phylum and **(D–F)** representing the Genera. **(A, D)** showing the fungal, **(B, E)** showing bacterial and **(C, F)** showing the archaeal diversity. (clear pictures are provided in Supplementary Material A–F: Figures S7–12).

0.25 mm, respectively, compared with that of the control (2.06 mm), but it did not affect the fruit shape index (Table 9).

The color value (de) and d (a/b) of the fruit color increased but did not reach a significant level compared with the control. The fruit surface brightness (dl) was the highest when 1.2 kg and 2.4 kg of biochar were added to each plant. The redness value (da) was highest at 6 kg of biochar per plant treatment. The yellow degree value (db) of each treatment was higher than that of the control, and the difference was significant (Table 10).

Table 11 shows that biochar can increase the soluble solids content/Titratable acid (SSC/TA), total sugar, reducing sugar, edible rate, and water content of "Shatangju", and reduce the content of Titratable acid (TA). It can also increase the soluble solids content(SSC) content, vitamin C, and juice yield, except for individual treatments. When the biochar amendments were 2.4 kg/plant and 3.6 kg/plant, the fruit quality was better than that under the other treatments. Compared with that of the control, the SSC content increased by 4.96% and 5.79%, TA decreased by 16.67% and 8.33%, soluble solids content/Titratable acid (SSC/TA) increased by 24.48% and 15.24%, vitamin C content increased by 13.30% and 18.18%, total sugar increased by 11.36% and 13.21%, reducing sugar increased by 7.37% and 22.35%, edible rate increased by 2.96% and 3.79%, juice yield increased by 8.96% and 5.86%, and water content increased by 0.52% and 0.63%. These results supported that proper biochar amendments had an obvious effect on improving fruit quality.

4 Discussion

In this experiment, the organic waste of an orchard was fully utilized to prepare biochar. Organic waste from orchards includes "Shatangju" branches from pruning twice a year and grass from mowing five times a year. A total of 1187 kg per mu produced 437 kg of biochar per mu. The simple biochar furnace that we developed and produced can handle the preparation of biochar and the reuse of organic waste in the "Shatangju" orchard. With obvious effects, the biochar output can meet the orchard requirements and support the organic carbon cycle in the orchard.

TABLE 9 Changes in physical fruit properties with different amounts of biochar amendment.

Treatments	Single fruitweight (g)	Proportion of middlefruits weight%	Proportion of middlefruits number%	Fruit shapeindex	Peel thick (mm)
Control	40.44±0.18b	52.62±0.10e	55.00±1.00e	0.78±0.01b	2.06±0.01a
C-1.2kg	39.83±0.25bc	79.97±0.19a	81.67±0.34a	0.82±0.00a	1.96±0.01bc
C-2.4kg	40.80±0.80b	69.49±0.16d	71.67±0.00c	0.80a±0.01b	1.75±0.01e
C-3.6kg	38.77±0.65cd	69.69±0.00d	68.33±1.00d	0.80±0.01ab	1.81±0.01d
C-4.8kg	42.89±0.31a	71.68±0.33c	75.00±0.50b	0.79±0.01ab	1.94±0.02c
C-6.0kg	37.44±0.10d	73.07±0.07b	70.00±0.00cd	0.80±0.01ab	2.00±0.02b

The lower case letters behind the values of the same indicator in each column are different, indicating that there is a significant difference between them(P<0.05).

TABLE 10 Changes of citrus peel visual with different biochar amendments.

Treatments	de	dl-	da+	db+	da/b
Control	74.57±0.07a	33.48±0.13b	27.85±0.07c	60.18±0.08e	0.46±0.02a
C-1.2kg	76.12±0.11a	32.25±0.11c	28.88±0.20b	62.46±0.11a	0.46±0.00a
C-2.4kg	75.55±0.97a	33.89±0.09a	28.97±0.18b	60.66±0.12d	0.48±0.02a
C-3.6kg	75.99±0.11a	34.25±0.10a	28.88±0.08b	61.12±0.13c	0.47±0.01a
C-4.8kg	75.78±0.52a	32.42±0.13c	28.22±0.17c	62.06±0.10b	0.46±0.01a
C-6.0kg	75.89±0.24a	34.09±0.09a	29.86±0.18a	60.34±0.04de	0.49±0.01a

The lower case letters behind the values of the same indicator in each column are different, indicating that there is a significant difference between them($P<0.05$).

Biochar is a kind of stable, insoluble and aromatic solid substance produced by the pyrolysis of agricultural solid wastes such as straw, rice husk, bamboo, wood and animal manure under at high temperature and anaerobic conditions (Tan et al., 2022). This study analyzed the effects of “Shatangju” branch biochar amendments on soil physical and chemical properties, soil and root microorganisms, leaf nutrition, and fruit quality of “Shatangju”(Tables 4–11). After biochar amendments, the soil bulk density decreased, and the soil water content, field capacity and capillary porosity increased significantly, consistent with previous research results (Wang et al., 2012a; Zeng et al., 2013; Li et al., 2014; Zhan et al., 2015). The physical properties of biochar determine these benefits. As a kind of carbon-rich microporous material, biochar has a large specific surface area, making its density far less than that of soil (Spokas et al., 2009). Biochar has a strong adsorption capacity and thus promotes the formation of soil aggregates, and its strong hydrophilicity can increase capillary porosity and improve soil water holding capacity (Downie et al., 2009). Biochar is an effective soil amendment (Glaser, 1998).

According to the sequencing analysis of soil and root microorganisms (Figures 2, 3), biochar amendments significantly increased the number of species and the quantity of soil and root microorganisms in pot and field tests. Other dominant genera replaced many dominant genera in the control after biochar amendments. In the pot experiment, the abundance of beneficial bacteria such as Fusarium, Ceratobasidium, Chloroplast_norank, Mitochondria_norank and Gemmatimonas was the highest, and the content of harmful bacteria such as Cladophialophora was reduced when 3% biochar was added in the appropriate treatment. This is beneficial in degrading soil pollutants such as nitrogen oxides and heavy metals, increasing organic matter in mineral soil and fixing atmospheric nitrogen. The orchard environment is much more complex than the pot experiment environment with rain protection measures. The relative abundance of beneficial bacteria such as Fusarium, Humicola, Chloroplast_norank and Nitrososphaera was high, and the species of microbial colonies were more abundant in orchard soil. The high stability of biochar, which is a suitable addition amount, can prolong its retention in soil, improve soil structure, and affect the diversity of soil and root microbial communities, although orchard soil has a large volume and strong buffering capacity. Biochar amendments increased the soil microbial biomass in the peach orchard, especially the utilization rate of microbial carbon sources. However, high carbon is unfavorable to microbial

TABLE 11 Changes in citrus fruit nutritional properties with different biochar amendments.

Treatments	SSC/%	TA/%	SSC/TA	Vitamin C (mg/100g)	Total sugar content /%	Reducing sugar content /%	Edible rate/%	Juice yield/%	Moisture content/%
Control	12.1 ±0.00c	0.48 ±0.01a	25.22 ±0.53d	21.43±0.03d	7.04±0.36c	4.34±0.04d	74.23±0.33c	51.92±0.70d	82.5±0.50a
C-1.2kg	12.5 ±0.10ab	0.43 ±0.00bc	29.07 ±0.23bc	22.98±0.46c	8.43±0.11ab	4.86±0.06b	75.17 ±0.10bc	50.19±0.10e	82.86±0.06a
C-2.4kg	12.7 ±0.10a	0.40 ±0.01d	31.78 ±1.04a	24.28±0.20b	7.84±0.25b	4.66±0.10bc	76.43 ±0.40ab	56.57±0.21b	82.93±0.58a
C-3.6kg	12.8 ±0.20a	0.44 ±0.01b	29.10 ±0.21b	25.33±0.30a	7.97±0.07ab	5.31±0.00a	77.04±0.52a	54.96±0.40c	83.02±0.02a
C-4.8kg	12.1 ±0.00c	0.44 ±0.00b	27.50 ±0.00c	23.74±0.20bc	8.43±0.03ab	4.75±0.05b	75.61 ±0.60bc	55.53 ±0.18bc	83.47±0.20a
C-6.0kg	12.2 ±0.00bc	0.41 ±0.01cd	29.77 ±0.73b	20.59±0.12d	8.61±0.07a	4.56±0.05c	76.28 ±0.32ab	58.25±0.27a	83.11±0.10a

de, the color of the peel; dl-, brightness of the peel; da+, redness of the peel; db+, yellowness of the peel; da/b, the ratio of Da and Db; SSC, soluble solids content; TA, Titratable acid. The lower case letters behind the values of the same indicator in each column are different, indicating that there is a significant difference between them($P<0.05$).

diversity (Lu et al., 2020). The pH value of potato rhizosphere soil is important for soil microbial biomass, followed by organic carbon and total nitrogen (Xu et al., 2020). Biochar has a large specific surface area and nonvolatile ash, providing a more suitable niche for soil microorganisms. Biochar directly affected the soil pH value and increased the soil organic carbon content. We speculated that soil pH stability is the main reason for the increase microbial diversity in the soil and rhizosphere of "Shatangju" in the orchard and pot tests based on the results reported by Zhalnina et al. (2015) and Shi et al. (2021).

Relevant studies have suggested that biochar can also improve soil fertility, reduce nutrient fixation and leaching, promote nutrient absorption by plants, increase fertilizer utilization rate, and improve growth and development of most crops, while avoiding the disadvantages caused by the lime (Magrini-Bair et al., 2009; Laird et al., 2010; Wang et al., 2012a; Chen et al., 2013; Zhang et al., 2013a). This experiment also proved that biochar has these advantages in the "Shatangju" orchard and pot tests (Tables 5, 8).

Biochar also exerts effects on improving the nutrient absorption of crops. Studies have shown that biochar amendments can improve the crop's capacity to absorb nitrogen, phosphorus, potassium and other nutrients, and the absorption rate increases with the number of biochar amendments, however, when it exceeds a certain amount, it inhibits the absorption of nutrients by crops (Chan et al., 2007; Li et al., 2014; Khan et al., 2020). Our study showed that the contents of nitrogen, phosphorus, potassium, calcium, magnesium and boron in the leaves of "Shatangju" after biochar amendments were slightly lower than those of the control (Tables 4,6), consistent with the results of (Zhang et al., 2013c). It may be that biochar amendments can improve the soil nutrient efficiency and then improve the nutrient absorption of crops. However, the increase in plant biomass and fruit amount, carbohydrates produced by photosynthesis, and the transfer of nutrients lead to the dilution of leaf nutrients and the reduction of element contents. Meanwhile, biochar increased the content of available phosphorus, potassium, calcium and magnesium and other mineral elements in the soil and increased the absorption of these elements.

Previous studies have demonstrated that (Fang et al., 2014; Zhang et al., 2014) biochar amendments can increase the aboveground dry matter accumulation and crop yield, but the effect on crop quality is rarely mentioned. The present experiment also proved the effect of biochar in the production of "Shatangju". The different proportions of biochar can improve "Shatangju" internal and external qualities to varying degrees, especially the proportion of medium fruit. The price of medium fruit of "Shatangju" is high so that biochar amendments can increase the economic benefits after harvest for the grower (Tables 9–11).

In this experiment, biochar amendments in pot and field tests significantly improved the soil pH value and organic matter contents (OMC), hydrolyzable alkali nitrogen, phosphorus, potassium, exchangeable calcium, exchangeable magnesium, zinc, available boron and CEC. Many pot tests have found similar findings and analyzed the related reasons (Kimetu and Lehmann, 2010; Gao et al., 2012; Han et al., 2012; Zhang et al., 2013a; Zhang et al., 2013c; Zhao et al., 2015; Zhu et al., 2015). However, there is not a complete design for the optimal amount of biochar. It is generally believed that the effect of biochar on crop growth, yield and quality is closely related to the biochar amount and soil properties (Khan et al., 2021a). Asai et al. (2009) found that rice yield increased with biochar amendments, but when biochar amendments reached 16 t/hm^2, rice yield did not increase due to nitrogen deficiency. In a pot test on sandy loam, Vaccari et al. (2011) showed that the biomass of ryegrass increased by 20% and 52% when biochar amendments were 30 t/hm^2 and 60 t/hm^2, respectively, but decreased when biochar amendments were 100 t/hm^2 and 200 t/hm^2 compared with that of the control group. This study found that in the pure soil test, whether or not chemical fertilizer is applied, 3% biochar amendments can provide a suitable pH value for "Shatangju" growth and are relatively stable. Due to the limited amount of planting soil in the pot test, whether or not fertilizer is applied, 1.5%-3% biochar can improve the soil. In the field test, the biochar at 2.4-3.6 kg/plant (approximately 4% - 6% of the mixed soil sample, namely, approximately it is about 4% - 6% of the soil in the fertilizing ditch 80 cm long, 30 cm wide and 30 cm deep) is suitable for the growth and development of "Shatangju" with proper soil pH value, organic matter content (OMC), large, medium and trace element content and leaf element content, and improved fruit quality. Therefore, the amount of biochar added in the open environment (if the garden) can be slightly adjusted according to the results of the closed environment test (pure soil test and pot test). Of course, the amount of biochar used in the field needs to be determined by the soil, variety, tree age and planting density, and it should be noted that the effect of not always better the amount is.

5 Conclusion

A simple small-scale biochar furnace is beneficial for the "Shatangju" orchard. It can convert the carbon fixed by "Shatangju" plants and orchard grasses into biochar and change the physical and chemical properties of soil and microbial colonies in the soil by applying 2.4-3.6 kg biochar per plant, thus affecting the absorption and utilization of soil nutrients by "Shatangju" roots, directly increasing the yield and improving the quality of fruit. The results of the closed environment test (pure soil test and pot test) and the open environment test (if it is a garden) can refer to each other in terms of the added biochar in order to obtain a model of the organic carbon cycle in the orchard. It provides a method deal with the waste in the orchard, address the problem of biochar shortage, and maintain the cycle of organic carbon in the orchard, which provides a theoretical basis for the fertilization, soil improvement and rational agriculture of biochar in "Shatangju" orchards.

Data availability statement

The original contributions presented in the study are publicly available. This data can be found here: NCBI, PRJNA889182.

Author contributions

YG: methodology, data curation, visualization and investigation, formal analysis and writing the original draft preparation. BQ: data curation, fund acquisition, project administration and resources. ZK: formal analysis and data curation. HJ: visualization and investigation. QJ: supervision, conceptualization, resources, writing, reviewing and editing, project administration, and funding acquisition. MK: conceptualization, software, writing, reviewing, and editing. QF: software, formal analysis and resources. All authors contributed to the article and approved the submitted version.

Funding

This study was supported by the Laboratory of Lingnan Modern Agriculture Project (NT2021003), China Agriculture Research System of MOF and MARA (CARS-26) and Guangdong Provincial Key Laboratory of Environmental Health and Land Resource (Grant No. 2020B121201014).

Conflict of interest

The authors declare that the research was conducted in the absence of any commercial or financial relationships that could be construed as a potential conflict of interest.

Publisher's note

All claims expressed in this article are solely those of the authors and do not necessarily represent those of their affiliated organizations, or those of the publisher, the editors and the reviewers. Any product that may be evaluated in this article, or claim that may be made by its manufacturer, is not guaranteed or endorsed by the publisher.

Supplementary material

The Supplementary Material for this article can be found online at: https://www.frontiersin.org/articles/10.3389/fpls.2022.1001740/full#supplementary-material

References

Ahmad, M., Lee, S. S., Lim, J. E., Lee, S. E., Cho, J. S., Moon, D. H., et al. (2014). Speciation and phytoavailability of lead and antimony in a small arms range soil amended with mussel shell, cow bone and biochar: EXAFS spectroscopy and chemical extractions. *Chemosphere* 95, 433–441. doi: 10.1016/j.chemosphere.2013.09.077

Ahmad, M., Ok, Y. S., Kim, B. Y., Ahn, J. H., Lee, Y. H., Zhang, M., et al. (2016). Impact of soybean stover- and pine needle-derived biochars on Pb and as mobility, microbial community, and carbon stability in a contaminated agricultural soil. *J. Environ. Manage.* 166, 131–139. doi: 10.1016/j.jenvman.2015.10.006

Asai, H., Samson, B. K., Stephan, H. M., Songyikhangsuthor, K., Homma, K., Kiyono, Y., et al. (2009). Biochar amendment techniques for upland rice production in northern laos. 1. soil physical properties, leaf SPAD and grain yield. *F. Crop Res.* 111, 81–84. doi: 10.1016/j.fcr.2008.10.008

Bao, S. (2005). *Soil agrochemical analysis. 3rd ed* (Beijing: China Agricultural Publishing).

Bashir, S., Rizwan, M. S., Salam, A., Fu, Q., Zhu, J., Shaaban, M., et al. (2018). Cadmium immobilization potential of rice straw-derived biochar, zeolite and rock phosphate: Extraction techniques and adsorption mechanism. *Bull. Environ. Contam. Toxicol.* 100, 727–732. doi: 10.1007/s00128-018-2310-z

Brahmakshatriya, R. D., and Donker, J. D. (1971). Five methods for determination of silage dry matter. *J. Dairy Sci.* 54, 1470–1474. doi: 10.3168/jds.S0022-0302(71)86049-6

Bruun, E. W., Petersen, C. T., Hansen, E., Holm, J. K., and Hauggaard-Nielsen, H. (2014). Biochar amendment to coarse sandy subsoil improves root growth and increases water retention. *Soil Use Manage.* 30, 109–118. doi: 10.1111/sum.12102

Chaisiri, C., Liu, X. Y., Yin, W. X., Luo, C. X., and Lin, Y. (2021). Morphology characterization, molecular phylogeny, and pathogenicity of diaporthe passifloricola on citrus reticulata cv. nanfengmiju in Jiangxi province, China. *Plants* 10, 1–20. doi: 10.3390/plants10020218

Chan, K. Y., Van Zwieten, L., Meszaros, I., Downie, A., and Joseph, S. (2007). Agronomic values of greenwaste biochar as a soil amendment. *Aust. J. Soil Res.* 45, 629–634. doi: 10.1071/SR07109

Chen, W., Zhang, W., and Meng, J. (2013). Advances and prospects in research of biochar utilization in agriculture. *Sci. Agric. Sin.* 46, 3324–3333. doi: 10.3864/j.issn.0578-1752.2013.16.003

Downie, A., Crosky, A., and Munroe, P. (2009). "Physical properties of biochar," in *Biochar for environmental management*, vol. 448 . Eds. J. Lehmann and S. Joseph (London: Taylor & Francis). doi: 10.4324/9781849770552

Du, Z-I., Ren, T-s., Hu, C-s., Zhang, Q-z., and Blanco-Canqui, H. (2013). Soil aggregate stability and aggregate-associated carbon under different tillage systems in the North China Plain. *J. Integr. Agric.* 12, 2114–2123. doi: 10.1016/S2095-3119(13)60428-1

Fang, B., Li, X., Zhao, B., and Zhong, L. (2014). Influence of biochar on soil physical and chemical properties and crop yields in rainfed field. *Ecol. Environ. Sci.* 23, 1292–1297. doi: 10.16258/j.cnki.1674-5906.2014.08.006

Gao, H., He, X., Chen, X., Zhang, W., and Geng, Z. (2012). Effect of biochar and biochar-based ammonium nitrate fertilizers on soil chemical properties and crop yield. *J. Agro-Environment Sci.* 31, 1948–1955.

Glaser, B. (1998). Black carbon in soils: the use of benzene carboxylic acids as specific markers. *Org. Geochem.* 29, 811–819. doi: 10.1016/S0146-6380(98)00194-6

Han, G. M., Meng, J., Zhang, W. M., and Chen, W. F. (2012). Effect of biochar on microorganisms quantity and soil physicochemical property in rhizosphere of spinach (Spinacia oleracea l.). *J. Shenyang Agric. Univ. (Social Ed.* 43, 515–520.

Iqbal, A., Liang, H., Mcbride, S. G., Yuan, P., Ali, I., Zeeshan, M., et al. (2022). Manure applications combined with chemical fertilizer improves soil functionality , microbial biomass and rice production in a paddy field. *Agron. J.* 114, 1–16. doi: 10.1002/agj2.20990

Jiang, H., Guo, Y., Guo, L., Zhou, X., Hu, Y., and Ji, Q. (2015). Soil nutrient and leaf nutrient status of yellow shatang orange orchard in xijiang river basin of guangdong province. *South China Fruits* 43, 59–63. doi: 10.13938/j.issn.1007-1431.20140598

Kang, C., Cao, J., Sun, J., Zheng, G., Wang, Y., Chen, K., et al. (2022). Comparison of physiochemical characteristics of citrus reticulata cv. shatangju fruit with different fruit sizes after storage. *Food Packag. Shelf Life* 31, 100774. doi: 10.1016/j.fpsl.2021.100774

Khan, Z., Khan, M. N., Zhang, K., Luo, T., Zhu, K., and Hu, L. (2021a). The application of biochar alleviated the adverse effects of drought on the growth, physiology, yield and quality of rapeseed through regulation of soil status and nutrients availability. *Ind. Crops Prod.* 171, 113878. doi: 10.1016/j.indcrop.2021.113878

Khan, Z., Nauman Khan, M., Luo, T., Zhang, K., Zhu, K., Rana, M. S., et al. (2021b). Compensation of high nitrogen toxicity and nitrogen deficiency with biochar amendment through enhancement of soil fertility and nitrogen use efficiency promoted rice growth and yield. *GCB Bioenergy* 13, 1765–1784. doi: 10.1111/gcbb.12884

Khan, Z., Zhang, K., Khan, M. N., Bi, J., Zhu, K., Luo, L., et al. (2022). How biochar affects nitrogen assimilation and dynamics by interacting soil and plant enzymatic activities: Quantitative assessment of 2 years potted study in a rapeseed-soil system. *Front. Plant Sci.* 13. doi: 10.3389/fpls.2022.853449

Khan, Z., Zhang, K., Khan, M. N., Fahad, S., Xu, Z., and Hu, L. (2020). Coupling of biochar with nitrogen supplements improve soil fertility, nitrogen utilization efficiency and rapeseed growth. *Agronomy* 10, 1661. doi: 10.3390/agronomy10111661

Kimetu, J. M., and Lehmann, J. (2010). Stability and stabilisation of biochar and green manure in soil with different organic carbon contents. *Aust. J. Soil Res.* 48, 577–585. doi: 10.1071/SR10036

Laird, D. A., Fleming, P., Davis, D. D., Horton, R., Wang, B., and Karlen, D. L. (2010). Impact of biochar amendments on the quality of a typical Midwestern agricultural soil. *Geoderma* 158, 443–449. doi: 10.1016/j.geoderma.2010.05.013

Lehmann, J., Rillig, M. C., Thies, J., Masiello, C. A., Hockaday, W. C., and Crowley, D. (2011). Biochar effects on soil biota - a review. *Soil Biol. Biochem.* 43, 1812–1836. doi: 10.1016/j.soilbio.2011.04.022

Li, H. (2000). *Principles and techniques of plant physiological and biochemical experiments* (Beijing: Higher Education Press).

Li, T., Shi, S., Goel, S., Shen, X., Xie, X., Chen, Z., et al. (2019). Recent advancements in mesoporous silica nanoparticles towards therapeutic applications for cancer. *Acta Biomat.* 89, 1–13. doi: 10.1016/j.actbio.2019.02.031

Liu, B., Xia, H., Jiang, C., Riaz, M., Yang, L., Chen, Y., et al. (2022). 14 year applications of chemical fertilizers and crop straw effects on soil labile organic carbon fractions, enzyme activities and microbial community in rice-wheat rotation of middle China. *Sci. Tot. Environ.* 841, 156608. doi: 10.1016/j.scitotenv.2022.156608

Li, Q., Wu, F., Li, T., Su, X., Jiang, G., Qu, H., et al. (2012).). 1-methylcyclopropene extends the shelf-life of "Shatangju" mandarin (Citrus reticulate blanco) fruit with attached leaves. *Postharvest Biol. Technol.* 67, 92–95. doi: 10.1016/j.postharvbio.2012.01.001

Li, X., Zhang, J., Li, L., Pan, G., Zhang, X., Zheng, J., et al. (2014). Effects of biochar amendment on maize growth and soil properties in Huang-Huai-Hai plain. *Soil* 46, 269–274. doi: 10.13758/j.cnki.tr.2014.02.012

Lu, H., Yan, M., Hung, M., Yin, W., Wang, Y., Wen, X., et al. (2020). Effects of biochar on soil microbial community and functional genes of a land fi ll cover three years after ecological restoration. *Sci. Tot. Environ.* 717, 137133. doi: 10.1016/j.scitotenv.2020.137133

Magrini-Bair, K. A., Czernik, S., Pilath, H. M., Evans, R. J., Maness, C., and Leventhal, J. (2009). Biomass derived, carbon sequestering, designed fertilizers. *Ann. Environ. Sci.* 3, 217–225.

Meng, L., Sun, T., Li, M., Saleem, M., Zhang, Q., and Wang, C. (2019). Soil-applied biochar increases microbial diversity and wheat plant performance under herbicide fomesafen stress. *Ecotoxicol. Environ. Saf.* 171, 75–83. doi: 10.1016/j.ecoenv.2018.12.065

Mikula, K., Izydorczyk, G., Skrzypczak, D., Mironiuk, M., Moustakas, K., Witek-Krowiak, A., et al (2019). Controlled release micronutrient fertilizers for precision agriculture – A review. *Sci. Total Environ.* 712, 1–8. doi: 10.1016/j.scitotenv.2019.136365

Oleszczuk, P., Jośko, I., Futa, B., Pasieczna-Patkowska, S., Pałys, E., and Kraska, P. (2014). Effect of pesticides on microorganisms, enzymatic activity and plant in biochar-amended soil. *Geoderma* 214–215, 10–18. doi: 10.1016/j.geoderma.2013.10.010

Oni, B. A., Oziegbe, O., and Olawole, O. O. (2019). Significance of biochar application to the environment and economy. *Ann. Agric. Sci.* 64, 222–236. doi: 10.1016/j.aoas.2019.12.006

Oshunsanya, S. O., and Aliku, O. O. (2016). "Biochar technology for sustainable organic farming," in *Organic farming - a promising way of food production*. Ed. P. Konvalina (London, United Kingdom: IntechOpen), 111–129. doi: 10.5772/61440

Pawlak-Kruczek, H., Niedzwiecki, L., Sieradzka, M., Mlonka-Mędrala, A., Baranowski, M., Serafin-Tkaczuk, M., et al. (2020). Hydrothermal carbonization of agricultural and municipal solid waste digestates – structure and energetic properties of the solid products. *Fuel* 275, 117837. doi: 10.1016/j.fuel.2020.117837

Puget, P., and Lal, R. (2005). Soil organic carbon and nitrogen in a mollisol in central Ohio as affected by tillage and land use. *Soil Tillage Res.* 80, 201–213. doi: 10.1016/j.still.2004.03.018

Shi, Y., Li, Y., Yang, T., and Chu, H. (2021). Threshold effects of soil pH on microbial co-occurrence structure in acidic and alkaline arable lands. *Sci. Tot. Environ.* 800, 149592. doi: 10.1016/j.scitotenv.2021.149592

Spokas, K. A., Koskinen, W. C., Baker, J. M., and Reicosky, D. C. (2009). Chemosphere impacts of woodchip biochar additions on greenhouse gas production and sorption / degradation of two herbicides in a Minnesota soil. *Chemosphere* 77, 574–581. doi: 10.1016/j.chemosphere.2009.06.053

Tan, S., Mathiyazhagan Narayanan, D. T. T. H., Ito, N., Unpaprom, Y., Pugazhendhi, A., Chi, N. T. L., et al. (2022). A perspective on the interaction between biochar and soil microbes: A way to regain soil eminence. *Environ. Int.* 214, 113832. doi: 10.1016/j.envres.2022.113832

Tardy, V., Spor, A., Mathieu, O., Lévèque, J., Terrat, S., Plassart, P., et al. (2015). Shifts in microbial diversity through land use intensity as drivers of carbon mineralization in soil. *Soil Biol. Biochem.* 90, 204–213. doi: 10.1016/j.soilbio.2015.08.010

Tian, S., Ning, T., Wang, Y., Liu, Z., Li, G., and Li, Z. (2016). Crop yield and soil carbon responses to tillage method changes in north China. *Soil Tillage Res.* 163, 207–213. doi: 10.1016/j.still.2016.06.005

Vaccari, F. P., Baronti, S., Lugato, E., Genesio, L., Castaldi, S., Fornasier, F., et al. (2011). Biochar as a strategy to sequester carbon and increase yield in durum wheat. *Eur. J. Agron.* 34, 231–238. doi: 10.1016/j.eja.2011.01.006

Wang, Z., Li, H., Lin, J., Tian, J., and Wu, Z. (2012b). Study on quality and storability of different size of shatangju fruits. *Storage Process* 12, 6–11.

Wang, Y., Yuan, Y., and Liu, S. (2009). Comparative study on determination methods of corn silage. *China Dairy Cattle* 2009, 14–17.

Wang, D., Zhang, X., Jiang, C., and Peng, S. (2012a). Biochar research advances regarding soil improvement and crop response. *Chin. J. Eco-Agricul0* 20, 963–967. doi: 10.3724/SP.J.1011.2012.00963

Wu, H., Zeng, G., Liang, J., Chen, J., Xu, J., Dai, J., et al. (2016). Responses of bacterial community and functional marker genes of nitrogen cycling to biochar, compost and combined amendments in soil. *Appl. Microbiol. Biotechnol.* 100, 8583–8591. doi: 10.1007/s00253-016-7614-5

Xia, H., Riaz, M., Zhang, M., Liu, B., El-desouki, Z., and Jiang, C. (2020). Biochar increases nitrogen use efficiency of maize by relieving aluminum toxicity and improving soil quality in acidic soil. *Ecotoxicol. Environ. Saf.* 196, 110531. doi: 10.1016/j.ecoenv.2020.110531

Xu, Y., Ma, S., Zhu, B., Zhang, X., Xing, Y., Duan, M., et al. (2020). Effects of the combined application of biochar and chemical fertilizer on fertility and microbial characteristics of purple soil and yield and quality of oilseed rape. *Acta Prataculturae Sin.* 29, 121–131. doi: 10.11686/cyyxb2019338

Yu, H., Zou, W., Chen, J., Chen, H., Yu, Z., Huang, J., et al. (2019). Biochar amendment improves crop production in problem soils: A review. *J. Environ. Manage.* 232, 8–21. doi: 10.1016/j.jenvman.2018.10.117

Zeng, A., Liao, Y., Zhang, J., Sui, Y., and Wen, X. (2013). Effects of biochar on soil moisture, organic carbon and available nutrient contents in manural loessial soils. *J. Agro-Environment Sci.* 32, 1009–1015. doi: 10.11654/jaes.2013.05.019

Zhalnina, K., Dias, R., de Quadros, P. D., Davis-Richardson, A., Camargo, F. A. O., Clark, I. M., et al. (2015). Soil pH determines microbial diversity and composition in the park grass experiment. *Microb. Ecol.* 69, 395–406. doi: 10.1007/s00248-014-0530-2

Zhang, N., Li, J., Liu, X., Liu, Y., Wang, Y., Liang, H., et al. (2014). Effects of biochar on growth and yield of summer maize. *J. Agro-Environment Sci.* 33, 1569–1574. doi: 10.11654/jaes.2014.08.015

Zhang, X., Wang, D., Jiang, C., and Peng, S. (2013b). Biochar and research advances of biochar in acidic soil improvement. *Hubei Agric. Sci.* 52, 997–1000. doi: 10.14088/j.cnki.issn0439-8114.2013.05.037

Zhang, X., Wang, D., Jiang, C.-C., Zhu, P., Lei, J., and Peng, S.-A. (2013a). Effect of biochar on physicochemical properties of red and yellow brown soils in the south China region. *Chin. J. Eco-Agricul0* 21, 979–984. doi: 10.3724/sp.j.1011.2013.00979

Zhang, X., Wang, D., Zhu, P., Jiang, C., and Peng, S. (2013c). Effects of biochar on improvement of acid red soil and growth of navel orange seedlings. *South China Fruits* 42, 38–41. doi: 10.13938/j.issn.1007-1431.2013.06.003

Zhan, X., Peng, J., Wang, Y., Liu, Y., Chen, K., Han, X., et al. (2015). Influences of application of biochar and biochar-based fertilizer on brown soil physiochemical properties and peanut yields. *Plant Nutr. Fertil Sci.* 21, 1633–1614. doi: 10.11674/zwyf.2015.0631

Zhao, Q., Meng, J., and Chen, W. (2015). Effect of biochar on growth of brassica campestris l. ssp. pekinesis (lour) olsson. *J. Agro-Environment Sci.* 34, 2394–2401.

Zhu, P., Ying, J., Peng, S., and Jiang, C. (2015). Effects of biochar and lime on soil physicochemical properties and tobacco seedling growth in red soil. *J. Agric. Resour. Environ.* 32, 590–595.

frontiers | Frontiers in Plant Science

TYPE Original Research
PUBLISHED 25 November 2022
DOI 10.3389/fpls.2022.1069624

Optimizing maize yields using growth stimulants under the strategy of replacing chemicals with biological fertilizers

Ahmed I. Abdo[1,2,3], El-Sayed E. A. El-Sobky[4] and Jiaen Zhang[1*]

[1]Department of Ecology, College of Natural Resources and Environment, South China Agricultural University, Guangzhou, China, [2]Henry Fok School of Biology and Agriculture, Shaoguan University, Shaoguan, China, [3]Soil Science Department, Faculty of Agriculture, Zagazig University, Zagazig, Egypt, [4]Agronomy Department, Faculty of Agriculture, Zagazig University, Zagazig, Egypt

OPEN ACCESS

EDITED BY
Amanullah,
University of Agriculture, Peshawar, Pakistan

REVIEWED BY
Zhiguang Liu,
Shandong Agricultural University, China
Yousef Alhaj Hamoud,
Hohai University, China

*CORRESPONDENCE
Jiaen Zhang
jeanzh@scau.edu.cn

SPECIALTY SECTION
This article was submitted to Plant Nutrition, a section of the journal Frontiers in Plant Science

RECEIVED 14 October 2022
ACCEPTED 07 November 2022
PUBLISHED 25 November 2022

CITATION
Abdo AI, El-Sobky E-SEA and Zhang J (2022) Optimizing maize yields using growth stimulants under the strategy of replacing chemicals with biological fertilizers.
Front. Plant Sci. 13:1069624.
doi: 10.3389/fpls.2022.1069624

Partial replacement of chemicals with biological fertilizers is a recommended strategy to reduce the adverse environmental effects of chemical fertilizer losses. Enhancing the reduced mineral with biological fertilizers strategy by foliar application of humic acid (HA) and amino acids (AA) can reduce environmental hazards, while improving maize (*Zea mays L.*) production under semiarid conditions. The recommended doses of N, P and K (e.g., 286 kg N ha^{-1}, 75 kg P_2O_5 ha^{-1} and 67 kg K_2O ha^{-1}) were applied as the first fertilization level (100% NPK) and were replaced with biofertilizers by 100%, 75%, 50% and 25% as levels of reducing mineral fertilization. These treatments were applied under four foliar applications of tap water (TW), HA, AA and a mixture of HA and AA. Our results reported significant reductions in all parameters, including maize ear yield attributes and grain nutrient uptake, when replacing the mineral NPK with biofertilizers by 25-100% replacement. However, these reductions were mitigated significantly under the application of growth stimulants in the descending order: HA and AA mixture>AA>HA>TA. Applying a mixture of HA and AA with 75% NPK + biofertilizers increased ear length, grain yield, grain uptake of N and K, and crude protein yield by 37, 3, 4, 11 and 7%, respectively as compared with 100% mineral fertilizer only. Moreover, all investigated parameters were maximized under the application of 75% NPK + biofertilizers combined with AA or the mixture of HA and AA, which reveals the importance of growth stimulants in enhancing the reduced chemical NPK strategy. It could be concluded that the mineral NPK rate can be reduced by 25% with biofertilization without any yield losses when combined with HA and AA under arid and semi-arid conditions. That achieves the dual goals of sustainable agriculture by improving yield, while reducing environmental adverse effects.

KEYWORDS
maize, mineral NPK fertilizers, biofertilizers, humic acid, amino acids

1 Introduction

Maize (*Zea mays L.*) is the most important staple crop worldwide with various basic uses, such as human diets, animal feeding and energy production. The global area of maize production was greater than 150×10^6 ha in 2010 (Bassu et al., 2014), and the demand is expected to double by 2050 (Ramirez-Cabral et al., 2017). In Egypt, maize is the second main crop (7.5×10^6 tons) with an area of 1.1×10^6 ha that is located in a semiarid region with low-fertility soil (FAO, 2020). On average, 290, 80 and 70 kg ha^{-1} of N, P_2O_5 and K_2O, respectively, are the conventional mineral fertilization to maize fields in Egypt with use efficiencies by 30, 36 and 20%, respectively (El-Etr and Mahmoud, 2011; El-Gedwy, 2020; El-Sobky and Abdo, 2020). This means that more than 60% of the applied synthetic fertilizers are lost to the environment, which causes environmental hazards and economic losses. Furthermore, intensive nitrogen fertilization can decrease crop yields owing to lodging (Corbin et al., 2016) in addition to inducing water and air pollution as a result of N losses (Huang et al., 2017) through nitrate leaching (Fan et al., 2012) and nitrous oxide and ammonia emissions (Hirel et al., 2011).

For cleaner production, intensive research work has been carried out to increase nutrient use efficiencies in parallel with reducing synthetic fertilizer usage and losses. Biofertilizers have been suggested as inputs for sustainable agricultural production, as they are eco-friendly and cost-effective materials (Kumawat, 2017). Biofertilizers are defined as the formulations containing living microorganisms or latent cells having the potential of colonizing roots of crops plants and promoting the growth by improving nutrients availability and acquisition (Lakshmi, 2014; du Jardin, 2015).

Chemical fertilizers provide root zone with readily available nutrients that are subject to losses, while biofertilizers increase nutrient uptake by fixing the nutrients that are vulnerable to loss and from outer sources (e.g., N_2 fixing bacteria) or by solubilizing unavailable nutrients (e.g., P and K solubilizing bacteria) (Pawar et al., 2019). Biofertilizers are sources of beneficial soil microorganisms, which enhance plant growth, yield and N use efficiency by increasing the availability and supply of essential nutrients (Kubheka et al., 2020a; Phares et al., 2022). Also, Biofertilizers improve plant resistance to environmental stress, including drought, temperature and saline conditions (Itelima et al., 2018). Maize yields were optimized under the reduced fertilization strategy when combined with N, P and K biofertilizers (Jilani et al., 2007; Yosefi et al., 2011). On the other hand, using biofertilizers improved maize yields by only 15.3% on average in a meta-analysis study (Schmidt and Gaudin, 2018). We hypothesized that applying growth stimulants, such as humic and amino acids, can enhance maize growth and yields under a reduced synthetic N strategy with biofertilizers.

Humic acid improves the morphological and yield attributes; metabolism (e.g., total soluble sugar, photosynthetic pigment, total carbohydrates, proline and total amino acids); nutrient contents, nutrients uptake and yields and yield attributes (Canellas et al., 2019; Khan et al., 2019; Yuan et al., 2022). Amino acids enhance plant functions such as photosynthesis, protein synthesis, phytohormone activators, stoma action, stress resistance and chelating effects (Matysiak et al., 2020). Amino acids are better than humic acid in improving the maize yield attributes and grain contents of N, P and K and have positive effects on the physicochemical processes and yield attributes (Ragheb, 2016). Amino acids are readily available sources of N, protein synthesis, and hormone precursors, including auxins and antistress agents, which in turn positively affect plant growth and yields. However, there was no documentation in the literature on the effects of the combined foliar application of humic and amino acids with partial replacement of NPK mineral fertilizers with biofertilizers on maize yield quantities and crop grain qualities.

Therefore, this study aimed to evaluate the possibility of reducing nutrient surplus by growth stimulants (amino or humic acid) to enhance maize yield attributes and nutrients uptake under replacement of synthetic fertilizers strategy with biofertilizers. This study also aimed to select the best combined rate of minerals and biofertilizers when using single or mixed humic and amino acids for optimal maize production under semiarid conditions. This study serves the efforts of achieving the dual goals of sustainable agriculture by maintaining optimal yields accompanied by less environmental effects, especially in arid and semi-arid regions.

2 Materials and methods

2.1 Experiment site

A two-season trial was carried out at the Experimental Station in Ghazala Village, Fac. of Agric., Zagazig Univ., Sharkia Governorate, Egypt (30.11°N, 31.41°E) during the summer seasons of 2019 and 2020. This site is described by hot weather, dry summer seasons (Table S1) with an average temperature of 32.1°C and no precipitation. Analysis of soil was carried according to Klute, (1986), the soil is alluvial clay in texture (FAO-UNESCO soil map) and consisted of 475.7 ± 2.2 and 476.6 ± 1.8 g kg^{-1} clay, 318.2 ± 0.8 and 318 ± 1.1 g kg^{-1} silt and 206.1 ± 1.2 and 205.4 ± 1.3 g kg^{-1} sand during the first and second seasons, respectively. The soil pH levels (1:2.5) were 8.05 ± 0.02 and 8.02 ± 0.05, respectively and the EC values (1:5) (dSm^{-1}) were 1.85 ± 0.1 and 1.92 ± 0.06 during the first and second seasons, respectively. The available N, P and K (mg kg^{-1}) concentrations were 21.12 ± 1.1 and 22.15 ± 0.9, 8.15 ± 0.9 and 8.22 ± 0.8, and 149.3 ± 1.5 and 148.7 ± 1.3 during the first and second seasons, respectively. The soil organic carbon contents were 7.45 ± 0.13 and 7.56 ± 0.04 g kg^{-1}, respectively.

2.2 Experimental design and study factors

In total, twenty treatments with three replicates were conducted in a randomized complete block split-plot design. Foliar spraying using growth stimulants was used for the main plot, and mineral and biofertilizer applications were used for the subplots. Three foliar sprays with humic acid (HA), amino acids (AA) and a mixture of HA+AA were applied at rates of 3 g L^{-1}, 3 ml L^{-1} and 3 g L^{-1}+3 ml L^{-1}, respectively. In parallel, tap water (TW) was sprayed as the control. Foliage-applied treatments were carried out using water (595 L ha^{-1} per spray) at 21, 35 and 55 days after planting (DAP). The foliar spraying of humic acid and amino acids was conducted by using solid and liquid commercial products, namely, K-humate (e.g., 860 g kg^{-1} humic acid, total organic matter 750 g kg^{-1}, pH 5.5–6.5 and 12 g kg^{-1} K_2O), as well as Aminocat star (Shoura, Alexandria, Egypt) as a source of amino acids containing 10 g kg^{-1} free amino acids, 3 g kg^{-1} N, 1 g kg^{-1} P_2O5 and 5 g kg^{-1} K_2O.

Five rates of mineral and biofertilizer application (e.g., NPK 100% (F1), NPK 75% plus biofertilizers (F2), NPK 50% plus biofertilizers (F3), NPK 25% plus biofertilizers (F4) and biofertilizers (F5)) were applied. The recommended doses of NPK (NPK 100%) were established by adding 286 kg N ha^{-1} ammonium nitrate (335 g kg^{-1} N), 75 kg P_2O_5 ha^{-1} superphosphate (155 g kg^{-1} P_2O_5) and 67 kg K_2O ha^{-1} potassium sulfate (48 g kg^{-1} K_2O). The recommended NPK doses are applied by maize producers for commercial production in the region. Before planting, the maize seeds were inoculated with a biofertilizer mixture (e.g., Nitrobein biofertilizer containing *Azotobacter* sp. and *Azospirillum* sp. as N_2-fixing bacteria, phosphorine biofertilizer containing *Bacillus megaterium* var. *phosphaticum* as phosphate-solubilizing bacteria, and potassiomage as K solubilizing bacteria). These biofertilizers were produced by the Agriculture Research Center, Giza, Egypt and were used at the recommended dose of 1 kg ha^{-1} for each biofertilizer. Superphosphate and potassium sulfate were applied basally before planting. Nitrogen fertilizer was applied in two equal splits before the first and second irrigation periods at 21 and 34 days after planting (DAP).

2.3 General agronomic practices

During the two seasons, maize was cultivated after wheat (*Triticumaestivum L.*) and the soil was plowed using a moldboard plow to a depth of 0.30 m and was divided into 60 plots. The area of each plot was 3.5 m x 5 m including 5 ridges with 70 cm apart. On May 15th and 20th of the first and second seasons, a single cross 178 yellow maize cultivar was planted. Seeds were sown by hand at a rate of 24 kg ha^{-1} in both seasons on one side of the ridge in hills that were 25 cm apart. Furrow flood irrigation was conducted at each 14-day interval with a total amount of 7140 m^3 ha^{-1}. The plants were thinned before the first irrigation (21 DAP) to one plant for each hill to a density of 57120 plants ha^{-1}. Soil samples were collected each season before planting at a depth of 0-30 cm to determine the soil physical and chemical properties.

2.4 Recorded data

2.4.1 Maize yields and yield attribute measurements

By late September of each year, the maize was harvested (120 DAP), and the following yield attributes were recorded using ten ears: ear length (cm), ear diameter, row number per ear, grain number per row, grain number/ear (calculated), 100-grain weight (g), and grain weight per ear (g). Additionally, the following final yield traits were recorded from the three central ridges at each plot and were converted into Mg ha^{-1}: grain yield at a grain moisture content of 15.5%, ear yield, stover yield and biological yield. The harvest index was calculated from the grain and total yields (Mg ha^{-1}) according to (Buresh et al., 1988) as follows:

$$\text{Harvest index (HI)} = \frac{\text{grain yield}}{\text{total yield}} \times 100$$

2.4.2 Determination of macronutrients content and uptake

The grain samples were dried at 70°C after harvest to determine their total N, P and K contents according to (Faithfull, 2002). The grain N, P and K uptakes (kg ha^{-1}) were calculated by multiplying the grain yields by the grain N, P and K percentages (Moll et al., 1962). The grain protein contents (%) were calculated by multiplying the grain N percentages by 5.70 (Bishnoi and Hughes, 1979). The crude protein yields (CPY) (kg ha^{-1}) were calculated by multiplying the grain yields (kg ha^{-1}) by the percentages of grain protein content (%).

2.5 Statistical analysis

The data were statistically analyzed using MSTAT-C Version 2.1, which was used also for analysis of variance (ANOVA) determinations (Gomez and Gomez, 1984). The treatment means were compared using the least significant differences (LSD) test at a 0.05 probability level (Snedecor and Cochran, 1989). The Pearson's simple correlation matrix for yields, yield attributes and uptake of nutrients in grains was also computed by SPSS 20. The path coefficient analysis was estimated. Path-coefficient analysis measures the direct effect of one predictor variable on another and has been widely used to determine the nature of the relationships among grain yields and their contributing components (Pavlov et al., 2015).

3 Results

3.1 Maize yield attributes and crude protein yield

The greatest ear length (EL) (20.32 cm) was reported under the application of 75% NPK + biofertilizers with HA and AA mixture during the first season, while the greatest ear length was (20.50 cm) during the second season under the application of 100% NPK and AA without biofertilizers (Table 1). On average, ELs exhibited their maximum (e.g., 17.99 and 18.83 cm) values under the application of 75% NPK + biofertilizers when compared with all other NPK and biofertilizer combinations during the first and second seasons, respectively. Additionally, ELs exhibited their maximum lengths (e.g., 17.74 and 17.71 cm) under HA and AA mixture when compared with the control [e.g., tap water (TW)] and the single application of HA or AA during the first and second seasons, respectively. Similarly, ear diameter (ED), number of grains per ear (NG/E) and grain weight per ear (GW/E) were maximized under the application of 75% NPK + biofertilizers and HA and AA mixture as compared with the other single applications of growth stimulants during both seasons (Tables 1, 2). The NG/Es had the highest values (e.g., 614.6 and 589.9) under the application of 50% NPK + biofertilizers with HA and AA mixture or 100% NPK and AA, respectively. In contrast, the EDs (cm) and GW/Es (g) exhibited their highest values (e.g., 4.38 and 4.48, 229.5 and 225.9, respectively) under the combined application of 75% NPK + biofertilizers and an HA and AA mixture during the first and second seasons, respectively. On the other hand, the application of 100% NPK with TW resulted in the highest 100-grain weights (e.g., 37.91 and 40.51 g) during the two seasons. On average, the 100-grain weights were maximized under the application of 75% NPK + biofertilizers with foliar application of the HA and AA mixture during the two seasons. The application of growth stimulants (HA and/or AA) significantly improved all ear parameters compared with TW, and the mixture exhibited the highest values. Application of these stimulants reduced the negative impact of replacing mineral fertilizer with biofertilizers on the ear parameters, while using only 25% NPK with biofertilizers under the application of an HA and AA mixture exhibited all investigated ear parameters to be higher, equal or have no significant reductions when compared with using 100% mineral fertilizer.

The grain yield (GY), stover yield (SY), biological yield (BY), harvest index (HI) and crude protein yield (CPY) responded

TABLE 1 Impact of foliar spraying of stimulants and chemical and bio fertilization treatments on ear length, ear diameter and number of grains per ear of maize.

Foliar spraying	EL						ED						NG/E					
	F1	F2	F3	F4	F5	Mean	F1	F2	F3	F4	F5	Mean	F1	F2	F3	F4	F5	Mean
2019 season																		
TW	14.88g	18.25bc	17.50cd	16.69de	15.57e:g	*16.58*^{c}	4.35a	3.98f:h	3.75ij	3.75ij	4.10c:f	*3.99*^{c}	543.3cd	457.4hi	450.8i	465.9g:i	490.9f:h	*481.6*^{d}
HA	17.25cd	16.63de	15.82e:g	17.25cd	15.25fg	*16.44*^{c}	4.17b:e	4.27a:c	4.03e:g	4.07d:g	3.82hi	*4.07*^{b}	533.6c:e	554.9c	457.4hi	490.9f:h	516.8d:f	*510.7*^{c}
AA	19.50ab	16.75de	16.50d:f	16.63de	16.50d:f	*17.18*^{b}	4.09d:f	4.33ab	4.08d:g	4.23a:d	3.60j	*4.06*^{b}	537.1c:e	606.6ab	505.2ef	559.1c	466.7g:i	*534.9*^{b}
HA+AA	16.75de	20.32a	15.63e:g	19.25ab	16.75de	*17.74*^{a}	3.92g:i	4.38a	4.27a:c	4.32ab	4.05e:g	*4.18*^{a}	500.1e:g	569.2bc	614.6a	558.1c	613.1a	*571.0*^{a}
Mean	17.09^{B}	17.99^{A}	16.36^{C}	17.45^{AB}	16.02^{C}		4.13^{B}	4.24^{A}	4.03^{C}	4.09^{BC}	3.89^{D}		528.5^{AB}	547.0^{A}	507.0^{C}	518.5^{BC}	521.9^{BC}	
2020 season																		
TW	14.63j	19.25ab	16.50e:h	17.57de	17.19ef	*17.03*^{b}	4.45ab	4.03e:g	3.55j	3.85g:i	4.00f:h	*3.98*^{c}	546.0c:f	519.0f:h	475.0i	494.8hi	525.6e:h	*512.1*^{c}
HA	17.75c:e	18.88bc	15.94f:i	16.75e:h	14.75ij	*16.81*^{b}	4.29bc	4.29bc	4.18c:e	3.99f:h	3.84hi	*4.12*^{ab}	525.6e:h	563.4a:c	496.3g:i	497.0g:i	508.2gh	*518.1*^{c}
AA	20.50a	17.25e	17.50de	16.88e:g	15.50h:j	*17.53*^{a}	4.07d:f	4.48a	4.03e:g	4.18c:e	3.70ij	*4.09*^{b}	589.9a	558.8a:d	554.2b:e	528.4d:g	439.3j	*534.1*^{b}
HA+AA	16.75e:h	19.94ab	15.88g:j	18.75b:d	17.25e	*17.71*^{a}	4.04ef	4.23cd	4.29bc	4.14c:f	4.15c:f	*4.17*^{a}	526.3d:h	567.0a:c	565.9a:c	583.4ab	577.2a:c	*563.9*^{a}
Mean	17.41^{B}	18.83^{A}	16.45^{C}	17.49^{B}	16.17^{C}		4.21^{A}	4.25^{A}	4.01^{BC}	4.04^{B}	3.92^{C}		546.9^{A}	552.1^{A}	522.8^{B}	525.9^{B}	512.5^{B}	

TW, tap water, HA, humic acid, AA, amino acids, HA + AA, mixture of humic acid + amino acids, F1, 100% NPK, F2, 75% NPK + biofertilizers, F3, 50% NPK + biofertilizers, F4, 25% NPK + biofertilizers, F5, biofertilizers, EL is ear length (cm), ED is ear diameter (cm) and NG/E is number of grains/ear. Means in italic refer to foliage applications, while none italic refer to fertilization treatments. Means followed by different letters in the same direction differ significantly by LSD ($p \leq 0.05$).

TABLE 2 Impact of foliar spraying of stimulants and chemical and bio fertilization treatments on grain weight per ear,100-grain weight and grain yield of maize.

Foliar spraying	GW/E F1	GW/E F2	GW/E F3	GW/E F4	GW/E F5	GW/E Mean
2019 season						
TW	206.0b	122.6ij	111.0j	109.9j	150.0f:h	*139.9*^{d}
HA	185.0c	175.9cd	156.1e:g	150.8f:h	125.2ij	*158.6*^{c}
AA	133.5hi	213.6ab	172.3ce	182.7c	139.5gi	*168.3*^{b}
HA+AA	159.3d:f	229.5a	171.5c:e	174.8cd	169.9c:e	*181.0*^{a}
Mean	170.9^{B}	185.4^{A}	152.7^{C}	154.5^{C}	146.1^{C}	
2020 season						
TW	221.2ab	118.0jk	106.8k	104.7k	130.2ij	*136.2*^{d}
HA	181.7de	183.0de	149.6gh	145.6gi	114.1jk	*154.8*^{c}
AA	137.7hi	225.9a	155.4f:h	169.7ef	137.5hi	*165.2*^{b}
HA+AA	155.4f:h	206.1bc	189.4cd	190.0cd	155.9fg	*179.3*^{a}
Mean	174.0^{A}	183.3^{A}	150.3^{B}	152.5^{B}	134.4^{C}	

Foliar spraying	100-GW F1	100-GW F2	100-GW F3	100-GW F4	100-GW F5	100-GW Mean
2019 season						
TW	37.91ab	26.81i:k	24.65jk	23.58k	30.55e:i	*28.70*^{b}
HA	34.66b:d	31.69c:g	34.14b:e	30.72d:h	24.20jk	*31.08*^{a}
AA	24.86jk	35.23bc	34.10b:e	32.72c:f	29.90f:i	*31.36*^{a}
HA+AA	31.84c:g	40.31a	28.03gj	31.30d:h	27.70h:j	*31.83*^{a}
Mean	32.32^{A}	33.51^{A}	30.23^{B}	29.58^{BC}	28.09^{C}	
2020 season						
TW	40.51a	22.74j	22.49j	21.16j	24.82h:j	*26.34*^{c}
HA	34.57bc	32.51c:e	30.19d:g	29.30e:g	22.44j	*29.80*^{b}
AA	23.34ij	40.43a	28.05f:h	32.11c:e	31.38c:f	*31.06*^{a}
HA+AA	29.56d:g	36.34b	33.49b:d	32.58b:e	27.01g:i	*31.79*^{a}
Mean	32.00^{A}	33.00^{A}	28.55^{B}	28.79^{B}	26.41^{C}	

Foliar spraying	GY F1	GY F2	GY F3	GY F4	GY F5	GY Mean
2019 season						
TW	8.79a:c	5.38g:i	4.88h	4.83h	5.64e:h	*5.90*^{c}
HA	6.91c:g	7.73b:d	6.36d:h	6.63d:h	4.95h	*6.51*^{bc}
AA	7.33c:g	9.39ab	7.57b:e	8.02b:d	5.63f:h	*7.59*^{ab}
HA+AA	7.00c:g	10.08a	7.54b:f	7.18c:g	6.96c:g	*7.75*^{a}
Mean	7.51^{AB}	8.15^{A}	6.59^{BC}	6.67^{BC}	5.80^{C}	
2020 season						
TW	9.72ab	5.20jk	4.70k	4.60k	5.73ij	*5.99*^{d}
HA	7.98de	8.04de	6.57gh	6.41gi	5.01jk	*6.80*^{c}
AA	6.05hi	9.93a	6.82f:h	7.46ef	6.05hi	*7.26*^{b}
HA+AA	6.82f:h	9.06bc	8.32cd	8.36cd	6.86fg	*7.88*^{a}
Mean	7.64^{A}	8.06^{A}	6.70^{B}	6.70^{B}	5.91^{C}	

TW, tap water, HA, humic acid, AA, amino acids, HA + AA, mixture of humic acid + amino acids, F1, 100% NPK, F2, 75% NPK + biofertilizers, F3, 50% NPK + biofertilizers, F4, 25% NPK + biofertilizers, F5, biofertilizers, GW/E is grain weight/ear (g), 100-GW is 100- grain weight (g) and GY is grain yield (Mg ha^{-1}). Means in italic refer to foliage applications, while none italic refer to fertilization treatments. Means followed by different letters in the same direction differ significantly by LSD ($p \le 0.05$).

differently to the combinations of minerals and biofertilizers and growth stimulants (Tables 2–4). The GYs and EYs (Mg ha^{-1}) exhibited their highest values (e.g., 10.03 and 9.93, 11.49 and 11.63, respectively) when applying 75% NPK + biofertilizers combined with the HA and AA mixture and the single application of AA during the first and second seasons, respectively. On average, the GYs and EYs recorded their maximum values under the application of 75% NPK + biofertilizers with foliar application of the HA and AA mixture during the two seasons. The maximum values of SY (Mg ha^{-1}) and BY (Mg ha^{-1}) during the first and second seasons (e.g., 21.72 and 20.19 and 32.61 and 30.60, respectively) were obtained when applying 75% NPK + biofertilizer treatment combined with AA during the first season and the mixture of HA and AA during the second season, respectively. In contrast, the HIs (%) reached their highest values (e.g., 45.60 and 45.42) under the application of AA combined with 25% NPK + biofertilizers in the first season and biofertilizers without mineral fertilization in the second season. Applying the 75% NPK + biofertilizer treatment combined with the application of HA and AA reported the highest improvements in GY, EY, SY and BY, which was followed by 100% NPK, with no significant differences. In contrast, the biofertilization treatment recorded the highest HI, while the lowest HI was exhibited under mineral fertilization (100% NPK) only. GY, SY and BY were sensitive to the replacement of mineral NPK with biofertilizers under TW, with average reductions of 44.44, 33.26 and 38.41%, respectively, when compared with mineral fertilizer with biofertilization. The maximum values of CPY (kg ha^{-1}) during the first and second seasons (e.g., 1064.2 and 1089, respectively) were reported under the 75% NPK + biofertilizer treatment combined with application of the HA and AA mixture during the first season and AA during the second season.

3.2 Macronutrient content and uptake

The application of 100% NPK with AA or 75% NPK + biofertilizer treatments with TW resulted in the highest N contents (e.g., 20.5 and 20.4 g kg^{-1}) during the 1st season and 21.3 and 20.9 g kg^{-1} during the 2nd season, respectively (Figure 1A). The N content decreased significantly with replacing the mineral NPK by more than 50%, where the N content decreased from 19.5 g kg^{-1} under 100% NPK with AA or 75% NPK + biofertilizer treatments to 14.5 g kg^{-1} under biofertilization only. The maximum P content (1.6 g kg^{-1}) was reported under the application of 100% NPK and 50% NPK + biofertilizers combined with AA or the application of biofertilizers combined with HA and AA mixture during both seasons (Figure 1B). On average, the P content was the highest (1.54 g kg^{-1}) when applying 100% NPK and decreased significantly with replacing the mineral fertilization until reaching 1.4 g kg^{-1} under the biofertilization treatment. The

TABLE 3 Impact of foliar spraying of stimulants and chemical and bio fertilization treatments on stover, ear and biological yields of maize.

Foliar spraying	SY						EY						BY					
	F1	F2	F3	F4	F5	Mean	F1	F2	F3	F4	F5	Mean	F1	F2	F3	F4	F5	Mean
2019 season																		
TW	13.57de	8.79f:j	9.64f:h	9.43f:i	5.06k	*9.30*^{c}	10.47b	6.16ij	5.63j	5.84j	7.61fg	*7.14*^{d}	24.04c	14.95g:i	15.27f:h	15.26f:h	12.67i	*16.44*^{c}
HA	17.63bc	15.76:d	9.12f:i	7.06h:k	6.58i:k	*11.23*^{bc}	9.47c	8.97c	7.86ef	7.72f	6.44h:j	*8.09*^{c}	27.10b	24.72bc	16.98e:g	14.77g:i	13.02hi	*19.32*^{b}
AA	11.20ef	21.72a	9.68f:h	8.34g:j	5.93jk	*11.37*^{b}	6.81g:i	10.89ab	8.80cd	9.26c	7.16f:h	*8.58*^{b}	18.01ef	32.61a	18.48de	17.60e:g	13.08hi	*19.96*^{b}
HA+AA	13.10de	19.42ab	18.00bc	10.70e:g	8.72f:j	*13.99*^{a}	7.96d:f	11.49a	8.71c:e	8.90cd	8.71c:e	*9.15*^{a}	21.06d	30.91a	26.71bc	19.59de	17.42e:g	*23.14*^{a}
Mean	13.87^{B}	16.42^{A}	11.61^{C}	8.88^{D}	6.57^{E}		8.67^{B}	9.37^{A}	7.75^{C}	7.93^{C}	7.48^{C}		22.55^{B}	25.80^{A}	19.36^{C}	16.81^{D}	14.05^{E}	
2020 season																		
TW	12.00d:f	8.96f:i	10.63e:g	8.48g:i	6.89hi	*9.39*^{d}	11.40a	5.96ij	5.47j	5.56j	6.76hj	*7.03*^{d}	23.40d	14.90i:l	16.10g:k	14.04kl	13.65kl	*16.42*^{d}
HA	9.21fgh	14.72cd	10.15e:g	8.42g:i	8.77g:i	*10.25*^{c}	9.44cd	9.28cd	7.63e:h	7.40f:h	5.89ij	*7.93*^{c}	18.65e:g	23.99cd	17.78e:h	15.81h:l	14.65j:l	*18.18*^{c}
AA	16.96bc	16.83bc	12.12de	8.85g:i	6.30i	*12.21*^{b}	7.00gh	11.63a	7.87e:g	8.54de	7.09f:h	*8.42*^{b}	23.96cd	28.46ab	19.99e	17.39e:i	13.39l	*20.64*^{b}
HA+AA	19.33ab	20.19a	16.43bc	9.88e:g	9.14f:i	*14.99*^{a}	7.86e:g	10.42b	9.65bc	9.72bc	7.92ef	*9.11*^{a}	27.19b	30.60a	26.08bc	19.60ef	17.06f:j	*24.10*^{a}
Mean	14.37^{A}	15.17^{A}	12.33^{B}	8.90^{C}	7.77^{C}		8.92^{A}	9.32^{A}	7.65^{B}	7.80^{B}	6.91^{C}		23.30^{A}	24.49^{A}	19.98^{B}	16.71^{C}	14.69^{D}	

TW, tap water, HA, humic acid, AA, amino acids, HA + AA, mixture of humic acid + amino acids, F1, 100% NPK, F2, 75% NPK + biofertilizers, F3, 50% NPK + biofertilizers, F4, 25% NPK + biofertilizers, F5, biofertilizers, SY is stover yield (Mg ha^{-1}), EY is ear yield (Mg ha^{-1}) and BY is biological yield (Mg ha^{-1}). Means in italic refer to foliage applications, while none italic refer to fertilization treatments. Means followed by different letters in the same direction differ significantly by LSD ($p \leq 0.05$).

AA was higher than HA and AA mixture followed by HA and finally TW for their effects on increasing P contents. The maximum K contents (10.4 and 10.8 g kg^{-1}) during the 1st and 2nd seasons, respectively, were exhibited with the application of 50% NPK + biofertilizers with HA (Figure 1C). The HA or AA resulted in the highest K contents (e.g., 9.2 and 9.7 g kg^{-1}, respectively), while TW exhibited the lowest K contents (e.g., 7.7 and 8.0 g kg^{-1}) during the 1st and 2nd seasons, respectively. The grain uptakes of N (GNU), P (GPU) and K (GKU) improved significantly in response to the application of growth stimulants, even with reductions in the mineral NPK application rates (Figure 2). GNU (kg kg^{-1}), GPU (kg kg^{-1}), GKU (kg kg^{-1}) and CPY (kg ha^{-1}) exhibited their maximum values (e.g., 181, 14.12 and 94.36, respectively) when 75% NPK + biofertilizers were applied combined with foliar application of the HA and AA mixture during the first season. While applying 75% NPK + biofertilizers combined with foliar application of AA maximized these parameters (e.g., 185.2, 14.9 and 99.75, respectively) during the 2nd season. Generally, a reduction by 47% was reported in these parameters under partial or complete replacement of mineral NPK without growth stimulants. However, the application of HA with AA or a single AA mitigated this reduction significantly, especially under 75% or 50% NPK with biofertilizer treatments.

3.3 Correlations and path coefficients among the studied variables

The EL was significantly and positively correlated with GN/E, stover and biological yields, crude protein yield, N (%) and GNU when the data were pooled over the two years (Table 5). Additionally, NG/E had positive and significant correlations with yield attributes, CPY, and macronutrient contents and uptake. The 100-grain weight exhibited positive and significant correlations with SY, EY, BY, CPY, K (%), GNU, GPU, GKU and GY. Moreover, SY was positively and significantly correlated (p< 0.01) with EY (0.554**) and BY (0.966**), while it exhibited negative and significant correlations with HI (-0.708**) and N concentration (-0.327**). The EY had positive and significant correlations with BY, CPY, macronutrient contents and uptake, and GY. The CPY was significantly and positively correlated with N (%), P (%), K (%), GNP, GPU, GKU and GY. In addition, grain N contents were positively and highly significantly correlated (p< 0.01) with P (%), K (%), GNP, GPU, GKU and GY. Similarly, grain P contents exhibited positive and significant correlations with K (%), nutrient uptake, and GY. There were positive correlations between grain K contents and GNU (0.426**), GPU (0.451**), GKU (0.697**) and GY (0.325**). The GNU was positively and strongly correlated (p< 0.01) with GPU (0.913**), GKU (0.882**) and GY (0.913**). The GKU had strong positive correlations (p< 0.01) with GY (0.900**). The GY exhibited positive and strong correlations (p< 0.01) with ED

TABLE 4 Impact of foliar spraying of stimulants and chemical and bio fertilization treatments on harvest index and crude protein yield of maize.

Foliar spraying	HI						CPY					
	F1	F2	F3	F4	F5	Mean	F1	F2	F3	F4	F5	Mean
2019 season												
TW	36.54a:e	36.01a:e	32.01c:e	31.69c:e	45.40a	*36.33*^{ab}	884.1a:c	643.8e:h	487.9f:i	416.2i	482.4f:i	*582.9*^{b}
HA	25.81e	31.28c:e	37.60a:e	44.97ab	38.19a:e	*35.57*^{ab}	754.2c:e	881.6a:c	452.2g:i	697.8c:f	457.1g:i	*648.6*^{b}
AA	40.53a:d	28.86de	40.96a:d	45.60a	43.23a:c	*39.83*^{a}	878.2a:d	1013.7ab	776.6cde	820.8b:e	436.8hi	*785.2*^{a}
HA+AA	33.31a:e	32.61b:e	28.25de	36.65a:e	39.95a:d	*34.15*^{b}	818.9b:e	1064.2a	662.8d:g	787.1cde	676.7c:f	*801.9*^{a}
Mean	34.05^{BC}	32.19^{C}	34.70^{BC}	39.73^{AB}	41.69^{A}		833.8^{A}	900.8^{A}	594.9^{BC}	680.5^{B}	513.2^{C}	
2020 season												
TW	41.52a:c	34.83c:g	29.18gh	32.77fg	42.01ab	*36.06*^{ab}	1000.0ab	636.2gh	412.2k	463.4jk	493.2jk	*601.0*^{d}
HA	42.85ab	33.52e:g	37.01b:f	40.58a:d	34.28d:g	*37.65*^{a}	884.0cd	942.9bc	705.1f:h	515.4ij	423.9jk	*694.2*^{c}
AA	25.37h	34.98c:g	34.68d:g	42.86ab	45.42a	*36.66*^{a}	757.7ef	1089.0a	705.7fg	777.6ef	476.5jk	*761.3*^{b}
HA+AA	25.16h	29.59gh	31.94f:h	42.66ab	40.18a:e	*33.91*^{b}	820.1de	961.4bc	927.6bc	747.1ef	610.1hi	*813.3*^{a}
Mean	33.72^{B}	33.23^{B}	33.20^{B}	39.72^{A}	40.47^{A}		865.5^{A}	907.4^{A}	687.7^{B}	625.9^{C}	500.9^{D}	

TW, tap water, HA, humic acid, AA, amino acids, HA + AA, mixture of humic acid + amino acids, F1, 100% NPK, F2, 75% NPK + biofertilizers, F3, 50% NPK + biofertilizers, F4, 25% NPK + biofertilizers, F5, biofertilizers, HI is harvest index (%) and CPY is crude protein yield (kgha^{-1}). Means in italic refer to foliage applications, while none italic refer to fertilization treatments. Means followed by different letters in the same direction differ significantly by LSD ($p \leq 0.05$).

(0.810**), GN/E (0.636**), GW/E (0.940**), 100-grain weight (0.830**), EY (0.939**), BY (0.560**), HI (0.735**), CPY (0.913**), N (%) (0.298**), P (%) (0.314**), K (%) (0.325**) and GNU (0.913**).

The direct and indirect effects of grain yield and the other yield components of maize across the two seasons are presented in Table 6. Grain weight/ear had positive and strong direct effects on grain yield (1.359), while the number of grains/ear and 100-grain weight exhibited negative effects (-0.144 and -0.361, respectively). For the indirect effects, only the number of grains/ear and 100-grain weight had positive effects on grain yield (0.874 and 1.229, respectively) through grain weight/ear.

4 Discussion

4.1 Response of maize yield attributes and crude protein yield to a reduced NPK strategy combined with biofertilizers and growth stimulants

Due to their vital roles in building plant tissues and all physiological processes, the decline in mineral N, P and K rates was accompanied by significant reductions in maize growth and ear parameters. Our results showed significant reductions in the ear parameters, including EL, ED, NG/E and GW/E, under partial replacement of mineral NPK fertilizers by biofertilizers. Replacing mineral fertilizers with biofertilizers has environmental importance by reducing the loss of chemical fertilizers to the environment but may have negative impacts on maize growth and yield (Gao et al., 2020). Higher reductions in GW/E were reported as compared with that in EL, ED and NG/E when using lower rates of NPK fertilizers, which indicates the importance of high rates of readily available NPK during grain filling (Zarabi et al., 2011). Biofertilizers are not direct sources of nutrient, but enhance the activity of soil microorganisms, which improves soil fertility by regulating the decomposition of organic matter, increasing nutrient solubility and protecting them against losses. This explains the reductions in ear parameters with the reduced NPK rates even when applying biofertilizers. We combined growth stimulants such as HA and AA to reduce the negative effect of reduced NPK rates on maize growth, and we found improvements in the maize ear parameters even under reduced NPK rates by 75%. The reductions in EL, ED, NG/E and GW/E were significantly affected by AA application, while the mixture of HA and AA with 75% NPK + biofertilizers increased those parameters over than applying 100% NPK. Under semiarid conditions, plants are subjected to drought periods during growth, which could reduce ear formation. In addition to containing N, P and K, the AA contains amino acids which enhance plant resistance to stress and reduce their effects on ear growth, grain formation and filling (Canellas et al. 2019). Additionally, HA contains organic substances and K, which promotes plant growth under stress conditions but does not contain high NPK like amino acids. Combining HA and AA exhibited superior effects on the ear parameters when compared with a single application of HA or AA. For cleaner maize production, we suggest combining lower rates of chemical NPK fertilizers with biofertilizers and HA and AA mixtures. On the other hand, GY, SY, EY, BY, HI and CPY recorded significant variations in their responses to the combined application of chemical NPK fertilizers, biofertilization and growth stimulants (HA and AA). Sharp

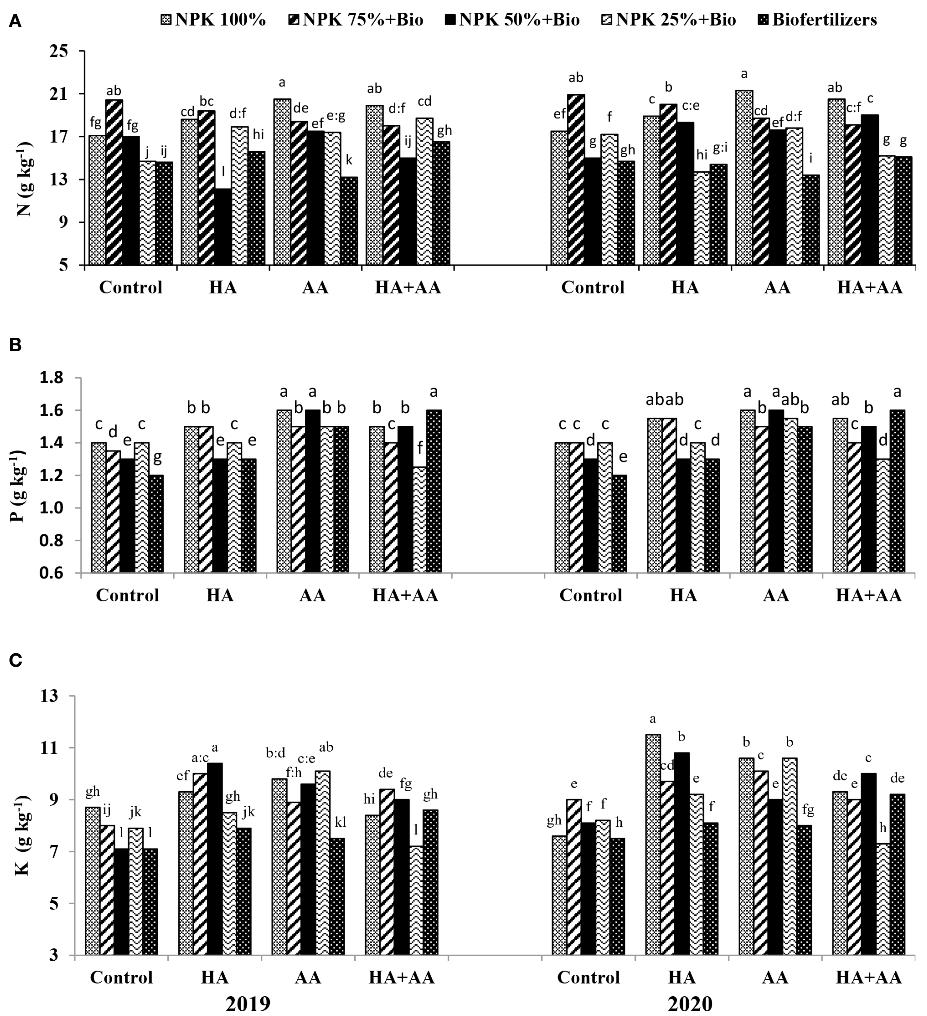

FIGURE 1
Impact of humic acid (HA), amino acids (AA) and the mixture (HA+AA) application on contents of nitrogen (%) **(A)**, phosphorous (%) **(B)** and potassium (%) **(C)** under chemical and bio fertilization treatments. Letters above columns refer to the significance LSD ($p \leq 0.05$).

reductions in these attributes were exhibited by reducing the mineral NPK rate by 25-100%, even with biofertilization. Similarly, increases in grain and stover yields with increasing N, P and K rates were reported (Gul et al., 2015). Higher N, P and K uptakes by maize plants produce higher LAIs, which activate photosynthesis and lead to greater dry matter production in terms of grain and stover yields (Canellas et al. 2019). Applying biofertilizers did not noticeably compensate for the sharp reductions in yield attributes that resulted from the reduced mineral fertilizer rate, which indicates less efficient of biofertilization under low NPK rates. Only an improvement by 12.5% in maize yields under biofertilization was reported by the meta-analysis study of Schmidt and Gaudin (2018). They found that biofertilizers were more effective under controlled conditions than under open field conditions, as field conditions might not be appropriate for microorganism activity, especially under semiarid conditions. Applying HA decreased the adverse effect of lower rates of mineral fertilization but not as much as AA or the mixture of HA and AA, because HA could only promote plant resistance to environmental stresses through its organic components. AA had the same effect as the HA and AA mixture on improving the yield attributes to exhibit higher GY, SY, EY and BY than by applying 100% NPK only. Similarly, there were increases in grain yields and yield attributes, as well as grain protein contents and GNU, with the application of HA or AA (Khan et al., 2019). In addition, AA is a direct source of N, P and K, which promotes plant resistance to stress under arid conditions (drought) and increases protein formation, photosynthesis and grain formation and filling (Szczepaniak et al., 2018). It is worth mentioning that HI recorded a contradictory response, for which the highest HI was reported when applying 25% NPK + biofertilizers, which

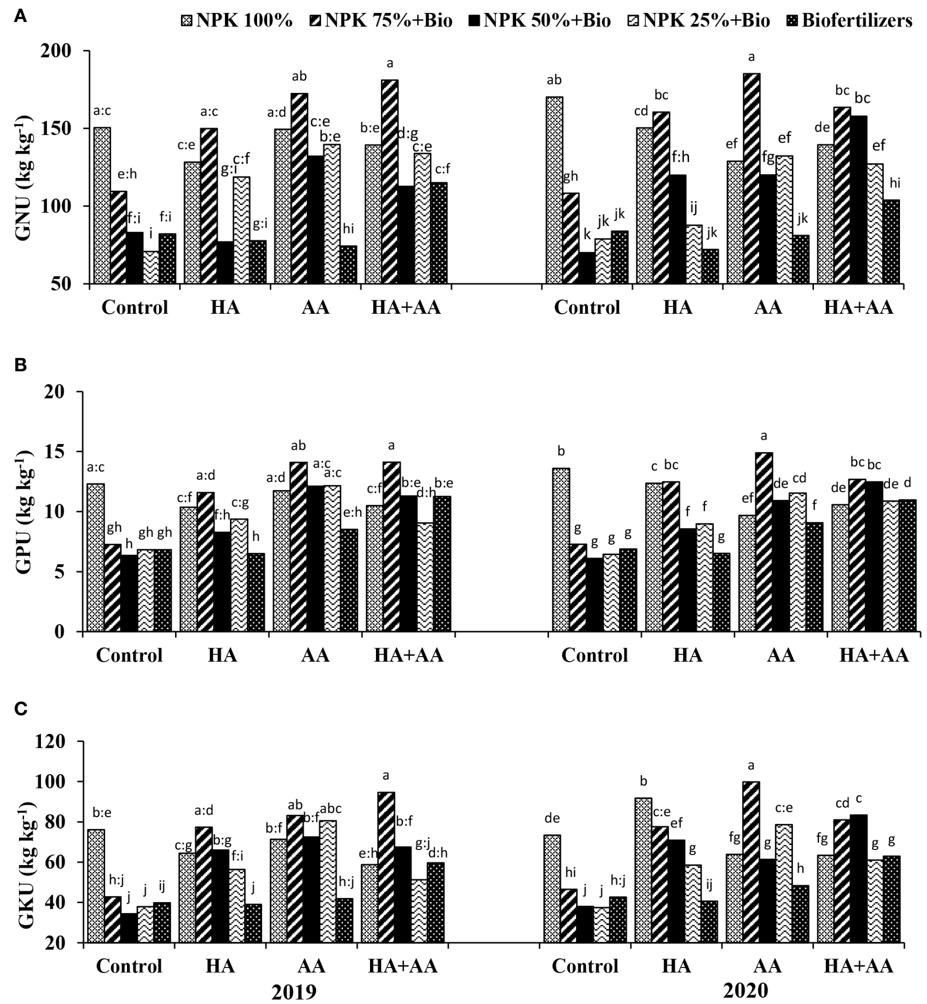

FIGURE 2
Impact of humic acid (HA), amino acids (AA) and the mixture (HA+AA) application on grain nitrogen uptake (GNU) **(A)**, grain phosphorus uptake (GPU) **(B)** and grain potassium uptake (GKU) **(C)** under five fertilization treatments. Letters above columns refer to the significance LSD ($p \leq 0.05$).

means higher grain formation against dry matter. The HI measures the relative investment of plant resources in their reproductive parts (Unkovich, 2010). The CPY increased with increasing the replacement of NPK fertilizer with biofertilizers combined with foliar application of HA and AA. This response could result from enhanced soil fertility with high organic matter and N contents, which increased grain yields (White, 2009; El-Sobky, 2016), amino acid formation (Jiang et al., 2019) and mineralization of soil organic N (Li et al., 2003), and accelerated the physiological and biochemical processes of the plants (Rawal and Kuligod, 2014). That increased the N concentration and N uptake. In addition, humic acid and amino acids enhance plant functions such as photosynthesis, protein synthesis, phytohormone activation, total amino acids and grain contents of N, P and K (Ragheb, 2016; Canellas et al., 2019; Khan et al., 2019).

4.2 Effect of reduced NPK rates combined with biofertilizers and growth stimulants on maize macronutrient contents and uptake

Nutrient contents and uptakes by maize grains have a strong positive correlation with mineral fertilization rates (Luan et al., 2020; Li et al., 2021). Significant reductions in N, P and K contents were exhibited under chemical NPK rates that were lower than 50% even combined with biofertilizers. Meanwhile, the nutrient uptakes and crude protein yields recorded sharp reductions with decreasing NPK rate of less than 100% with biofertilizers. These results were correlated with the previous sharp reductions in grain yield, which demonstrated the role of biofertilizers for continuous, but not rapid or high supply with NPK like chemical fertilizers to maximize yield (Sarajuoghi et al.,

TABLE 5 Correlations (Pearson correlation coefficient) between the study traits in maize as calculated from the combined data across two years.

Characters	ED	NG/E	GW/E	100-GW	SY	EY	BY	HI	CPY	N	P	K	GNU	GPU	GKU	GY
EL	0.168	0.261*	0.057	-0.08	0.264*	0.044	0.224*	-0.207	0.296**	0.507**	0.166	0.17	0.296**	0.136	0.163	0.114
ED		0.680**	0.821**	0.664**	0.507**	0.821**	0.657**	-0.007	0.812**	0.426**	0.201	0.427**	0.812**	0.759**	0.799**	0.810**
NG/E			0.643**	0.260*	0.585**	0.646**	0.665**	-0.198	0.636**	0.335**	0.393**	0.278*	0.636**	0.670**	0.598**	0.636**
GW/E				0.904**	0.564**	0.998**	0.757**	0.035	0.837**	0.231*	0.258*	0.288**	0.837**	0.886**	0.838**	0.940**
100-GW					0.376**	0.899**	0.577**	0.169	0.696**	0.101	0.132	0.233*	0.696**	0.748**	0.730**	0.830**
SY						0.554**	0.966**	-0.708**	-0.052	-0.327**	-0.108	-0.145	-0.052	0.078	0.029	0.129
EY							0.749**	0.041	0.833**	0.222*	0.257*	0.284*	0.833**	0.885**	0.836**	0.939**
BY								-0.551**	0.654**	0.481**	0.334**	0.331**	0.654**	0.580**	0.572**	0.560**
HI									0.777**	0.451**	0.345**	0.351**	0.777**	0.735**	0.713**	0.735**
CPY										0.656**	0.413**	0.426**	1.000**	0.913**	0.882**	0.913**
N											0.389**	0.394**	0.656**	0.375**	0.399**	0.298**
P												0.550**	0.413**	0.576**	0.480**	0.314**
K													0.426**	0.451**	0.697**	0.325**
GNU														0.913**	0.882**	0.913**
GPU															0.925**	0.955**
GKU																0.900**

*, ** Significant at P=0.05 and P= 0.01, respectively. EL is ear length (cm), ED is ear diameter (cm) and NG/E is number of grains/ear, GW/E is grain weight/ear (g), 100-GW is 100- grain weight (g), SY is stover yield (Mg ha^{-1}), EY is ear yield (Mg ha^{-1}) and BY is biological yield (Mg ha^{-1}), HI is harvest index (%) and CPY is crude protein yield (kg ha^{-1}), GNU is grain N uptake (kg ha^{-1}), GPU is grain P uptake(kg ha^{-1}), GKU is grain K uptake(kg ha^{-1})and GY is grain yield (Mg ha^{-1}).

2013; Kubheka et al., 2020a). We applied a biofertilizer mixture of N_2-fixing bacteria and P- and K-solubilizing bacteria, which increased soil macronutrient availability and uptake by plants (Goebel et al., 2016). The biofertilizers produced a compound that could be synthesized by bacteria or facilitate nutrient uptake from the environment. The application of growth stimulants, especially AA, under 75% NPK + biofertilizers, caused significant increases in the N and P contents and their uptakes to have the same values like that of 100% NPK. On the other hand, the K contents and uptakes recorded their highest values when applying 50% NPK + biofertilizers with HA. These results demonstrate the role of AA-containing amino acids and N and P nutrients in improving the assimilation of these nutrients in grains, which also proves the stronger effect of AA on grain yield compared with other stimulants (Hegab et al., 2020). There were increments in grain N concentrations and total N uptakes of maize with N fertilizer applications (Niaz et al., 2016). The HA is a source of organic acids and K, which could prevent sharp reductions in grain yield under environmental stress and can significantly supply plants with K only, which is consistent with our results. Increased K contents with the reduction of NPK rate by 50% refer to the antagonistic effect of high N rates on K uptake by maize grains. There are no previous studies on the combined effect of HA and/or AA on the N, P and K contents and uptakes by maize grains; however, there were increments in grain N and P contents by 21.3 and 15.2%, respectively, under AA application when compared with HA (Hegab et al., 2020). The K contents increased by 22.7% under HA application compared with AA application.

4.3 Correlations and path coefficients among grain yields and yield attributes and macronutrient contents and uptake

The correlations among the examined traits may be due to the consequence of the genetic associations among the studied parameters. The correlation and path analysis (Table 5) revealed that grain yield had significant relationships with the yield components, macronutrient content and nutrient uptake. These findings suggested that the improvement in maize grain yields is linked to an increase in those traits that might have positive impacts on grain yield. Similarly, significant positive correlations among maize grain yields and yield attributes as well

TABLE 6 Direct (Diagonal) and indirect effect of yield components on maize grain yield across two years relative to correlation.

Characters	Number of grains/ear	Grain weight/ear (g)	100-grain weight (g)	Correlation with grain yield (Mg ha^{-1})
Number of grains/ear	-0.144	0.874	-0.094	0.636
Grain weight/ear (g)	-0.093	1.359	-0.327	0.940
100-grain weight (g)	-0.037	1.229	-0.361	0.830

as with grain quality were reported [Ali (2016); Reddy and Jabeen (2016)]. The results revealed that grain weight/ear was considered to be the major yield component that maize breeders should consider to produce high-yielding maize. Similar results have been reported by several investigators (Nataraj et al., 2014; Ali, 2016; Reddy and Jabeen, 2016).

5 Conclusions

The efforts to obtain cleaner production are continuously increasing due to the environmental hazards that are caused by the intensive application of chemical fertilizers, especially N, P and K. Although the replacement of these chemicals with biofertilizers is a strongly recommended strategy, numerous findings have indicated that such replacements are an inefficient economic strategy. As shown by our study, there were sharp reductions in the maize yield attributes when replacing chemical NPK fertilizer by 25% to 100% with biofertilizers. For example, the grain yield was halved when reducing the recommendation rate of NPK fertilizers by 25%. Bio-stimulants, including humic (HA) and amino acids (AA), act against these reductions and significantly improved the maize yield quantities and qualities under 75% NPK more than for the recommended NPK rate. Moreover, the best yield attributes were obtained under the application of 75% NPK with HA and AA as compared with 100% of NPK fertilizers. Generally, the mixture of HA and AA reported the greatest effects, which was followed by AA and then HA. We strongly recommend combining the reduced amounts of chemical fertilizers with biological fertilizer, and HA and AA as strategies to obtain optimal maize yields and quality under semiarid conditions with less environmental hazards.

Data availability statement

The original contributions presented in the study are included in the article/Supplementary Material. Further inquiries can be directed to the corresponding author.

Author contributions

AA: Investigation, methodology, data curation, writing - original draft. E-SE-S: Data curation, resources, investigation, methodology, validation, writing - original draft. JZ: Writing – review & editing, funding acquisition. All authors contributed to the article and approved the submitted version.

Acknowledgments

The present study was supported by Guangdong Provincial Special Project of Rural Revitalization Strategy (Document No. [2021] 12), Science and Technology Planning Project of Guangdong Province of China (grant number 2019B030301007) and Guangdong Laboratory for Lingnan Modern Agriculture (NT2021010).

Conflict of interest

The authors declare that the research was conducted in the absence of any commercial or financial relationships that could be construed as a potential conflict of interest.

Publisher's note

All claims expressed in this article are solely those of the authors and do not necessarily represent those of their affiliated organizations, or those of the publisher, the editors and the reviewers. Any product that may be evaluated in this article, or claim that may be made by its manufacturer, is not guaranteed or endorsed by the publisher.

Supplementary material

The Supplementary Material for this article can be found online at: https://www.frontiersin.org/articles/10.3389/fpls.2022.1069624/full#supplementary-material

References

Ali, M. (2016). Estimation of some breeding parameters for improvement grain yield in yellow maize under water stress. *J. Plant Production* 7, 1509–1521. doi: 10.21608/jpp.2016.47111

Bassu, S., Brisson, N., Durand, J. L., Boote, K., Lizaso, J., Jones, J. W., et al. (2014). How do various maize crop models vary in their responses to climate change factors? *Global Change Biol* 20 (7), 2301–2320. doi: 10.1111/gcb.12520

Bishnoi, U. R., and Hughes, J. L. (1979). Agronomic performance and protein content of fall-planted triticale, wheat, and rye. *Agron. J.* 71, 359–360. doi: 10.2134/agronj1979.00021962007100020032x

Buresh, R. J., Datta, S., Padilla, J. L., and Chua, T. T. (1988). Potential of inhibitors for increasing response of lowland rice to urea fertilization. *Agron. J.* 80, 947–952. doi: 10.2134/agronj1988.00021962008000060022x

Canellas, L. P., Olivares, F. L., Canellas, N., Mazzei, P., and Piccolo, A. (2019). Humic acids increase the maize seedlings exudation yield. *Chem. Biol. Technol. Agric.* 6, 3. doi: 10.1186/s40538-018-0139-7

Corbin, J. L., Orlowski, J. M., Harrell, D. L., Golden, B. R., Larry, F., Jason, K. L., et al. (2016). Nitrogen strategy and seeding rate affect rice lodging, yield, and economic returns in the midsouthern united states. *Agron. J.* 108, 1938. doi: 10.2134/agronj2016.03.0128 du Jardin, P. (2015). Plant biostimulants: Definition, concept, main categories and regulation. *Scientia Hortic.* 196, 3–14. doi: 10.1016/j.scienta.2015.09.021

El-Etr,, and Mahmoud, A. A. (2011). Improving phosphorus use efficiency and its effect on the productivity of some crops. *J. Soil Sci. Agric. Eng.* 2, 1019–1034. doi: 10.21608/jssae.2011.55708

El-Gedwy, E. S. (2020). Effect of Water Stress, Nitrogen and Potassium Fertilizers on Maize Yield Productivity. *Ann. Agric. Sci. Moshtohor* 58, 515–534. doi: 10.21608/assjm.2020.122030

El-Sobky, E. (2016). Response of yellow maize yield to preceding crop effect and NP fertilization level. *J. Agron.* 38, 153–171. doi: 10.1080/01904167.2020.1845369

El-Sobky, E., and Abdo, A. I. (2020). Efficacy of using biochar, phosphorous and nitrogen fertilizers for improving maize yield and nitrogen use efficiencies under alkali clay soil. *J. Plant Nutr.* 44, 1–19. doi: 10.1080/01904167.2020.1845369

Faithfull, N. T. (2002). *Methods in agricultural chemical analysis. A practical handbook* (Wallingford: CABI Publishing) 84–95. doi: 10.1079/9780851996080.0000

Fan, M., Shen, J., Yuan, L., Jiang, R., and Zhang, F. (2012). Improving crop productivity and resource use efficiency to ensure food security and environmental quality in China. *J. Exp. Bot.* 63, 13–24. doi: 10.1093/jxb/err248

FAO (2020) Food and Agriculture Organization of the United Nations. *Statistical Database*. Available at: http://www.fao.org/faostat/en/#data.

Gao, C., El-Sawah, A. M., Ali, D., Hamoud, Y., and Sheteiwy, M. S. (2020). The integration of bio and organic fertilizers improve plant growth, grain yield, quality and metabolism of hybrid maize (Zea mays l.). *Agron. J.* 10, 319. doi: 10.3390/agronomy10030319

Goebel, N. L., Edwards, C. A., Follows, M. J., and Zehr, J. P. (2016). Modeled diversity effects on microbial ecosystem functions of primary production, nutrient uptake, and remineralization. *Ecology* 95, 153–163. doi: 10.1890/13-0421.1

Gomez, K. N., and Gomez, A. A. (1984). *Statistical procedures for agricultural research* Vol. 68 (New York: John Wiley and Sons).

Gul, S., Khan, M. H., Khanday, B. A., and Nabi, S. (2015). Effect of sowing methods and NPK levels on growth and yield of rainfed maize (Zea mays l.). *Scientifica* 2015, 1–6. doi: 10.1155/2015/198575

Hegab, R. H., Fawy, E. A., and Habib, A. (2020). Evaluates effect of amino acids, humic acid and antioxidants as foliar application on the biochemical content and productivity of wheat under north Sinai soils conditions. *Am. J. Agric. Forestry* 8, 167. doi: 10.11648/j.ajaf.20200804.19

Hirel, B., Tétu, T., Lea, P. J., and Dubois, F. (2011). Improving nitrogen use efficiency in crops for sustainable agriculture. *Sustainability* 3, 1452–1485. doi: 10.3390/su3091452

Huang, Y., Zhang, L., Wang, H., Liang, M., and Zheng, W. (2017). Assessment of ammonia volatilization losses and nitrogen utilization during the rice growing season in alkaline salt-affected soils. *Sustainability* 9 (1), 132. doi: 10.3390/ su9010132

Itelima, J. U., Bang, W. J., Sila, M., Onyimba, I. A., and Egbere, O. J. (2018). A review: Biofertilizer - a key player in enhancing soil fertility and crop productivity. *J Microbiol Biotechnol Rep.* 2 (1), 22–28.

Jiang, D., Hao, M., Fu, J., Liu, K., and Yan, X. (2019). Potential bioethanol production from sweet sorghum on marginal land in China. *J. Cleaner Production* 220, 225–234. doi: 10.1016/j.jclepro.2019.01.294

Jilani, G., Akram, A., Raja, M., and Hafeez, Y. F. (2007). Enhancing crop growth, nutrients availability, economics and beneficial rhizosphere microflora through organic and biofertilizers. *Ann. Microbiol* 57 (2), 177–184. doi: 10.1007/BF03175204

Khan, S. A., U-Khan, S., Qayyum, A., Khan, A., and Z-Amin, B. A. (2019). Integration of humic acid with nitrogen wields an auxiliary impact on physiological traits, growth and yield of maize (zea mays l.) varieties. *Appl. Ecol. Environ. Res.* 17, 6783–6799. doi: 10.15666/aeer/1703_67836799

Klute, A. (1986). Methods of soil analysis. part 1. *Phys. mineralogical Methods Soil Sci.* 146, 138. doi: 10.2136/sssabookser5.1.2ed

Kubheka, B. P., Laing, M., and Yobo, K. S. (2020a). Combinations of a biofertilizer with micro-dosed chemical fertilizers increased yield of maize in a high acid saturated soil. *Rhizosphere* 13, 100189. doi: 10.1016/j.rhisph.2020.100189

Kumawat, N. (2017). Role of biofertilizers in agriculture. *Pop Kheti* 5, 6.

Lakshmi, P. (2014). Comparative study of vermicast and charcoal used as a carrier inoculums to the biofertilizer preparation. *BMR Biotechnoloy* 1, 1–6.

Li, G., Cheng, Q., Li, L., Lu, D., and Lu, W. (2021). N, p and K use efficiency and maize yield responses to fertilization modes and densities - ScienceDirect. *J. Integr. Agric.* 20, 78–86. doi: 10.1016/S2095-3119(20)63214-2

Li, H., Han, Y., and Cai, Z. (2003). Nitrogen mineralization in paddy soils of the taihu region of China under anaerobic conditions: Dynamics and model fitting - ScienceDirect. *Geoderma* 115, 161–175. doi: 10.1016/S0016-7061(02)00358-0

Luan, P., Tjca, B., Ras, C., Fhg, B., Gbr, B., Lzp, D., et al. (2020). Effect of hairy vetch cover crop on maize nitrogen supply and productivity at varying yield environments in southern Brazil. *Sci. Total Environ.* 759, 144313. doi: 10.1016/j.scitotenv.2020.144313

Matysiak, K., Kierzek, R., Siatkowski, I., Kowalska, J., Krawczyk, R., and Miziniak, W. (2020). Effect of exogenous application of amino acids l-arginine and glycine on maize under temperature stress. *Agronomy* 10, 769. doi: 10.3390/agronomy10060769

Moll, R. H., Kamprath, E. J., and Jackson, W. A. (1962). Analysis and interpretation of factors which contribute to efficiency of nitrogen utilization. *Agron. J.* 74, 562–564. doi: 10.2134/agronj1982.00021962007400030037x

Nataraj, V., Shahi, J. P., and Agarwal, V. (2014). Correlation and path analysis in certain inbred genotypes of maize (Zea mays l.) at varanasi. *Int. J. innovative Res. Dev.* 3, 14–17.

Niaz, A., Yaseen, M., Shakar, M., Sultana, S., and Nazarat, A. (2016). Maize production and nitrogen use efficiency in response to nitrogen application with and without humic acid. *J. Anim. Plant Sci.* 26, 1641.

Pavlov, J., Delic, N., Markovic, K., Crevar, M., and Stevanovic, M. (2015). Path analysis for morphological traits in maize (Zea mays l.). *Genetika* 0534-0012) 47, 295–301. doi: 10.2298/GENSR1501295P

Pawar, J., Kumar, P., and Khanna, R. (2019). Efficiency of biofertilizers in increasing the production potential of cereals and pulses: A review. *J. Pharmacognosy Phytochem.* 8, 183–188.

Phares, C. A., Amoakwah, E., Danquah, A., Afrifa, A., Beyaw, L. R., and Frimpong, K. A. (2022). Biochar and NPK fertilizer co-applied with plant growth promoting bacteria (PGPB) enhanced maize grain yield and nutrient use efficiency of inorganic fertilizer. *J. Agric. Food Res.* 10, 100434. doi: 10.1016/j.jafr.2022.100434

Ragheb, E. E. (2016). Sweet corn as affected by foliar application with amino – and humic acids under different fertilizer sources. *Egypt. J. Hortic.* 43, 441–456. doi: 10.21608/ejoh.2016.3564

Ramirez-Cabral, N., Kumar, L., and Shabani, F. (2017). Global alterations in areas of suitability for maize production from climate change and using a mechanistic species distribution model (CLIMEX). *Sci. Rep.* 7, 5910. doi: 10.1038/s41598-017-05804-0

Rawal, R., and Kuligod, V. B. (2014). Influence of graded doses of nitrogen on nutrient uptake and grain yield of maize (Zea mays) under varying levels of soil salinity*. *Karnataka J. Agric. Sci.* 27, 22–24.

Reddy, V. R., and Jabeen, F. (2016). Narrow sense heritability, correlation and path analysis in maize (Zea mays l.). *Sabrao J. Breed. Genet.* 48, 120–126.

Sarajuoghi, M., Ardakani, M. R., Nurmohammadi, G., Kashani, A., and Mafakheri, S. (2013). Response of yield and yield components of maize (Zea mays l.) to different biofertilizers and chemical fertilizers. *Am. Eurasian J. Agric. Environ. Sci.* 1, 1068–1077.

Schmidt, J. E., and Gaudin, A. (2018). What is the agronomic potential of biofertilizers for maize? A meta-analysis. *FEMS Microbiol. Ecol.* 7, fiy094. doi: 10.1093/femsec/fiy094

Snedecor, G. W., and Cochran, W. G. (1989). *Statistical Methods. 8th* Edition. (Ames: Iowa State University Press).

Szczepaniak, W., Potarzycki, J., Grzebisz, W., and Nowicki, B. (2018). Zinc and amino acids impact on nutrient status of maize during the 'critical window'. *Plant Soil Environ.* 64, 126–131. doi: 10.17221/19/2018-PSE

Unkovich, M. (2010). Variability in harvest index of grain crops and potential significance for carbon accounting. *Adv. Agron.* 105, 173–219. doi: 10.1016/S0065-2113(10)05005-4

White, P. J. (2009). *The use of nutrients in crop plants* Vol. 45 (FL, USA: CRC Pres), 380–380.

Yosefi, K., Galavi, M., Ramrodi, M., and Mousavi, S. R. (2011). Effect of bio-phosphate and chemical phosphorus fertilizer accompanied with micronutrient foliar application on growth, yield and yield components of maize (Single cross 704). *Aust. J. Crop Sci.* 5, 175–180. doi: 10.5539/jas.v3n4p22

Yuan, Y., Gai, S., Tang, C., Jin, Y., Cheng, K., Antonietti, M., et al. (2022). Artificial humic acid improves maize growth and soil phosphorus utilization efficiency. *Appl. Soil Ecol.* 179, 104587. doi: 10.1016/j.apsoil.2022.104587

Zarabi, M., Alahdadi, I., Akbari, G. A., and Akbari, G. A. (2011). A study on the effects of different biofertilizer combinations on yield, its components and growth indices of corn (Zea mays l.) under drought stress condition. *Afr. J. Agric. Res.* 6, 681–685. doi: 10.5897/AJAR10.870

frontiers | Frontiers in Plant Science

TYPE Original Research
PUBLISHED 08 December 2022
DOI 10.3389/fpls.2022.1041924

OPEN ACCESS

EDITED BY
Gabrijel Ondrasek,
University of Zagreb, Croatia

REVIEWED BY
Krishan K. Verma,
Guangxi Academy of Agricultural Sciences, China
Abdul Wakeel,
University of Agriculture, Pakistan

*CORRESPONDENCE
Vitalij Dombinov
v.dombinov@fz-juelich.de

SPECIALTY SECTION
This article was submitted to Plant Nutrition, a section of the journal Frontiers in Plant Science

RECEIVED 11 September 2022
ACCEPTED 11 November 2022
PUBLISHED 08 December 2022

CITATION
Dombinov V, Herzel H, Meiller M, Müller F, Willbold S, Zang JW, da Fonseca-Zang WA, Adam C, Klose H, Poorter H, Jablonowski ND and Schrey SD (2022) Sugarcane bagasse ash as fertilizer for soybeans: Effects of added residues on ash composition, mineralogy, phosphorus extractability and plant availability.
Front. Plant Sci. 13:1041924.
doi: 10.3389/fpls.2022.1041924

Sugarcane bagasse ash as fertilizer for soybeans: Effects of added residues on ash composition, mineralogy, phosphorus extractability and plant availability

Vitalij Dombinov[1*], Hannes Herzel[2], Martin Meiller[3], Felix Müller[4], Sabine Willbold[5], Joachim W. Zang[6], Warde A. da Fonseca-Zang[6], Christian Adam[2], Holger Klose[1,7], Hendrik Poorter[1,8], Nicolai D. Jablonowski[1] and Silvia D. Schrey[1]

[1]Institute of Bio- and Geosciences, IBG-2: Plant Sciences, Forschungszentrum Jülich GmbH, Jülich, Germany, [2]Thermochemical Residues Treatment and Resource Recovery, Bundesanstalt für Materialforschung und -prüfung (BAM), Berlin, Germany, [3]Renewable Energy, Fraunhofer Institute for Environmental, Safety, and Energy Technology UMSICHT, Sulzbach-Rosenberg, Germany, [4]Thermal Process Technology, TU Clausthal (CUTEC), Clausthal-Zellerfeld, Germany, [5]Central Institute for Engineering, Electronics and Analytics, Analytics (ZEA-3), Forschungszentrum Jülich GmbH, Jülich, Germany, [6]Instituto Federal de Educação, Ciência e Tecnologia de Goiás (IFG), Goiânia, Brazil, [7]RWTH Aachen University, Aachen, Germany, [8]Department of Natural Sciences, Macquarie University, Sydney, Australia

Sugarcane bagasse is commonly combusted to generate energy. Unfortunately, recycling strategies rarely consider the resulting ash as a potential fertilizer. To evaluate this recycling strategy for a sustainable circular economy, we characterized bagasse ash as a fertilizer and measured the effects of co-gasification and co-combustion of bagasse with either chicken manure or sewage sludge: on the phosphorus (P) mass fraction, P-extractability, and mineral P phases. Furthermore, we investigated the ashes as fertilizer for soybeans under greenhouse conditions. All methods in combination are reliable indicators helping to assess and predict P availability from ashes to soybeans. The fertilizer efficiency of pure bagasse ash increased with the ash amount supplied to the substrate. Nevertheless, it was not as effective as fertilization with triple-superphosphate and K_2SO_4, which we attributed to lower P availability. Co-gasification and co-combustion increased the P mass fraction in all bagasse-based ashes, but its extractability and availability to soybeans increased only when co-processed with chicken manure, because it enabled the formation of readily available Ca-alkali phosphates. Therefore, we recommend co-combusting biomass with alkali-rich residues to increase the availability of P from the ash to plants.

KEYWORDS

combustion and gasification, ^{31}P-NMR spectroscopy, X-ray diffraction (XRD), phosphate extractability and availability, greenhouse experiments

Introduction

In tropical and subtropical countries, the combustion of sugarcane bagasse and leaves is used to generate heat and electricity (Raza et al., 2021). This combustion can be considered sustainable (Ondrasek et al., 2021), as it releases only carbon that has been sequestered from the atmosphere (Mendiara et al., 2017). In Brazil, about 6% of electricity is generated from the combustion of sugarcane leaves and bagasse (Watanabe et al., 2020), resulting in up to 10 million tons of ash annually (Herzel et al., 2020). However, sustainability also depends on appropriately recycling valuable elements found in the ash, such as phosphorus (P) and potassium (K). Although bagasse ash has been recognized as a potential fertilizer because it contains P and K (Pita et al., 2012; Gonfa et al., 2018), it is often disposed of as waste in landfills (Xu et al., 2018; Silva et al., 2019). This is due to both a lack of reliable information on nutrient availability compared to conventional fertilizers, and because the ash is partly produced in the rainy season, which makes transport to the field difficult. Biomass combustion and use of the resulting ash in agriculture is a promising strategy for sustainable energy production, disposing of ash at low-cost while recycling valuable nutrients (Patterson et al., 2004). Ultimately, such practices will help to achieve global goals for climate change mitigation by making efficient use of resources (EU, 2016; Li et al., 2016; Müller-Stöver et al., 2018; EU, 2019; Chojnacka et al., 2020).

While K from biomass ash is comparable to that found in mineral fertilizers (Li et al., 2017; Tran et al., 2018), the availability of P from ashes to plants depends, among other factors, on the origin and composition of the biomass. This can be modified by joint processing with other (nutrient-rich) residues, and by varying thermal processing conditions (Demeyer et al., 2001; Schiemenz and Eichler-Löbermann, 2010; Müller-Stöver et al., 2018). Following thermal processing, organic P oxidizes and reacts with other metals, including alkaline earth metals and alkali metals such as aluminum (Al) and iron (Fe), calcium (Ca), and sodium (Na), forming a mixture of oxides and phosphates (Tan and Lagerkvist, 2011). The solubility of phosphates from ash and their availability to plants depends on mineral P types formed during the thermal processing of biomass (Brod et al., 2015; Kratz et al., 2019; Luyckx et al., 2021). To our knowledge, there is currently only limited information available on the P mineralogy of bagasse ash, and thus the fertilization effects of these ashes are not well understood.

Abbreviations: cB, combusted bagasse; cBS, combusted bagasse sewage sludge; cBM, combusted bagasse chicken manure; gB, gasified bagasse; gBM, gasified bagasse chicken manure; TSP, triple superphosphate; XRD, X-ray diffraction; NMR, nuclear magnetic resonance spectroscopy; P, elemental phosphorus; K, elemental potassium.

The objectives of the present study were to produce ashes by combusting and gasifying sugarcane bagasse alone and in combination either with chicken manure or sewage sludge. The goal of these variations was to i) change the elementary composition of bagasse ash and ii) use laboratory and greenhouse analyses to understand and predict plant P availability as well as subsequent fertilization effects. Chicken manure and sewage sludge were used because they both have high P mass fractions, while otherwise differing in Ca, Na, K, Fe, and Al content. The co-processing also aimed to show the benefits of using bagasse ash as a fertilizer. We chose soybean as a model plant because it is one of the most widely cultivated crops in Brazil (FAOSTAT, 2022) and is often cultivated in rotation with sugarcane (Bordonal et al., 2018; Withers et al., 2018). In this study, we conducted laboratory and greenhouse experiments to understand and predict the plant P availability from different bagasse-based ashes and their fertilization effects on soybeans.

Material and methods

Ash preparations

Bagasse ashes from the sugarcane factory 'Usina Nova Gália Ltda.' (Paraúna, Goiás state, Brazil), hereafter named cB ash, as well as five bagasse-based ashes resulting from small-scale combustion and gasification, were used in this study. On a small-scale, bagasse pellets were gasified alone (gB) or as a blend with chicken manure pellets (gBM), and co-combusted either with chicken manure pellets (cBM) or sewage sludge (cBS; Supplementary Material S1, S2). The ratios of bagasse pellets to chicken manure pellets and sewage sludge were 80 to 20 (w/w). All sugarcane bagasse-based ashes were dried to constant weights at 60°C (TR 1050, Nabertherm GmbH, Lilienthal, Germany). The ashes, as well as triple superphosphate (TSP; Triferto Fertilizers, Doetinchem, Netherlands), were milled (≤ 250 µm, Retsch ZM 1, Retsch GmbH, Haan, Germany) before analyses and use in greenhouse pot experiments.

Ash characterizations

Elementary compositions

All bagasse-based ashes and TSP were analyzed for their elemental composition. Carbon (C) and nitrogen (N) were measured in a Vario El Cube, CHNS elemental analyzer (CHNS mode, Elementar Analyzensysteme GmbH, Langenselbold, Germany) by combusting 0.1 g of each fertilizer. Another 0.1 g of fertilizer was mixed with 0.25 g lithium borate and digested at 1000°C in a muffle furnace for 30 min. The molten phase was diluted in 30 ml of 5% hydrochloric acid (HCl) and filled up to 50 ml with ultra-pure water (Milli-Q Reference, Merck, Darmstadt, Germany). Subsamples for P, K, Ca, Na, Fe, Al, magnesium (Mg) and silicon (Si) determination were then diluted with ultra-pure water at a ratio of 1:20 (*v*/*v*) and measured in inductively coupled plasma atomic emission spectroscopy (iCAP 6500, Fisher Scientific, Schwerte, Germany).

Sequential phosphorus extraction

The sequential P extractions from cB, gB, gBM, cBM and cBS ashes followed the protocol of Hieltjes and Lijklema (1980), modified by Qian et al. (2009). In brief, 0.5 g of each ash were sequentially extracted with 20 mL of distilled deionized water (ddH_2O), 1 M ammonium chloride (NH_4Cl) at pH 7, 0.1 M sodium hydroxide (NaOH), and twice with 0.5 M hydrochloric acid (HCl) solutions. Samples were shaken (Turbula T2c, Willy A. Bachofen AG, Muttenz, Switzerland) for 2 hours (h), 2 h, 17 h, and 2x 24 h, respectively, and centrifuged at 15000 *g* (Hermle Z326K, HERMLE Labortechnik GmbH, Wehingen, Germany) for 5 min. before collecting supernatants. Phosphorus in supernatants was measured using inductively coupled plasma atomic emission spectroscopy (Thermo iCAP 7400, Dreieich, Germany) according to Brod et al. (2015).

Phosphorus and potassium extraction in citric acid

Phosphorus and K were extracted with 2% citric acid from all bagasse-based ashes and TSP following the protocol of Herzel et al. (2020). Briefly, 1.0 g ± 0.1 g of ashes or TSP were mixed with 100 mL of 2% citric acid solution (1:100 *w/v*), then shaken for 30 min. in an overhead shaker (35 rpm, RA20, Gerhardt, Königswinter, Germany) and filtered *via* a folded filter (type 2015, particle retention 5-8 µm, Labsolute, Renningen, Germany). Phosphorus and K concentrations in the filtrates were analyzed by inductively coupled plasma atomic emission spectroscopy (Thermo iCAP 7400, Dreieich, Germany).

Powder X-ray diffraction analysis

The powder X-ray diffraction (XRD) measurements were based on the protocol described by Herzel et al. (2020). Measurements focused on P phases in cB, gB, gBM, cBM and cBS ashes and were combined with P extractions in 2% citric acid, 2% formic acid, 0.1 M NaOH and 0.5 M HCl to verify the disappearance of reflexes due to pH changes. Ash measurements were performed in Bragg-Brentano geometry over a 2θ range from 5° to 80° with a step size of 0.02° employing a D8 Advance Bruker AXS (Bruker, Billerica, USA) before and after P extraction in 0.1 M NaOH and 0.5 M HCl solutions, respectively. Diffraction patterns were collected using Cu Kα1 and Cu Kα2 ($\lambda 1$ = 1.54056 Å, $\lambda 2$ = 1.54443 Å) radiation and recorded with a Lynxeye detector. Qualitative identification of the crystalline phases was performed using the MATCH! Software (version 3.6) in combination with the ICDD PDF2 database.

Plant trials under greenhouse conditions

Two independent greenhouse pot experiments were conducted at the Institute of Bio- and Geosciences, IBG-2: Plant Sciences, Forschungszentrum Jülich, Germany (50°54'36''N, 6° 24'49''E), to evaluate the fertilizing effect (Exp. 1) and plant P availability (Exp. 2) from bagasse-based ashes to soybeans.

Soybeans (*Glycine max* (L.) Merr., RGT Shouna) were cultivated as described in Herzel et al. (2020) to provide homogeneous plant material at the start of the experiments. Soybeans were germinated on moist filter paper in the dark, and after 3 days (d) seedlings with comparable radicle length were transplanted into the substrate, i.e., sand and a greenhouse substrate low in nutrients (*Null-Erde*, Balster Einheitserdewerk, Fröndenberg, Germany) in a volume ratio of 1:1 (Supplementary Material S3) until the unifoliate leaves were fully expanded. At this stage, the roots were washed and plantlets with comparable morphologies were identified. Five plantlets were harvested to analyze the initial K and P contents (referred to as the first harvest in Eq. 2 and 3). Roots of remaining plantlets were inoculated with N_2-fixing *Bradyrhizobium japonicum* (NPPL HI Stick, BASF SE, 180 Ludwigshafen, Germany). Plantlets were then transplanted into pots containing 1150 gram (g), i.e. 1.25 liter (L), of substrate treated with the different fertilizers. The selection of the potting medium was based on additional analyses (Supplementary Material S3). The substrate chosen as the potting medium was selected because it contained only a small mass fraction of P, and its physical and chemical properties were not significantly affected by high doses of bagasse ash, unlike either Brazilian soil from the field or quartz sand. This enabled analyses of ash as fertilizer and of P availability from ashes to soybeans under highly controlled conditions.

Soybean plants received 16 h d^{-1} light from natural and artificial light sources (minimum 400 µmol s^{-1} m^{-2}, SON-T AGRO 400, Philips) regulated by an automated light system. The pots were watered to 70% of their water holding capacity weekly. The substrate was covered with white plastic granulate to reduce water evaporation. Pots were randomized each week to minimize edge effects.

Experiment 1: Soybean response to increasing doses of cB ash

A dose-response experiment using cB ash (Table 1) as fertilizer for soybeans was conducted from August to September. The aim of this experiment was to analyze the efficiency of pure bagasse ash as fertilizer for soybeans under greenhouse conditions. Six doses of cB ash, ranging from 0 g to 31.6 g cB ash kilogram^{-1} (kg^{-1}) substrate, were homogeneously incorporated into the substrate and delivered 0 mg to 120 mg P and 0 mg to 385 mg K kg^{-1} of substrate. Positive control treatment received readily available P and K at optimal doses for soybeans, i.e., 30 mg P kg^{-1} from TSP and 225 mg K kg^{-1} from potassium sulphate (K_2SO_4), determined in pre-experiments (data not shown). According to the recommendation for soybean

TABLE 1 Chemical compositions of cB, gB, gBM, cBM and cBS ashes and triple superphosphate (TSP).

Elements	Unit	cB ash B Comb.	gB ash B Gas.	gBM ash B/M (80:20) Gas.	cBM ash B/M (80:20) Comb.	cBS ash B/S (80:20) Comb.	TSP
C	wt%	5.05	53.7	40.5	1.07	0.21	
N	wt%	0.1	0.05	0.08	0.03	0.02	
P	wt%	0.38	0.41	1.66	2.05	3.02	19.48
K	wt%	1.21	1.04	2.41	3.15	0.64	0.04
Ca	wt%	1.26	0.99	5.15	9.12	3.99	13.74
Mg	wt%	0.46	0.57	1.14	1.01	0.67	0.23
Na	wt%	0.1	0.04	0.19	0.24	0.11	
Fe	wt%	5.38	3.32	2.46	1.44	3.86	0.28
Al	wt%	3.86	2.98	2.72	1.14	4.18	0.23
Si	wt%	14.62	0.56	0.72	0.04	0.01	
$pH_{1:2.5}$		7.1	9.9	11.5	12.8	7.7	2.6
P_{CA}	mg P g^{-1}	1.86	3.97	15.6	17.34	9.02	183.09
K_{CA}	mg K g^{-1}	6.05	3.64	14.46	16.7	-	-

The pH values were measured in 0.01 M $CaCl_2$ solution (1:2.5 w/v). P_{CA} and K_{CA} indicate the mass fractions of P and K from ash, TSP and K_2SO_4 soluble in 2% citric acid. B, bagasse; M, chicken manure; S, sewage sludge; Comb., combustion; Gas., gasification.

cultivation under field conditions, soybean plantlets were inoculated with the symbiotic microbe *Bradyrhizobium japonicum* (2.3) and no mineral N fertilizer was added (Mendes et al., 2003).

Each fertilizer treatment contained five biological replicates, which were harvested after 44 d of growth. During plant growth the average relative air humidity was 52/66% (day/night) and the temperature was 25/20°C (day/night). The plants received an average of 9.8 mol photons m^{-2} d^{-1} light irradiance.

Experiment 2: Effect of thermal co-processing bagasse pellets with nutrient rich residues on P-availability to soybeans

Over the period from April to June, we evaluated the P availability from gB, gBM, cBM and cBS ashes (Table 1) to soybeans. The soybeans were fertilized with 54 mg P kg^{-1} of substrate. Phosphorus dose was based on the dose response experiment discussed in Effect of industrially produced bagasse ash as fertilizer. Absolute amounts of applied bagasse-based ashes were 13.2 g of gB, 3.2 g of gBM, 2.2 g cBM, and 1.9 g cBS ashes kg^{-1} substrate. For all treatments, the concentration of K was adjusted with K_2SO_4 to 244 mg kg^{-1} and with ammonium nitrate to 23 mg of N kg^{-1} of substrate to exclude K and N limitation when comparing plant P availability from gB, gBM, cBM and cBS ashes.

Each fertilizer treatment contained five biological replicates, which were harvested after 42 d of growth. Average relative air humidity was 47/62% (day/night) and the temperature was 25/19°C (day/night). The plants received an average of 11.2 mol photons m^{-2} d^{-1} light irradiance.

Non-invasive shoot growth measurements

In Experiment 1, the shoot areas of soybean plants were regularly imaged using the plant phenotyping "ScreenHouse" platform available at IBG-2 Plant Sciences, Forschungszentrum Jülich GmbH, Germany, as described in Nakhforoosh et al. (2016) and Herzel et al. (2020) to depict the shoot growth dynamics. In brief, the shoots were automatically imaged at a 45° angle from four sides of the pot, i.e., 0°, 90°, 180°, and 270° (Point Gray Grasshopper2, 5MP color camera, by FLIR Integrated Imaging Solutions Inc., Richmond, British Columbia, Canada). The sum of the four images represented the projected shoot area of the plant. Shoot areas were imaged weekly for 26 d, starting on day 6 after transplanting the plantlets into the fertilized substrate. Imaged shoot area was significantly correlated with leaf area of soybeans after plant harvest (R = 0.96, Supplementary Material S4), allowing an estimation of projected leaf area over time. The factor used to convert the projected shoot areas from px to projected leaf areas in cm^2 was 1792 and was based on a calibration curve (Supplementary Material S4).

Destructive analyses

In experiment 1, roots and shoots were harvested separately and numbers of root nodules were counted to evaluate the evenness of root nodulation between treatments. In both experiments 1 and 2, roots and shoots were separately dried at 65°C to constant weight (TR 1050, Nabertherm GmbH, Lilienthal, Germany). The dry masses (DM) were determined (PG503-S, Mettler Toledo GmbH, Gießen, Germany) and the root mass fractions (RMF) were calculated, defined as dry mass of nodulated roots (DM_{Roots}) relative to the total dry mass (DM_{Total}) of the plant from shoot and root organs (Eq. 1).

$$RMF\ \ (g\ \ g^{-1}) = \frac{DM_{Root}\ \ (g)}{DM_{Total}(g)} \quad \text{(Eq. 1)}$$

Before washing the roots, 250 g of homogenized substrate were sampled, dried at 30°C to constant weight and used for pH measurements (Supplementary Material S5).

Chemical biomass analyses

Shoot and root material was ground (MM 400, Retsch GmbH, Haan, Germany) separately in experiment 1, and collectively in experiment 2. Phosphorus and K were analyzed as follows: 50 g of dry biomass were digested in a microwave (Mars 5, Prg. Pflanzen160 X-Press, Kamp-Lintfort, Germany) with 2 mL of HNO_3 and 1 mL of H_2O_2 for 35 min. including heating and residence time in triplicate. The samples were then diluted with ultra-pure water (Milli-Q Reference, Merck, Darmstadt, Germany) to a total volume of 14 mL. Before measurement by inductively coupled plasma atomic emission spectroscopy (iCAP 6500, Fisher Scientific, Schwerte, Germany), subsamples were diluted to a ratio of 1:20. The subsamples were measured for P in both experiments and additionally for K in experiment 1, which focused on the fertilization effect of cB ash as a PK fertilizer rather than only on plant P availability from the ashes as in experiment 2. Phosphorus and K uptakes were calculated as described by Herzel et al. (2020), i.e., as the differences in total P and K in total dry matter of soybeans after 44 d (see Experiment 1: Soybean response to increasing doses of cB ash) and 42 d (see Experiment 2: Effect of thermal co-processing bagasse pellets with nutrient rich residues on P-availability to soybeans) of growth in fertilized substrates (referred to as final harvest) and before fertilization beginning (see Plant trials under greenhouse conditions), i.e., first harvest (Eq. 2 and Eq. 3).

$$\Delta P_{Uptake}\ (mmol) = P_{final\ harvest}\ (mmol) - P_{first\ harvest}\ (mmol) \qquad \text{(Eq. 2)}$$

$$\Delta K_{Uptake}\ (mmol) = K_{final\ harvest}\ (mmol) - K_{first\ harvest}\ (mmol) \qquad \text{(Eq. 3)}$$

To evaluate the potential substitution of commercial P and K from TSP and K_2SO_4 by cB ash, the relative agronomic effectiveness (RAE) of P and K from cB ash was calculated according to Bogdan et al. (2021). RAE is based on the uptakes of P and K from cB ash (P_{cB}), TSP (P_{TSP}), K_2SO_4 (K_{K2SO4}) and unfertilized substrate (P_0, K_0) following the Eq. 4 and Eq. 5.

$$RAE\ (\%\ P\ from\ TSP) = \frac{P_{cB}\ (mmol) - P_0\ (mmol)}{P_{TSP}\ (mmol) - P_0\ (mmol)} \times 100 \qquad \text{(Eq. 4)}$$

$$RAE\ (\%\ K\ from\ K_2SO_4) = \frac{K_{cB}\ (mmol) - K_0\ (mmol)}{P_{K2SO4}\ (mmol) - K_0\ (mmol)} \times 100 \qquad \text{(Eq. 5)}$$

Statistics

Randomization of pots and statistical analyses were performed with RStudio, version 1.2.1355 (2019), using the package "agricolae" (Mendiburu, 2022). Data were calculated as arithmetic means ± standard error of the means of the biological replicates and visualized using the R package "ggplot2" (Wickham, 2016) and "ggpattern" (Langlais et al., 2020). Data were subjected to Levene tests for normality using the R package "heplots" (Fox et al., 2021) before a one-way analysis of variance (ANOVA) was performed. Replicate means were compared by Tukey's honest significance test. Pearson correlations were performed using the R package "corrplot" (Wei et al., 2017). The R package "FactoMineR" (Husson et al., 2022) with the function "factoextra" (Kassambara and Mundt, 2020) was used to perform the principal component analyses and to visualize the results. The data set for principal component analyses included P extractable with H_2O, NH_4Cl, NaOH and HCl, as well as the mass fractions of K, Na, Ca, Mg, Fe and Al (Supplementary Material S6), because these elements may form phosphates in the ash and affect P extractability.

Results and discussion

Ash characterizations

Elementary compositions of bagasse-based ashes

Bagasse-based ashes were analyzed for mass fractions of N, P and K, which are the most important for plant nutrition, as well as for Ca, Mg, Na, Al and Fe, which influence the availability of P from ashes to plants. All ashes contained low mass fractions of N, which is due to N emission during thermal processing of the biomass (Mayer et al., 2022). cB and gB ashes contained similar P and K but different C mass fractions, which is due to different fuel to air ratios during thermal biomass processing. Other elements in cB and gB ashes likely differed due to soil contamination in the cB ash as it was sampled from the landfill. The chemical compositions of bagasse-based ashes were strongly modified by thermal co-processing (co-gasification and co-combustion) of bagasse pellets with the additional feedstocks of chicken manure or sewage sludge (see 2.1). In regard to P, the mass fractions increased from 0.4 wt% in ash from gasification of bagasse pellets alone (gB), to 1.7 and 2.0 wt% in gBM and cBM ashes (co-gasified and co-combusted bagasse pellets with chicken manure pellets), to 3.0 wt% in cBS ash (co-combusted bagasse pellets with sewage sludge; Table 1). Thus, thermal co-processing of bagasse pellets with nutrient rich chicken manure pellets or sewage sludge increased the P mass fraction in bagasse-based ashes to values also described for low grade phosphate rock (Zapata and Roy, 2004). According to

European regulations (EU, 2019), gBM and cBM ashes can thus be classified as PK fertilizers since they contained more than 1.3 wt% P and 1.6 wt% K, while cBS ash could be classified as P fertilizer because of the low K content of 0.64 wt% (Table 1).

The extractability of P from ashes is highly affected by elemental composition and P forms (Luyckx et al., 2021). Calcium, Mg, Na, K, Fe and Al are of great importance for phosphate formation and its solubility in various extraction solutions (Kratz et al., 2019). Combining 20 wt% chicken manure pellets with 60 wt% bagasse pellets (gBM and cBM ashes), increased the mass fractions of P, K, Ca, Mg and Na in gBM and cBM ashes up to 5.0, 3.0, 9.2, 1.8 and 6.0 fold, respectively. In contrast, the mass fractions of Fe and Al decreased as much as 2.3 and 2.6 fold, compared to pure gB ash (Table 1). When bagasse pellets were co-combusted with sewage sludge, the mass fractions of P, Ca, Mg and Na in cBS ash increased 7.4, 4.0, 1.2 and 2.8 fold, while K mass fraction decreased 1.6 fold compared to gB ash. In contrast to chicken manure as additional feedstock, Fe was not reduced and Al even increased following the addition of sewage sludge (Table 1).

Phosphorus extractability from bagasse-based ashes

To distinguish between extractable P forms, we conducted a sequential P extraction with water, 1 M NH_4Cl at pH 7, 0.1 M NaOH and 0.5 M HCl. The pH dependence of the extraction is thought to represent water dissolvable P, labile P, Fe-/Al-bound P and Ca-/Mg-bound P fractions (Qian et al., 2009; Brod et al., 2015). The total P content extracted by this procedure was 75% from gBM ash and cBM ash, 68% from cBS ash and 56% from cB and gB ashes (Figure 1A). The extractability of P from all bagasse-based ashes with 0.5 HCl was higher than all other extraction solutions (Figure 1A). This is consistent with previous studies reporting that P soluble in HCl is the major P fraction in various ashes (Brod et al., 2015; Lemming et al., 2020). Luyckx et al. (2021) explained this by the presence of Ca-phosphates (e.g. apatite and whitlockite), which dissolve in acidic solutions.

Only low amounts of P were soluble in 0.1 M NaOH. The highest solubility was found in cBS ash with around 7% of total P (Figure 1A). The different P solubility in 0.1 M NaOH was probably due to different Fe and Al mass fractions in the ashes (Table 1; Qian et al., 2009). The overall lowest P extractability was achieved with 1 M NH_4Cl at pH 7 ($\leq$ 3% of total P) and with H_2O (<1% of total P; Figure 1A).

P extractability in 2% citric acid is commonly considered to predict P availability from a fertilizer for a plant (Bergfeldt et al., 2018; Herzel et al., 2020). In this study, P was extracted with 2% citric acid, yielding similar values for gBM ash (96.8%) as for TSP (98.0%), while cBM ash (85%), gB ash (78%) and cB ash (49%) contained less extractable P (% of P from total P; Figure 1B). This extractability of P was higher than in 0.5 M HCl, probably due to complexing agents in citric acid (Herzel et al., 2020; Luyckx et al., 2021). The lowest amount of P extracted with 2% citric acid was measured in cBS ash (30%; Figure 1B). Contrary to gB, gBM and cBM ashes, the extractability of P in citric acid from cBS ash was half of that seen in 0.5 M HCl, indicating the presence of different P forms in cBS ash than in other bagasse-based ashes, as well as the necessity of harsh acidic conditions for P solubilization from cBS ash.

Principal component and correlation analyses

To understand P extractability in bagasse-based ashes, principal component analyses (PCA) were performed for P soluble in water, 1 M NH_4Cl at pH 7, 0.1 M NaOH and 0.5 M HCl, and the mass fractions of Ca, Mg, Fe, Al, K and Na, which can form phosphates in the ash. The first two principal components, named dimension 1 (Dim1) and dimension 2 (Dim2), together explain 94.90% (Dim1: 83.4% and Dim2 11.5%) of the total variance (Figure 2). Interestingly, Na, K,

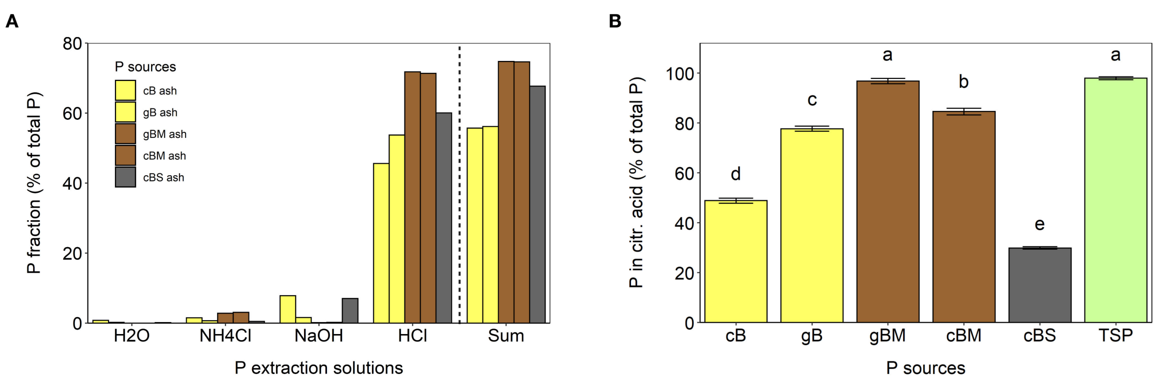

FIGURE 1
Phosphorus extractability from cB, gB, gBM, cBM and cBS ashes in various solutions. **(A)** Sequential P extractability in water, 1 M NH_4Cl at pH 7, 0.1 M NaOH and in 0.5 M HCl. **(B)** Phosphorus extractability with 2% citric acid. The error bars represent standard errors of the means. Different letters indicate statistical differences between P extractabilities (Tukey's HSD test, $p \leq 0.05$, n = 3).

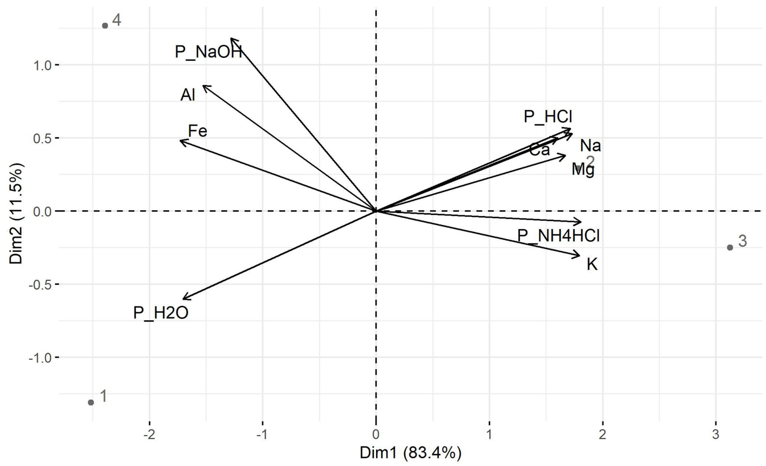

FIGURE 2
Biplot of component 1 (Dim1) and 2 (Dim2) of the Principle Component Analyses (PCA) for P soluble in water (P_{H2O}), 1 M NH_4Cl at pH 7 (P_{NH4Cl}), 0.1 M NaOH (P_{NaOH}), and 0.5 M HCl (P_{HCl}), mass fractions of potassium (K), sodium (Na), calcium (Ca), magnesium (Mg), iron (Fe) and aluminum (Al) with gB (1), gBM (2), cBM (3) and cBS (4) ashes as sub-data set.

Mg, Ca, P_{HCl} and P_{NH4Cl} formed a group with gBM and cBM ashes, while Fe, Al, P_{NaOH} and P_{H2O} formed a group with cBS and gB ashes (Figure 2). This indicated a close relationship between the pH of the solutions for P extraction and the mass fractions of Na, K, Mg, Ca, Fe and Al in the ashes.

Further analyses revealed that P soluble in HCl positively correlated with total Mg ($R^2 = 0.96$, $p \leq 0.01$), Ca ($R^2 = 0.86$, $p< 0.10$) and Na ($R^2 = 0.82$, $p< 0.10$) mass fractions (Table 2A) suggesting the presence of Mg-/Ca-phosphates and/or Mg-/Ca-Na phosphates in bagasse-based ashes. The positive correlation of K ($R^2 = 0.97$, $p \leq 0.01$), Na ($R^2 = 0.90$, $p \leq 0.05$) and Mg ($R^2 = 0.81$, $p \leq 0.10$) mass fractions with P soluble in 1 M NH_4Cl hints at the presence of Mg-alkali phosphates in the ashes (Table 2A). Calcium- and Mg-alkali phosphates likely occurred in cBM and gBM ashes due to higher mass fractions of K and Na in the ashes compared to gB and cBS ashes (Table 1). High mass fractions of Fe (3.86 wt%) and Al (4.18 wt%; Table 1), as well as strong positive correlations with Fe ($R^2 = 0.89$, $p< 0.05$) and Al mass fractions ($R^2 = 0.83$, $p< 0.1$) with P soluble in 0.1 M NaOH (Table 2A) suggest the presence of Fe- and Al-phosphates in cBS ash.

Crystalline P phases in bagasse-based ashes

Phosphorus phases were analyzed by X-ray diffraction (XRD) to understand P extractability from bagasse-based ashes. The crystalline P phases detected by XRD in any of the ashes contained predominantly orthophosphate and only small amounts of pyrophosphate (Table 3, Supplementary Material S7). This is in line with ^{31}P nuclear magnetic resonance (NMR) analyses conducted in our study (Supplementary Material S8) and in a previous study by Herzel et al. (2020). The combination of ^{31}P NMR analyses with sequential extraction revealed further

TABLE 2 Pearson's correlation between sequentially extracted P with distilled deionized water (P_{H2O}), 1 M NH_4Cl at pH 7 (P_{NH4Cl}), 0.1 M NaOH (P_{NaOH}), and 0.5 M HCl (P_{HCl}) from gB, gBM, cBM and cBS ashes with total mass fractions of potassium (K), sodium (Na), calcium (Ca), magnesium (Mg), iron (Fe) and aluminum (Al) in the ashes (A), and with phosphorus (P) uptake from the ashes (B).

Variables		(A) K	Na	Ca	Mg	Fe	Al	(B) P uptake
P_{H2O}	p-value	0.42	0.39	0.22	0.12	0.04	0.34	0.05
	correlation	-0.48	-0.50	-0.67	-0.78	0.89	0.55	-0.82
P_{NH4Cl}	p-value	<0.01	0.03	0.14	0.10	0.24	0.12	0.62
	correlation	0.97	0.90	0.76	0.81	-0.64	-0.78	0.26
P_{NaOH}	p-value	0.15	0.40	0.35	0.14	0.04	0.08	0.18
	correlation	-0.74	-0.49	-0.53	-0.76	0.89	0.83	-0.63
P_{HCl}	p-value	0.14	0.09	0.06	<0.01	0.03	0.21	0.03
	correlation	0.76	0.82	0.86	0.96	-0.91	-0.68	0.86

TABLE 3 Overview of crystalline P phases in gB, gBM, cBM and cBS ashes based on Supplementary Material S7.

P phases	gB ash	gBM ash	cBM ash	cBS ash
$AlPO_4$				X
Whitlockite ≈ $Ca_9M(PO_4)_7$	X	XX	X	XX
$CaK_2P_2O_7$	X	X	X	X
Two undefined P phases		X	X	
$Ca(Na,K)PO_4$			XX	

Number of "X" indicates the amount of semi-quantified P phases. The placeholder "M" in whitlockite is commonly Ca, Fe, and/or Mg (Herzel et al., 2020). Two undefined P phases were extractable in formic and/or citric acids. All crystalline P phases were soluble in 0.5 M HCl solution, while $AlPO_4$ was also soluble in 0.1 M NaOH.

undefined P species in the fertilizers that were not extractable with the standard extraction solution of 0.25 M NaOH and 50 mM Na_2EDTA for ^{31}P NMR analyses (Supplementary Material S8).

The P phase formation depends on the chemical elements present in the biomass before thermal processing as previously reported by Hannl et al. (2022) in sewage sludge-based ashes. In the cBS ash, high mass fractions of Fe and Al from sewage sludge (Supplementary Material S1) facilitated the formation of $AlPO_4$, which was soluble in 0.1 M NaOH and 0.5 M HCl. High mass fractions of alkali and earth alkali metals from chicken manure favored the formation of $Ca(Na,K)PO_4$ in cBM ash, and two, as yet undefined, P phases in both cBM and gBM ashes (Table 3, Supplementary Material S7). We assume that the formation of Ca-alkali phosphates in bagasse-based ashes was due to the principle of thermochemical post-treatment of ashes. In this process, ashes and alkaline additives such as Na_2SO_4 or K_2SO_4 are combusted at 1000°C for 30 min. to form Ca-alkali phosphates (Steckenmesser et al., 2017; Herzel et al., 2020). The formation of different P phases in cBM and gBP ashes may have been due to the different thermal processing environments, as illustrated by Bergfeldt et al. (2018) in ash and biochar after combustion and pyrolysis of chicken manure. All bagasse-based ashes from small-scale processing contained $CaK_2P_2O_7$ and whitlockite ($Ca_9M(PO4)_7$), which most commonly contain Ca, K, Fe, and/or Mg at the placeholder "M"; (Herzel et al., 2020). In an earlier study, Hannl et al. (2022) detected K-whitlockite in alkali-rich ash and (Mg, Fe)-whitlockite and $AlPO_4$ in Fe-and Al-rich ash. In cB ash, amorphous phases masked potential P phases (Supplementary Material S7).

According to earlier studies, the extractability and/or plant availability of P from $AlPO_4$ and Ca-based phosphates is as follows: $Ca(Na,K)PO_4 > CaK_2P_2O_7 > Ca_9M(PO4)_7 > AlPO_4$ (Vogel and Adam, 2011; Kratz et al., 2019; Herzel et al., 2020). Further analyses of the undefined P phases and detailed elucidation of whitlockite structure in bagasse-based ashes will help to identify the factors behind the fertilizers´ efficiency. Consequently, variation of crystalline P phases might enable prediction of plant P availability from bagasse-based ashes. Based on P extractability in 2% citric acid and XRD analyses, we predict that the fertilizer effectiveness of bagasse-based ashes for soybeans will be as follows: cBM ≥ gBM > gB > cBS > cB.

Ash fertilization effects under greenhouse conditions

Effects of industrially produced bagasse ash as fertilizer

In experiment 1, bagasse ash (cB ash) from a sugarcane factory in Goiás, Brazil, was investigated as a fertilizer for soybeans. Compared to the non-fertilized control plants, substrate fertility was significantly increased by the addition of the ash. The measurements showing the fertilization effects included soybean shoot size, projected leaf area, dry biomass accumulation, biomass allocation to the roots, and uptakes of P and K (Figure 3). In general, shoot size, leaf area, biomass, and nutrient uptake increase as nutrient availability increases, while the biomass allocation to the roots decreases as plants need to forage less for nutrients in the soil (Poorter et al., 2012; Herzel et al., 2020). The positive fertilization effect of cB ash on the employed soybean is in line with earlier studies reported for various other crops, such as wheat (Gonfa et al., 2018), bean, and Chinese kale (Webber III et al., 2017).

Despite the positive fertilization effects of cB ash described above, it was less effective as fertilizer for soybeans, although 7.9 g cB ash kg^{-1} substrate provided the same dose of P as in the positive control treatment using triple-superphosphate (TSP). When compared to plants provided TSP, those receiving cB ash displayed significantly slower shoot growth 16 d after the beginning of the treatment, lower total plant dry mass, and a larger root mass fraction as well as lower P and K uptakes after harvesting the plants (Figures 3A–F). We assume that the fertilization effects of cB ash depended on plant P rather than K availability and N_2 fixation, because K extractability in 2% citric acid was higher than that of P (Table 1), and the number of root nodules and mass fractions of N in roots did not significantly differ across treatments (Supplementary Material S9). The relative agronomic efficiency of P from cB ash, which presents the fertilizer effectiveness relative to referenced fertilizer (TSP in the present study), was only 22% of that of TSP (Figure 3E). The low efficiency is in line with P extractability in 2% citric acid (Figure 3B). In a study by Bogdan et al. (2021), P uptake from ashes produced by combustion of two different sewage sludges was shown to increase the relative agronomic P efficiency during seven months of ryegrass (*Lolium perenne*)

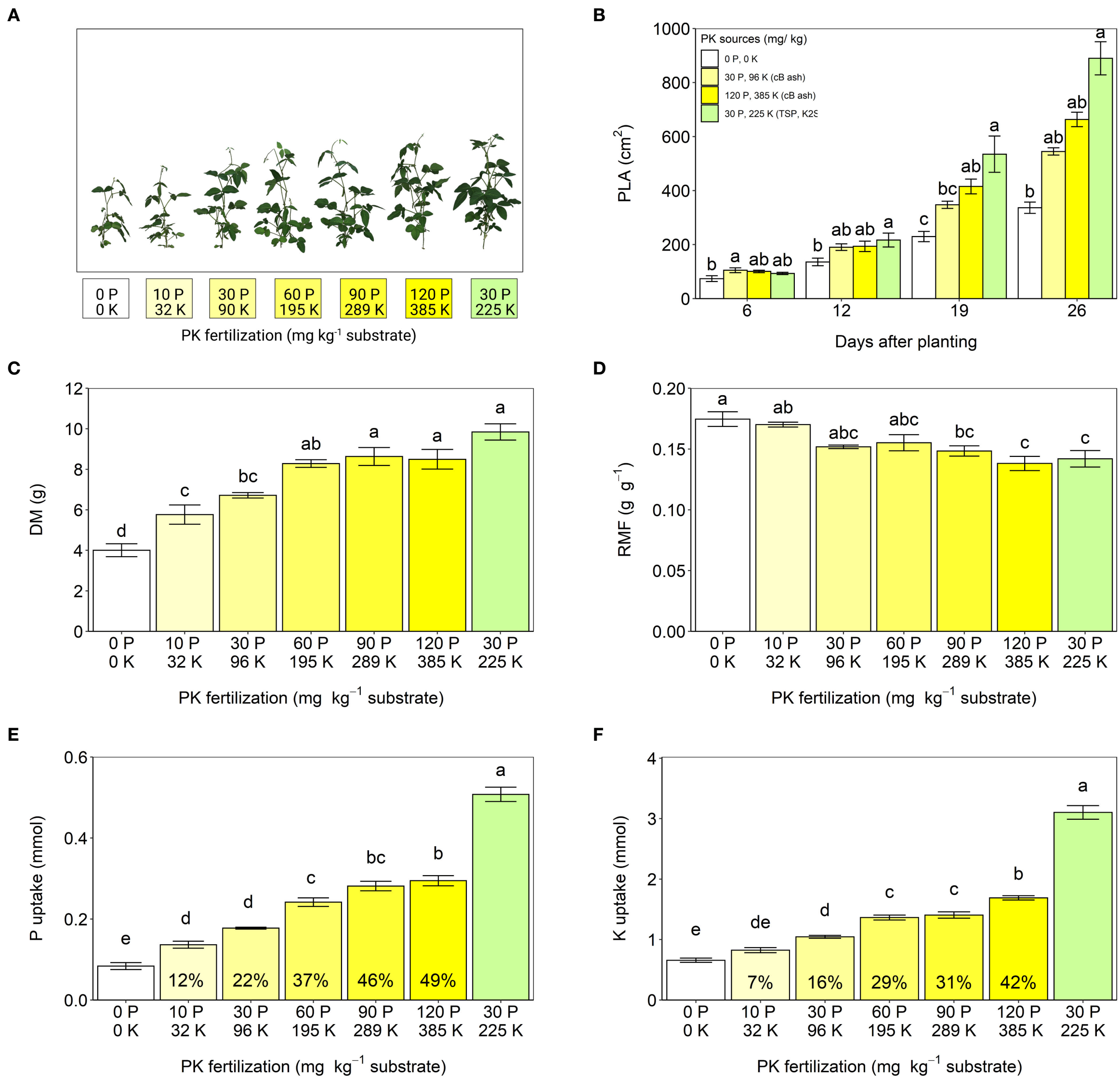

FIGURE 3
Effects of increasing cB ash doses on soybean growth (experiment 1). **(A)** Shoot phenotypes, **(B)** projected leaf areas (PLA), **(C)** total plant dry mass (DM) from shoot and root organs, **(D)** root mass fractions (RMF), **(E)** uptake of phosphorus (P) and **(F)** uptake of potassium (K) during 44 d growth. All values are given per plant. Phosphorus and potassium were provided by cB ash (yellow bars and labels) and triple-superphosphate (TSP) and K_2SO_4 (green bars and labels). The values within the bars **(E, F)** represent relative agronomic effectiveness compared to P and K from TSP and K_2SO_4. The error bars represent standard errors of the means. Identical letters indicate no statistical differences between the fertilizer treatments (Tukey's HSD test, $p \le 0.05$, n = 5).

growth. A long-term experiment with a perennial plant that can be harvested above ground in regular intervals, could aid in better understanding P uptake dynamics from bagasse ash and thus offer insight into the use of bagasse ash as a slow-release P fertilizer.

Increasing doses of cB ash enhanced fertilizer efficacy. Fertilization with 90 mg P/289 mg K kg^{-1} and 120 mg P/385 mg K kg^{-1} from cB ash even produced biomass yields comparable to TSP fertilization (Figure 3C), although P uptake again remained significantly lower than with TSP (Figure 3E). The use of large quantities of ash has been suggested to result in nutrient imbalances in the substrate that do not conform to crop requirements (Müller-Stöver et al., 2018). A detailed study on nutrient content in plants fertilized with increasing amounts of ash would clarify whether large cB ash doses can cause nutrient imbalances in the substrate that hinder P uptake by plants.

The pure bagasse ash tested here was not able to compete with TSP and K_2SO_4 for fertilizer efficiency. Future studies should investigate the effects of different local combustion conditions, times, and storage conditions on the composition, as well as the P availability from bagasse ashes to crops. This would allow better insight into how the ash could be effectively used in agriculture and industry, rather than being disposed of in landfills.

Effect of thermal co-processing bagasse pellets with nutrient rich residues on P-availability to soybeans

In the following, bagasse pellets were gasified (λ = 0.4) alone (gB) and in combination with chicken manure (gBM) as well as co-combusted (λ = 2.2) with chicken manure (cBM) or sewage sludge (cBS) to obtain different ashes for testing as fertilizer for soybeans under greenhouse conditions. Plant P availability from bagasse-based ashes varied and depended on the biomass used for ash production, which is in line with previous studies (Schiemenz and Eichler-Löbermann, 2010; Müller-Stöver et al., 2018).

The effects of pH and/or availability of other plant nutrients on plant P availability from ashes, as suggested by Schiemenz and Eichler-Löbermann (2010), were negligible in this study. The pH values in the selected substrate did not statistically differ, regardless of fertilizer treatment (Supplementary Material S2, S4), and N and K were not limiting due to the additional supply (see 2.3.2). Compared to gB and cBS ashes, soybeans receiving P from gBM and cBM ashes accumulated significantly more total dry biomass and took up more P (Figures 4A–D), indicating better plant P availability (Herzel et al., 2020). This was probably due to more Ca-/Mg-phosphates in the ashes, since P uptake is positively correlated with P soluble in 0.5 M HCl (R^2 = 0.86, p< 0.05; Table 2B). Lemming et al. (2020) assumed that Ca-phosphates determine the overall level of plant P availability. Although amounts of plant dry biomass and P uptake from ashes showed evidence of different plant P availabilities, biomass allocation to the roots, which also indicates plant P availability (Poorter et al., 2012; Herzel et al., 2020), was not statistically different (Figure 4C). We recommend 1) further studies in arable soil to investigate plant P availability from bagasse-based ashes under field conditions and 2) the use of other crops that respond differently to ash, as shown by Schiemenz and Eichler-Löbermann (2010). Previously, Ferreira et al. (2012) reported that P extractability in Mehlich I solution from Brazilian arable soil (classified as Ferralsol) increased after fertilization with a residual ash from the co-combustion of bagasse with bovine residues.

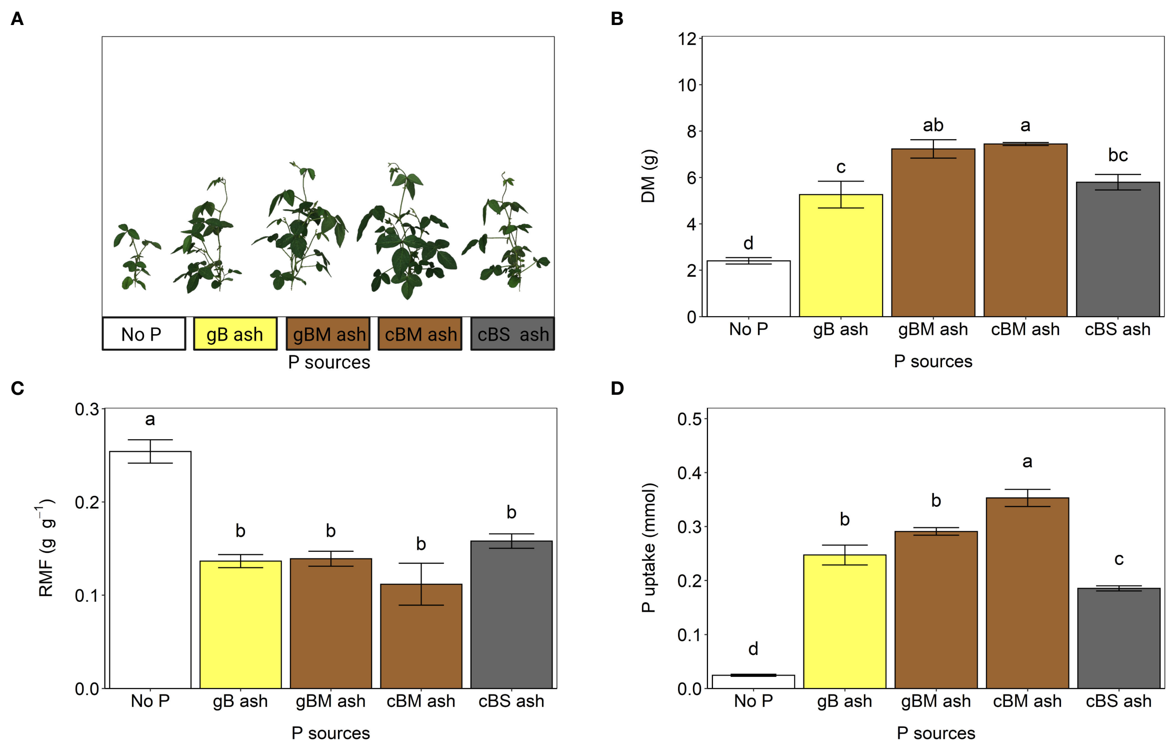

FIGURE 4
Fertilization effects of gB, gBM, cBM and cBS ashes on soybean (experiment 2). **(A)** Shoot phenotypes, **(B)** total plant dry mass (DM), **(C)** root mass fractions (RMF), and **(D)** uptakes of phosphorus (P) from the ashes. All values are given per plant. The error bars indicate standard errors of the means. Identical letters indicate no statistical differences between the fertilizer treatments (Tukey's HSD test, p ≤ 0.05, n = 5).

Extraction of P from bagasse-based ashes with 2% citric acid provided a reasonable estimate for plant P availability, as indicated by plant growth analyses (Figure 1B, Figure 4). However, it tended to underestimate or overestimate P availability depending on the P phases in the ash. Phosphorus extraction in 2% citric acid predicted the lowest available P in cBS ash, which is in line with the results described above. The same extraction procedure also indicated that gBM ash should contain significantly more plant available P than cBM ash (Figure 1), which was not observed in the pot experiment using soybeans. Here, more P was taken up following cBM ash fertilization than with gBM ash (Figure 4C). The better plant P availability from cBM ash was probably due to the $Ca(Na,K)PO_4$ phase in cBM ash, as it is more plant available than whitlockite (Herzel et al., 2020), which dominated in gBM ash (Table 3, Supplementary Material S7). Thus, both extraction of P in 2% citric acid and mineralogical P phase analyses are good estimates of plant P availability, although the mineralogical analyses provide a better prediction than P extractability in 2% citric acid.

The question arises whether co-processing of the low-P containing bagasse with nutrient-rich residues makes sense. Chicken manure is a valuable fertilizer in and of itself. However, the high solubility of P from chicken manure could lead to pollution of surface waters, while its combustion could reduce P solubility in water and while retaining its availability to plants (Codling, 2006; Codling, 2019). Sewage sludge ash contains high amounts of P which would only be diluted by co-processing with bagasse. In this study, these resources were used as they provided contrasting chemical compositions and were instrumental in helping to understand the P mineralogy of the bagasse-based ashes. However, careful selection of locally available residues that are produced in sufficient amounts and are otherwise potentially disposed of (as the bagasse ash itself) is indispensable for showing the benefits of using bagasse ash as a fertilizer. Finally, when such a process is implemented, life cycle analyses and economic assessments need to be conducted to investigate the environmental impacts of producing and using bagasse-based ashes as fertilizers, particularly with respect to their economic and ecological advantage over finite rock-based fertilizers.

Conclusion

Bagasse ash represents a valuable resource that deserves attention in further studies as a potential fertilizer, with the goal of reducing the dependence on rock-based sources in fertilizer production. While the use of pure bagasse ash as a fertilizer for soybeans was limited by the low P mass fraction and plant P availability, thermal co-processing of bagasse with either chicken manure or sewage sludge increased the overall P mass fraction in the ashes to the levels of low-grade phosphate rock. The plant P availability was even shown to increase when bagasse was co-combusted with chicken manure due to the formation of plant available Ca-alkali phosphates. Thus, we recommend co-processing bagasse with alkali-rich residues to increase the P availability from bagasse-based ashes to soybeans.

Data availability statement

The raw data supporting the conclusions of this article will be made available by the authors, without undue reservation.

Author contributions

VD: Conceptualization, Methodology, Validation, Investigation, Writing - Original Draft. HH: Validation, Investigation, Visualization, Writing – Review & Editing. SW: Methodology, Investigation, Visualization, Writing – Review & Editing. WF-Z: Resources, Writing – Review & Editing. JWZ: Resources, Writing – Review & Editing. MM: Resources, Writing – Review & Editing, Project Administration. FM: Resources, Writing – Review & Editing. CA: Funding Acquisition, Writing – Review & Editing. HK: Writing – Review & Editing. HP: Conceptualization, Methodology, Writing – Review & Editing. NDJ: Conceptualization, Methodology, Writing – Review & Editing, Supervision, Project Administration, Funding Acquisition. SDS: Conceptualization, Methodology, Writing – Original Draft, Supervision, Project Administration. All authors contributed to the article and approved the submitted version.

Funding

This work was supported by the German Federal Ministry of Education and Research (BMBF), within the German-Brazilian collaboration project ASHES (grant number 031A288).

Acknowledgments

The data and scientific findings presented in this manuscript have partly been published earlier as part of the doctoral thesis by the corresponding author VD (Dombinov, 2021). The figures were compiled with BioRender.com. We are grateful for the help in plant harvest by Marlene Müller, Edelgard Schölgens and Lucy Harrison. The authors thank the team of Nova Gália sugarcane industry USINOVA in Paraúna (Goiás, Brazil) for providing information about the process, as well as for bagasse and ash samples. The authors also wish to thank Sarah Kenyon for critically reading and editing the manuscript. The authors appreciate critical reading and feedback by the referees.

Conflict of interest

The authors declare that the research was conducted in the absence of any commercial or financial relationships that could be construed as a potential conflict of interest.

Publisher's note

All claims expressed in this article are solely those of the authors and do not necessarily represent those of their affiliated organizations, or those of the publisher, the editors and the reviewers. Any product that may be evaluated in this article, or claim that may be made by its manufacturer, is not guaranteed or endorsed by the publisher.

Supplementary material

The Supplementary Material for this article can be found online at: https://www.frontiersin.org/articles/10.3389/fpls.2022.1041924/full#supplementary-material

References

Bergfeldt, B., Tomasi Morgano, M., Leibold, H., Richter, F., and Stapf, D. (2018). Recovery of phosphorus and other nutrients during pyrolysis of chicken manure. *Agric. (Basel)* 8, 187. doi: 10.3390/agriculture8120187

Bogdan, A., Donell, C. O., Robles Aguilar, A. A., Sigurnjak, I., Power, N., Michels, E., et al. (2021). Impact of time and phosphorus application rate on phosphorus bioavailability and efficiency of secondary fertilizers recovered from municipal wastewater. *Chemosphere* 183, 131017. doi: 10.1016/j.chemosphere.2021.131017

Bordonal, R., Carvalho, J. L. N., Lal, R., Figueiredo, E. B., de, Oliveira, B. G., and de, La Scala, N. (2018). Sustainability of sugarcane production in Brazil. *A review. Agron. Sustain. Dev.* 38, 574. doi: 10.1007/s13593-018-0490-x

Brod, E., Øgaard, A. F., Hansen, E., Wragg, D., Haraldsen, T. K., and Krogstad, T. (2015). Waste products as alternative phosphorus fertilisers part I: Inorganic p species affect fertilisation effects depending on soil pH. *Nutr. Cycl. Agroecosyst.* 103, 167–185. doi: 10.1007/s10705-015-9734-1

Chojnacka, K., Moustakas, K., and Witek-Krowiak, A. (2020). Bio-based fertilizers: A practical approach towards circular economy. *Bioresour. Technol.* 295, 122223. doi: 10.1016/j.biortech.2019.122223

Codling, E. E. (2006). Laboratory characterization of extractable phosphorus in poultry litter and poultry litter ash. *Soil Sci. (Alphen aan den Rijn Niederlande)* 171, 858–864. doi: 10.1097/01.ss.0000228059.38581.97

Codling, E. E. (2019). Effects of phosphorus amended low phosphorus soil on soybean (*Glycine max* l.) and wheat (*Titicum aestivum* l.) yield and phosphorus uptake. *J. Plant Nutr.* 42, 891–899. doi: 10.1080/01904167.2019.1589506

Demeyer, A., Voundi Nkana, J. C., and Verloo, M. G. (2001). Characteristics of wood ash and influence on soil properties and nutrient uptake: An overview. *Biores. Technol.* 77, 287–295. doi: 10.1016/S0960-8524(00)00043-2

Dombinov, V. (2021) *From lab to field - investigations of phosphorus availability from sugarcane bagasse ash to soybeans. [dissertation]* (Universitäts- und Landesbibliothek Bonn) (Accessed September 08, 2022).

EU (2016) *Paris Agreement - UN framework convention on climate change - EUR-lex*. Available at: https://eur-lex.europa.eu/content/paris-agreement/paris-agreement.html (Accessed September 07, 2022).

EU (2019) *Regulation (EU) 2019/1009 of the European parliament and of the council of 5 June 2019 laying down rules on the making available on the market of EU fertilising products and amending regulations (EC) no 1069/2009 and (EC) no 1107/2009 and repealing regulation (EC) no 2003/2003. 1-114. L170/1* (Brussels, Belgium: EU). Available at: https://eur-lex.europa.eu/legal-content/EN/TXT/?uri=celex%3A32019R1009 (Accessed September 07, 2022). O.J.o.t.E.U., Ed.

FAOSTAT (2022) *FAOSTAT*. Available at: http://www.fao.org/faostat/en/#compare (Accessed September 07, 2022).

Ferreira, E., Fageriae, N. K., and Didonet, A. D. (2012). Chemical properties of an oxisol under organic management as influenced by application of sugarcane bagasse ash. *Ciênc. Agron.* 43, 228–236. doi: 10.1590/S1806-66902012000200004

Fox, J., Friendly, M., and Monette, G. (2021) *{heplots}: Visualizing tests in multivariate linear models. r package version 1.3-8*. Available at: https://CRAN.R-project.org/package=heplots (Accessed September 08, 2022).

Gonfa, A., Bedadi, B., and Argaw, A. (2018). Effect of bagasse ash and filter cake amendments on wheat (*Triticum turgidum* l.var. *durum*) yield and yield components in nitisol. *Int. J. Recycl. Org. Waste. Agricult.* 7, 231–240. doi: 10.1007/s40093-018-0209-7

Hannl, T. K., Häggström, G., Hedayati, A., Skoglund, N., Kuba, M., and Öhman, M. (2022). Ash transformation during single-pellet gasification of sewage sludge and mixtures with agricultural residues with a focus on phosphorus. *Fuel Process. Technol.* 227, 107102. doi: 10.1016/j.fuproc.2021.107102

Herzel, H., Dombinov, V., Vogel, C., Willbold, S., Levandowski, G. V., Meiller, M., et al. (2020). Soybean fertilized by p-phases from bagasse-based materials: P-extraction procedures, diffusive gradients in thin films (DGT), and X-ray diffraction analysis (XRD). *Agron. (Basel)* 10, 895. doi: 10.3390/agronomy10060895

Hieltjes, A. H. M., and Lijklema, L. (1980). Fractionation of inorganic phosphates in calcareous sediments. *J. Environ. Qual.* 9, 405–407. doi: 10.2134/jeq1980.00472425000900030015x

Husson, F., Josse, J., Le, S., and Mazet, J. (2022)FactoMineR: Multivariate exploratory data analysis and data mining. In: *Comprehensive r archive network (CRAN)*. Available at: https://cran.r-project.org/web/packages/FactoMineR/index.html (Accessed September 07, 2022).

Kassambara, A., and Mundt, F. (2020) *Extract and visualize the results of multivariate data analyses [R package factoextra version 1.0.7]*. Available at: https://cran.r-project.org/web/packages/factoextra/index.html (Accessed September 07, 2022).

Kratz, S., Vogel, C., and Adam, C. (2019). Agronomic performance of p recycling fertilizers and methods to predict it: A review. *Nutr. Cycl Agroecosyst.* 115, 1–39. doi: 10.1007/s10705-019-10010-7

Langlais, B., Klanderman, M., Noble, B., and Dueck, A. (2020) *ProAE: Tools for PRO-CTCAE scoring, analysis, and graphical display*. Available at: https://CRAN.R-project.org/ (Accessed September 07, 2022).

Lemming, C., Simmelsgaard Nielsen, M. T., Jensen, L. S., Schetz, C., and Magid, J. (2020). Phosphorus availability of sewage sludges and ashes in soils of contrasting pH. *J. Plant Nutr. Soil Sci.* 183, 682–694. doi: 10.1002/jpln.201900323

Li, X., Rubæk, G. H., and Sørensen, P. (2016). High plant availability of phosphorus and low availability of cadmium in four biomass combustion ashes. *Sci. Total Environ.* 557-558, 851–860. doi: 10.1016/j.scitotenv.2016.03.077

Li, X., Rubæk, G. H., and Sørensen, P. (2017). Availability of potassium in biomass combustion ashes and gasification biochars after application to soils with variable pH and clay content. *Arch. Agron. Soil Sci.* 64, 1119–1130. doi: 10.1080/03650340.2017.1414198

Luyckx, L., Sousa Correia, D. S., and van Caneghem, J. (2021). Linking phosphorus extraction from different types of biomass incineration ash to ash mineralogy, ash composition and chemical characteristics of various types of extraction liquids. *Waste Biomass Valorization* 12, 5235–5248. doi: 10.1007/s12649-021-01368-3

Mayer, E., Eichermüller, J., Endriss, F., Baumgarten, B., Kirchhof, R., Tejada, J., et al. (2022). Utilization and recycling of wood ashes from industrial heat and power plants regarding fertilizer use. *Waste Manag.* 141, 92–103. doi: 10.1016/j.wasman.2022.01.027

Mendes, I. C., Hungria, M., and Vargas, M. A. T. (2003). Soybean response to starter nitrogen and *Bradyrhizobium* inoculation on a cerrado oxisol under no-tillage and conventional tillage systems. *Rev. Bras. Ciênc. Solo* 27, 81–87. doi: 10.1590/S0100-06832003000100009

Mendiara, T., Gayán, P., García-Labiano, F. , de Diego, L. F., Pérez-Astray, A., Izquierdo, M. T., et al. (2017). Chemical looping combustion of biomass: An approach to BECCS. *Energy Proc.* 114, 6021–6029. doi: 10.1016/j.egypro.2017.03.1737

Mendiburu, F. (2022)Agricolae: Statistical procedures for agricultural research. Available at: https://cran.r-project.org/web/packages/agricolae/index.html (Accessed September 07, 2022).

Müller-Stöver, D. S., Jakobsen, I., Grønlund, M., Rolsted, M. M. M., Magid, J., Hauggaard-Nielsen, H., et al. (2018). Phosphorus bioavailability in ash from straw and sewage sludge processed by low-temperature biomass gasification. *Soil Use Manage.* 34, 9–17. doi: 10.1111/sum.12399

Nakhforoosh, A., Bodewein, T., Fiorani, F., and Bodner, G. (2016). Identification of water use strategies at early growth stages in durum wheat from shoot phenotyping and physiological measurements. *Front. Plant Sci.* 7. doi: 10.3389/fpls.2016.01155

Ondrasek, G., Kranjčec, F., Filipović, L., Filipović, V., Bubalo Kovačić, M., Badovinac, I. J., et al. (2021). Biomass bottom ash & dolomite similarly ameliorate an acidic low-nutrient soil, improve phytonutrition and growth, but increase cd accumulation in radish. *Sci. Total Environ.* 753, 141902. doi: 10.1016/j.scitotenv.2020.141902

Patterson, S. J., Acharya, S. N., Thomas, J. E., Bertschi, A. B., and Rothwell, R. L. (2004). Barley biomass and grain yield and canola seed yield response to land application of wood ash. *Agron. J.* 96, 971–977. doi: 10.2134/agronj2004.0971

Pita, V., Vasconcelos, E., Cabral, F., and Ribeiro, H. M. (2012). Effect of ash from sugarcane bagasse and wood co-combustion on corn growth and soil properties. *Arch. Agron. Soil Sci.* 58, 206–212. doi: 10.1080/03650340.2012.698000

Poorter, H., Niklas, K. J., Reich, P. B., Oleksyn, J., Poot, P., and Mommer, L. (2012). Biomass allocation to leaves, stems and roots: Meta-analyses of interspecific variation and environmental control. *New Phytol.* 193, 30–50. doi: 10.1111/j.1469-8137.2011.03952.x

Qian, Y., Miao, S. L., Gu, B., and Li, Y. C. (2009). Effects of burn temperature on ash nutrient forms and availability from cattail (*Typha domingensis*) and sawgrass (*Cladium jamaicense*) in the Florida Everglades. *J. Environ. Qual.* 38, 451–464. doi: 10.2134/jeq2008.0126

Raza, Q.-U.-A., Bashir, M. A., Rehim, A., Sial, M. U., Ali Raza, H. M., Atif, H. M., et al. (2021). Sugarcane industrial byproducts as challenges to environmental safety and their remedies: A review. *Water (Basel)* 13, 3495. doi: 10.3390/w13243495

Schiemenz, K., and Eichler-Löbermann, B. (2010). Biomass ashes and their phosphorus fertilizing effect on different crops. *Nutr. Cycl. Agroecosyst.* 87, 471–482. doi: 10.1007/s10705-010-9353-9

Silva, F. C., Cruz, N. C., Tarelho, L. A. C., and Rodrigues, S. M. (2019). Use of biomass ash-based materials as soil fertilisers: Critical review of the existing regulatory framework. *J. Clean. Prod.* 214, 112–124. doi: 10.1016/j.jclepro.2018.12.268

Steckenmesser, D., Vogel, C., Adam, C., and Steffens, D. (2017). Effect of various types of thermochemical processing of sewage sludges on phosphorus speciation, solubility, and fertilization performance. *Waste Manage.* 62, 194–203. doi: 10.1016/j.wasman.2017.02.019

Tan, Z., and Lagerkvist, A. (2011). Phosphorus recovery from the biomass ash: A review. *Renew. Sustain. Energy Rev.* 15, 3588–3602. doi: 10.1016/j.rser.2011.05.016

Tran, Q. T., Maeda, M., Oshita, K., Takaoka, M., and Saito, K. (2018). Phosphorus and potassium availability from cattle manure ash in relation to their extractability and grass tetany hazard. *Soil Sci. Plant Nutr.* 64, 415–422. doi: 10.1080/00380768.2018.1433958

Vogel, C., and Adam, C. (2011). Heavy metal removal from sewage sludge ash by thermochemical treatment with gaseous hydrochloric acid. *Environ. Sci. Technol.* 45, 7445–7450. doi: 10.1021/es2007319

Watanabe, M. D. B., Morais, E. R., Cardoso, T. F., Chagas, M. F., Junqueira, T. L., Carvalho, D. J., et al. (2020). Process simulation of renewable electricity from sugarcane straw: Techno-economic assessment of retrofit scenarios in Brazil. *J. Clean. Prod.* 254, 120081. doi: 10.1016/j.jclepro.2020.120081

Webber, C. L.III, White, P. M.Jr., Spaunhorst, D. J., and Petrie, E. C. (2017). Impact of sugarcane bagasse ash as an amendment on the physical properties, nutrient content and seedling growth of a certified organic greenhouse growing media. *J. Agric. Sci. (Belihuloya)* 9, 1. doi: 10.5539/jas.v9n7p1

Wei, T., Simko, V., Levy, M., Xie, Y., Jin, Y., and Zemla, J. (2017) *Visualization of a correlation matrix [R package corrplot version 0.84]*. Available at: https://cran.r-project.org/web/packages/corrplot/index.html (Accessed September 07, 2022).

Wickham, H. (2016). *ggplot2: Elegant graphics for data analysis* (Cham: Springer), 221–240. doi: 10.1007/978-3-319-24277-4

Withers, P. J. A., Rodrigues, M., Soltangheisi, A., de Carvalho, T. S., Guilherme, L. R. G., Benites, V., et al. (2018). Transitions to sustainable management of phosphorus in Brazilian agriculture. *Sci. Rep.* 8, 2537. doi: 10.1038/s41598-018-20887-z

Xu, Q., Ji, T., Gao, S.-J., Yang, Z., and Wu, N. (2018). Characteristics and applications of sugar cane bagasse ash waste in cementitious materials. *Mater. (Basel Switzerland)*, 12, 1. doi: 10.3390/ma12010039

Zapata, E., and Roy, R. N. (2004). "Phosphate rocks as raw materials for p-fertilizer manufacturing," in *Use of phosphat rocks for sustainable agriculture* (Rome: Food and Agriculture Organization of the United Nations), 148.

frontiers | Frontiers in Plant Science

TYPE Original Research
PUBLISHED 10 January 2023
DOI 10.3389/fpls.2022.1092610

OPEN ACCESS

EDITED BY
Abdel Rahman Mohmmad Said Al -Tawaha,
Al-Hussein Bin Talal University, Jordan

REVIEWED BY
Yanjie Li,
Research Institute of Subtropical Forestry, Chinese Academy of Forestry, China
Zuolin Xiao,
Chongqing Normal University, China

*CORRESPONDENCE
Zhuyun Yan
yanzhuyun@cdutcm.edu.cn

SPECIALTY SECTION
This article was submitted to Plant Nutrition, a section of the journal Frontiers in Plant Science

RECEIVED 08 November 2022
ACCEPTED 20 December 2023
PUBLISHED 10 January 2023

CITATION
Li W, Wang K, Han G, Wang H, Tan N and Yan Z (2023) Integrated diagnosis and time-series sensitivity evaluation of nutrient deficiencies in medicinal plant (*Ligusticum chuanxiong* Hort.) based on UAV multispectral sensors. *Front. Plant Sci.* 13:1092610. doi: 10.3389/fpls.2022.1092610

Integrated diagnosis and time-series sensitivity evaluation of nutrient deficiencies in medicinal plant (*Ligusticum chuanxiong* Hort.) based on UAV multispectral sensors

Wenbo Li[1], Ke Wang[2], Guiqi Han[1], Hai Wang[1], Ningbo Tan[2] and Zhuyun Yan[1]*

[1]State Key Laboratory of Southwestern Chinese Medicine Resources, Chengdu University of Traditional Chinese Medicine, Chengdu, China, [2]School of Big Data and Artificial Intelligence, Chengdu Technological University, Chengdu, China

Background: Nitrogen(N), phosphorus(P), and potassium(K) are essential elements that are highly deficient during plant growth. Existing diagnostic methods are not suitable for rapid diagnosis of large-scale planting areas. Near-ground remote sensing technology based on unmanned aerial vehicle (UAV) and sensor is often applied to crop growth condition monitoring and agricultural management. It has been proven to be used for monitoring plant N, P, and K content. However, its integrated diagnostic model has been less studied.

Methods: In this study, we collected UAV multispectral images of Ligusticum chuanxiong Hort. in different periods of nutritional stress and constructed recognition models with different heights and algorithms. The optimal model variables were selected, and the effects of different sampling heights and modeling algorithms on the model efficiency under the time span were evaluated. At the same time, we evaluated the timeliness of the model based on leaf element content determination and SPAD. It was also validated in field crop production.

Results: The results showed that the LR algorithm's model had optimal performance at all periods and flight altitudes. The optimal accuracy of N-deficient plants identification reached 100%, P/K-deficient plants reached 92.4%, and normal plants reached 91.7%. The results of UAV multispectral diagnosis, chemical diagnosis, and SPAD value diagnosis were consistent in the diagnosis of N deficiency, and the diagnosis of P and K deficiency was slightly lagging behind that of chemical diagnosis.

Conclusions: This research uses UAV remote sensing technology to establish an efficient, fast, and timely nutritional diagnosis method for L. Chuanxiong, which is applied in production. Meanwhile, the standardized production of medicinal plant resources provides new solutions.

KEYWORDS

nutrient deficiency, symptom identification, unmanned aerial vehicle (UAV), canopy reflectance, medicinal plants, *ligusticum chuanxiong* Hort

1 Introduction

There are 14 essential mineral nutrients in the whole life cycle of plants (de Bang et al., 2021), among which nitrogen(N), phosphorus(P), and potassium(K) are closely related to the yield and quality of cultivated crops and are more likely to be deficient (Sanchez et al., 2020). N is a component of plant proteins, nucleic acids, chlorophyll, and other substances. N deficiency can cause phenotypic symptoms such as stunted growth, yellowing old leaves, small leaves, and reduced branching and flowering (Rahayu et al., 2005). P is an element involved in energy metabolism (ATP, NADPH), nucleic acids, and membrane phospholipid composition (Kamerlin et al., 2013). P deficiency causes a reduction in cell division and elongation, reddish-purple or dark green plant leaves, and stunted plant growth and development (Hughes and Lev-Yadun, 2015). K regulates plant growth in plants by affecting electroneutrality, osmoregulation, anion-cation balance, and biochemical pH status, and K+ reduces the production of reactive oxygen species (ROS) by suppressing the number of electrons used for side reactions with oxygen, such that potassium deficiency can lead to local necrosis of the plant foliage (Pottosin and Shabala, 2016). K deficiency also predisposes the plant to collapse by hindering cell wall development (Anschutz et al., 2014). Identifying and replenishing N, P, and K deficiencies at an early stage of plant deficiency is the key to ensuring proper plant growth. Therefore, N, P, and K are the plant nutrients that need to be monitored as a priority in field production management.

Ligusticum chuanxiong Hort. is one of the commonly used medicinal plants of the Umbelliferae family, which has been cultivated in China for more than 1500 years (Ran et al., 2011). Its roots are widely used in China, Japan, Korea, Singapore, and other Asian regions for treating and preventing cardiovascular and gynecological diseases (Chen et al., 2018). Currently, the cultivation area of L. chuanxiong in the Chengdu Plain of China is more than 6000 hm^2 year-round, with an annual production of 1.8×107~20×107 kg (Peng et al., 2020). However, irrational fertilization exists in the process of large-scale cultivation. This causes a waste of resources (Krasilnikov et al., 2022), environmental pollution and damages the quality of Chuanxiong herbs (Liu, 2009; Chen et al., 2022).On the other hand, due to the specificity of their use, medicinal plants are often subject to strict requirements in terms of growing environment and cultivation management, which requires a large amount of labor. With the urbanization and aging of China's population, labor management costs have increased. Therefore, in the context of large-scale cultivation and rising labor costs, there is an urgent need for efficient and reliable tools to assist medicinal growers in management and decision-making.

In the process of crop planting and production, due to the differences in soil properties and nutrient content, as well as temperature changes, rainfall conditions, etc., the nutrient loss is different (St Luce et al., 2011). Adequate fertilization is an important factor to ensure crop yield and quality (Imran et al., 2021). Therefore, it is necessary to monitor the nutritional status of the key stages of crop growth to take timely remedial measures. At present, the nutritional diagnosis of crops mainly includes sensory empirical, chemical, and spectral. Sensory experience diagnosis is highly subjective. Chemical diagnosis relies on laboratory conditions, and the operation process is cumbersome and time-consuming (Daughtry et al., 2000). The spectral diagnosis method established by using the close correlation between crop nutritional status and its spectral characteristics is fast, non-destructive, and easy to grasp (Balasubramanian et al., 1998; Toth and Jozkow, 2016; Sanchez et al., 2020). Although the existing proximal spectral diagnosis technology identifies more types of element deficiencies with high accuracy (Rustioni et al., 2018; Sanchez et al., 2020), the collection efficiency is low and cannot meet the real-time monitoring of large-scale agricultural fields. And with the development of UAV technology, it is equipped with different sensors such as RGB, Multispectral, Hyperspectral, Thermal Sensor, Light Detection and Ranging (Sun et al., 2022). Appropriate sensors can be selected according to the application (Zhu et al., 2021), thus providing a new solution for crop growth monitoring (Toth and Jozkow, 2016). UAVs are equipped with optical sensors to collect and quantify light attenuation caused by photon scattering, absorption, and transmission caused by the interaction of light with plant canopy tissue. These interrelationships are closely related to the physical and chemical properties of the plant, thus obtaining crop phenotypic parameters to provide an accurate and timely assessment of the crop development status (Homolova et al., 2013), such as the assessment of crop nutrition, disease, pest incidence, weeds, biomass, etc. (Osco et al., 2020; de Castro et al., 2021; Rehman et al., 2022). At present, the acquisition of near-Earth spectral image technology based on UAV has attracted the attention of many scholars due to its high efficiency, real-time and non-destructive characteristics.

The sustainable development of agroecosystems needs to be considered in crop growth detection. Non-destructive, low-cost, and high-efficiency UAV multispectral technology solves the problem. Multispectral cameras have three or more discrete bands. The choice of bands depends on the need for vegetation indices (VI) associated with crop phenotypes, which are more sensitive to vegetation characteristics than a single wavelength. Among them, indices such as Normalized Difference VI (NDVI), Green Normalized Difference VI (GNDVI), Normalized Difference Red-edge Index (NDRE), and soil-adjusted VI (SAVI) are considered to be closely related to the nutritional status of plants (Osco et al., 2020). Rehman et al. (2022) used NDVI and NDRE to establish a prediction model for rice nitrogen and yield in different locations and time spans. Gordillo-Salinas et al. (2021) found that GNDVI and Blue Normalized Difference Vegetation Index (BNDVI) had better prediction effects on the nitrogen content of wheat in different phenological periods. Furlanetto et al. (2021) found that GNDVI, NDVI, Ratio between Infrared and Green (GRVI), Ratio between Green and Infrared (GNIR), Ratio between Red and Infrared (RNIR), and Ratio between Infrared and Red (RVI) can effectively differentiate adequate K supply maize plants under treatment with severe potassium deficiency. Gracia-Romero et al. (2017) found that the NDVI, SAVI, Renormalized difference vegetation index (RDVI), Enhanced vegetation index (EVI) and other indices of corn plants with and without phosphate fertilizer had significant changes. Given this, we believe that UAV multispectral technology has the potential for integrated diagnosis of plant N, P, and K deficiency and can meet the needs of future crop cultivation and production self-energy and intelligence.

This study aimed to verify the possibility of distinguishing N, P and K deficiency in plants using UAV multispectral technology. And we will evaluate the impact of different algorithms and flight altitudes on classification accuracy as well as the timing of the diagnosis compared to other diagnostic methods. We expect that UAV multispectral technology with a suitable algorithm and flight altitude can accurately identify deficient plants and can detect the deficiency symptoms of plants as early as possible.

2 Materials and methods

The method is described in three main stages: a) experimental design and data collection; b) digital image processing and data analysis; c) Chemical analysis of leaf tissue and determination of growth indicators. The specific steps of each phase are organized in a workflow (Figure 1) and detailed below.

2.1 Experimental design and data collection

2.1.1 Study area and experimental design

The field experiment was conducted in the Medicinal Botanical Garden of Chengdu University of Traditional Chinese Medicine (30°69'N, 103°81'E, 524m ASL) located in Chengdu City, Sichuan Province, China, from January 2022 to June 2022 (Figure 2A). The region has a humid subtropical monsoonal climate. The average temperature during the experiment was 13.7°C, and the accumulated rainfall was 316.99 mm. The cultivation medium is made of yellow loam, perlite, and coconut coir in a volume of 5:3:2. The yellow soil was collected from long-term unfertilized plots (pH 6.98, organic matter content of 18.4 g/kg, available nitrogen content of 43.71 mg/kg, available phosphorus content of 19.57 mg/kg, and available potassium content of 51.92 mg/kg). After the soil was air-dried for several days, it was crushed and passed through a 5 mm sieve (Rajkovich et al., 2011). The mixed cultivation medium was packed into polypropylene pots with quartz sand at the bottom, and 2/3 of the pots were buried in the soil and kept at the same height.

The germplasm material was crop rhizomes harvested from Fengdui Village, Dujiangyan City, Sichuan Province. The area is a Geo-Authentic product area of L. chuanxiong. Before planting, remove the aerial parts and fibrous roots according to traditional planting habits. After 3 days of placement, choose rhizomes of even size for planting. Two in each pot are one sample, totaling 196 samples. Hoagland's nutrient solution was watered weekly after planting to ensure normal growth in the early stages (Hoagland and Arnon, 1950). Until April 1, samples were divided into control (CK), N deficient (ND), P deficient (PD), and K deficient (KD) groups. Each processed 48 samples. Every 7 days, 500 ml of the corresponding nutrient solution was poured, CK was poured with Hoagland's nutrient solution, and the stress group was poured with Hoagland's nutrient solution with the relative mineral elements completely removed. The deficient nutrient solution was prepared according to the method of Xu and Mou (2016). Watering the soil with sufficient water to remove the pre-watering Hoagland's solution before starting the treatment. After 30 days of treatment, 24 samples were divided from ND, PD, and KD as nitrogen supplementation group (NS), phosphorus supplementation group (PS), and potassium supplementation group (KS), respectively, and changed to watering with whole Hoagland nutrient solution (Figure 2B).

2.1.2 Remote sensing image acquisition

A total of nine missions were conducted during the experiment in April-May 2022 to capture multispectral images between 11:00 and 13:00 in cloudless and windless weather. The interval between each capture was about 7 days. The drone used is the DJI Phantom 4 Multispectral (DJI, Shenzhen, China), which was equipped with a multispectral lens having six CMOS sensors, including one RGB sensor for visible imaging and five single-band sensors (B: 450 ± 16 nm, G: 560 ± 16 nm, R: 650 ± 16 nm, RE: 730 ± 16 nm, NIR: 850 ± 26 nm). Missions were uploaded to the drone *via* DJI GS Pro. Above ground level (AGL) was set to 5 and 10 meters. Under this AGL, the drone did not affect the crop canopy, and the orthoimage stitching was normal. The ground sampling distance (GSD) was 0.265 cm/pixel (5m AGL) and 0.529 cm/pixel (10m AGL). The camera was connected to the drone with a gimbal, and shooting angle was 90° from the ground. The for-ward overlap rate was 80%, and the side overlap rate was 75%. Image geographic coordinates determined by Real Time Kinematic (RTK) GPS with an error of less than 1 cm in the horizontal direction and less than 1.5 cm in

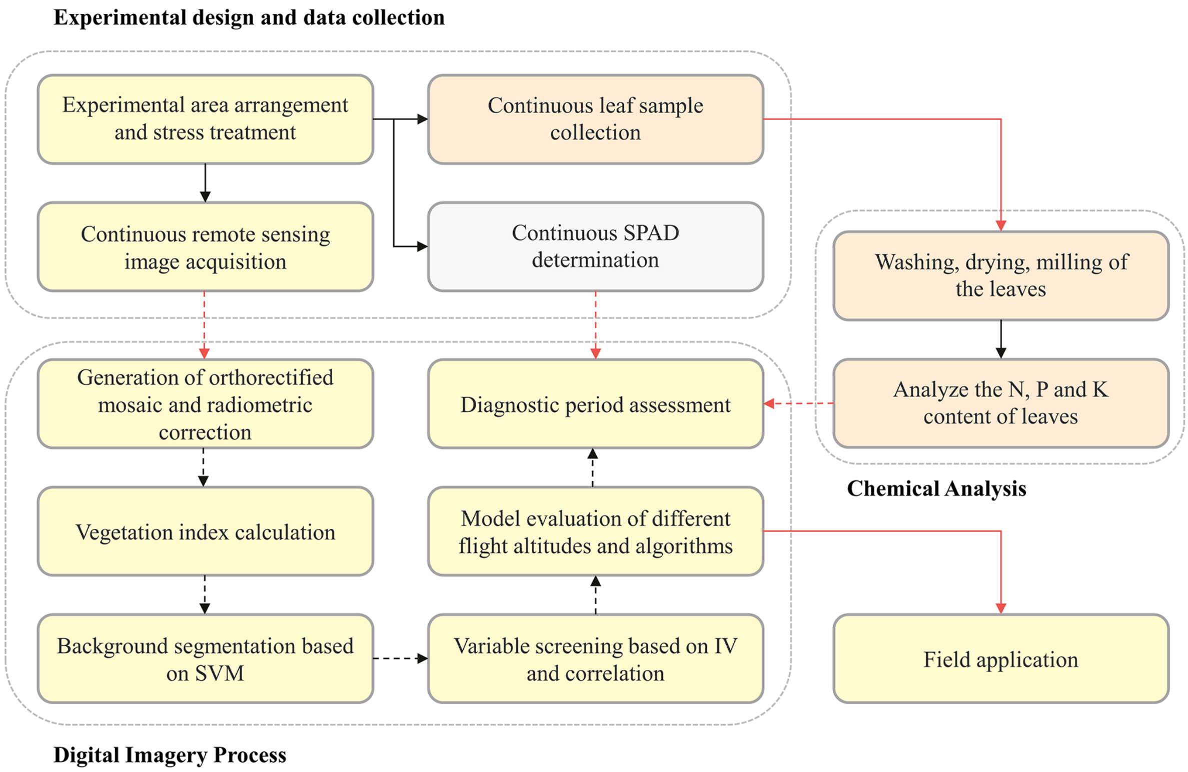

FIGURE 1
Workflow of the process performed in this study.

the vertical direction. The 10% and 90% radiometric calibration plates (JINGYI, Guangzhou, China) were placed in the center of the plot before the mission begin. It was used to verify the radiometric calibration effect.

2.2 Digital image processing and data analysis

2.2.1 Generation of orthorectified mosaic and radiometric correction

The generation of orthorectified mosaic was done on DJI Terra (DJI, Shenzhen, China) and the steps include radiometric calibration, image alignment, dark angle compensation, and aberration calibration. The radiometric calibration was calculated as follows (DJ-Innovations, 2020):

$$X_{ref} = \frac{X_{DN} \times pCam_X}{X_{LS} \times pLS_X} \times \rho_{NIR} \tag{1}$$

Where X is the response band, X_{DN} is the brightness value of the image element in this band, X_{LS} is the light-sensitive signal obtained by the light intensity sensor, ρ_{NIR} is the parameter that regulates the interconversion between the NIR image signal and the multispectral light intensity sensor, and $pCam_X$ and pLS_X are the calibration parameters obtained by the multispectral light intensity sensor in other bands with reference to the NIR band.

2.2.2 Feature extraction and variable screening

Mask images were made using the support vector machine (SVM) algorithm (Figure 3), and vegetation indices were calculated (Table 1). Then the image was segmented, and mask extracted the sample mean reflectance and vegetation index (Hassanzadeh et al., 2020), then removed redundant variables through the information value (IV) and correlation between variables (Zaghwan and Gunawan, 2021). Correlation coefficients between variables were calculated by person correlation analysis, and 90% was used as the correlation threshold to remove redundant variables (Hassanzadeh et al., 2020). The IV is used primarily to evaluate the predictive ability of variables in the classification model. The higher the IV value, the higher the information contribution of the variable. Before calculating IV, the data needs to be discretized. The calculation formula is as follows (Zhang et al., 2017):

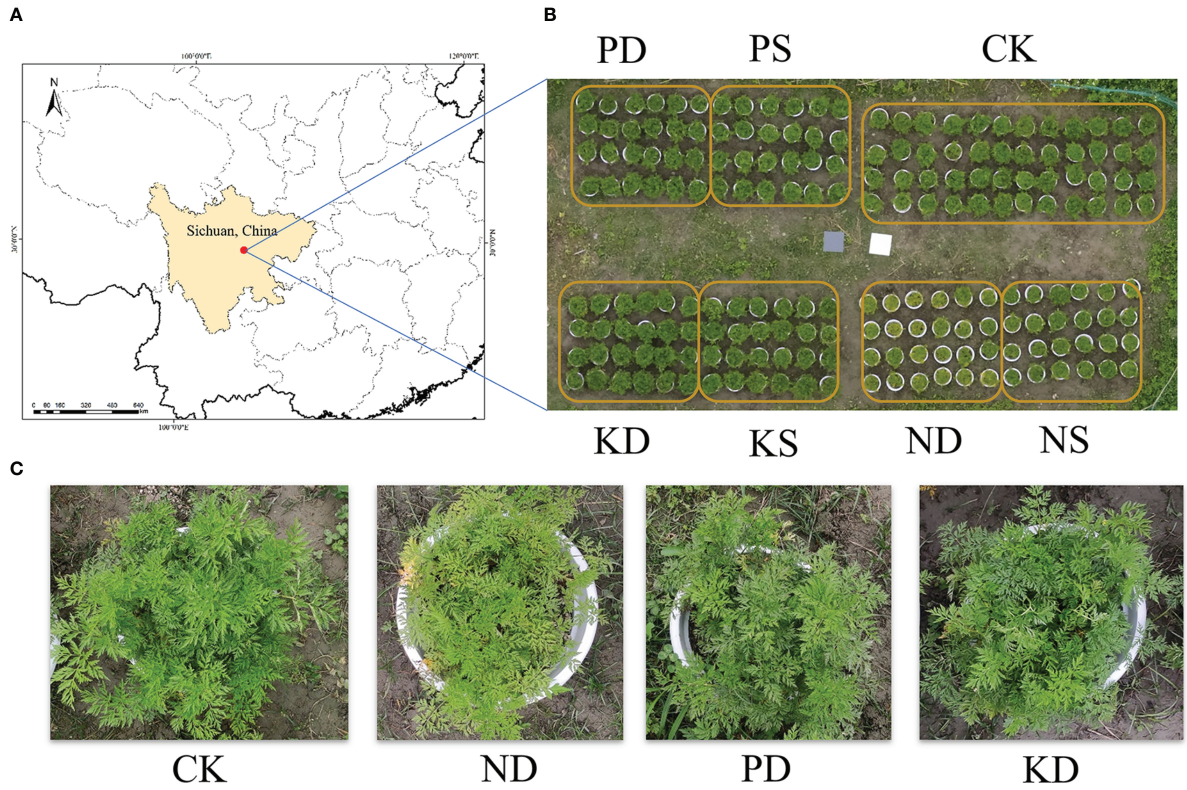

FIGURE 2
Study site, experimental design, and stress characterization. **(A)** Study area location, **(B)** Study area, **(C)**, Stress characterization. CK, control group, ND, nitrogen deficiency group, PD, phosphorus deficiency group, KD, potassium deficiency group, NS, nitrogen supplementation group, PS, phosphorus supplementation group, KS, potassium supplementation group.

$$IV = \sum_{i}^{n}\left((y_i/y_T - n_i/nT) \times ln(\frac{y_i/n_i}{y_T/nT})\right) \quad (2)$$

Where n is the number of groups, set to 10; i represents the ith group; y_i is the number of positive samples in this group; n_i is the number of negative samples in this group; y_T is the number of all positive samples in the sample; nT is the number of all negative samples in the sample; to prevent extreme values, if the number of positive samples or negative samples in the variable group is 0, it is adjusted to 1.

2.2.3 Data analysis and evaluation

Data processing and evaluation were performed in Python 3.8. Divide the data into training and test sets according to 7:3. Standardize and PCA dimensionality reduction of selected variables (Abdi and Williams, 2010). Since the dataset is an unbalanced sample, the SMOTE algorithm was used to oversample the training set data (Zhu et al., 2017). And then, the model was trained using K-Nearest Neighbor (KNN), Logistic Regression (LR), Naive Bayesian Model (NBM), Support Vector Machine (SVM), Decision Tree (DT), and Random Forest (RF) algorithms. The optimal parameters of the model were determined by grid search and five-fold cross-validation. Model performance was evaluated by AUC (Area under the Curve), precision, recall, and f1-score. All evaluation metrics were averaged over ten random divisions of the training and test sets obtained (Hossin and Sulaiman, 2015). AUC is the area under the ROC curve, which is applicable to the evaluation of classification models with unbalanced samples. The closer the AUC is to 1, the better the model is; close to 0.5, the model has no predictive value. Precision indicates the proportion of true cases among positive cases, recall indicates the proportion of true cases among all positive cases, f1-score neutralizes the precision and recall for evaluation, and the calculation equation is as follows (Wu et al., 2022):

$$precision = \frac{TP}{TP + FP} \quad (3)$$

$$recall = \frac{TP}{TP + FN} \quad (4)$$

$$F1\_score = \frac{2 \times precision \times recall}{precision + recall} \quad (5)$$

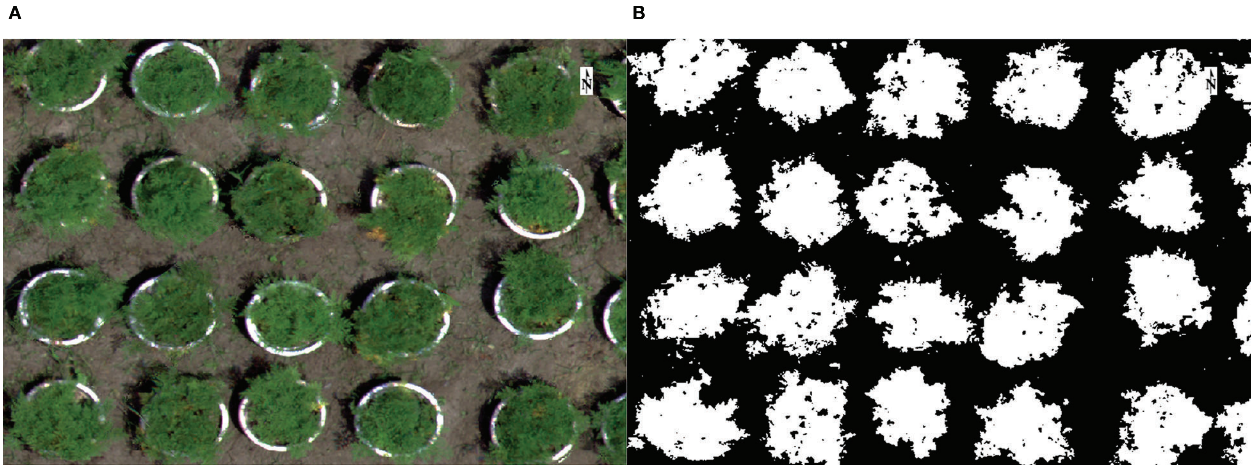

FIGURE 3
Mask extraction. Support vector machines (SVM) separated the crop crown from the background. **(A)** RGB image. **(B)** Mask.

Where TP is the number of samples where the instance is a positive class and is predicted to be positive, TN is the number of samples where the instance is a negative class and is predicted to be negative, FN is the number of samples where the instance is a positive class and is predicted to be negative, and FP is the number of samples where the instance is a negative class and is predicted to be positive.

2.3 Ground sampling and chemical analysis

Ground sampling activities were conducted before each nutrient watering (16:00-18:00 on the same day), and nine sampling sessions were conducted. SPAD was measured with MultispeQ V2 (PhotosynQ, USA) by selecting the first fully

TABLE 1 Vegetation indices, equations, and sources used in the study.

VIs	Name	Formula	References
NDVI	Normalized Difference VI	$NDVI=(NIR-R)/(NIR+R)$	(Rousel et al., 1973)
RVI	Red Ratio VI	$RVI=NIR/R$	(Jordan, 1969)
EVI	Enhanced VI	$EVI = 2.5(\frac{NIR-R}{NIR+6R-7.5B+1})$	(Huete et al., 2002)
DVI	Difference VI	$DVI=NIR-R$	(Richardson et al., 1977)
RDVI	Renormalized Difference VI	$RDVI = (NIR-R)/\sqrt{NIR-R}$	(Roujean and Breon, 1995)
SAVI	Soil Adjusted VI	$SAVI=1.5(NIR-R)/(NIR+R+0.5)$	(Huete, 1988)
GNDVI	Green Normalized Difference VI	$GNDVI=(NIR-G)/(NIR+G)$	(Gitelson et al., 1996)
NDRE	Normalized Difference Red-edge VI	$NDRE=(NIR-RE)/(NIR+RE)$	(Gitelson et al., 1994)
OSAVI	Optimization of Soil-Adjusted VI	$OSAVI=(NIR-R)/((NIR+R+0.16)$	(Rondeaux et al., 1996)
GRVI	Green Ratio VI	$GRVI=NIR/G$	(Xue et al., 2004)
LCI	Leaf Chlorophyll Index	$LCI=(NIR-RE)/(NIR-R)$	(Datt, 1999)
NDWI	Normalized Difference Water Index	$NDWI=(G-NIR)/(G+NIR)$	(Gao, 1996)
BNDVI	Blue Normalized Difference VI	$BNDVI=(NIR-B)/(NIR+B)$	(Peñuelas et al., 1995)
BVI	Blue Ratio VI	$BVI=NIR/B$	(Jordan, 1969)
BRVI	Simple Blue Ratio Index	$BRVI=R/B$	(Peñuelas et al., 1994)

expanded leaf below the terminal branch and measuring the mean of five parts of the leaf on both sides of the base, both sides of the middle, and the tip. Each treatment was randomly sampled 10 times. At the same time, the first fully expanded leaf was collected for chemical analysis of nutrient element content, all samples were collected, and each 8 replicate samples were mixed into 1 sample (about 0.25 g). A minimum of 3 samples per treatment were used for chemical analysis. After collection, they were placed in ice boxes and brought back to the laboratory for chemical assays, washed 2-3 times using RO water dripping, deenzymated at 105°C for 30 min, and dried at 65°C to constant weight. Digest with H_2SO_4 -H_2O_2, Kjeldahl analyzer (BUCHI K-360, FOSS, Sweden) was used to determine the total K, UV-Vis spectrophotometer (A580, AOE, China) for total P determination, and total K was determined using a flame photometer (6400A, shjingmi, China) (PRC, 2011).

After the last flight mission, dry biomass and leaf-to-stem ratio (LSR) were determined by the weighing method (Smart et al., 2004), and chlorophyll and carotenoid contents in leaves were determined by the acetone extraction colorimetric method (Arnon, 1949).

3 Results

3.1 Effect of nutritional deficiency on the growth of *L. chuanxiong*

Samples were collected after 58 days of stress and measured for biomass, chlorophyll content, carotenoid content, and leaf-to-stem ratio (Table 2). Except for KS, all treatment groups showed a significant decrease in biomass compared to CK, with ND showing the largest decrease of 43.52%, PD and KD decreasing by 21.15% and 14.33%. And biomass increased in all groups after supplementation with deficient nutrients compared to those with complete deficiency. For chlorophyll content, only ND showed significant differences with CK. PD (P=0.121) and KD (P=0.078) showed an increasing trend in chlorophyll content, but there was no significant difference. For carotenoid content, ND was significantly reduced, and PD significantly increased compared to CK. For LSR, all treatment groups showed a decrease compared to CK. The decreases were 52.27%, 42.05% and 18.18% in the KD, ND and PD groups. And LSR increased after supplementation with deficient nutrients compared to the deficient treatment. Collectively, all stress groups caused a reduction in biomass compared to the control group, with ND>PD>KD. Only ND significantly reduced chlorophyll and carotenoid contents. All the stress groups caused a reduction in the leaf-to-stem ratio, where KD>ND>PD.

3.2 Model building and evaluation

3.2.1 Variable filtering

Including single-band reflectance and vegetation index, we counted 20 indicators as pre-selected variables (Figure S1). To remove redundant information and simplify the workflow by information value (IV) and Pearson correlation analysis. We used IV as the degree of variable contribution and 0.9 as the correlation threshold (Figure 4) and finally determined the GRVI, LCI, BRVI, RVI, GREEN band, RED band, RE band, OSAVI, BVI, EVI as the input variable.

We removed the background of the selected variables and conducted PCA dimension reduction. As shown in Figure 5, with increasing stress time, phenotypic changes were first seen in the ND group (After 15 days). After 22 days of stress, the PD and KD groups began to show differences from the CK group. After 30 days of stress, we set up a supplemental fertilizer treatment, and the supplemental fertilizer treatment group gradually returned to the level of the CK group.

3.2.2 Different algorithms and AGL evaluation

The classification effects of different algorithms under 5 m and 10 m AGL were compared (Figures 6A, B), with AUC as the evaluation criterion. LR maintains the optimal classification performance under different stress stages and heights; NBM,

TABLE 2 Effect of different treatments on plant biomass, chlorophyll content, carotenoid content, and leaf-to-stem ratio.

Group	Dry biomass (g/pot)	Chlorophyll (mg/g)	Carotenoid (mg/g)	Leaf-to-stem ratio
CK	69.75 ± 8.41	0.83 ± 0.15	0.19 ± 0.02	0.88 ± 0.14
ND	39.39 ± 5.25**	0.54 ± 0.15**	0.14 ± 0.02**	0.51 ± 0.09**
NS	48.73 ± 5.53**	0.8 ± 0.18	0.18 ± 0.03	0.66 ± 0.16**
PD	55.002 ± 9.50**	0.91 ± 0.14	0.22 ± 0.03*	0.72 ± 0.05*
PS	57.26 ± 4.97*	0.85 ± 0.2	0.21 ± 0.03	0.71 ± 0.12*
KD	59.75 ± 11.09*	0.92 ± 0.13	0.21 ± 0.03	0.42 ± 0.06**
KS	61.44 ± 10.51	0.85 ± 0.16	0.20 ± 0.03	0.52 ± 0.07**

* (P<0.05) and **(P<0.01) represent significant differences from the control group. Statistical methods used were Student's t-test.

SVM, and RT also have high classification performance, while Decision Tree and KNN perform poorly. After 23 days of stress, the AUC values of the models constructed by LR, NBM, SVM, and RT algorithms reached or approached 0.9. The classification effect was the best at 38 and 45 days of stress, and the AUC values of the LR models exceeded 0.99. After 52 days, the classification performance of all algorithms and flight altitude models decreased. Overall, LR is best for building models.

Comparison of the LR algorithm at different heights (Figure 6C). The classification effect of 5m AGL was higher than that of 10m AGL before 22 days of stress. The AUC reached above 0.9 after 15 days of stress, while the AUC exceeded 0.9 after 22 days with 10 m AGL. Both models had similar classification performance after 31 days. AUC all reached above 0.99 after 45 days of stress. Overall, modeling efficacy was similar for 5m and 10m collection data after 30 days of stress, but 5m AGL modeling was more sensitive to nutrient deficiency.

3.2.3 Model evaluation

Based on the results in the above sections, we choose to use the LR algorithm to build the model under 5m AGL and perform PCA dimensionality reduction visualization for samples in different stress periods (Figure 7). After 15 days of stress, the ND group was gradually separate from the CK and PD\KD groups (Figure 7C), and the prediction accuracy was 78.48%. And the accuracy rate reached 97.77% after 22 days. From 38 to 58 days, the prediction precision and recall rate both reached 100% (Table 3). After 22 days of stress, there were differences between PD\KD group and CK group (Figure 7D), the

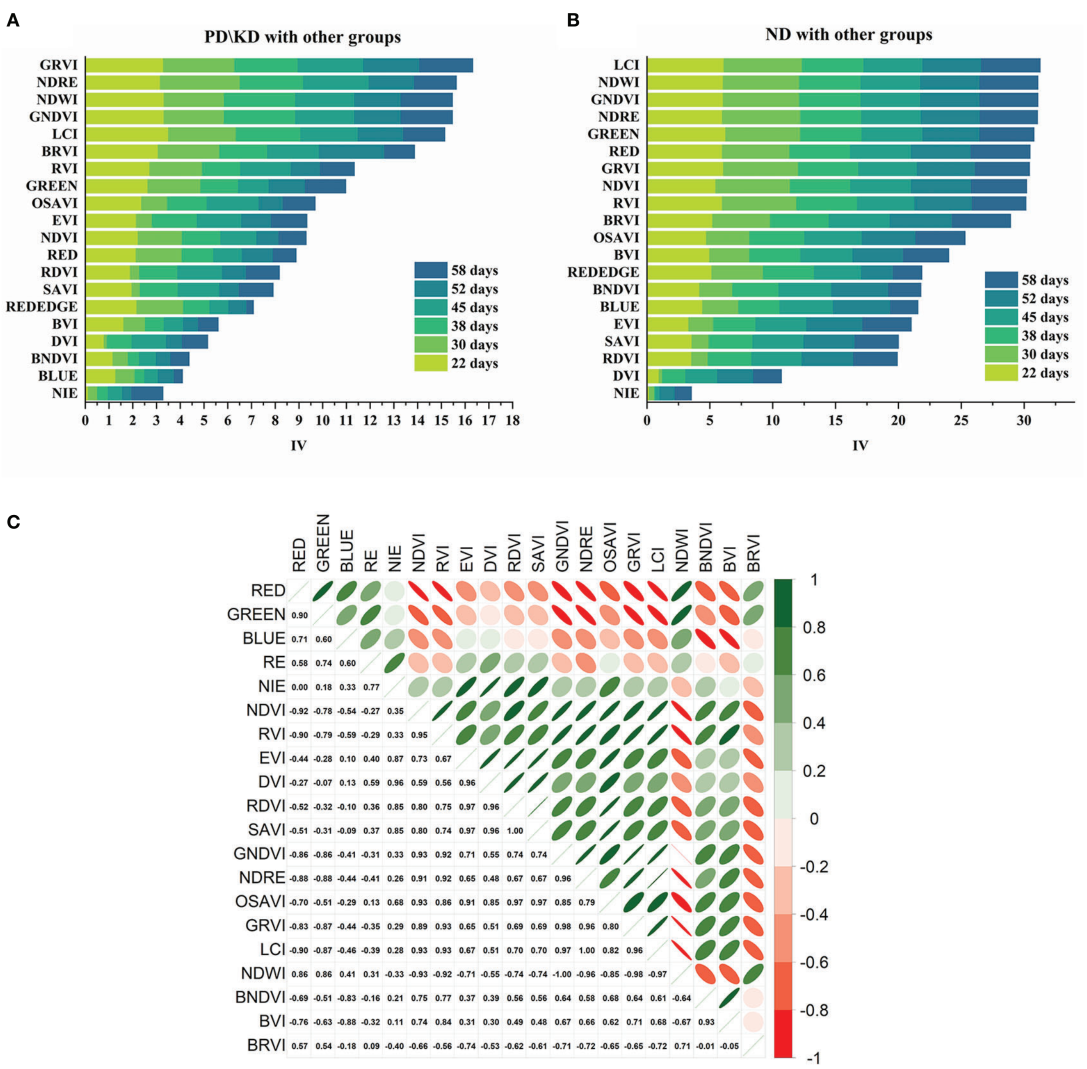

FIGURE 4
Variable screening based on IV and correlation. **(A)** The IV was calculated with PD\KD as the positive sample and the other treatment groups as the negative sample. **(B)** The IV was calculated with the ND as the positive sample and the other treatment groups as the negative sample. **(C)** Heat map of vegetation index correlation.

recognition precision rate reached 87.1%, and the recall rate was 82.08%. The recognition accuracy rate between 30 and 45 days was between 87.3% and 92.35%, the recall rate was between 86.37% and 89.03%, and the recognition effect was the best (Table 3). The recognition rate decreased in both ND and PD \KD groups after 52-58 days of stress.

3.3 Comparison with other diagnostic methods and field validation

Diagnosis of each treatment group was performed by chemically measuring the elemental content of the plant leaves and SPAD (Figure 8). There was a significant difference compared to the CK group, indicating that the diagnostic method could make a valid diagnosis of stress in that period. For the ND group, both chemical diagnosis and SPAD diagnosis showed significant differences from the CK group after 15 days of stress (Figures 8A, D); After 15 days of stress, the images of RGB, GRVI, and results of PCA were different from those of CK group (Figures 5, 7C). For the P deficiency treatment, leaf P content was significantly different between the CK group after 15 days (Figure 8B), while there was no difference in SPAD compared to the CK group. There was a difference between PCA images after 22 days of stress (Figure 5), which was further proved by PCA scatter plot (Figure 7). For the K deficiency treatment, leaf K content was significantly reduced after 8 days of stress compared to the CK group, and there was no significant difference in SPAD. The diagnosis period of potassium-deficient plants by multispectral

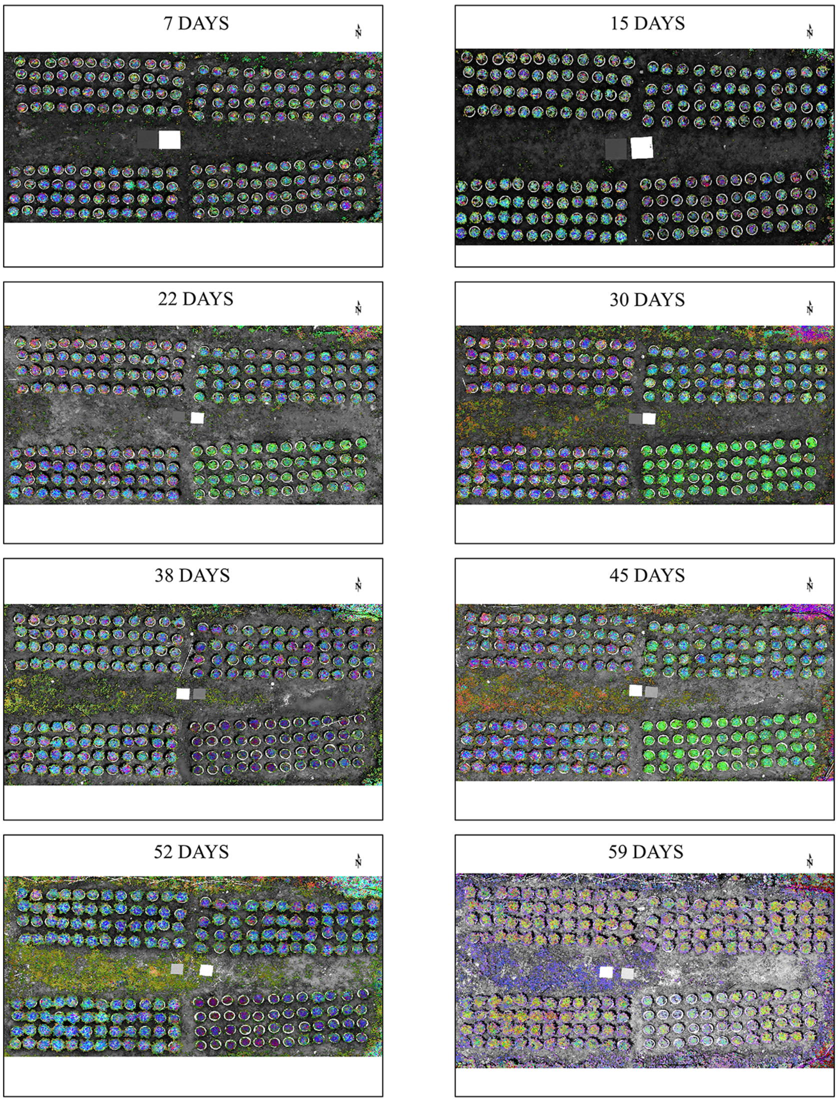

FIGURE 5
Dimensionality reduction images at different stress times. The remote sensing images of selected variables were subjected to PCA downscaling. b: PC1, g: PC2, r: PC3.

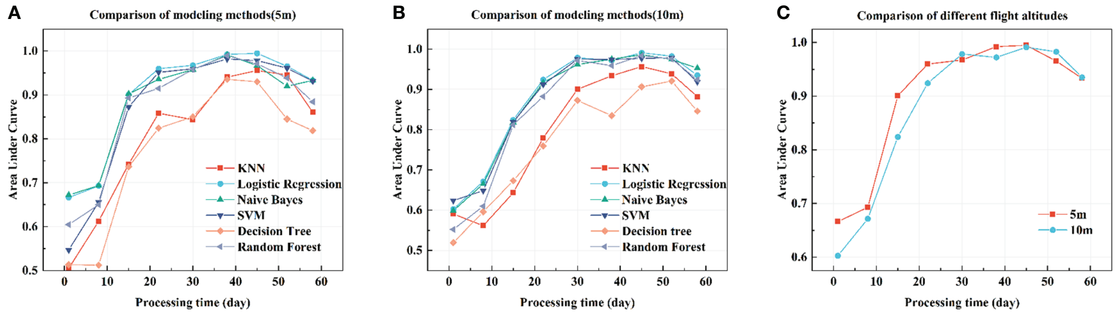

FIGURE 6
Different modeling algorithms and AGL evaluation. AUC is the evaluation metric of the model as the average of area of the ROC curves for each classification sample. **(A)** performance evaluation of different algorithms at 5 m AGL, **(B)** evaluation of different algorithms at 10 m AGL, **(C)** evaluation of logistic regression algorithms at different AGL.

imaging was 15 to 22 days after stress. Based on this, multispectral diagnosis is similar to chemical diagnosis in the diagnosis period of nitrogen deficiency, while phosphorus and potassium deficiency are slightly lagged behind.

As shown in Figure 9, we predicted the nutrient status of the field vegetation in *L. Chuanxiong* planted fields with the model developed during the same period (after 38 days of stress). In this image acquisition, potted plants of ND, PD, and KD groups were placed in the open area of the field. We collected leaves from N deficient area and normal field, and N content of the leaves in this area was significantly lower than that of normal field leaves. Moreover, the results predicted by the model were similar to the ND group of crops (Figure 9B). Crops in most areas and the CK group were predicted to be healthy vegetation (Figure 9A). Crops in the roadside area were predicted to be phosphorus or potassium deficient, similar to the results predicted for the PD and KD groups (Figure 9C).

4 Discussion

4.1 Effect of N deficiency on crop phenotype and canopy spectrum

N is an essential nutrient for plants' main physiological metabolic functions and is closely related to chlorophyll synthesis and light metabolism. Under our experimental conditions, nitrogen deficiency produced distinct symptomatic features with uniform yellow leaves and slow plant growth (Figure 2C). Yellowing symptoms occurred first in the basal leaves and later caused the yellowing of the whole plant.

In agreement with Have et al. (2017), N deficiency caused a decrease in chlorophyll and carotenoid content in the leaves (Table 2), while a decrease in the pigment content of canopy leaves followed by an increase in visible light reflectance was the key to identifying N-deficient plants. N deficiency caused slow crop growth and a significant reduction in LSR (Table 2), which resulted in sparse vegetation canopy foliage. Although background segmentation was performed prior to data processing, mixed image elements still resulted in spectral differences (Benincasa et al., 2017), which is also an important factor in identifying N-deficient plants. Therefore, the key to distinguishing N-deficient plants is the canopy pigment content and the number of canopy leaves.

The indices LCI, NDWI, GNDVI, and NDRE in our study contributed more information gain to the identification of N-deficient plants than single bands (Figure 4A). This is consistent with the finding of Osco et al. (2020) that vegetation indices contributed more to the prediction of leaf N content than spectral bands. Meanwhile, the green and red band reflectance provided a high information gain (Figure 4A) and a weak correlation with the vegetation index (Figure 4C), which is also consistent with the finding of Li et al. (2022) that the combination of vegetation index plus spectral band variables can improve the accuracy of the model. In addition, we verified by supplementing the treatments with deficient elements that the change was indeed due to differences in N deficiency. All indices and bands except the red-edge band tended to move closer to the control after the N supplementation treatment (Figure 5, Figure S1), with indices such as OSAVI and RVI being more sensitive to the response of N supplementation.

4.2 Effect of P and K deficiencies on crop phenotype and spectrum

Plants are usually subjected to P deficiency conditions, where the reduction in cell division and elongation leads to high chlorophyll concentration and further causes anthocyanin accumulation, giving the leaves a purplish-red color (de Bang

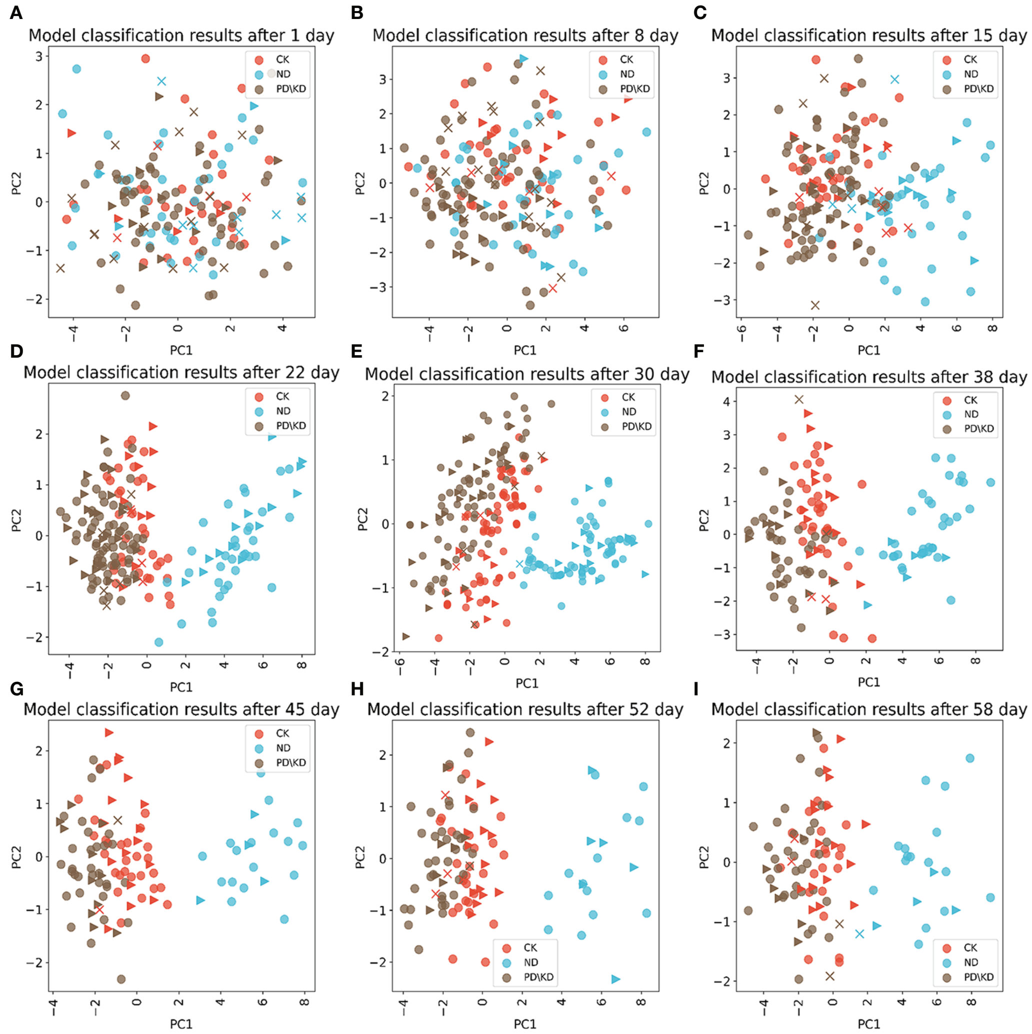

FIGURE 7
Classification results of logistic regression(LR) models under different stress time models. PCA dimensionality reduction and visualization of sample data collected at 5 m height. **(A-I)** were the classification results after 1, 8, 15, 22, 30, 38, 45, 52 and 58 days of stress successively. The LR algorithm predicts the test samples. ▼ are the correctly predicted samples in the test set, x are the incorrectly predicted samples in the test set, and • are the training set samples.

et al., 2021). However, Hughes and Lev-Yadun (2015) found that reddening leaf margins were not a common symptom of all P deficiencies. For example, in sugar beet, rice, and potato, P deficiency symptoms only manifested as stunted growth with dark blue/green leaf coloration. Under our experimental conditions, only a few plants were observed to have reddish-purple leaves in the early stages of stress, but the leaves were dark green with little new leaf emergence (Figure 1C).

The present study differs from Gracia-Romero et al. (2017)'s study in that P deficiency increased NDVI, GNDVI, LCI, and other indices (Figure S1). The difference could be the accumulation of more chlorophyll under P-deficient conditions and the reduction in the number of new leaf sprouts in the canopy or the difference in the GSD, making the previous spectral images contain more information about the soil background.

Under K-deficient conditions, plants generally exhibit symptoms of chlorosis or necrosis from the tip to the edge of old leaves (Ueno et al., 2018) and loose leaves and stems. In this experiment, the symptoms of edge necrosis of old leaves were not easily detected, but the plants showed obvious relaxation of leaves and stems (Figure 1C). At the same time, the number of new leaf germinations was significantly reduced compared with normal plants.

K deficiency greatly reduced the leaf-to-stem ratio of crops (Table 2), indicating that K deficiency limited the reduction of crop new leaf germination, and the reflectance of new leaves in the visible light band is lower than that of mature leaves (Nakaji et al., 2019; Wu et al., 2022). The reduction of the visible light

TABLE 3 Evaluation index of models in different stress stages.

Processing time(day)	CK			ND			PD\KD		
	precision	recall	f1-score	precision	recall	f1-score	precision	recall	f1-score
1	0.4834	0.46178	0.46028	0.37892	0.46428	0.4129	0.5881	0.51908	0.55046
8	0.31558	0.30658	0.3061	0.45906	0.5562	0.50048	0.57894	0.51332	0.54098
15	0.3868	0.4857	0.42704	0.7848	0.72878	0.7511	0.68514	0.63372	0.65652
22	0.66568	0.7395	0.69776	0.97772	0.98824	0.98284	0.871	0.8208	0.8439
30	0.71898	0.82944	0.76458	0.98888	0.92174	0.9526	0.92354	0.86366	0.88972
38	0.91042	0.90094	0.90274	1	1	1	0.87308	0.8903	0.87636
45	0.89516	0.91098	0.90098	1	1	1	0.91516	0.87378	0.89086
52	0.91714	0.83096	0.8659	1	1	1	0.83254	0.9159	0.86614
58	0.77534	0.8472	0.80246	1	0.89642	0.93846	0.85016	0.81076	0.82456

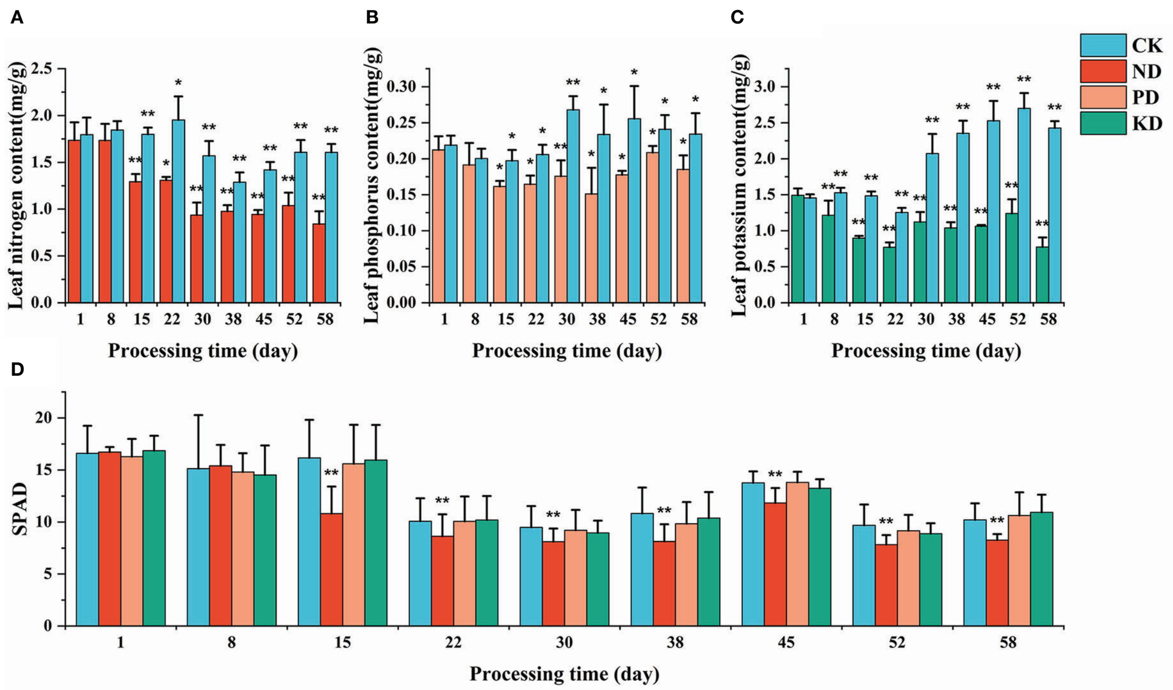

FIGURE 8
Chemical diagnosis and SPAD diagnosis results. **(A)** Leaf N content. **(B)**: leaf P content. **(C)** leaf K content. **(D)** SPAD values; * (P<0.05) and ** (P<0.01) represent significant differences from the control group. Statistical methods used were Student's t-test and ANOVA.

band in the canopy of K-deficient plants was related to the decrease in the proportion of young leaves in the canopy caused by K deficiency. This spectral change is similar to that of Severtson et al. (2016) for diagnosing K deficiency in rapeseed by a drone-carrying canopy sensor. Unlike the study of Furlanetto et al. (2021), the former study found that the chlorophyll concentration, GNDVI, RVI, and GRVI of maize decreased in severe K deficiency. In this study, the chlorophyll concentration of crops did not decrease under the state of P deficiency but increased compared with normal plants; the GNDVI, RVI, GRVI, and other indices were significantly higher than normal plants. This may be related to the reduction of the new leaf germination of *L. chuanxiong* and the higher spatial resolution in this study. It is worth noting that GRVI obtained the best regression model between K content in the former study and the maize growth stage, and in this study, GRVI was also the best index to distinguish PD\KD groups from other groups (Figure 2B).

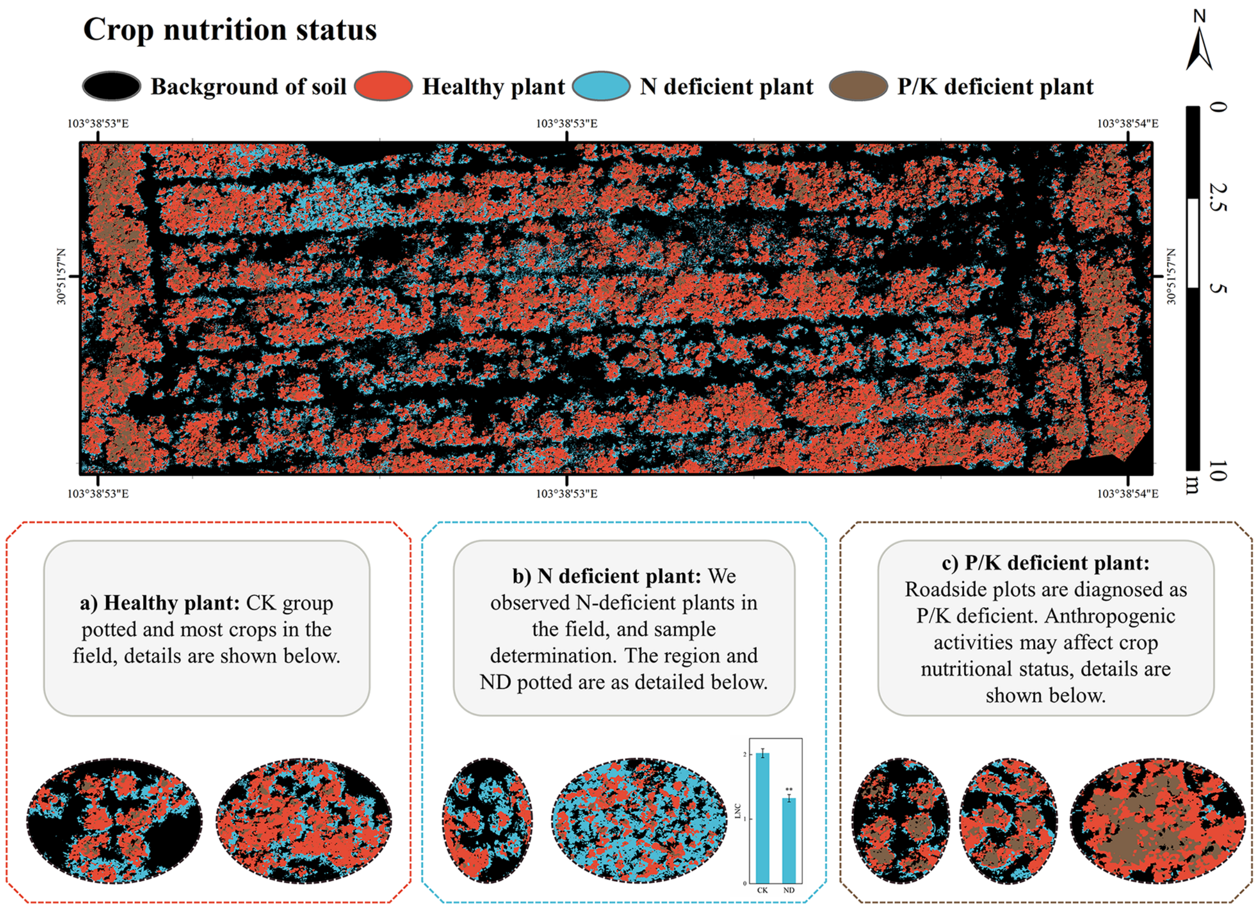

FIGURE 9
Field verification (5m). **(P<0.01) represent significant differences from the control group. Statistical methods used were Student's t-test.

In the model constructed in this study, PD and KD groups were set as one category because the canopy of *L. chuanxiong* under P and K deficiency treatments had similar spectral characteristics and phenotypic changes. However, compared with potassium deficiency, phosphorus deficiency did not severely limit the germination of new leaves. The reason for the spectral change may be the dark green overall appearance of the plant due to the accumulation of pigment. Increasing the band of the multispectral camera or adding texture information may be the solution. In practice, this method should be applied for initial diagnosis in large-scale production and combined with other means to further determine phosphorus or potassium deficiency.

4.3 Effects of GSD and classifiers on model performance

Background information, such as exposed soil and vegetation shading, may significantly impact the vegetation index, especially in the case of small canopy coverage (Benincasa et al., 2017). Removing the background does not always improve the results, and the solution to the problem is usually to increase the image's resolution (Corti et al., 2018). In the present study, lower AGL improved the model's accuracy at an early stage (15-22 days of stress). However, the higher recognition accuracy (1-8 days of stress) before differences in chemical assays led us to consider that lower AGL are more susceptible to noise. While the model constructed with 10 m AGL had lower classification performance in the early stage, it achieved similar classification performance after 30 days of stress (Figure 6C). There was also no significant change in accuracy when Vega et al. (2015) used multispectral images to monitor sunflower nitrogen status with GSDs ranging from 1 to 100 cm/pixel. We argued that different GSD does not affect the accuracy of model recognition, and using a lower AGL only means increasing the model sensitivity at the early stage of stress, but it may also reduce the model noise resistance.

We compared the model performance of KNN, LR, NBM, SVM, DT, and RF with AUC as the evaluation index and found that LR, NBM, SVM, and RF all achieved better prediction accuracy at 5m and 10m AGL. Among them, the LR algorithm achieved the best results in each stress period and flight altitude, but the model sensitivity was high and easily affected by noise at 5m AGL. Both NBM and RT have such problems, while SVM performs better on this problem. The study by Zermas et al. (2015) also showed that the LR algorithm showed higher sensitivity than the SVM algorithm in distinguishing N-defective leaves. KNN performs classification by measuring the distance method between different feature values. NBM is a probabilistic classification method proposed by Pearl based on Bayes' theorem. DT judges the attributes of samples sequentially based on knowing the probability of occurrence of various situations until the final result is derived. RF is an integrated algorithm consisting of multiple decision trees. SVM and LR are classification methods based on linear models, and the results of the two algorithms are very close in most experiments. The SVM is a structural risk minimization model, which is not easily affected by outliers. This is why SVM was not affected by noise in this study, but it also means that it is not sensitive to vegetation diagnosis at the initial stage of stress. Classifiers based on linear discriminant always achieve better classification results in the classification of remote sensing images, such as SVM and LDA (Ang and Seng, 2021; Zhang et al., 2021), and the same is true in this study. All classifiers showed a decrease in performance at the later stage of stress, which is related to plant physiological characteristics.

4.4 Consistency inspection with traditional diagnostic methods and field validation

In previous studies, vegetation indices such as NDVI, GNDVI, and NDRE showed high sensitivity to leaf nitrogen content (Gordillo-Salinas et al., 2021; Rehman et al., 2022), while P and K deficiency treatments only responded to severe deficits (Gracia-Romero et al., 2017; Furlanetto et al., 2021). The present study's spectral responses of P and K deficiency treatments also showed delayed diagnosis time. We diagnosed K deficiency symptoms after 7 days of stress and P and N deficiency symptoms after 15 days of stress by chemical assays (Figure 8). The spectral response of the ND group appeared at the same time as the difference in leaf N content. The spectral response of the PD and KD groups appeared 7 to 14 days after the appearance of the elemental difference (after 22 days of stress). It can be seen that UAV multispectral technology lags behind the chemical diagnosis of P and K deficiency symptoms but can diagnose N-deficient plants promptly. Although the remote sensing image diagnosis method in this study is relatively slow in the diagnosis of phosphorus and potassium deficiency, it is more suitable for large-scale agricultural production than the chemical diagnosis method, which needs to rely on a laboratory environment and complex operation.

We verified the feasibility of the practical application of the model in field. Unfortunately, areas predicted by the model to be phosphorus or potassium deficient were not sampled, resulting in our inability to rule out whether the crop in that area was affected by other factors that influenced the results. However, the model successfully identified crops of ND, PD, and KD groups in fields. We cannot strictly control soil nutrient conditions in the field, so constructing an accurate remote sensing nutrient deficiency diagnostic model is difficult. The method used in the paper can provide a solution bill for this purpose, but it is difficult to achieve large-scale cultivation, so it needs to be collected at a lower flight altitude. However, higher flight altitude means higher efficiency, so the question of how models built at lower flight altitudes can be applied at higher flight altitudes will be a further research direction.

5 Conclusions

In conclusion, this study developed a nutrient deficit recognition technology based on UAV multispectral images in *L. Chuanxiong* and completed the process from nutrient deficiency model construction to field application. Moreover, we evaluated the influence of different algorithms and flight altitude on the recognition model during the full growth period. It can provide a reference for the application of UAV remote sensing technology in intelligent agriculture and help *L. Chuanxiong* cultivation personnel and botanists to make decisions. In addition, with the rapid development of UAV remote sensing technology, UAV with different sensors will play a greater role in the development and utilization of medicinal plant resources and regulate the production methods of medicinal plant resources in a more reasonable and efficient way.

Data availability statement

The original contributions presented in the study are included in the article/Supplementary Material. Further inquiries can be directed to the corresponding author.

Author contributions

WL and ZY contributed the central idea, analysed most of the data, and wrote the initial draft of the paper. The remaining authors contributed to refining the ideas, carrying out additional analyses and finalizing this paper. All authors contributed to the article and approved the submitted version.

Funding

This research was funded by Science and Technology Department of Sichuan Province (2021YFS0045).

Conflict of interest

The authors declare that the research was conducted in the absence of any commercial or financial relationships that could be construed as a potential conflict of interest.

Publisher's note

Supplementary material

The Supplementary Material for this article can be found online at: https://www.frontiersin.org/articles/10.3389/fpls.2022.1092610/full#supplementary-material

References

Abdi, H., and Williams, L. (2010). Principal component analysis. *Wiley Interdiscip. Rev: Comput. Stat* 2 (4), 433–459. doi: 10.1002/wics.101

Ang, K. L. M., and Seng, J. K. P. (2021). Big data and machine learning with hyperspectral information in agriculture. *IEEE Access* 9, 36699–36718. doi: 10.1109/access.2021.3051196

Anschutz, U., Becker, D., and Shabala, S. (2014). Going beyond nutrition: Regulation of potassium homoeostasis as a common denominator of plant adaptive responses to environment. *J. Plant Physiol.* 171 (9), 670–687. doi: 10.1016/j.jplph.2014.01.009

Arnon, D. I. (1949). Copper enzymes in isolated chloroplasts. polyphenoloxidase in beta vulgaris. *Plant Physiol.* 24 (1), 1.

Balasubramanian, V., Morales, A. C., Cruz, R. T., and Abdulrachman, S. (1998). On-farm adaptation of knowledge-intensive nitrogen management technologies for rice systems. *Nutrient Cycling Agroecosystems* 53 (1), 59–69. doi: 10.1023/a:1009744605920

Benincasa, P., Antognelli, S., Brunetti, L., Fabbri, C. A., Natale, A., Sartoretti, V., et al. (2017). Reliability of ndvi derived by high resolution satellite and uav compared to in-field methods for the evaluation of early crop n status and grain yield in wheat. *Exp. Agric.* 54 (4), 604–622. doi: 10.1017/s0014479717000278

Chen, Y. Y., Peng, F. F., Tao, S., Yuan, C., Wu, Y., Shi, T. T., et al. (2022). Effects of combined application of n, p and K on the growth and active components of ligusticum chuanxiong. *Modern Agric. Sci. Technol.* 06, 32–37. doi: 10.3969/j.issn.1007-5739.2022.06.010

Chen, Z., Zhang, C., Gao, F., Fu, Q., Fu, C., He, Y., et al. (2018). A systematic review on the rhizome of ligusticum chuanxiong hort. *(Chuanxiong) Food Chem. Toxicol.* 119, 309–325. doi: 10.1016/j.fct.2018.02.050

Corti, M., Cavalli, D., Cabassi, G., Vigoni, A., Degano, L., and Marino Gallina, P. (2018). Application of a low-cost camera on a UAV to estimate maize nitrogen-related variables. *Precis. Agric.* 20 (4), 675–696. doi: 10.1007/s11119-018-9609-y

Datt, B. (1999). A new reflectance index for remote sensing of chlorophyll content in higher plants: Tests using eucalyptus leaves. *J. Plant Physiol.* 154 (1), 30–36. doi: 10.1016/S0176-1617(99)80314-9

Daughtry, C. S., Walthall, C., Kim, M., De Colstoun, E. B., and McMurtrey Iii, J. (2000). Estimating corn leaf chlorophyll concentration from leaf and canopy reflectance. *Remote Sens. Environ.* 74 (2), 229–239. doi: 10.1016/S0034-4257(00)00113-9

de Bang, T. C., Husted, S., Laursen, K. H., Persson, D. P., and Schjoerring, J. K. (2021). The molecular-physiological functions of mineral macronutrients and their consequences for deficiency symptoms in plants. *New Phytol.* 229 (5), 2446–2469. doi: 10.1111/nph.17074

de Castro, A. I., Shi, Y., Maja, J. M., and Peña, J. M. (2021). UAVs for vegetation monitoring: Overview and recent scientific contributions. *Remote Sens.* 13 (11), 2139. doi: 10.3390/rs13112139

DJ-Innovations (2020). P4 multispectral image processing guide CHS. Available at: https://dl.djicdn.com/downloads/p4-multispectral/20200717/P4_Multispectral_Image_Processing_Guide_CHS.pdf. [Accessed June 1, 2022]

Furlanetto, R. H., Rafael Nanni, M., Guilherme Teixeira Crusiol, L., Silva, G. F. C., Junior, A., and Sibaldelli, R. N. R. (2021). Identification and quantification of potassium (K+) deficiency in maize plants using an unmanned aerial vehicle and visible / near-infrared semi-professional digital camera. *Int. J. Remote Sens.* 42 (23), 8783–8804. doi: 10.1080/01431161.2020.1871091

Gao, B.-C. (1996). NDWI–a normalized difference water index for remote sensing of vegetation liquid water from space. *Remote Sens. Environ.* 58 (3), 257–266. doi: 10.1016/S0034-4257(96)00067-3

Gitelson, A. A., Kaufman, Y. J., and Merzlyak, M. N. (1996). Use of a green channel in remote sensing of global vegetation from EOS-MODIS. *Remote Sens. Environ.* 58 (3), 289–298. doi: 10.1016/S0034-4257(96)00072-7

Gitelson, A., Merzlyak, M. N., and Biology, P. B. (1994). Quantitative estimation of chlorophyll-a using reflectance spectra: Experiments with autumn chestnut and maple leaves. *J. Photochem.* 22 (3), 247–252. doi: 10.1016/1011-1344(93)06963-4

Gordillo-Salinas, V. M., Flores-Magdaleno, H., Ortiz-Solorio, C. A., and Arteaga-Ramírez, R. (2021). Evaluation of nitrogen status in a wheat crop using unmanned aerial vehicle images. *Chilean J. Agric. Res.* 81 (3), 408–419. doi: 10.4067/s0718-58392021000300408

Gracia-Romero, A., Kefauver, S. C., Vergara-Diaz, O., Zaman-Allah, M. A., Prasanna, B. M., Cairns, J. E., et al. (2017). Comparative performance of ground vs. aerially assessed RGB and multispectral indices for early-growth evaluation of maize performance under phosphorus fertilization. *Front. Plant Sci.* 8. doi: 10.3389/fpls.2017.02004

Hassanzadeh, A., Murphy, S. P., Pethybridge, S. J., and van Aardt, J. (2020). Growth stage classification and harvest scheduling of snap bean using hyperspectral sensing: A greenhouse study. *Remote Sens.* 12 (22), 3809. doi: 10.3390/rs12223809

Have, M., Marmagne, A., Chardon, F., and Masclaux-Daubresse, C. (2017). Nitrogen remobilization during leaf senescence: Lessons from arabidopsis to crops. *J. Exp. Bot.* 68 (10), 2513–2529. doi: 10.1093/jxb/erw365

Hoagland, D. R., and Arnon, D. I. (1950). The water-culture method for growing plants without soil. *Circular. California agricultural experiment station* 347(*2nd* edit), 32.

Homolova, L., Maenovsky, Z., Clevers, J. G. P. W., Garcia-Santos, G., and Schaeprnan, M. E. (2013). Review of optical-based remote sensing for plant trait mapping. *Ecol. Complexity* 15, 1–16. doi: 10.1016/j.ecocom.2013.06.003

Hossin, M., and Sulaiman, M. N. (2015). A review on evaluation metrics for data classification evaluations. *Int. J. Data Min. Knowledge Manage. Process* 5 (2), 1. doi: 10.5121/ijdkp.2015.5201

Huete, A. R. (1988). A soil-adjusted vegetation index (SAVI). *Remote Sens. Environ.* 25 (3), 295–309. doi: 10.1016/0034-4257(88)90106-X

Huete, A., Didan, K., Miura, T., Rodriguez, E. P., Gao, X., and Ferreira, L. G. (2002). Overview of the radiometric and biophysical performance of the MODIS vegetation indices. *Remote Sens. Environ.* 83 (1-2), 195–213. doi: 10.1016/S0034-4257(02)00096-2

Hughes, N. M., and Lev-Yadun, S. (2015). Red/purple leaf margin coloration: Potential ecological and physiological functions. *Environ. Exp. Bot.* 119, 27–39. doi: 10.1016/j.envexpbot.2015.05.015

Imran, A., Ali khan, A., Mahmood, T., Al Tawaha, A. R., and Khanum, S. (2021). Adequate fertilization, application method and sowing techniques improve maize yield and related traits. *Commun. Soil Sci. Plant Anal.* 52 (19), 2318–2330. doi: 10.1080/00103624.2021.1925688

Jordan, C. (1969). Derivation of leaf-area index from quality of light on the forest floor. *Ecology* 50 (4), 663–666. doi: 10.2307/1936256

Kamerlin, S. C. L., Sharma, P. K., Prasad, R. B., and Warshel, A. (2013). Why nature really chose phosphate. *Q. Rev. Biophys* 46 (1), 1–132. doi: 10.1017/S0033583512000157

Krasilnikov, P., Taboada, M. A., and Amanullah, (2022). Fertilizer use, soil health and agricultural sustainability. *Agriculture* 12 (4), 462. doi: 10.3390/agriculture12040462

Li, X., Ba, Y., Zhang, M., Nong, M., Yang, C., and Zhang, S. (2022). Sugarcane nitrogen concentration and irrigation level prediction based on UAV multispectral imagery. *Sens (Basel)* 22 (7), 2711. doi: 10.3390/s22072711

Liu, L. (2009). *Effects of nitrogen application period and nitrogen application rate in spring on physiological characteristics and yield of ligusticum chuanxiong* (Chengdu: Sichuan Agricultural University).

Ministry of Agriculture of the PRC (2011). Determination of nitrogen, phosphorus and potassium in plants. https://std.samr.gov.cn/hb/search/stdHBDetailed?id=B01B6E44148F87D8E05397BE0A0A5EC7 [Accessed Feb 15, 2022]

Nakaji, T., Oguma, H., Nakamura, M., Kachina, P., Asanok, L., Marod, D., et al. (2019). Estimation of six leaf traits of East Asian forest tree species by leaf spectroscopy and partial least square regression. *Remote Sensing of Environment* 233, 111381. doi: 10.1016/j.rse.2019.111381.

Osco, L. P., Junior, J. M., Ramos, A. P. M., Furuya, D. E. G., Santana, D. C., Teodoro, L. P. R., et al. (2020). Leaf nitrogen concentration and plant height prediction for maize using UAV-based multispectral imagery and machine learning techniques. *Remote Sens.* 12 (19), 3237. doi: 10.3390/rs12193237

Peng, F., Chen, Y., Tao, S., Yan, C., Wu, Y., Shi, T., et al. (2020). Investigation and evaluation on cultivation status of ligusticum chuanxiong in sichuan province. *Chin. J. Exp. Tradit Med. Formulae* 26 (02), 181–189. doi: 10.13422/j.cnki.syfjx.20200114

Peñuelas, J., Filella, I., and Gamon, J. (1995). Assessment of photosynthetic radiation-use efficiency with spectral reflectance. *New Phytol.* 131 (3), 291–296. doi: 10.1111/j.1469-8137.1995.tb03064.x

Peñuelas, J., Gamon, J., Fredeen, A., Merino, J., and Field, C. (1994). Reflectance indices associated with physiological changes in nitrogen-and water-limited sunflower leaves. *Remote Sens. Environ.* 48 (2), 135–146. doi: 10.1016/0034-4257(94)90136-8

Pottosin, I., and Shabala, S. (2016). Transport across chloroplast membranes: Optimizing photosynthesis for adverse environmental conditions. *Mol. Plant* 9 (3), 356–370. doi: 10.1016/j.molp.2015.10.006

Rahayu, Y. S., Walch-Liu, P., Neumann, G., Römheld, V., von Wirén, N., and Bangerth, F. (2005). Root-derived cytokinins as long-distance signals for NO3–induced stimulation of leaf growth. *J. Exp. Bot.* 56 (414), 1143–1152. doi: 10.1093/jxb/eri107

Rajkovich, S., Enders, A., Hanley, K., Hyland, C., Zimmerman, A. R., and Lehmann, J. (2011). Corn growth and nitrogen nutrition after additions of biochars with varying properties to a temperate soil. *Biol. Fertil Soils* 48 (3), 271–284. doi: 10.1007/s00374-011-0624-7

Ran, X., Ma, L., Peng, C., Zhang, H., and Qin, L. P. (2011). Ligusticum chuanxiong hort: A review of chemistry and pharmacology. *Pharm. Biol.* 49 (11), 1180–1189. doi: 10.3109/13880209.2011.576346

Rehman, T. H., Lundy, M. E., and Linquist, B. A. (2022). Comparative sensitivity of vegetation indices measured *via* proximal and aerial sensors for assessing n status and predicting grain yield in rice cropping systems. *Remote Sens.* 14 (12), 2770. doi: 10.3390/rs14122770

Richardson, A. J., Wiegand, C., and sensing, R. (1977). Distinguishing vegetation from soil background information. *Photogrammetric Eng.* 43 (12), 1541–1552.

Rondeaux, G., Steven, M., and Baret, F. (1996). Optimization of soil-adjusted vegetation indices. *Remote Sens. Environ.* 55 (2), 95–107. doi: 10.1016/0034-4257(95)00186-7

Roujean, J.-L., and Breon, F.-M. (1995). Estimating PAR absorbed by vegetation from bidirectional reflectance measurements. *Remote Sens. Environ.* 51 (3), 375–384. doi: 10.1016/0034-4257(94)00114-3

Rousel, J., Haas, R., Schell, J., and Deering, D. (1973). Monitoring vegetation systems in the great plains with ERTS. *NASA Spec* 351, 309–317.

Rustioni, L., Grossi, D., Brancadoro, L., and Failla, O. (2018). Iron, magnesium, nitrogen and potassium deficiency symptom discrimination by reflectance spectroscopy in grapevine leaves. *Scientia Hortic.* 241, 152–159. doi: 10.1016/j.scienta.2018.06.097

Sanchez, L., Ermolenkov, A., Biswas, S., Septiningsih, E. M., and Kurouski, D. (2020). Raman spectroscopy enables non-invasive and confirmatory diagnostics of salinity stresses, nitrogen, phosphorus, and potassium deficiencies in rice. *Front. Plant Sci.* 11. doi: 10.3389/fpls.2020.573321

Severtson, D., Callow, N., Flower, K., Neuhaus, A., Olejnik, M., and Nansen, C. (2016). Unmanned aerial vehicle canopy reflectance data detects potassium deficiency and green peach aphid susceptibility in canola. *Precis. Agric.* 17 (6), 659–677. doi: 10.1007/s11119-016-9442-0

Smart, A. J., Schacht, W. H., Moser, L. E., and Volesky, J. D. (2004). PREDICTION OF LEAF/STEM RATIO USING NEAR-INFRARED REFLECTANCE SPECTROSCOPY (NIRS) a TECHNICAL NOTE. *Agron. J.* 96 (1), 316–318. doi: 10.2134/agronj2004.3160

St Luce, M., Whalen, J. K., Ziadi, N., and Zebarth, B. J. (2011). Nitrogen dynamics and indices to predict soil nitrogen supply in humid temperate soils. *Adv. Agron.* 112 112, 55–102. doi: 10.1016/B978-0-12-385538-1.00002-0

Sun, D. W., Robbins, K., Morales, N., Shu, Q. Y., and Cen, H. Y. (2022). Advances in optical phenotyping of cereal crops. *Trends Plant Sci.* 27 (2), 191–208. doi: 10.1016/j.tplants.2021.07.015

Toth, C., and Jozkow, G. (2016). Remote sensing platforms and sensors: A survey. *Isprs J. Photogrammetry Remote Sens.* 115, 22–36. doi: 10.1016/j.isprsjprs.2015.10.004

Ueno, H., Maeda, T., Katsuyama, N., Katou, Y., Matsuo, S., Yano, K., et al. (2018). Cation measurements and gene expression analysis suggest tomato leaf marginal necrosis is caused by a jasmonate signal induced by k+ starvation in the tip region of leaflets. *Horticult J.* 87 (2), 206–213. doi: 10.2503/hortj.OKD-101

Vega, F. A., Ramirez, F. C., Saiz, M. P., and Rosua, F. O. (2015). Multi-temporal imaging using an unmanned aerial vehicle for monitoring a sunflower crop. *Biosyst. Eng.* 132, 19–27. doi: 10.1016/j.biosystemseng.2015.01.008

Wu, H., Song, Z., Niu, X., Liu, J., Jiang, J., and Li, Y. (2022). Classification of toona sinensis young leaves using machine learning and UAV-borne hyperspectral imagery. *Front. Plant Sci.* 13. doi: 10.3389/fpls.2022.940327

Xue, L., Cao, W., Luo, W., Dai, T., and Zhu, Y. (2004). Monitoring leaf nitrogen status in rice with canopy spectral reflectance. *Agron. J.* 96 (1), 135–142. doi: 10.2134/agronj2004.1350

Xu, C. P., and Mou, B. Q. (2016). Responses of spinach to salinity and nutrient deficiency in growth, physiology, and nutritional value. *J. Am. Soc. Hortic. Sci.* 141 (1), 12–21. doi: 10.21273/Jashs.141.1.12

Zaghwan, A., and Gunawan, I. (2021). Energy loss impact in electrical smart grid systems in Australia. *Sustainability* 13 (13), 7221. doi: 10.3390/su13137221

Zermas, D., Teng, D., Stanitsas, P., Bazakos, M., Kaiser, D., Morellas, V., et al. (2015). Automation solutions for the evaluation of plant health in corn fields, 2015 IEEE/RSJ International Conference on Intelligent Robots and Systems (IROS). 2015, 6521–6527. doi: 10.1109/IROS.2015.7354309

Zhang, Y. H., Chu, G., Li, P. P., Hu, X. G., and Wu, X. D. (2017). Three-layer concept drifting detection in text data streams. *Neurocomputing* 260, 393–403. doi: 10.1016/j.neucom.2017.04.047

Zhang, Y. C., Yang, W., Sun, Y., Chang, C., Yu, J. Y., and Zhang, W. B. (2021). Fusion of multispectral aerial imagery and vegetation indices for machine learning-based ground classification. *Remote Sens.* 13 (8), 1411. doi: 10.3390/rs13081411

Zhu, T., Lin, Y., and Liu, Y. (2017). Synthetic minority oversampling technique for multiclass imbalance problems. *Pattern Recog* 72, 327–340. doi: 10.1016/j.patcog.2017.07.024

Zhu, W., Sun, Z., Huang, Y., Yang, T., Li, J., Zhu, K., et al. (2021). Optimization of multi-source UAV RS agro-monitoring schemes designed for field-scale crop phenotyping. *Precis. Agric.* 22 (6), 1768–1802. doi: 10.1007/s11119-021-09811-0

frontiers | Frontiers in Plant Science

TYPE Original Research
PUBLISHED 23 January 2023
DOI 10.3389/fpls.2023.1034421

Check for updates

OPEN ACCESS

EDITED BY
Gabrijel Ondrasek,
University of Zagreb, Croatia

REVIEWED BY
Muhammad Musa Khan,
Zhejiang University, China
Weina Zhang,
Huanghuai University, China

*CORRESPONDENCE
Bryan G. Hopkins
hopkins@byu.edu

SPECIALTY SECTION
This article was submitted to Plant Nutrition, a section of the journal Frontiers in Plant Science

RECEIVED 01 September 2022
ACCEPTED 03 January 2023
PUBLISHED 23 January 2023

CITATION
Jamal A, Saeed MF, Mihoub A, Hopkins BG, Ahmad I and Naeem A (2023) Integrated use of phosphorus fertilizer and farmyard manure improves wheat productivity by improving soil quality and P availability in calcareous soil under subhumid conditions. *Front. Plant Sci.* 14:1034421. doi: 10.3389/fpls.2023.1034421

Integrated use of phosphorus fertilizer and farmyard manure improves wheat productivity by improving soil quality and P availability in calcareous soil under subhumid conditions

Aftab Jamal[1], Muhammad F. Saeed[2], Adil Mihoub[3], Bryan G. Hopkins[4*], Iftikhar Ahmad[2] and Asif Naeem[5]

[1]Department of Soil and Environmental Sciences, Faculty of Crop Production Sciences, University of Agriculture, Peshawar, Pakistan, [2]Department of Environmental Science, COMSATS University, Islamabad, Vehari Campus, Vehari, Pakistan, [3]Center for Scientific and Technical Research on Arid Regions, Biophysical Environment Station, Touggourt, Algeria, [4]Department of Plant and Wildlife Sciences, Brigham Young University, Provo, Utah, United States, [5]Soil and Environmental Sciences Division, Nuclear Institute for Agriculture and Biology, Faisalabad, Pakistan

Introduction: Low soil fertility and high fertilizer costs are constraints to wheat production, which may be resolved with integrating fertilizer phosphorus (P) and farm-yard manure (FYM). Study objectives were to evaluate P source impacts on soil, P efficiency, and wheat growth in a calcareous soil.

Methods: Treatments included P fertilizer (0, 17, 26, or 39 kg P ha-1) and/or FYM (0 or 10 T ha-1) in a: 1) incubation experiment and 2) wheat (Triticum aestivum spp.) field experiment.

Results and Discussion: Soil organic matter increased (30-72%) linearly for both fertilizer and FYM, whereas pH decreased (0.1-0.3 units) with fertilizer only. Addition of fertilizer and FYM increased plant available P (AB-DTPA extractable soil P) an average of 0.5 mg P kg-1 soil week-1 with incubation. The initial increase was 1-9 mg P kg-1, with further increase after 84 d of ~3-17 mg P kg-1. There was also a significant increase of available P in the soil supporting plants in the field study, although the magnitude of the increase was only 2 mg kg-1 at most for the highest fertilizer rate + FYM. Grain (66 to 119%) and straw (25-65%) yield increased significantly, peaking at 26 kg P ha-1 + FYM. The P Absorption Efficiency (PAE), P Balance (PB), and P Uptake (PU) increased linearly with P rate, with the highest levels at the highest P rate. The P Use Efficiency (PUE) was highest at the lowest rates of P, with general decreases with increasing P, although not consistently. Principal component analysis revealed that 94.34 % of the total variance was accounted for with PC1 (84.04 %) and PC2 (10.33 %), with grain straw yield significantly correlated to SOM, PU, and PAE. Regression analysis showed highly significant correlation of PB with P-input (R2= 0.99), plant available P (R2= 0.85), and PU (R2= 0.80). The combination of FYM at the rate of 10 T ha-1 and fertilizer P at 26 kg P ha-1 was found as the optimum dose that significantly increased yield. It is concluded that FYM concoction with fertilizer-P not only improved SOM and residual soil P, but also enhanced wheat yields with reasonable P efficiency.

KEYWORDS

manure, phosphorus, wheat, calcareous, phosphorus absorption efficiency, phosphorus balance, phosphorus uptake, phosphorus use efficiency

1 Introduction

Wheat (*Triticum aestivum* L.) is the world's leading agronomic crop in production value and acreage (Hopkins and Hansen, 2019). Wheat is Pakistan's most important cereal crop, accounting for 8.7% of agricultural value addition and 1.7% of the gross domestic product (GDP) (Khan et al., 2022).

Although Pakistan's soil and climate conditions are favorable and high-yielding cultivars are available, wheat grain production is reduced due to the calcareous nature of most Pakistani soils and poor nutrient management, particularly that of phosphorus (P) (Ul-Allah et al., 2018). Low soil fertility due to continuous cropping, with little or no external inputs and crop residue removal, are other causes of low production (NFDC, 2001).

Plants require P as an essential macronutrient to complete their life cycles (Marschner, 2012; Hopkins, 2015; Ding et al., 2020; Hopkins, 2020). In calcareous soils, a majority of applied P fertilizer is adsorbed on the calcite surface and becomes temporarily unavailable to plants, which can cause a yield reduction (Hopkins, 2015; Saeed et al., 2021). Plant-available P in soil is affected by soil chemistry properties, especially pH and limestone content (Lindsay, 2001; Fixen and Bruulsema, 2014). Calcareous soils are commonly deficient in plant-available P due to poor solubility as a result of fixation and sorption (Lindsay, 2001; Manzoor, 2013; Hopkins et al., 2014; Mihoub and Boukhalfa-Deraoui, 2014; Deraoui et al., 2015; Hopkins, 2020). The resulting effect of low P solubility is relatively poor fertilizer P efficiency (Jamal et al., 2018; Mihoub et al., 2019). Thus, a great majority of calcareous soils need relatively high amounts of extraneous supplementation of P for sustained crop yield (Fixen and Bruulsema, 2014; Hopkins et al., 2014; Hopkins and Hansen, 2019; Pradhan et al., 2021). Therefore, P dynamics in these soils must be known to evaluate their availability to plants (Manzoor, 2013).

Furthermore, the present price boost in P fertilizers is reflected in its decreased application to crops by resource-poor farmers, potentially resulting in reduced crop production (Aboukila et al., 2018). In some regions, including Pakistan, it is difficult to convince the farming community to apply full-recommended fertilizer doses for wheat, but it seems possible to improve fertilizer P use efficiency (PUE) in calcareous soils by selecting efficient P sources and adopting appropriate time and methods of application. To address the aforementioned issues, cost-effective, environmentally friendly, and more productive farming technologies must be developed (Hopkins, 2015; Mihoub et al., 2019; Hopkins, 2020).

Yields have steadily increased since the onset of the Green Revolution, and as a result, there is an increasing need to efficiently supply P to plants while minimizing negative impacts on the environment (Hopkins and Hansen, 2019; Khan et al., 2022). Many studies have shown that organic manures may partially or entirely substitute chemical fertilizers, reducing dependency on limited rock phosphate reserves (Khan et al., 2022; Mihoub et al., 2022). Manure (commonly referred to as "farmyard manure" (FYM) in some regions, including Pakistan) is less concentrated, and P is bound to various molecules that must be decomposed to convert it to inorganic phosphates that plants can take up (Hopkins, 2015; Mihoub et al., 2022). However, an advantage of the FYM is that it also contains all other essential plant nutrients, which can reduce the possibility of P-induced deficiencies of other nutrients (Barben et al., 2011). It is also considered a slow-release source of P (Hopkins, 2015). The FYM also contains a wide variety of other molecules, including organic acids, that can be beneficial as they improve P movement through soil and bioavailability (Hill et al., 2015a; Hill et al., 2015b; Hopkins, 2015; Summerhays et al., 2015). The addition of soil organic matter (SOM) may improve soil chemical, physical, and biological properties, which can then positively impact nutrient cycling and provide an enhanced environment for vegetation growth (Wu et al., 2013).

As previously mentioned, animal manures are considered a valuable nutrient source when applied to the soil with proper management (Pradhan et al., 2021), although it has also been reported that the sole application of organic amendments could hamper nutrient availability due to fixation (Hazra et al., 2018). Its decomposition rate is relatively faster than many other organic nutrient sources (Rehim et al., 2020), but this decomposition can lead to increases in SOM. This process can play a prominent role in improving soil structure, which in turn provides favorable environments for root development (Zhang et al., 2014) and improves soil water-holding capacity (Wu et al., 2013). It has been reported as a valuable fertilizer for wheat (*Triticum aestivum* L.) production by increasing SOM content (Rehim et al., 2020).

In this regard, the integration of traditional chemical P fertilizers and organic amendments, such as FYM, could be a possible option for improving the efficiency of fertilizer P use in highly calcareous P-sorbing soils (Hopkins, 2015). Although there are many studies examining chemical fertilizer and manure P in wheat, there needs to be an evaluation of the changes in P transformations and grain yield of bread wheat induced by the combined application of FYM and chemical P fertilizer. Moreover, it needs to be clarified how P fertilizer in combination with FYM may affect nutrient balance and the need for, or not, chemical fertilizers in calcareous soils. This point is considered one of the most important recent trends in studies related to soil quality and soil-plant relations regarding P under these conditions.

Therefore, studies were conducted to determine whether the combination of P fertilizer with FYM in calcareous soils under subhumid climatic conditions found in Pakistan can: (1) improve soil properties and P availability; (2) improve phosphorus absorption efficiency (PAE), phosphorus balance (PB), phosphorus uptake (PU), and PUE in wheat; and (3) increase wheat productivity. For this study, it was hypothesized that the application of inorganic P in combination with FYM improves wheat grain yield by improving soil properties, PAE, PB, PU, and PUE in calcareous soils.

2 Materials and methods

2.1 Experimental site and soil characteristics

The experiment was carried out at a greenhouse and a field location immediately next to each other located at the Institute of Biotechnology and Genetic Engineering at the University of Agriculture, Peshawar, Pakistan (34° 01′, 14.2″ N and 71° 28′, 52.6″ E). The preceding crop in the location was maize (*Zea mays* L.). This region lies 340 m above sea level and is classified as a warm-temperate zone. The average annual temperature is ~22°C, with the highest average in June at ~33°C and the lowest in January at ~10°C. The average annual precipitation is 640 mm, with the least amount of rainfall occurring in November.

A composite soil sample was collected at 0–20 cm depth before the experiment with the following results: pH = 8.4 (Richards, 1954), salinity as electrical conductivity (EC) = 0.25 dS m^{-1} (Richards, 1954), SOM = 5.9 g kg^{-1} (Nelson and Sommers, 1982), total nitrogen (N) = 5 mg kg^{-1}, and plant-available P and potassium (K) = 4.7 and 130 mg kg^{-1}, respectively, as determined through extraction with ammonium bicarbonate-diethylenetriamine pentaacetate (AB-DTPA) (Soltanpour, 1985).

2.2 Experimental design and measurements

2.2.1 Treatments: Laboratory incubation and field experiment

Four chemical P fertilizer rates were applied without or with 10 T FYM ha^{-1} in both studies (Table 1). The chemical fertilizer was single superphosphate (SSP; 8% P). The FYM was derived from well-decomposed cattle (*Bos taurus*) excreta (dung and urine) mixed with some crop residues, such as rice and cotton straw. The physiochemical properties and nutrient constituents of FYM were as follows: brown to black color, pH = 8.0, EC = 2.1 dS m^{-1}, total N = 13.6 g kg^{-1}, total P = 1.5 g kg^{-1}, and total K = 8.4 g kg^{-1}.

2.2.2 Soil P release dynamics and mineralization potential: Laboratory incubation

A laboratory experiment was carried out by applying fertilizer and/or FYM (Table 1) to 1 kg of soil in plastic pots with no drainage holes. Before filling the soil in pots, the soil and the fertilizer and/or FYM were thoroughly mixed. Each treatment had three replicates, and the pots were arranged in a completely randomized design (CRD) and incubated under laboratory conditions of a 16-h light and 8-h dark cycle at 25°C ± 1°C and 55%–65% relative humidity for 84 days. Distilled water (DW) was added as needed to maintain adequate soil moisture at near-field capacity.

Triplicate soil samples from each treatment were spectrophotometrically analyzed for plant-available P after 0, 7, 14, 28, 56, and 84 days of incubation. The change in P content (weekly turnover) was calculated by subtracting the initial plant-available P at 0 days from the final P at 84 days and dividing by the total number of weeks (12). Mineralization potential (kg ha^{-1} $week^{-1}$) was calculated by multiplying weekly turnover in milligrams of P per kilogram of soil per week (the assumption is that the weight of 1-ha soil is approximately 2×10^6 kg; Sarir et al., 2006).

TABLE 1 Phosphorus (P) treatment rates (kg ha^{-1}) applied as single superphosphate (SSP) and/or farmyard manure (FYM) for a laboratory and a field experiment.

Treatment	Chemical fertilizer (F)		Manure fertilizer (M)		Total P applied
ID	P (kg ha^{-1})	SSP (kg ha^{-1})	P (kg ha^{-1})	FYM (T ha^{-1})	P (kg ha^{-1})
F_0M_0	0	0	0	0	0
F_0M_{15}	0	0	15	10	15
$F_{17}M_0$	17	220	0	0	17
$F_{17}M_{15}$	17	220	15	10	32
$F_{26}M_0$	26	330	0	0	26
$F_{26}M_{15}$	26	330	15	10	41
$F_{39}M_0$	39	500	0	0	39
$F_{39}M_{15}$	39	500	15	10	54

The ID is derived from the rates of SSP fertilizer (F) at 0, 17, 26, or 39 kg P ha^{-1} and manure (M) at 0 or 10 T FYM ha^{-1} with 0 or 15 kg P ha^{-1}, respectively (FYM = 0.15% P).

2.2.3 P efficiency and yield: Field experiment

A field study was conducted by applying the same fertilizer/FYM treatments as described in experiment 1 (Table 1). The experimental field was plowed to a 30-cm depth using a rotavator, and then the SSP and/or FYM were applied to the soil in respective plots, each of 10 m^2, before crop sowing with tillage. The experimental treatments were arranged in a randomized complete block design (RCBD) with three replicates. The seeds of the wheat variety ATTA-HABIB-2010 were surface disinfected with 1% sodium hypochlorite (NaOCl) to minimize microorganism growth on the seed and then rinsed two to three times with DW. The disinfected seeds were then sown at a seeding rate of 120 kg ha^{-1} with a 25-cm row spacing.

The plots were furrow-irrigated. Fertilizer K was applied as potassium sulfate (K_2SO_4) to all plots prior to the first irrigation at 22 kg K ha^{-1}. At the first and second irrigations, fertilizer N was split and applied in two equal doses as urea [$CO(NH_2)_2$] to all plots at 110 kg N ha^{-1}. The N and K were not balanced, with plots receiving FYM having an additional 136 and 84 kg ha^{-1} of N and K, respectively. However, there was no evidence of deficiency or excess of either of these or other nutrients, and, therefore, it is assumed that these nutrients had no effect on the treatments.

The crop was generally raised using the best agronomic and cultural management practices. The crop was largely free of insect and disease damage. No pesticides were applied. Weeds were pulled by hand as and when required. The wheat was hand-harvested using a sickle.

At maturity, whole plant samples were randomly collected from each plot to determine P concentration and accumulation by wheat plants (Jackson, 1973). The total dry matter yield of each plot was recorded; wheat grains were separated using a micro-plot thresher (Kissan wheat thresher, Gojra, Pakistan), and grain yield was recorded. Postharvest soil samples were collected from each plot and the soil properties measured prior to planting were determined again.

To assess changes in the efficiency of applied P fertilizer in the presence of FYM, P uptake (PU; kg ha^{-1}) was calculated by multiplying the nutrient concentration values with the total dry matter yield (Eq. 1).

$$PU = P\ \text{content in plant tissue} \times \text{total plant dry matter} \quad (1)$$

In addition, the percent P uptake efficiency (PUE) was calculated by subtracting the PU in unfertilized soil from fertilized soil and dividing by the P applied (Eq. 2) (Syers et al., 2008).

$$PUE = \frac{\text{PU in fertilized soil} - \text{PU in unfertilized soil}}{\text{P applied to the soil}} \quad (2)$$

The PAE (mg mg^{-1}) was calculated by dividing PU by available soil P (Eq. 3) (adapted from Castillo et al., 2013):

$$PAE = \frac{PU}{\text{Available P}} \quad (3)$$

Finally, the PB (kg ha^{-1}) was calculated by subtracting the P output in the harvested wheat crop (measured as PU) from the total P input (P in fertilizer + P in FYM) (Eq. 4) (Sun et al., 2018).

$$PB = P\ \text{input} - PU \quad (4)$$

2.3 Statistical analysis

The experimental data were statistically evaluated using the statistical software MSTATC 8.1. A two-way ANOVA (in randomized blocks) was used to analyze data, considering the application rates of mineral fertilizer (SSP) and organic amendment (FYM) as the two factors. The significant differences between treatments were compared by critical difference at a 5% level of probability using the *F*-test. A principal component analysis (PCA) was done to classify the treatments according to the measured parameters and to identify the parameters that determine yield increases and P efficiency. A cluster analysis (CA) was performed using Ward's method to determine the most important traits related to grain yield. A simple linear regression was performed to show the

TABLE 2 Laboratory incubation: effect of fertilizer phosphorus (P) and farmyard manure (FYM) applications on soil AB-DTPA extractable P transformation during 12 weeks of incubation.

Trts	Incubation period (day)						Mean	Net increase
	0	7	14	28	56	84		
	Plant-available P (AB-DTPA extractable; mg P kg^{-1} soil)							
F_0M_0	6.13 ± 0.15 g	6.54 ± 0.55 e	6.38 ± 0.91 e	5.95 ± 0.19 d	6.48 ± 0.57 g	6.56 ± 0.31 g	6.34 ± 0.24 h	0.43d
F_0M_{15}	6.86 ± 0.14 f	7.73 ± 0.05 d	8.17 ± 0.04 d	8.84 ± 0.13 c	8.98 ± 0.22 f	9.14 ± 0.17 f	8.28 ± 0.88 g	2.28c
$F_{17}M_0$	9.30 ± 0.68 e	8.90 ± 0.27 c	7.55 ± 0.47 d	9.85 ± 0.24 c	10.70 ± 0.52 e	11.52 ± 0.29 e	9.63 ± 1.39 f	2.22c
$F_{17}M_{15}$	10.99 ± 0.22 d	9.25 ± 0.32 c	10.44 ± 0.86 c	13.40 ± 0.47 b	14.18 ± 0.19 d	14.48 ± 0.15 d	12.1 ± 2.18 e	3.49bc
$F_{26}M_0$	12.10 ± 0.10 c	11.02 ± 0.18 b	9.85 ± 0.13 c	13.17 ± 0.26 b	15.31 ± 0.26 c	16.23 ± 0.53 c	12.94 ± 2.46 d	4.13b
$F_{26}M_{15}$	13.94 ± 1.0 ab	12.44 ± 10.08 a	13.60 ± 0.39 a	15.89 ± 1.79 a	17.87 ± 0.98 b	18.43 ± 0.61 b	15.36 ± 2.43 b	4.49b
$F_{39}M_0$	15.21 ± 0.07 a	13.11 ± 0.01 a	12.10 ± 0.10 b	16.25 ± 0.04 a	20.22 ± 0.02 a	23.40 ± 0.01 a	16.71 ± 4.33 a	8.19a
$F_{39}M_{15}$	13.27 b ± 0.1 b	11.22 ± 0.01 b	12.38 ± 0.01 b	15.44 ± 0.01 a	18.44 ± 0.01 b	19.12 ± 0.01 b	14.97 ± 3.26 c	5.85b

Means within each column with different letters per column are significantly different at $p< 0.05$. In the treatment (Trts) column, the letters represent fertilizer (F) and FYM (M), while the numbers represent the rate of P in kilograms per hectare. Data are shown as means ± SD ($n = 3$).

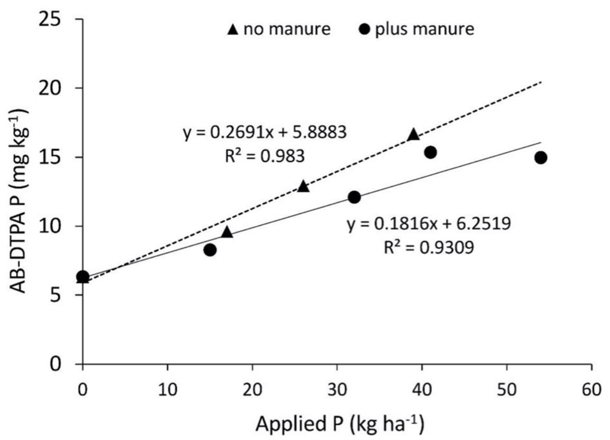

FIGURE 1
Correlations between plant-available P (extracted with ammonium bicarbonate-diethylenetriamine pentaacetate (AB-DTPA)) and applied P for soil incubated under laboratory conditions. The applied P was chemical fertilizer applied as a single superphosphate (SSP) and/or manure (farmyard manure (FYM)).

relationship of PB with PU, plant-available P (AB-DTPA), and P input (Excel 2007 software). The PCA and CA analyses were performed using the XLSTAT statistical package software (ver. 2022.1.1.1251, Excel Add-ins).

3 Results

3.1 Weekly turnover and mineralization potential of P: Laboratory incubation

There were several statistical differences in the laboratory incubation trial (Supplementary Table S1). In the control treatment (F_0M_0), the plant-available P had only minor fluctuations over time (Table 2). Initially (day 0 of incubation), there were significant increases (~1–9 mg P kg^{-1}) in plant-available P that were mostly proportional to the applied P rate. By the end of the study (84 days), the differences had increased (~3–17 mg P kg^{-1}) as the fertilizer and FYM P moved towards equilibrium with the soil.

The rate of this increase was gradual over the incubation time when the soil was treated with only FYM at 10 T ha^{-1} (F_0M_{15}). The remaining fertilized treatments, regardless of whether they were applied with FYM or not, tended to have a slight decrease in available P during the initial phase of incubation and thereafter an increase. The correlations between available and applied P was very high, especially when no FYM was applied (Figure 1).

The application of fertilizer P alone, as well as in conjunction with FYM, significantly affected the weekly turnover and mineralization potential of P in these calcareous soils (Supplementary Table S2; Table 3). The average change of plant-available P (weekly turnover) with applied P was 0.49 mg P kg^{-1} soil, which was significantly greater than the control. The increase in weekly turnover P against 17 to 26 kg P ha^{-1} was 56% and 19%, respectively. A decline in weekly turnover P was recorded when the soil was treated with the highest fertilizer P at 39 kg P ha^{-1} in conjunction with FYM. The application of FYM significantly increased mineralization potential at 0, 17, 39, and 26 kg P ha^{-1} (Supplementary Table S3). A maximum mineralization potential of 32.8 kg P ha^{-1} was recorded in the treatment ($F_{39}M_0$) followed by treatments ($F_{39}M_{15}$) and ($F_{26}M_{15}$) with values of 22.5 and 19.5 kg P ha^{-1}, respectively.

3.2 Straw and grain yields: Field experiment

There were significant differences in grain and straw yields (Table 4) for both P sources, as well as their interaction (fertilizer, FYM, and fertilizer × FYM). There were increases in grain and straw yields over the control for all fertilized treatments (Figure 2).

A significant increase in grain yield was observed with the addition of fertilizer P alone and in combination with FYM, as compared with the control treatment (Figure 2). Maximum grain yield was produced with the highest rate of fertilizer (39 kg P ha^{-1}), whether FYM was added or not. However, FYM allowed a statistically equivalent yield where it peaked at the second-highest rate of fertilizer (26 kg P ha^{-1}) when FYM was also included, which was higher than the yield at this same rate of fertilizer without FYM and all other lower fertilizer rates. Applications of 26 and 39 kg P ha^{-1}, reinforced with 10 T ha^{-1} FYM, increased grain yield by 33% and 28%, respectively, as compared with the same amount of fertilizer P applied alone.

TABLE 3 Laboratory incubation: effect of fertilizer phosphorus (P) and farmyard manure (FYM) application on weekly turnover P and mineralization potential.

Trts	Weekly P turnover (mg P kg^{-1} soil week^{-1})	Mineralization potential (kg P ha^{-1} season^{-1})
F_0M_0	0.03 ± 0.01 f	1.65 ± 0.70 f
F_0M_{15}	0.19 ± 0.01 e	9.12 ± 0.52 e
$F_{17}M_0$	0.18 ± 0.07 e	8.85 ± 3.59 e
$F_{17}M_{15}$	0.29 ± 0.09 d	13.73 ± 0.38 e
$F_{26}M_0$	0.34 ± 0.03 d	16.49 ± 1.79 d
$F_{26}M_{15}$	0.40 ± 0.03 c	19.50 ± 1.82 c
$F_{39}M_0$	0.68 ± 0.06 a	32.78 ± 0.266 a
$F_{39}M_{15}$	0.46 ± 0.03 b	22.49 ± 1.57 b

Means with different letters in the columns are significantly different at $p< 0.05$. The treatments (Trts) with F0, F17, F26, and F39 are 0, 17, 26, or 39 kg ha^{-1} of fertilizer P application, respectively, and with M0 or M15 are 0 and 10 t ha^{-1} of farmyard manure (FYM), respectively (10 T FYM ha^{-1} possesses 0.15% P or 15 kg ha^{-1}). Data are shown as means ± SD (n = 3).

TABLE 4 Field study: Statistics (F-Values with P-value significance indicated) for soil properties, yields, and P efficiency.

SOV	DF	SOM	pH	GY	SY	Soil P	PU	PUE	PAE	PB
Fertilizer (F)	3	4.4**	5.4**	23.5**	133.7**	24**	348.7**	13.7**	38.8**	4,408.2**
Manure (M)	1	5.1**	3.5^{ns}	24.3**	90.8**	6.6*	292.3**	60.7**	59**	3,485.5**
F × M	3	0.3^{ns}	0.8^{ns}	3.3*	7.9**	0.9^{ns}	45**	171.7**	17.2**	45**

SOV, source of variation; DF, degrees of freedom; SOM, soil organic matter; GY, grain yield; SY, straw yield; soil P, plant-available P as measured by AB-DTPA extractable soil P; PU, phosphorus uptake; PUE, P use efficiency; PAE, P acquisition efficiency; PB, P balance. *p < 0.05; **p < 0.01; *ns*, not significant.

Similarly, the maximum straw yield was achieved with the second-highest fertilizer P rate (26 kg P ha^{-1}) with FYM (Figure 2). However, this was again statistically similar to that of the highest fertilizer rate (39 kg P ha^{-1}).

3.3 P efficiency: Field experiment

There were significant differences in PU, PB, PUE, and PAE (Table 4) for both P sources, as well as their interaction (fertilizer, FYM, and fertilizer × FYM). There were increases in PU, PB, and PAE over the control for all fertilized treatments (Table 5; Figure 3). As is typical, the PUE was highest at the lowest rates of P (Table 5).

Not surprisingly, the PB, PU, and PAE increased somewhat linearly with the P rate and were significantly highest at the highest P rate ($F_{39}M_{15}$) (Table 5; Figure 3). When comparing with and without FYM, these parameters were higher with FYM at every fertilizer rate except PU and PAE at 17 kg P ha^{-1}. It was observed that in the control treatment (F_0M_0), the PU exceeded the P additions, leading to a slightly negative PB, whereas for all the other treatments, the PB was positive (Figure 3). This indicates residual P in the soil, which may benefit subsequent crops and soil P fertility. The PU followed similar trends as straw yield.

As expected, the maximum PUE was observed with the lowest P fertilizer level with FYM only (F_0M_{15}) as compared to the untreated control and was less for the low fertilizer rate ($F_{17}M_0$) (Table 5). The PUE decreased as fertilizer increased from 17 to 26 kg P ha^{-1} ($F_{17}M_0$ and $F_{26}M_0$, respectively). Surprisingly, the PUE did not decrease further at the highest P rate ($F_{39}M_0$). When FYM was added, the PUE decreased at the low fertilizer rate ($F_{17}M_0$ vs. $F_{17}M_{15}$), but curiously increased at the next highest rate ($F_{26}M_0$ vs. $F_{26}M_{15}$), and there was no difference at the highest rate ($F_{39}M_0$ vs. $F_{39}M_{15}$). Unexpectedly, the lowest PUE was at the lowest fertilizer rate with FYM ($F_{17}M_{15}$).

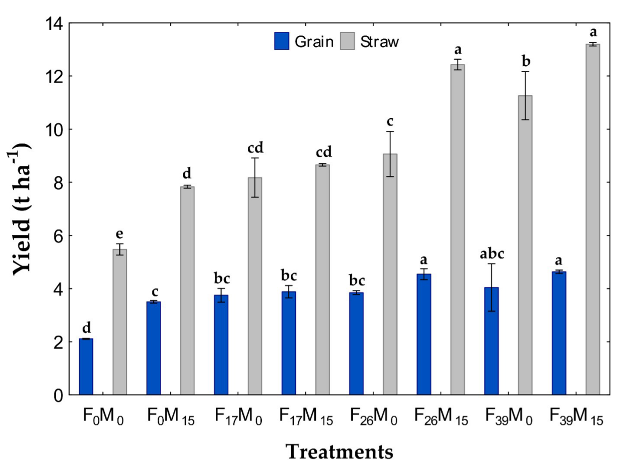

FIGURE 2
Wheat grain and straw yield as affected by P application from fertilizer (F) and/or farmyard manure (FYM). Fertilizer was applied at 0, 17, 26, or 39 kg P ha^{-1}, and FYM was applied at 0 or 10 T ha^{-1} with 0 or 15 kg P ha^{-1}, respectively (FYM = 0.15% P). Treatment means with different letters are significantly different at p< 0.05. Data are shown as means ± SD (n = 3).

3.4 Postharvest soil properties: Field experiment

There were highly significant differences in SOM (Table 4) for both P sources (fertilizer and FYM) but not for the interaction. For fertilizer (F), combined across FYM treatments, the increase was mostly linear and significant at the two highest P rates (Figure 4A). For FYM (M), combined across fertilizer rates, the increase was also significant (Figure 4B).

There were highly significant differences in pH (Table 4) for fertilizer P but not FYM or the interaction. For F, combined across FYM treatments, the decrease was mostly linear for the first two fertilizer rates but then plateaued across the highest two rates (Figure 4A). For FYM (M), there was a trend for a pH decrease with the FYM application, but the difference was not significant (Figure 4B).

There were highly significant differences in plant-available P, as measured by AB-DTPA-extractable soil P (Table 4), for both P sources (fertilizer and FYM), but not for the interaction. Application of P alone, as well as in combination with FYM, modestly increased postharvest available P over the control, with a general increase as the P rate increased (Table 5). The highest P rate resulted in a significant increase over the control (p< 0.05).

3.5 PCA and correlation: Field experiment

The PCA was computed to detect interrelationships among measured traits and to determine the importance of the measured traits on the evaluation of grain yield and P efficiency; the PCA was conducted using the experimental dataset including all eight treatments and 11 variables to reduce the dimensionality of the data and to reveal the potential relationships among the measured traits. The PCA results identified that the first two principal components (PCs) with eigenvalues of >1 were accounted for (Table 6). The measured traits are appropriate for accounting 94.34% of the total variance: PC1 (84.04%) and PC2 (10.33%). The PC1 was mainly explained by: SOM, pH, grain yield (GY), straw (SY),

TABLE 5 Field study: effect of fertilizer phosphorus (P) and farmyard manure (FYM) application on postharvest plant-available P (AB-DTPA extractable P), P uptake (PU), P use efficiency (PUE), and P acquisition efficiency (PAE).

Trts	AB-DTPA P (mg P kg^{-1} soil)	PU (kg P ha^{-1})	PUE (%)	PAE (mg mg^{-1} soil P)
F_0M_0	4.27 ± 0.04 d	7.00 ± 0.2 f	–	1.66 ± 0.04 e
F_0M_{15}	4.48 ± 0.04 cd	19.30 ± 0.3 de	35.6 ± 1.0 a	4.31± 0.08 cd
$F_{17}M_0$	4.67 ± 0.02 cd	18.70 ± 1.4 de	28.9 ± 3.7 b	4.02 ± 0.29 cd
$F_{17}M_{15}$	5.06 ± 0.71 bc	18.00 ± 0.1 e	14.6 ± 0.2 d	3.63 ± 0.52 d
$F_{26}M_0$	5.29 ± 0.12 b	20.80 ± 0.8 d	22.7 ± 1.4 c	3.94 ± 0.07 cd
$F_{26}M_{15}$	6.19 ± 0.004 a	32.40 ± 1.2 b	27.0 ± 1.2 b	5.24 ± 0.19 ab
$F_{39}M_0$	6.11 ± 0.18 a	28.10 ± 1.2 c	23.2 ± 1.4 c	4.61 ± 0.20 bc
$F_{39}M_{15}$	6.35 ± 0.61 a	35.50 ± 0.3 a	22.8 ± 0.2 c	5.65 ± 0.51 a

Means within each column with different letters per column are significantly different at $p< 0.05$. In the treatment (Trts) column, the letters represent fertilizer (F) and FYM (M), while the numbers represent the rate of P in kilograms per hectare. Data are shown as means ± SD (n = 3).

plant-available P (AB-DTPA), PU, PB, P Transf, and week T. The PC2 showed a high correlation with only PAE and PUE.

Grain yield and straw yield were significantly correlated to SOM, PU, and PAE (Figure 5). Moreover, the superimposition of various treatments on the variable plot showed that wheat treated with the $F_{26}M_{15}$ and $F_{39}M_{15}$ treatments represented a higher correlation with soil P, weekly turnover, PB, SOM, PU, straw, and grain yield (Figure 5). In contrast, fertilizer-only P (up to 26) or FYM application showed a negative association with various parameters.

The information obtained from the application of PCA allowed the identification of the most important traits related to wheat yield. The PCA conferred the positive effects of mineral-P concoction with FYM on SOM, soil P, PU, and wheat yield. This notation is further sustained by the CA results, which revealed that most traits of the PC1 were located in the same group (cluster I) (Figure 6). This suggests that those traits clustered together could contribute the most to influencing wheat yield under our study conditions.

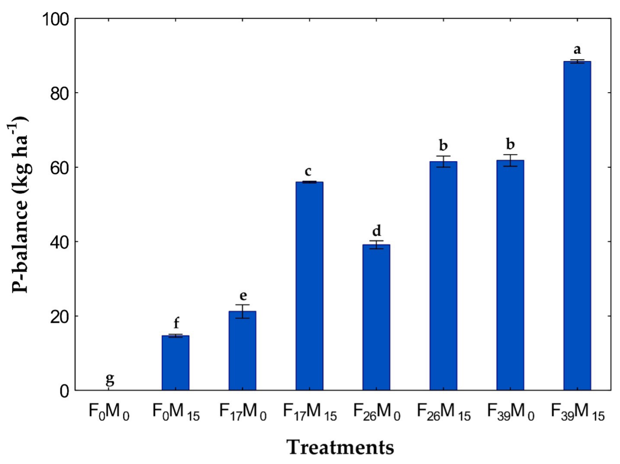

FIGURE 3
P balance (PB) is affected by P application from fertilizer (F) and/or farmyard manure (FYM). Fertilizer was applied at 0, 17, 26, or 39 kg P ha^{-1}, and FYM was applied at 0 or 10 T ha^{-1} with 0 or 15 kg P ha^{-1}, respectively (FYM = 0.15% P). Treatment means with different letters are significantly different at $p< 0.05$. Data are shown as means ± SD (n = 3).

A strong positive regression coefficient ($y = 0.782x - 8.439$, $R^2 = 0.98$) was observed between total P input and PB (Figure 7A). Positive values of PB are similar to the accumulation of P in soil and are good for soil fertility improvement, while negative values (such as for the zero P rate) indicate crop P starvation and suggest that the soil is being "mined" of soil P. This may result in a reduction in fertility (exhaustion). Similarly, there was a strong correlation between PB with plant-available P (AB-DTPA) ($y = 0.024x + 4.271$, $R^2 = 0.84$) (Figure 7B) and PU in plants ($y = 0.2644x + 11.362$, $R^2 = 0.80$) (Figure 7C). These observations indicate that PB is directly linked with the external application of P, which not only increased plant-available P (AB-DTPA) but was also helpful in the assimilation of P in growing plants.

4 Discussion

4.1 Plant-available P and mineralization potential

We generally observed a slow and gradual increase in plant-available P (AB-DTPA) with the addition of fertilizer P and FYM, which increased further with the incubation time. In general, FYM application has appreciable and dynamic impacts on the chemical fractions of P because P from FYM gradually turns into available forms over time (Hopkins, 2015; Ma et al., 2020).

It has been reported by Amin (2018) that the addition of FYM to calcareous soils significantly increased plant-available P (AB-DTPA). The increase in available P in our study might be due to the release of significant quantities of CO_2 during FYM decomposition (Andriamananjara et al., 2019) and the complexing of cations such as Ca^{+2}, thus reducing P fixation in calcareous soils (Lindsay, 2001; Fixen and Bruulsema, 2014; Jamal et al., 2018). The FYM contains organic acids, which are known to complex P and increase its solubility (Hill et al., 2015a; Hill et al., 2015b; Hopkins, 2015; Summerhays et al., 2015). Furthermore, FYM application, in conjunction with fertilizer P, increased the plant-available P throughout the incubation period. The application of animal manure, similar to the FYM used in this study, may increase the

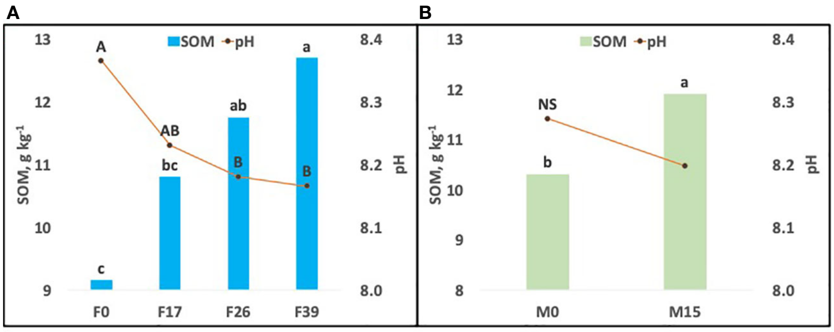

FIGURE 4
Postharvest soil pH and soil organic matter (SOM) as affected by P application from fertilizer (F) and/or farmyard manure (FYM). As the F × FYM interaction was not significant, the fertilizer graph **(A)** was averaged across FYM rates, and the FYM graph **(B)** was averaged across fertilizer rates. Fertilizer was applied at 0, 17, 26, or 39 kg P ha^{-1}, and FYM was applied at 0 or 10 T ha^{-1} with 0 or 15 kg P ha^{-1}, respectively (FYM = 0.15% P). Treatment means with different letters are significantly different at $p< 0.05$. Data are shown as means ± SD (n = 3).

bioavailability of soil P by improving the concentrations of soil-dissolved organic carbon (Jamal et al., 2018). Our results are in line with the study of Yan et al. (2016), who reported that manure application increased the proportion of plant-available P due to the transformation of stable P to labile P.

In our study, the mineralization potential was found to increase with increasing levels of fertilizer P. There is also some evidence of it increasing with FYM application, but only at the 0- and 26-kg P ha^{-1} fertilizer rates. However, the highest mineralization potential was achieved at the highest fertilizer P rate without FYM application, being significantly greater than all other treatments. Amin (2018) also found that high levels of FYM addition enhanced P mineralization in calcareous soils.

4.2 Postharvest soil properties

The application of fertilizer P generally increased SOM (Figure 4A). The addition of FYM also increased SOM. The increase in SOM with FYM treatment may be partially due to the input of organic matter found in the FYM (Rehim et al., 2020), although the increase in SOM with chemical fertilizer would not be explained by this as it contains no organic material. Rather, this increase is likely related to increased plant biomass in the current year's crop.

Other researchers have found that FYM not only reduced the oxidation stability of SOM but also improved the SOM content of the soil up to 1.2–2.9 kg ha^{-1} (Li et al., 2017; Ding et al., 2020). Furthermore, the addition of FYM with a combination of inorganic

TABLE 6 Field study: Principal component analysis (PCA) of the selected trials showing the amount of variance explained by individual principal components (PC) with PCA values.

Component	PC1	PC2
Eigenvalue	9.24	1.14
Variability %	84.04	10.33
Cumulative %	84.04	94.37
Parameters	Factor loadings	
SOM	0.837[a]	0.505
pH	−0.756[a]	−0.601
Grain yield	0.755[a]	0.628
Straw yield	0.901[a]	0.397
Plant-available P (AB-DTPA)	0.968[a]	0.189
PU	0.835[a]	0.513
PUE	0.063	0.969[a]
PAE	0.676	0.728[a]
PB	0.937[a]	0.253
P Transf	0.949[a]	0.201
Week T	0.885[a]	0.175

[a]Traits for the suggested factor.

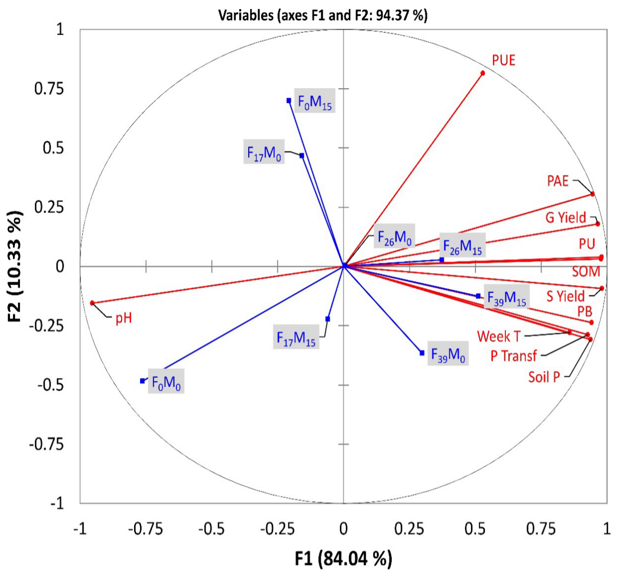

FIGURE 5
Principal component analysis (PCA) indicating the impact of treatments and their relationships with various soil properties and yield. Treatments (in blue font) are described in Table 1. Measured parameters (in red font) include phosphorus (P) use efficiency (PUE), P acquisition efficiency (PAE), grain yield (G yield), P uptake (PU), soil organic matter (SOM), straw yield (S yield), P balance (PB), and plant-available P (AB-DTPA) (soil P).

fertilizers to soil has been reported to increase the efficiency of applied fertilizers (Elgharably, 2020). Moreover, the addition of FYM with inorganic fertilizers can increase SOM and consequently soil water and nutrient holding capacity (Urbaniak et al., 2017).

The addition of FYM did not significantly decrease soil pH in our study, but it trended downward. Rehim et al. (2020) found that the addition of FYM decreased soil pH in calcareous sandy soil. The soil pH could have been reduced due to the chemical oxidation and microbiological decomposition of FYM in soil, which produced acidic compounds that help reduce soil pH. The production of organic acids (amino acid, glycine, cysteine, and humic acid) during the mineralization (ammonization and ammonification) of organic materials by heterotrophs and nitrification by autotrophs can also cause a decrease in soil pH (Kumar et al., 2020). We did measure a significant decrease in pH with the application of SSP fertilizer. During the mineralization and chemical transformations of organic and inorganic fertilizers, the H^+ ions released can decrease soil pH if the soil is not highly buffered with carbonates or similar substances (Hopkins, 2015; Ding et al., 2020).

The combined application of P fertilizers and organic amendments significantly increased P accumulation in soil, which agrees with the findings of various researchers (Hopkins, 2015; Qaswar et al., 2020; Rehim et al., 2020; Pradhan et al., 2021; Mihoub et al., 2022). This may be due to low levels of P in the soils and inputs from both organic and inorganic P sources (Shah et al., 2013).

Postharvest plant-available P (AB-DTPA) significantly increased with the application of fertilizer P. The addition of FYM increased this further, but only at one rate (possibly due to the great PU in the plant and less remaining in the soil). This effect may be attributed to the release of both P and low molecular weight organic acids during organic amendment decomposition (Pradhan et al., 2021). The organic acids/anions can dissolve insoluble P and compete with phosphate for adsorption sites on the surfaces of soil particles, thus increasing P availability (Jamal et al., 2018). Furthermore, organic amendments enhance soil biological and enzyme activities and increase organism abundance, thus enhancing P availability through dissolved organic carbon in the soil (Wu et al., 2013). The studied soil was highly calcareous, and the Ca–P was the most abundant fraction in these soils due to the high content of Ca^{2+} that forms calcium phosphates with P and hampers the availability of P (Saeed et al., 2021). The organic compounds can decrease the formation of Ca–P due to calcium solubilization by decreasing the soil pH due to the release of organic acids from SOM decomposition (Kumar et al., 2020). Additionally, these molecules, found in manure and similarly in ancient deposits of formerly living materials (e.g., Leonardite), or even with manmade molecules, can complex P to improve its solubility and mobility (Hopkins, 2013; Hill et al., 2015a; Hill et al., 2015b; Hopkins, 2015; Summerhays et al., 2015; Hopkins et al., 2018). For these reasons, manures can improve soil P availability and uptake by plants.

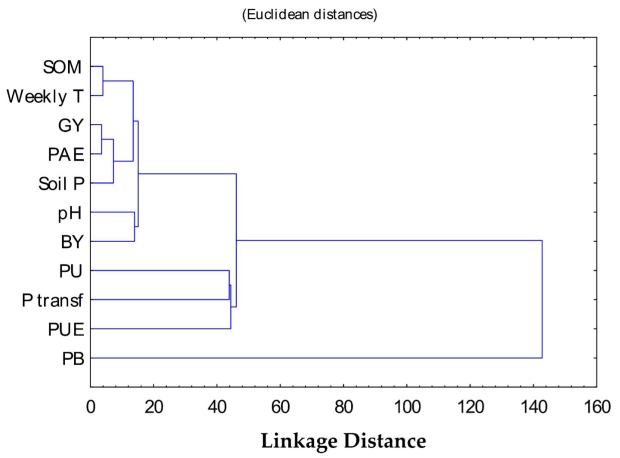

FIGURE 6
Cluster analysis (CA) of 11 traits of soil and wheat grown under calcareous conditions. Measured parameters include soil organic matter (SOM), grain yield (GY), P acquisition efficiency (PAE), plant-available P (AB-DTPA) (soil P), P uptake (PU), and phosphorus (P) use efficiency (PUE).

4.3 Yields and P Efficiency

Maximum wheat grain yield was achieved at the highest rate of P fertilizer (39 kg P ha^{-1}), regardless of whether FYM was applied or not. However, an equivalently high yield was achieved at the next lower rate of P fertilizer (26 kg P ha^{-1}) when FYM was also applied. Similarly, the findings of Ibrahim et al. (2008) revealed that FYM and different levels of compost have significantly increased wheat grain yield due to improved soil physical conditions, enhanced soil fertility, and improved stand establishment.

In the present study, the uptake of P by wheat was increased with P fertilizer and FYM. The increased uptake of P by wheat at an increased level of chemical P fertilizer and FYM could be due to the

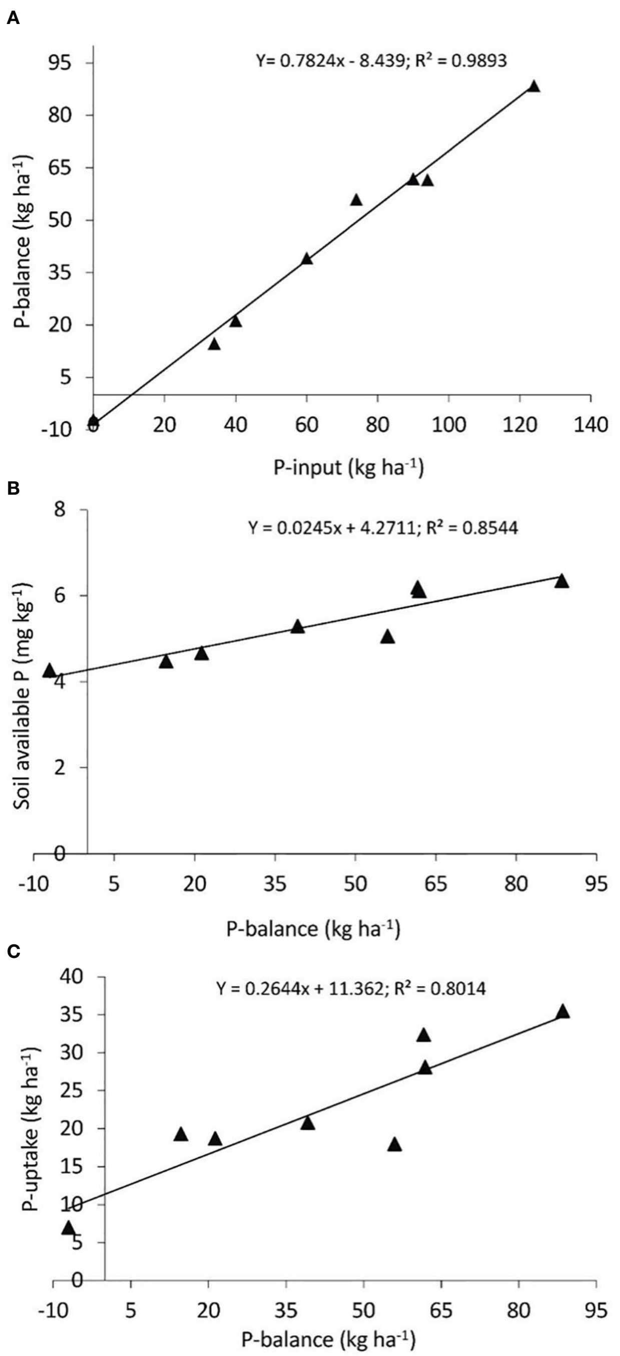

FIGURE 7
Simple linear regression analysis shows the relationship of P balance (PB) with P input **(A)**, soil (plant)-available P as AB-DTPA with PB **(B)**, and P uptake with PB **(C)**.

fact that FYM releases more nutrients over time, so that nutrient loss is less, which might have resulted in more plant PU. Furthermore, it could be due to the balanced and steady supply of nutrients to plants at all stages of crop growth.

Efficiencies for P, such as PAE and PUE, were determined in this study. PAE denotes the aptitude of crops to take up P from the soil, and PUE is the ability to produce biomass using the acquired P. Improving P efficiency can be reached by improving the acquisition and utilization of P (Parentoni and Lopez de Souza, 2008). In general, inorganic P caused an increase in PUE when applied in combination with FYM; however, PUE values decreased at higher FYM application rates. These results were in agreement with the findings by Rahim et al. (2010) and Castillo et al. (2013), who found that the PUE of wheat decreased significantly at a higher P rate.

We observed positive PB for all the treatments except the control. This shows that even the low levels of P fertilizer used in the present study resulted in a building of residual soil P. It has been reported by many that application of FYM alone or in combination with inorganic fertilizer increases the soil nutrient balance (Blake et al., 2000; Meena et al., 2017; Pradhan et al., 2021). Furthermore, we observed (Figure 3) strong correlations between P input vs. PB (R^2 = 0.98), PB vs. plant-available P (AB-DTPA) (R^2 = 0.84), and PB vs. PU (R^2 = 0.80). The PCA analysis also clustered various plant growth parameters with P26 and P39 along with FYM and conferred positive effects of applied treatments on soil properties and wheat yield (Figure 5). These positive linear relationships might be due to the cause of positive PB in these soils (Tang et al., 2008). These values have been successfully used as a tool for predicting the change in the soil P status and recommending the amount of P application practically (Blake et al., 2000). Plant-available P (AB-DTPA) in these highly alkaline calcareous soils has very low availability due to high fixation, and slow diffusion, thus limiting plant growth and crop yield. The addition of FYM alone or in combination with inorganic fertilizers decreases P fixation owing to the inactivation of Fe and Al ions thus improving the adsorption capacity of P in soil (Jamal et al., 2018; Saeed et al., 2021).

We note that, in terms of environmental considerations, the highest PUE was at the lowest rate of P (F_0M_{15}). However, this rate does not enable sufficient overall sustainability as the yields were so low. Agricultural producers have the responsibility to provide food, fuel, and fiber for the eight billion people on Earth. Low yields result in an increase in the amount of arable land. Thus, a combination of reasonable yields along with good P efficiency is a vital consideration. In our study, the second highest PUE was at the statistically highest grain and straw yield, providing for farm, environmental, and societal sustainability.

5 Conclusion

The SOM increased linearly for both fertilizer and FYM, whereas the pH decreased with fertilizer only. The addition of fertilizer and FYM increased plant-available P by an average of 0.5 mg P kg^{-1} soil week^{-1} with incubation. With this, plant-available P (AB-DTPA) increased initially (~1–9 mg P kg^{-1}), with further gains by the end of the incubation (~3–17 mg P kg^{-1}). In the field study, there was also a significant increase of available P in the soil supporting plants, although the magnitude of the increase was much smaller, with a maximum 2 mg kg^{-1} significant increase for the highest fertilizer rate with FYM. The increased plant-available P resulted in significant increases in grain and straw yields, which peaked with fertilizer at 26 kg P ha^{-1} plus FYM. The PU, PB, and PAE increased linearly with the P rate, with the highest levels at the highest P rate. In general, efficiency increased with FYM. The PUE was highest at the lowest rates of P, with general decreases with increasing P, although not consistently. The PCA revealed that 94.34% of the total variance was accounted for by PC1 (84.04%) and PC2 (10.33%), with grain straw yield significantly correlated to SOM, PU, and PAE. A strong positive regression coefficient was observed between PB and total P input, plant-available P (AB-DTPA), and PU. The outcomes of our study would help to update recommendations for P fertilizer application in calcareous soils while sustaining soil fertility and simultaneously reducing fertilizer costs and conserving limited resources.

Data availability statement

The raw data supporting the conclusions of this article will be made available by the authors, without undue reservation.

Author contributions

AJ: Planned research work and write-up of first drafts. MFS: Supervised the research and improved the first draft. AM: Performed conceptualization, improving draft and helped in data analysis. BH: Review, writing/improving draft. IA: Co-supervised research. AN: Helped in methodology, data curation. All authors contributed to the article and approved the submitted version.

Funding

We acknowledge the Higher Education Commission (HEC), Pakistan, for funding under the SRGP-HEC project and Brigham Young University for assistance with publication funding.

Conflict of interest

The authors declare that the research was conducted in the absence of any commercial or financial relationships that could be construed as a potential conflict of interest.

Publisher's note

All claims expressed in this article are solely those of the authors and do not necessarily represent those of their affiliated organizations, or those of the publisher, the editors and the reviewers. Any product that may be evaluated in this article, or claim that may be made by its manufacturer, is not guaranteed or endorsed by the publisher.

Supplementary material

The Supplementary Material for this article can be found online at: https://www.frontiersin.org/articles/10.3389/fpls.2023.1034421/full#supplementary-material

References

Aboukila, E. F., Nassar, I. N., Rashad, M., Hafez, M., and Norton, J. B. (2018). Reclamation of calcareous soil and improvement of squash growth using brewers' spent grain and compost. *J. Saudi Soc Ag. Sci.* 17, 390–397. doi: 10.1016/j.jssas.2016.09.005

Amin, A. E. E. A. Z. (2018). Availability and transformations of phosphorus in calcareous sandy soil as affected by farmyard manure and elemental sulfur applications. *Alex. Sci. Exch.* 39, 98–111. doi: 10.21608/asejaiqjsae.2018.5795

Andriamananjara, A., Rakotoson, T., Razafimbelo, T., Rabeharisoa, L., Razafimanantsoa, P., and Masse, D. (2019). Farmyard manure improves phosphorus use efficiency in weathered p deficient soil. *Nutr. Cycl. Agroecosyst.* 115, 407–425. doi: 10.1007/s10705-019-10022-3

Barben, S. A., Hopkins, B. G., Jolley, V. D., Webb, B. L., Nichols, B. A., and Buxton, E. A. (2011). Zinc, manganese and phosphorus interrelationships and their effects on iron and copper in chelator-buffered solution grown russet Burbank potato. *J. Plant Nutr.* 34, 1144–1163. doi: 10.1080/01904167.2011.558158

Blake, L., Mercik, S., Koerschens, M., Moskal, S., Poulton, P. R., Goulding, K. W. T., et al. (2000). Phosphorus content in soil, uptake by plants and balance in three European long-term field experiments. *Nutr. Cycl. Agroecosyst.* 56, 263–275. doi: 10.1023/A:1009841603931

Castillo, C., Acuña, H., Zagal, E., and Inostroza, L. (2013). Phosphorus absorption and use efficiency by lotus spp. under water stress conditions in two soils: A pot experiment. *Chil. J. Agric. Res.* 31–40, 73. doi: 10.4067/S0718-58392013000100005

Deraoui, N. B., Mekliche, L. H., and Mihoub, A. (2015). Effect of incubation period of phosphorus fertilizer on some properties of sandy soil with low calcareous content. southern Algeria. *Asian J. Agric. Res.* 9, 123–131. doi: 10.3923/ajar.2015.123.131

Ding, Z., Kheir, A. M., Ali, M. G., Ali, O. A., Abdelaal, A. I., Zhou, Z., et al. (2020). The integrated effect of salinity, organic amendments, phosphorus fertilizers, and deficit irrigation on soil properties, phosphorus fractionation and wheat productivity. *Sci. Rep.* 10, 1–13. doi: 10.1038/s41598-020-59650-8

Elgharably, A. (2020). Effects of rock phosphate added with farm yard manure or sugar juice residues on wheat growth and uptake of certain nutrients and heavy metals. *J. Soil. Sediments* 20, 3931–3940. doi: 10.1007/s11368-020-02683-3

Fixen, P. E., and Bruulsema, T. W. (2014). Potato management challenges created by phosphorus chemistry and plant roots. *Am. J. Potato Res.* 91, 121–131. doi: 10.1007/s12230-014-9374-z

Hazra, K. K., Swain, D. K., Bohra, A., Singh, S. S., Kumar, N., and Nath, C. P. (2018). Organic rice: Potential production strategies, challenges and prospects. *Org. Agric.* 8 (1), 39–56. doi: 10.1007/s13165-016-0172-4

Hill, M. W., Hopkins, B. G., and Jolley, V. D. (2015a). Maize in-season growth response to organic acid-bonded phosphorus fertilizer (Carbond p®). *J. Plant Nutr.* 38, 1398–1415. doi: 10.1080/01904167.2014.973040

Hill, M. W., Hopkins, B. G., Jolley, V. D., and Webb, B. L. (2015b). Phosphorus mobility through soil increased with organic acid-bonded phosphorus fertilizer (Carbond® p). *J. Plant Nutr.* 38, 1416–1426. doi: 10.1080/01904167.2014.973041

Hopkins, B. G. (2013). Russet Burbank potato phosphorus fertilization with dicarboxylic acid copolymer additive (AVAIL®). *J. Plant Nutr.* 36, 1287–1306. doi: 10.1080/01904167.2013.785565

Hopkins, B. G. (2015). "Phosphorus in plant nutrition," in *Plant nutrition handbook, 2nd edition*. Eds. D. J. Pilbeam and A. V. Barker (Boca Raton, FL, USA: CRC Press; Taylor & Francis Group), 65–126.

Hopkins, B. G. (2020). "Developments in the use of fertilizers," in *Achieving sustainable crop nutrition*. Ed. Z. Rengel (Cambridge, UK: Burleigh Dodds Science Publishing), 555–588. Available at: www.bdspublishing.com, ISBN: .

Hopkins, B. G., Fernelius, K. J., Hansen, N. C., and Eggett, D. L. (2018). AVAIL phosphorus fertilizer enhancer: Meta-analysis of 503 field evaluations. *Agron. J.* 110, 389–398. doi: 10.2134/agronj2017.07.0385

Hopkins, B. G., and Hansen, N. C. (2019). Phosphorus management in high-yield systems. *J. Environ. Qual.* 48, 1265–1280. doi: 10.2134/jeq2019.03.0130

Hopkins, B. G., Horneck, D. A., and MacGuidwin, A. E. (2014). Improving phosphorus use efficiency through potato rhizosphere modification and extension. *Am. J. Potato Res.* 91, 161–174. doi: 10.1007/s12230-014-9370-3

Ibrahim, M., Hassan, A., Iqbal, M., and Valeem, E. E. (2008). Response of wheat growth and yield to various levels of compost and organic manure. *Pak. J. Bot.* 40, 2135–2141.

Jackson, M. L. (1973). *Soil chemical analysis* (New Delhi: Prentice Hall of India Ltd), 219–221.

Jamal, A., Muhammad, D., and Jamal, H. (2018). Application of adsorption isotherms in evaluating the influence of humic acid and farmyard manure on phosphorous adsorption and desorption capacity of calcareous soil. *World Sci. News* 107, 136–149.

Khan, I., Jamal, A., Mihoub, A., Farooq, O., Farhan Saeed, M., Roberto, M., et al. (2022). Partial substitution of chemical fertilizers with organic supplements increased wheat productivity and profitability under limited and assured irrigation regimes. *Agriculture* 12, 1754. doi: 10.3390/agriculture12111754

Kumar, V., Sharma, P. K., Jatav, H. S., Singh, S. K., Rai, A., Kant, S., et al. (2020). Organic amendments application increases yield and nutrient uptake of mustard (*Brassica juncea*) grown in chromium-contaminated soils. *Commun. Soil Sci. Plant Anal.* 51, 149–159. doi: 10.1080/00103624.2019.1695831

Li, S., Li, J., Li, G., Li, Y., Yuan, J., and Li, D. (2017). Effect of different organic fertilizers application on soil organic matter properties. *Compost. Sci. Util.* 25, 31–36. doi: 10.1038/s41598-017-17219-y

Lindsay, W. L. (2001). *Chemical equilibria in soils* (Caldwell, ID, USA: The Blackburn Press).

Manzoor, A. (2013). Critical soil solution phosphorus concentration essential for plant growth in calcareous soil series (Pakistan: SES Department, the University of Agriculture Peshawar).

Marschner, P. (2012). *Mineral nutrition of higher plants. 3rd edition* (San Diego, CA, USA: Elsevier).

Ma, Q., Wen, Y., Ma, J., Macdonald, A., Hill, P. W., Chadwick, D. R., et al. (2020). Long-term farmyard manure application affects soil organic phosphorus cycling: A combined metagenomics and 33P/14C labelling study. *Soil Biol. Biochem.* 149, 107959. doi: 10.1016/j.soilbio.2020.107959

Meena, H. M., Sharma, R. P., Sankhyan, N. K., and Sepehya, S. (2017). Effect of continuous application of fertilizers, farmyard manure and lime on soil fertility and productivity of the maize-wheat system in an acid alfisols. *Commun. Soil Sci. Plant Anal.* 48, 1552–1563. doi: 10.1080/00103624.2017.1373800

Mihoub, A., Amin, A. E. E. A. Z., Naeem, A., and Bouhoun, M. D. (2019). Improvement in phosphorus nutrition of wheat plants grown in a calcareous sandy soil by incorporating chemical phosphorus fertilizer with some selected organic substances. *Acta Agric. Slov.* 113, 263–272. doi: 10.14720/aas.2019.113.2.7

Mihoub, A., and Boukhalfa-Deraoui, N. (2014). Performance of different phosphorus fertilizer types on wheat grown in calcareous sandy soil of El-menia, southern Algeria. *Asian J. Crop Sci.* 6, 383–391. doi: 10.3923/ajcs.2014.383.391

Mihoub, A., Naeem, A., Amin, A. E. E. A. Z., Jamal, A., and Saeed, M. F. (2022). Pigeon manure tea improves phosphorus availability and wheat growth through decreasing p adsorption in a calcareous sandy soil. *Commun. Soil Sci. Plant Anal.* 53, 2596–2607. doi: 10.1080/00103624.2022.2072859

Nelson, D. W., and Sommers, L. (1982). "Total carbon, organic carbon, and organic matter," in *Methods of soil analysis. part 2. chemical and microbiological properties*. Ed. D. Sparks (Madison, WI, USA: Soil Science Society of America), 539–579.

NFDC (2001). "Balanced fertilization through phosphate promotion," in *Project terminal report* (Islamabad, Pakistan: National Fertilizer Development Center).

Parentoni, S. N., and Lopez de Souza, ,.C.Jr. (2008). Phosphorus acquisition and internal utilization efficiency in tropical maize genotypes. *Pesqui. Agropecu. Bras.* 43, 893–901. doi: 10.1590/S0100-204X2008000700014

Pradhan, S. N., Ghosh, A., Nema, A., Ram, S., and Pal, Y. (2021). Changes in soil phosphorus forms in a long-term cropping system as influenced by fertilization and tillage. *Arch. Agron. Soil Sci.* 67, 822–835. doi: 10.1080/03650340.2020.1759800

Qaswar, M., Jing, H., Ahmed, W., Dongchu, L., Shujun, L., Lu, Z., et al. (2020). Yield sustainability, soil organic carbon sequestration and nutrients balance under long-term combined application of manure and inorganic fertilizers in acidic paddy soil. *Soil Tillage Res.* 198, 104569. doi: 10.1016/j.still.2019.104569

Rahim, A., Ranjha, A. M., and Waraich, E. A. (2010). Effect of phosphorus application and irrigation scheduling on wheat yield and phosphorus use efficiency. *Soil Environ.* 29, 15–22.

Rehim, A., Khan, M., Imran, M., Bashir, M. A., Ul-Allah, S., Khan, M. N., et al. (2020). Integrated use of farm manure and synthetic nitrogen fertilizer improves nitrogen use efficiency, yield and grain quality in wheat. *Ital. J. Agron.* 15, 29–34. doi: 10.4081/ija.2020.1360

Richards, L. A. (1954). Diagnosis and improvement of saline and alkali soils. *Soil Science* 78, 2, 154. doi: 10.1097/00010694-195408000-00012

Saeed, M. F., Jamal, A., Muhammad, D., Shah, G. M., Bakhat, H. F., Ahmad, I., et al. (2021). Optimizing phosphorus levels in wheat grown in a calcareous soil with the use of adsorption isotherm models. *J. Soil Sci. Plant Nutr.* 21, 81–94. doi: 10.1007/s42729-020-00344-5

Sarir, M. S., Durrani, M. I., and Mian, I. A. (2006). Effect of the source and rate of humic acid on phosphorus transformations. *J. Agric. Biol. Sci.* 1, 29–31.

Shah, Z., Haq, I. U., Rehman, A., Khan, A., and Afzal, M. (2013). Soil amendments and seed priming influence nutrients uptake, soil properties, yield and yield components of wheat (*Triticum aestivum* l.) in alkali soils. *Soil Sci. Plant Nutr.* 59, 262–270. doi: 10.1080/00380768.2012.762634

Soltanpour, P. N. (1985). Use of ammonium bicarbonate DTPA soil test to evaluate elemental availability and toxicity. *Commun. Soil Sci. Plant Anal.* 16, 323–338. doi: 10.1080/00103628509367607

Summerhays, J. S. C., Hopkins, B. G., Jolley, V. D., Hill, M. W., Ransom, C. J., and Brown, T. R. (2015). Enhanced phosphorus fertilizer (Carbond p®) supplied to maize in moderate and high organic matter soils. *J. Plant Nutr.* 38, 1359–1371. doi: 10.1080/01904167.2014.973039

Sun, B., Cui, Q., Guo, Y., Yang, X., Zhang, S., Gao, M., et al. (2018). Soil phosphorus and relationship to phosphorus balance under long-term fertilization. *Plant Soil Environ.* 64, 214–220. doi: 10.17221/709/2017-PSE

Syers, J. K., Johnston, A. E., and Curtin, D. (2008). Efficiency of soil and fertilizer phosphorus use. *FAO Fert. Plant Nutr. Bull.* 18 (108).

Tang, X., Li, J., Ma, Y., Hao, X., and Li, X. (2008). Phosphorus efficiency in long-term (15 years) wheat–maize cropping systems with various soil and climate conditions. *Field Crops Res.* 108, 231–237. doi: 10.1016/j.fcr.2008.05.007

Ul-Allah, S., Iqbal, M., Maqsood, S., Naeem, M., Ijaz, M., Ashfaq, W., et al. (2018). Improving the performance of bread wheat genotypes by managing irrigation and nitrogen under semi-arid conditions. *Arch. Agron. Soil Sci.* 64, 1678–1689. doi: 10.1080/03650340.2018.1450974

Urbaniak, M., Wyrwicka, A., Tołoczko, W., Serwecińska, L., and Zieliński, M. (2017). The effect of sewage sludge application on soil properties and willow (Salix sp.) cultivation. *Sci. Total Environ.* 586, 66–75. doi: 10.1016/j.scitotenv.2017.02.012

Wu, Y., Li, Y., Zheng, C., Zhang, Y., and Sun, Z. (2013). Organic amendent application influence soil organism abundance in saline alkali soil. *Eur. J. Soil. Biol.* 54, 32–40. doi: 10.1016/j.ejsobi.2012.10.006

Yan, Z., Chen, S., Li, J., Alva, A., and Chen, Q. (2016). Manure and nitrogen application enhances soil phosphorus mobility in calcareous soil in greenhouses. *J. Environ. Manage.* 181, 26–35. doi: 10.1016/j.jenvman.2016.05.081

Zhang, J. B., Yang, J. S., Yao, R. J., Yu, S. P., Li, F. R., and Hou, X. J. (2014). The effects of farmyard manure and mulch on soil physical properties in a reclaimed coastal tidal flat salt-affected soil. *J. Integr. Agric.* 13, 1782–1790. doi: 10.1016/S2095-3119(13)60530-4

TYPE Original Research
PUBLISHED 24 January 2023
DOI 10.3389/fpls.2023.1072216

Soil amendment with cow dung modifies the soil nutrition and microbiota to reduce the ginseng replanting problem

Setu Bazie Tagele[1,2], Ryeong-Hui Kim[3], Minsoo Jeong[1], Kyeongmo Lim[1], Da-Ryung Jung[1], Dokyung Lee[3], Wanro Kim[1] and Jae-Ho Shin[1,2,3]*

[1]Department of Applied Biosciences, Kyungpook National University, Daegu, Republic of Korea, [2]NGS core facility, Kyungpook National University, Daegu, Republic of Korea, [3]Department of Integrative Biology, Kyungpook National University, Daegu, Republic of Korea

Check for updates

OPEN ACCESS

EDITED BY
Anoop Kumar Srivastava,
Central Citrus Research Institute (ICAR), India

REVIEWED BY
Ugo De Corato,
Energy and Sustainable Economic Development (ENEA), Italy
Youn-Sig Kwak,
Gyeongsang National University, South Korea

*CORRESPONDENCE
Jae-Ho Shin
jhshin@knu.ac.kr

SPECIALTY SECTION
This article was submitted to Plant Nutrition, a section of the journal Frontiers in Plant Science

RECEIVED 17 October 2022
ACCEPTED 11 January 2023
PUBLISHED 24 January 2023

CITATION
Tagele SB, Kim R-H, Jeong M, Lim K, Jung D-R, Lee D, Kim W and Shin J-H (2023) Soil amendment with cow dung modifies the soil nutrition and microbiota to reduce the ginseng replanting problem. *Front. Plant Sci.* 14:1072216.
doi: 10.3389/fpls.2023.1072216

Ginseng is a profitable crop worldwide; however, the ginseng replanting problem (GRP) is a major threat to its production. Soil amendment is a non-chemical method that is gaining popularity for alleviating continuous cropping obstacles, such as GRP. However, the impact of soil amendment with either cow dung or canola on GRP reduction and the associated soil microbiota remains unclear. In the present study, we evaluated the effect of soil amendment with cow dung, canola seed powder, and without amendment (control), on the survival of ginseng seedling transplants, the soil bacterial and fungal communities, and their associated metabolic functions. The results showed that cow dung increased ginseng seedling survival rate by 100 percent and had a remarkable positive effect on ginseng plant growth compared to control, whereas canola did not. Cow dung improved soil nutritional status in terms of pH, electrical conductivity, NO_3^-, total carbon, total phosphorus, and available phosphorus. The amplicon sequencing results using Illumina MiSeq showed that canola had the strongest negative effect in reducing soil bacterial and fungal diversity. On the other hand, cow dung stimulated beneficial soil microbes, including *Bacillus*, *Rhodanobacter*, *Streptomyces*, and *Chaetomium*, while suppressing Acidobacteriota. Community-level physiological profiling analysis using Biolog Ecoplates containing 31 different carbon sources showed that cow dung soil had a different metabolic activity with higher utilization rates of carbohydrates and polymer carbon sources, mainly Tween 40 and beta-methyl-d-glucoside. These carbon sources were most highly associated with Bacillota. Furthermore, predicted ecological function analyses of bacterial and fungal communities showed that cow dung had a higher predicted function of fermentation and fewer functions related to plant pathogens and fungal parasites, signifying its potential to enhance soil suppressiveness. Co-occurrence network analysis based on random matrix theory (RMT) revealed that cow dung transformed the soil microbial network into a highly connected and complex network. This study is the first to report the alleviation of GRP using cow dung as a soil amendment, and the study contributes significantly to our understanding of how the soil microbiota and metabolic alterations *via* cow dung can aid in GRP alleviation.

KEYWORDS

co-occurrence network, functional prediction, ginseng, illumina miseq, replant failure, soil microbiome

1 Introduction

Ginseng (*Panax ginseng* C. A. Meyer) is an economically important medicinal plant in South Korea; however, its production is challenged by the ginseng replanting problem (GRP), which is caused by a variety of abiotic and biotic factors (Lee et al., 2015; Yang et al., 2015; Seo et al., 2019). Recent studies have documented that the changes in soil chemical properties, of which soil pH is the main factor, significantly contribute to GRP (Zhang et al., 2020). The soil microbiota plays a key role in determining plant health and productivity by channeling various crucial soil functionalities, including mineralization and plant disease control (Srivastava et al., 2022). Manipulating the soil microbiota is an effective way to alleviate GRP (Lee et al., 2015; Dong et al., 2018; Seo et al., 2019). Several agricultural practices can shape the soil microbial structure (Romdhane et al., 2022), which can result in either positive (Qi et al., 2020) or negative outcomes on plant health (Bziuk et al., 2021). For example, continuous cropping of ginseng affects the taxonomic and functional diversity of the soil microbial population and the potential pathogenic genera, increasing the risk of soil conduciveness (Zhang et al., 2020; Tong et al., 2021). On the other hand, various methods such as crop rotation (Zhao et al., 2017; Ji et al., 2021b), chemical fumigation (Liu et al., 2022), and high-temperature steaming (Yang et al., 2019) have been documented to reduce the replanting problem.

Soil amendment is an environmentally benign alternative approach to chemical fumigation that is efficient in suppressing soil-borne diseases (Zhou et al., 2019; Lopes et al., 2022). Soil amendment involves soil incorporation with organic materials and covering it with a polyethylene film for at least two weeks at an optimal temperature (Momma et al., 2006). Soil amendment improves soil suppressiveness by reshaping the soil microbiome and soil physicochemical properties (Lopes et al., 2022), which ultimately results in the enrichment of beneficial microbes for plant disease control, direct suppression of bacterial and fungal pathogens (Zhou et al., 2019; Zhao et al., 2020), and modulation of the plant immune system (Jayaraman et al., 2021).

Soil amendment successfully mitigates replanting problems in apples, prunus, and strawberries (Browne et al., 2018; DuPont et al., 2021; Giovannini et al., 2021). However, the efficacy of soil amendment varies with the type of carbon source utilized for incorporation (Zhao et al., 2020) and is mediated by the microbiota, which impacts the emission of volatile compounds toxic to soil-borne pathogens (Poret-Peterson et al., 2019; Lopes et al., 2022). More importantly, cow dung, an organic amendment, is a cheap and easily available resource that improves plant and soil health, resulting in sustainable crop production (Gupta et al., 2016). Integrating soil amendment and biofumigants, such as *Brassica* spp., effectively control apple replanting problems (Wang and Mazzola, 2019). However, the effect of soil amendment with either cow dung or canola (biofumigant) on GRP and the taxonomic and functional diversity of the associated bacterial and fungal communities remains unclear. Thus, we aimed to determine the impact of cow dung, and canola on soil microbial communities and GRP reduction in six-year-old ginseng cultivated soil, which had a significant GRP.

2 Materials and methods

2.1 Materials, study design, and sampling

In this study, we obtained the soil from a six-year-old continuously cultivated ginseng farm in Punggi, Gyeongsangbuk-do Province, South Korea (36°48′37′′N,128°32′28′′E). The farm was abandoned because of the high GRP. Cow dung (pH = 8, electrical conductivity (EC) = 0.823) was obtained from a dairy farm in Daegu, Kyungpook-do Province, South Korea (32°32′27′′N,126°35′27′′E). Canola seed meal was acquired from the FarmHannong Bio Company in Seoul, Yeongdeungpo-gu, South Korea.

An 8-mm sieve was used to homogenize the collected soil thoroughly. Cow dung and canola seed powder were mixed separately with the soil at 1% in a plastic box (0.5 × 0.5 m in width and length). Non-amended soil served as the control. The treatments, including control, were watered at 70% field capacity and covered with plastic transparent polythene film for 40 days. The soil was left for a month at air temperature, and the polythene film was uncovered and air-dried in a greenhouse for one month. The greenhouse pots (31 cm height, 15 cm diameter) were filled with 2 kg of soil. Three one-year-old baby ginseng plants were transplanted into each plastic pot. All the soil amendments were arranged in a completely randomized design. The experiment was replicated three times, each containing five pots. Ginseng was grown for three months in a greenhouse. The seedlings were irrigated once a week.

Soil for DNA extraction was sampled by removing the top 2 cm of soil at a depth of approximately 5 cm from 7 cm away from each transplanted ginseng seedling at three points from each pot immediately before ginseng seedling transplanting (0 days after transplanting, 0DAT) and at the end of the experiment (90 days after seedling transplanting, 90DAT) (Figure 1A). The samples were pooled to obtain three samples (replicates) for each treatment and stored at −80°C until used for DNA extraction. For chemical property profiling, soil samples were collected at 0DAT.

The emergence rate was calculated as the number of emerging transplants divided by the total number of transplants. Ginseng replanting problem (GRP) was determined in each replication by dividing the number of surviving transplants by the total number of transplanted seedlings at 90DAT (Li et al., 2019). The GRP was expressed as percent seedling survival.

2.2 Soil chemical property analysis

The soil chemical properties were analyzed according to NIAST (2010) at Kyungpook National University, South Korea. A pH and EC meter (SP2000, Skalar BV, Netherlands) was used to measure the soil

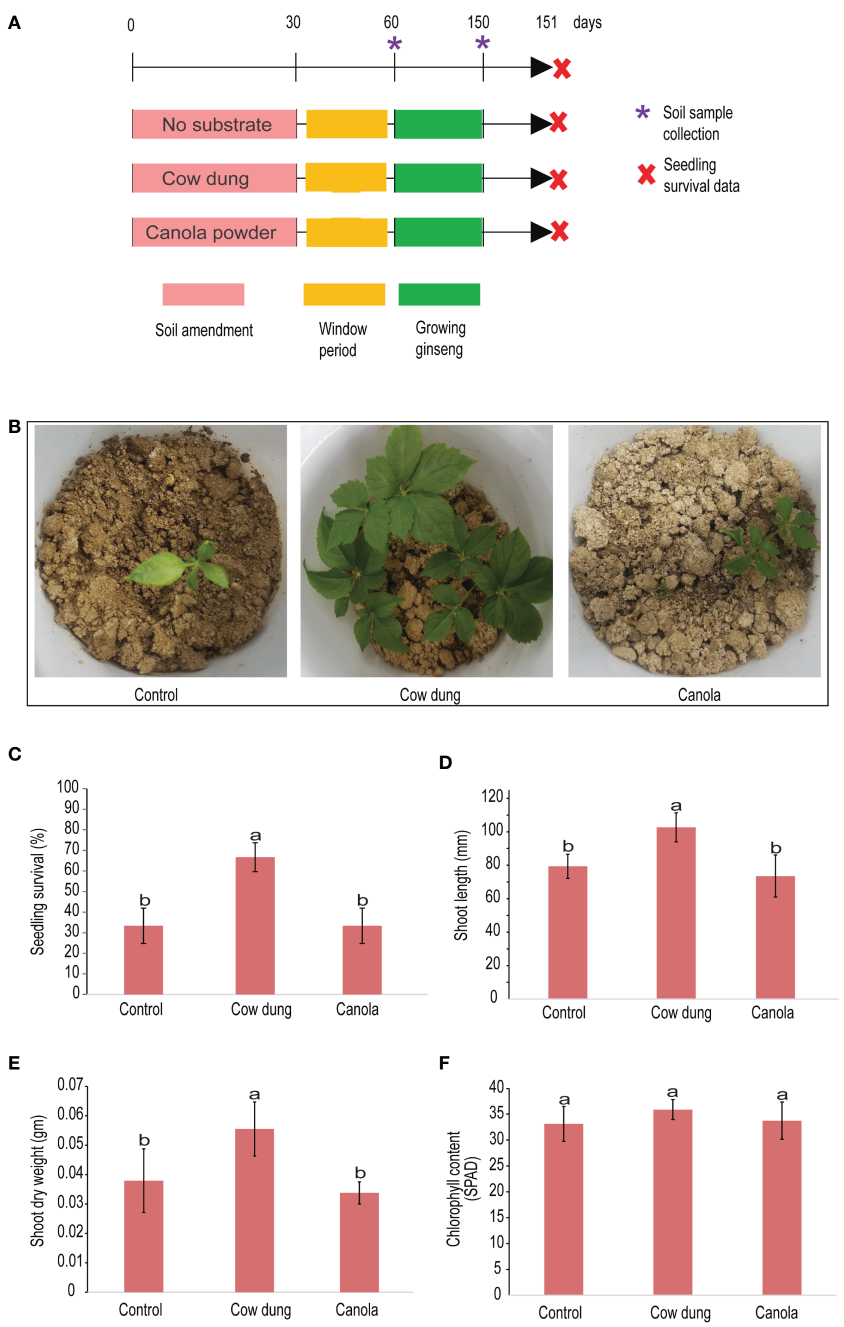

FIGURE 1
Impact of soil amendment on ginseng survival and plant growth properties. Pictorial view of the experimental scheme **(A)** and survived transplanted ginseng seedlings **(B)**. Graph showing the effect of different soil amendments on ginseng growth parameters during the three months after transplanting: the survival rate of transplanted ginseng seedlings **(C)**, shoot length **(D)**, shoot dry weight **(E)**, and chlorophyll content **(F)**. Mean values having the same letter(s) are not significantly different ($p < 0.05$). Error bars indicate standard deviation (n = 18).

pH and EC. A titration method using an automatic titrator (Metrohm 888, Switzerland) was employed to assess the soil organic matter (SOM) content. Soil ammonium (NH_4^+) and nitrate (NO_3^-) concentrations were measured using cadmium reduction and salicylate colorimetric methods, respectively, using BLTEC QuAAtro (BLTEC KK, Osaka, Japan). The method employed by Dumas was used to determine the total nitrogen (TN) concentration with S832DR (Leco, USA). The concentrations of exchangeable potassium (K) and available P_2O_5 (AP) in the soil were measured using a PerkinElmer Optima 8300 ICP-OES (PerkinElmer, MA, USA) and SKALAR San++ system autoanalyzer (Skalar Analytical B.V., Breda, Netherlands), respectively. The soil cation exchange capacity (CEC) was measured using the $BaCl_2$-H_2SO_4 exchange method.

2.3 Community-level physiological profiling

The change in the metabolic activity of the microbial communities in soil amendments was determined using the community-level physiological profiling (CLPP) method with Biolog EcoPlates with three replications. The EcoPlates had 31 kinds of carbon sources (Biolog, Hayward, CA, USA). Briefly, a one-gram soil was mixed with 99 mL of sterile distilled water. The mixture was vortex-homogenized for 20 min, and the soil particles were allowed to settle at 4°C for 30 min. The clay particles suspended in the supernatant were removed using one-gram $CaCo_3$ and $CaCl_2$. The supernatant (150 µL) was then dispensed into each well of a Biolog EcoPlate. The plates were then incubated at 25°C for 120 h under dark conditions. The color readings were measured at 590 nm and 750 nm wavelengths every 24 h using a Biolog microplate reader with Biolog MicroLog™ Software and MicroStation™. The absorbance value of each carbon source well was calculated by subtracting the value obtained from the control well at each time point. The carbon source utilization of the microbiota in each soil amendment was determined based on the percentage of total carbon utilization.

2.4 DNA extraction, library preparation, and sequencing

The DNeasy® PowerSoil® Pro Kit (Qiagen, Hilden, Germany) extracted microbial DNA from 0.5 g soil samples according to the manufacturer's guidelines. DNA purity was checked with UV spectrophotometry (NanoDrop™ One^C spectrophotometer, Thermo Fisher Scientific) and double-checked using gel electrophoresis. DNA quantity was measured using a Qubit® 2.0 Fluorometer (Life Technologies, Carlsbad, CA, USA). The DNA samples were kept at −80°C until used for library preparation for Illumina MiSeq sequencing.

The extracted DNA template was amplified using two-step PCR with universal primers 515F/907R for the bacterial 16S rRNA gene and ITS86F/ITS4R for the fungal internal transcribed spacer ITS (ITS1) region. Detailed descriptions of the primers and PCR conditions are provided in Table S1. The AMPure XP bead purification kit (Beckman Coulter, CA, USA) and Nextera®XT Index Kit (Illumina, San Diego, CA, USA) were used for the cleanup library and ligation processes, respectively. The pooled library was quality checking using an Agilent 2100 Bioanalyzer (Santa Clara, CA, USA). Sequencing was performed using the Illumina MiSeq platform (Illumina) at Kyungpook National University's NGS Core Facility (Daegu, South Korea).

2.5 Bioinformatics analysis

The QIIME2 pipeline (https://qiime2.org) was used to demultiplex the raw sequences of bacteria and fungi from each sample. The reads were denoised using DADA2 in QIIME2 (Callahan et al., 2016) by removing singletons and chimeric sequences. Taxonomic assignment of the representative sequences, which were truncated and had high-quality scores, was performed using a classify-sklearn-based QIIME feature classifier trained on reference databases. SILVA (version 138.1) 99% full-length database (Quast et al., 2013) and UNITE database (version 8.3) (Nilsson et al., 2019) were used for bacteria and fungi, respectively. Taxonomy-assigned contaminants of chloroplasts, mitochondria, and kingdom-level unclassified taxa of ASVs (amplicon sequence variants) were excluded from downstream analysis. The sample reads were rarefied to an equal size (Figure S1) to a subsampling depth of the smallest 5551 and 20753 reads per sample of bacteria and fungi, respectively, to enable similarity comparison between treatments and avoid variation attributed to the DNA extraction method as well as library preparation. The normalized dataset contained 2102 and 232 ASVs.

The ecological functions of bacterial, fungal, and communities following soil amendment were determined using the functional annotation of prokaryotic taxa (FAPROTAX) (Louca et al., 2016), fungi functional guild (FUNGuild) (Nguyen et al., 2016), respectively.

2.6 Statistical data analysis

The R statistical software (version 4.1.3) performed all downstream statistical data analyses (R Core Team, 2022). Different R packages, ggplot (Wickham, 2016) and ComplexHeatmap (neatmap v2.1.0) (Gu et al., 2016), were used to visualize the data. Levene's test (Oksanen et al., 2020) and PERMDISP (Anderson et al., 2011) were employed to determine the homogeneity of the variance and multivariate homogeneity of dispersion, respectively. The Shapiro–Wilk test was used to validate the data normality assumption. Comparison of the statistical difference between soil amendments in ginseng emergence, survival rate, and alpha diversity indices (at ASV level) was performed with ANOVA, and means comparison was performed with the least significant difference using the dplyr package. Factorial analysis was performed to additionally take into account the impact of the soil sampling time. The statistical differences among soil amendments in terms of bacterial and fungal community assembly were analyzed using permutational multivariate ANOVA (PERMANOVA) (Adonis; vegan, version 2.5.7) (Dixon, 2003). Differential abundance tools, such as ALDEx2 (Fernandes et al., 2013), LEfSe (Segata et al., 2011), metastat (White et al., 2009), metagenomeSeq (Paulson et al., 2013), and random forest in R (Beck and Foster, 2014) were used investigate potential microbial biomarkers in different soil amendments.

Random matrix theory (RMT) analysis based on the correlation method (Spearman's rank correlation) from compositional data at the ASV level was employed to construct a network of bacterial and fungal communities. ASVs were rarefied, values less than 0.1% relative abundance were filtered out, and the default correlation coefficient cutoff point was set to 0.7 at $p< 0.01$. Gephi (version 0.9.2) software (Bastian et al., 2009) was used to visualize the co-occurrence network.

3 Results

3.1 Effects of soil amendments on soil nutritional content and ginseng survival rate

The impact of cow dung and canola on the soil nutritional content of six-year-old ginseng cultivated soil with a known problem with ginseng replanting is illustrated in Table 1. Although each treatment began with a single composite sick soil sample, the cow dung and canola soil amendments improved the soil's nutritional status in terms of pH, EC, total carbon, total phosphorus, and available phosphorus. In addition, cow dung outperformed canola and control considerably ($p \leq 0.05$) in terms of soil NO_3^-, whereas canola exceeded in TN, NH_4^+, and exchangeable potassium (K).

Our study also revealed that, between treatments, the ginseng survival rate, shoot length, and shoot dry weight varied significantly ($p \leq 0.05$) (Figures 1B–F) at 90DAT. When compared to the control, cow dung significantly ($p \leq 0.05$) increased ginseng survival by 100%, whereas canola showed no discernible difference (Figures 1B, C). Cow dung also had a significantly ($p \leq 0.05$) high positive impact on ginseng seedling growth in terms of shoot length and weight (Figures 1D, E). The difference in chlorophyll content among the treatments was found to be insignificant ($p > 0.05$) (Figure 1F). Notably, there was no difference in ginseng emergence rate between treatments at the beginning; all had 100% emergence (data not shown), indicating that the soil amendments had no phytotoxic effects.

3.2 Microbial diversity and community composition changes following soil amendments

Most alpha diversity indices revealed a significantly ($p \leq 0.05$) high variation between the soil amendments, but not with sampling time (Figures 2A, B; Table S2). Furthermore, factorial ANOVA revealed that there was no significant ($p>0.05$) interaction effect between treatments and sampling time in most alpha diversity indices (Table S2), implying that the degree of soil amendment impact on these diversity indices did not vary across sampling times. Canola had a high negative effect on alpha diversity compared to cow dung and control (Figures 2A, B; Table S2). At 90DAT, there was a slight recovery of fungal and bacterial diversity in canola. Soil amendments also showed substantial variation in bacterial ($R^2 = 0.54$, $p \leq 0.001$) and fungal ($R^2 = 0.78$, $p \leq 0.001$) community composition (Figures 2C, D; Table 2). However, the shift in bacterial composition following cow dung and canola amendments across sampling periods varied, as revealed by the highly significant interaction effect between sampling time and treatment ($R^2 = 0.16$, $p \leq 0.001$) (Table 2). At 90DAT, the bacterial composition shift in cow dung was stable, whereas in canola, the microbial profile showed no return to that of 0DAT (Figure 2C, Table 2).

Cow dung and canola had a remarkable impact on taxonomic composition at 0DAT and 90DAT, and they severely depleted members of the phylum Acidobacteriota, one of the dominant phyla in control (Figures 2E, F; Table S3). Following the canola amendment, Pseudomonadota, mainly Gammaproteobacteria, was

TABLE 1 Effects of soil amendment with cow dung and canola on soil chemical properties of ginseng soil with replanting problem[a].

	Treatment		
	Control	Cow dung	Canola
pH	6.2 ± 0.00[c]	7.0 ± 0.06[a]	6.7 ± 0.06[b]
EC (dS m^{-1})	0.30 ± 0.03[b]	0.60 ± 0.12[a]	0.80 ± 0.10[a]
CEC (cmol$_c$ kg^{-1})	9.9 ± 0.16[b]	10.3 ± 0.17[b]	10.9 ± 0.07[a]
Total N (g kg^{-1})	0.10 ± 0.01[c]	0.10 ± 0.00[b]	0.20 ± 0.01[a]
Total C (g kg^{-1})	0.5 ± 0.01[c]	0.7 ± 0.01[b]	1.5 ± 0.01[a]
Total P (g kg^{-1})	279.9 ± 3.79[b]	360.6 ± 10.27[a]	377.5 ± 11.91[a]
AP (mg kg^{-1})	47.6 ± 3.2[c]	142 ± 7.6[a]	90.1 ± 1.1[b]
NO_3^- (mg kg^{-1})	7.9 ± 3.04[b]	22.1 ± 6.33[a]	0.5 ± 0.06[b]
NH_4^+ (mg kg^{-1})	7.8 ± 1.05[b]	7 ± 0.43[b]	87.7 ± 13.04[a]
K (cmol$_c$ kg^{-1})	0.2 ± 0.01[c]	0.2 ± 0.01[b]	0.5 ± 0.02[a]

Electrical conductivity (EC), cation exchange capacity (CEC), total nitrogen (Total N), total carbon (Total C), total phosphate (Total P), nitrate nitrogen (NO_3^-), ammonium nitrogen (NH_4^+), available P_2O_5 (AP), and exchangeable potassium (K).
Mean values followed by different letters (s) in a row represent significant differences at $P \leq 0.05$, LSD test.

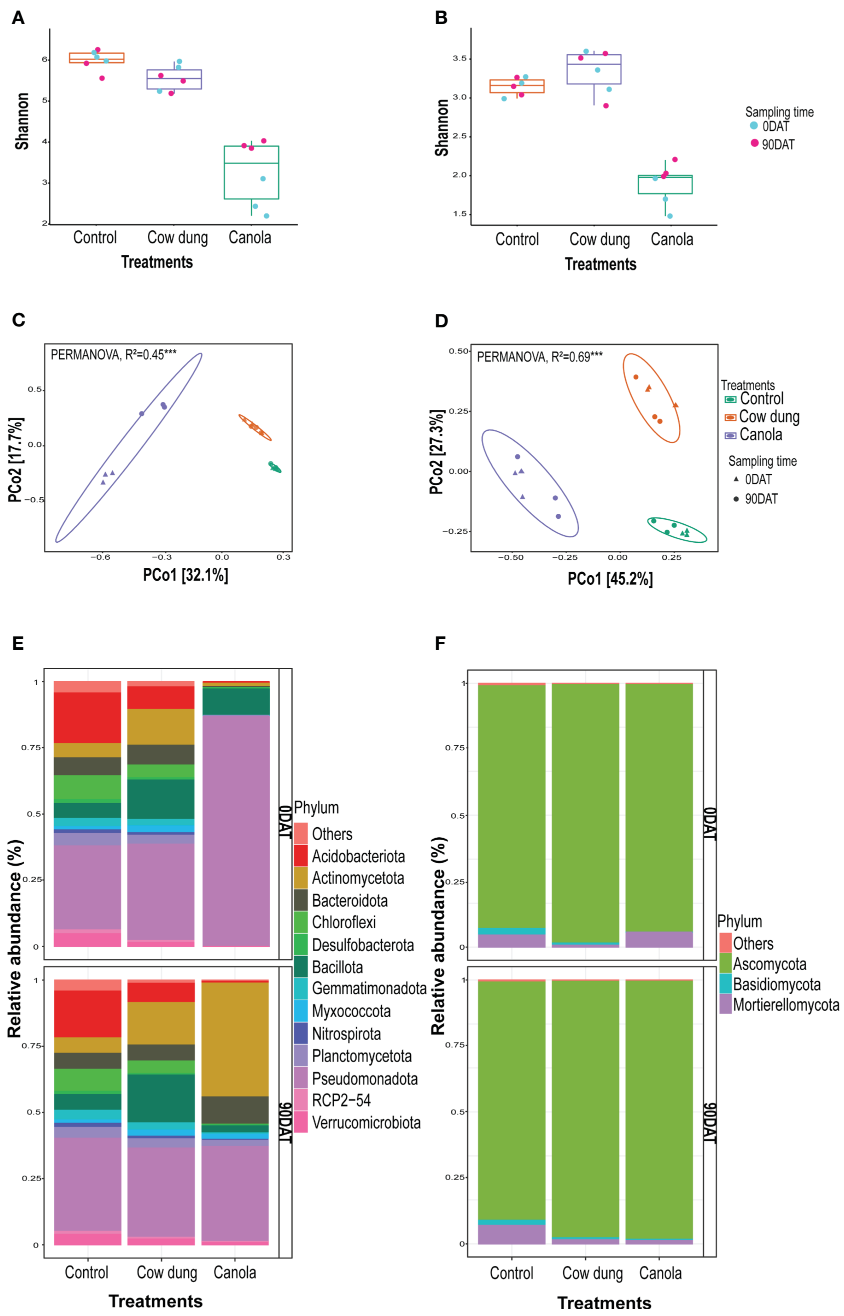

FIGURE 2
Impact of soil amendments on soil microbial diversity and community structure. Alpha bacterial **(A)** and fungal **(B)** diversities. Beta diversity of bacteria **(C)** and fungi **(D)** showing community structure of the treatments. Bacterial **(E)** and fungal **(F)** community composition (>1%) of treatments at phylum level on two sampling times.

the dominant population in the bacterial communities; however, Pseudomonadota was largely replaced by Actinomycetota at 90DAT (Figure 2E; Table S3). In addition, canola showed a severe transient negative impact on Bacteroidota abundance, although there was a complete recovery at 90DAT. In contrast, the cow dung amendment increased Bacillota and Actinomycetota. The increase in Bacillota abundance after cow dung could be partly attributed to the incorporation of cow dung as it was originally dominated by the Bacillota population (Figure S2). This effect persisted even after ginseng transplantation at 90DAT. Certain phyla, such as Armatimonadota and Desulfobacterota, vanished following canola treatment, and no members of this phylum were detected even at 90DAT. Myxococcota and Planctomcetota disappeared temporarily after canola treatment but later recovered three months later, at 90DAT. Ascomycota dominated the fungal community, with a relative abundance of over 85% across all treatments and sampling dates (Figure 2F). Among the other phyla, Basidiomycota was significantly negatively affected by the canola application. The second most abundant fungal phylum, Mortierellomycota, in control declined after cow dung and canola application at 90DAT. Ascomycota was the largest group of true fungi and comprised both pathogenic and saprophytic members. The fungal classes

TABLE 2 PERMANOVA analysis of soil treatment effects on bacterial and fungal community composition structure based on weighted uniFrac distance.

Source of variation		16S		ITS	
	df	F. Model	R^2	F. Model	R^2
Soil amendment	2	8.62	0.45***	19.66	0.69***
Sampling time	1	2.83	0.07**	1.80	0.03
Soil amendment*Sampling time	2	2.98	0.16***	2.10	0.07
Residuals	12		0.32		0.21
Total	17		1.0		1.0

PERMANOVA: Permutational multivariate analysis of variance. Sampling time includes 0DAT (immediately before ginseng transplanting) and 90DAT (90 days after ginseng transplanting). df: degree of freedom. 16S: bacterial community based on the V4-V5 hypervariable region of the 16S rRNA gene. ITS: fungal community based on the internal transcribed spacer 1 (ITS1) region. *p ≤0.05; **p ≤0.01; ***p ≤0.001.

Leotiomycetes and Sordariomycetes dominated control. On both sampling dates, the relative abundance of Leotiomycetes decreased dramatically in cow dung (Figure S3).

3.3 Identification of potential microbial biomarkers enriched in soil amendments

ALDEx2, LEfSe analysis (LDA values > 4), the random forest model, metastat, and metagenomeSeq were used to identify potential microbial biomarkers discriminating the bacterial and fungal communities between the treatments. The results showed that over 464 bacterial and 75 fungal taxa were key discriminatory microbes between the treatment groups (Figure 3; Supplementary material 2). *Bacillus*, *Turicibacter*, *Streptomyces*, *Rhodanobacter*, and *Paeniclostridium* were the most highly stimulated bacterial genera in cow dung, as consistently detected by most biomarker selection tools (Figures 3A, C, E). Several features from Pseudomonadota, such as *Stenotrophomonas* and *Pseudomonas*, were the key bacteria found to be enriched in canola (Figure 3A). In control, the relevant members of p_Acidobacteriota and p_Chloroflexi were comparatively more abundant.

In the fungal community, most biomarker tools detected *Chaetomium* as the most significantly enriched genus in the cow dung application (Figures 3B, D, F), signifying that *Chaetomium* can be considered a key biomarker. Furthermore, f_ Stachybotryaceae, and *Trichoderma* were abundant in the canola treatment (Figures 3B, D). Members of c-Leotiomycetes (including *Pseudeurotium*), *Talaromyces*, *Mrakia*, and *Curvularia* were differentially abundant in control than in the substrate-amended soils (Figures 3B, D, Supplementary material 2).

3.4 Microbial co-occurrence network patterns and functional diversity alterations by soil amendments

RMT-based analysis was employed to construct co-correlation networks for the soil amendments. The results revealed that soil amendments showed a remarkable variation in bacterial-fungal network topologies (Figures 4A–C and Table 3). Cow dung shifted the microbial community assembly of the six-year-old ginseng soil to a highly connected (total links, avWD) and less modularized network (Table 3). It is worth noting that cow dung had a lower percentage of negative links, indicating better co-occurrence than the co-exclusion of bacteria and fungi. In contrast, in canola, the number of nodes, total links, avWD, modularity, GD, and modules were lower than in cow dung and control, implying that the impact of soil amendments on the complexity of the microbial co-occurrence network highly depends on the type of amendment. A negative relationship was found in the intra- and inter-phylum (Figures 4A–C).

Given the shift in soil microbial communities after soil amendment with cow dung and canola, FAPROTAX analysis was performed to determine functional changes. Chemoheterotrophy and aerobic chemoheterotrophy putative functions were the most dominant in all treatments (Figure 4D). The canola amendment enhanced functions related to nitrate reduction and nitrate/nitrogen respiration, which are often called dissimilatory nitrate reduction and lead to the accumulation of NH_4^+ (Picazo et al., 2021) (Figure 4D). There was also a remarkable reduction in the functions related to animal parasites and human-associated and human pathogens following canola. Furthermore, fermentation and chitinolysis were enhanced in cow dung (Figure 4D). The change in fungal ecological guild following soil amendments was parsed using FUNGuild (Figure 4E). The functional profiles of ginseng soil changed with the soil amendments based on the trophic mode. Cow dung-amended soil and cow dung were enriched with dung saprotrophs, epiphytes, and plant saprophytes. In addition, the same treatment was less enriched with functions related to plant pathogens and fungal parasites than canola and control, indicating its potential to enhance soil suppressiveness. The genera that contributed to plant pathogens were *Acremonium*, *Alternaria*, *Calonectria*, *Colletotrichum*, *Coniochaeta*, *Cladosporium*, *Curvularia*, *Dendryphion*, *Fusarium*, *Microascus*, *Monilinia*, *Neofusicoccum*, *Neonectria*, *Rhexocercosporidium*, *Stagonospora*, and *Trichoderma*.

3.5 CLPP analysis and the soil microbiota-soil nutrient relationship

CLPP analysis using 31 different carbon sources in Biolog EcoPlates showed that cow dung induced significant functional changes related to carbon utilization (Figures 5A, B). The distribution of carbon source

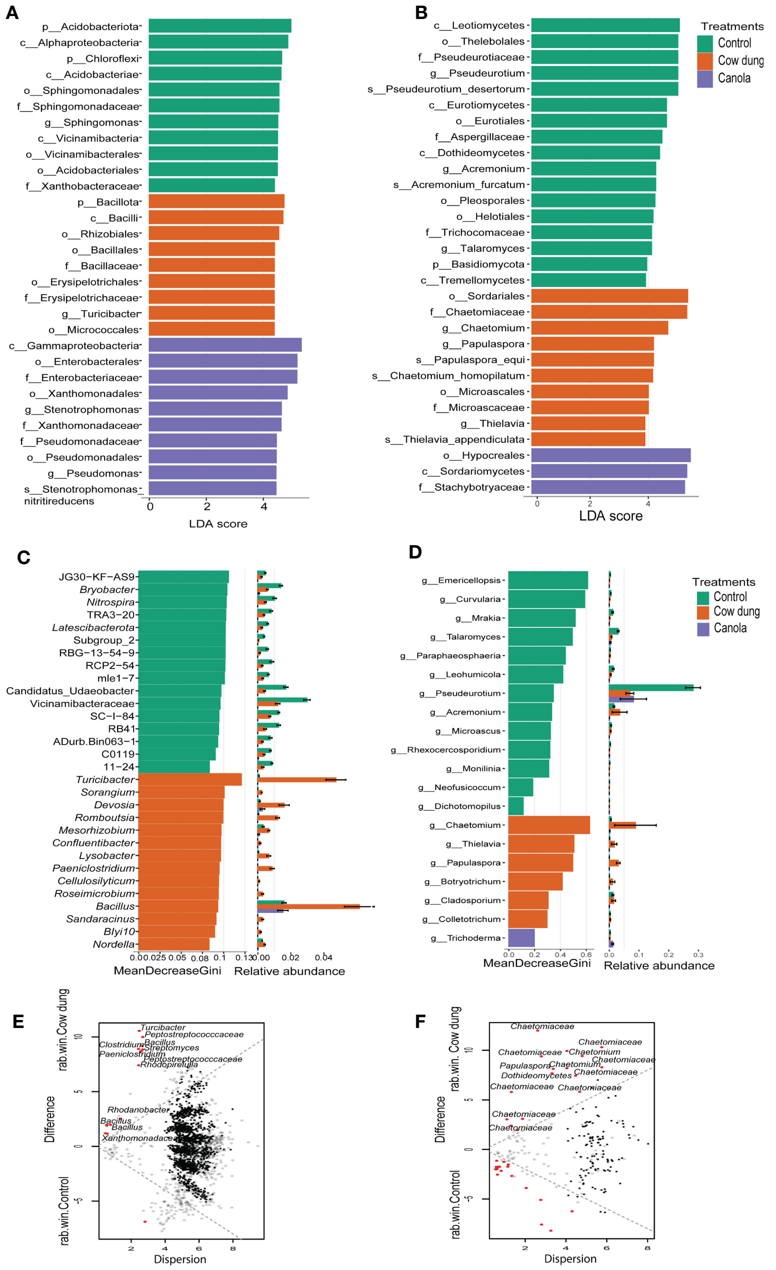

FIGURE 3
Differential abundance analysis of bacterial and fungal taxa after soil amendments. LEfSe analysis (LDA score > 4.0) displaying differentially abundant bacterial **(A)** and fungal **(B)** taxa among the treatments. Taxon names are abbreviated as p: phylum, c: class, o: order, f: family, and g: genus. Random forest model displaying the most predictive bacterial **(C)** and fungal **(D)** genera following soil amendments. Bland-Altman plot showing ALDEx2 analysis between cow dung and control of bacteria **(E)** and fungi **(F)**. ASVs with a larger difference and small dispersion are considered differentially abundant (q ≤ 0.1) and are indicated by red dots. Black and grey dots represent rare and abundant taxa, respectively.

utilization in the soil amendments differed (Figure 5C). Amines/amides were the least utilized carbon groups by the soil microbial communities in the soil amendments. More importantly, compared to control and canola, the cow dung-amended soil had higher utilization rates of carbohydrates and polymer carbon sources. Among the polymers and carbohydrates, Tween 40 and beta-methyl-D-glucoside were the most utilized carbon sources in cow dung (Figure S4). These carbon sources were highly associated with Bacillota (Figure 5D). In contrast, cow dung showed less catabolic activity of carboxylic and acetic acids than canola. Canola showed higher metabolic activities of D-galactonic acid and D-galacturonic acid, which were positively associated with Pseudomonadota (Figure 5D). Such differences in metabolic activity following the change in microbial community assembly may be linked to modifications in soil nutritional content after soil amendment. Most soil chemical properties, including TN, total carbon, and CEC, strongly influenced the soil microbial community structure, where improved soil pH and AP had a cow dung-mediated positive influence on Bacillota (Figure 5E; Table S4). Similarly, most soil factors were consistently found to be determinant factors in the fungal community assembly (Table S4).

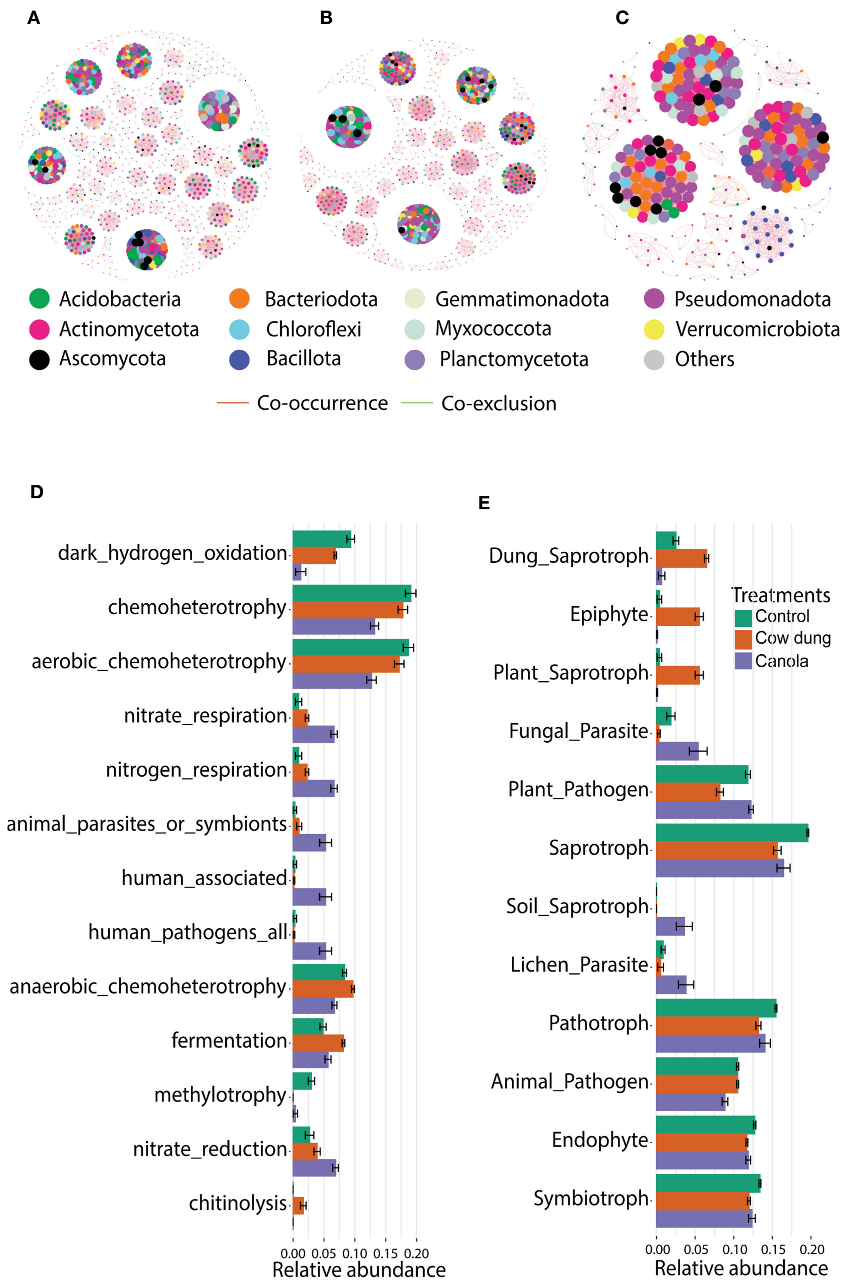

FIGURE 4
Impact of soil amendments on microbial co-occurrence network patterns and functional diversity. Co-occurrence networks of bacterial and fungal communities in treatments based on RMT analysis at the ASV level (Spearman's rank correlation (corr_cut = 0.7), p< 0.05): control **(A)**, cow dung **(B)** and canola **(C)**. Node size in each treatment is proportional to the degree. Predicted functions of bacterial **(D)** and fungal communities **(E)** in different treatments based on the FAPROTAX database and fungal guild tools, respectively. LEfSe analysis (LDA score > 4.0) showed differentially enriched predicted functions across treatments.

4 Discussion

The GRP is a major concern for ginseng farmers throughout much of the world, including South Korea. Soil microbiota imbalance and accumulation of toxic substances are the major causes of GRP (Lee et al., 2015; Liu et al., 2021b). Several agricultural interventions have the potential to shift the microbiota structure and induce disease suppression (Qi et al., 2020) (Jayaraman et al., 2021). soil amendment is an environmentally benign non-chemical approach that is effective in reshaping the soil microbiota, resulting in reduced continuous cropping obstacles (Lopes et al., 2022) owing to the introduction or activation of beneficial microbes for soil-borne disease control (Zhao et al., 2020). However, the impact of cow dung and canola on GRP has not been previously investigated, and the shift in taxonomic and functional diversity of soil bacterial and fungal communities after cow dung remains unclear. Therefore, the present study investigated the effect of cow dung and canola on GRP reduction, soil nutrition, and microbiota.

The survival rate of transplanted ginseng seedlings grown in cow dung-treated soil was 100% higher than that of control, whereas canola had no significant effect. In support of our results, numerous studies have documented that soil amendment alleviates the

TABLE 3 Co-occurrence network topological properties of bacterial-fungal communities in soil amendments.

	Soil amendment		
	Control	Cow dung	Canola
Total nodes	1303	1203	307
Total links[a]	20568	35544	5167
Total positive links (%)	99.9	99.97	99.94
Total negative links (%)	0.1	0.03	0.06
avWD[b]	31.57	59.09	33.66
Graph density (GD)	0.024	0.049	0.11
Modularity	0.875	0.784	0.723
Modules	172	124	31

[a]Links: pairwise correlation of nodes.
[b]Average weighted degree (avWD): average number of links per treatment.

replanting problems of different plants (Browne et al., 2018). Li et al. (2019) also applied soil disinfestation with bean dregs and sugarcane bagasse and found a reduction in the replant failure of ginseng plants. However, we believe that this study is the first to document the alleviation of GRP using a soil amendment with cow dung as a substrate. Changes in soil microbiota are one of the major contributing factors affecting the occurrence of GRP (Dong et al., 2018). Thus, understanding and manipulating the soil microbiota with pre-planting agronomic practices is a novel approach to microbiome-assisted strategies to enhance soil suppressiveness for suitable organic farming systems (Dong et al., 2018; De Corato, 2020).The direct exogenous microbial input from the incorporated cow dung may have contributed to the alteration in microbial community structure assembly (Sun et al., 2015). More importantly, the enhanced soil nutrient content after incorporating cow dung as a carbon source could provide diverse microhabitats for soil microbial growth and colonization (Suleiman et al., 2016; Zhou et al., 2019; Ye et al., 2021), inducing substantial changes in the soil bacterial and fungal community structures (Hu et al., 2018; Liu et al., 2021b). Our findings are in agreement with previous reports that soil nutrients, such as pH, TC, and TN, were the major factors shaping soil microbial community in the ginseng field and alleviating GRP (Zhang et al., 2020; Ji et al., 2021b; Liu et al., 2021b).

Chloroflexi and Acidobacteriota are oligotrophic bacteria that specifically adapt to low available resources (Eo and Park, 2016; Liang et al., 2018; Ye et al., 2021), and low soil pH often decreases their abundance after organic amendments (Ye et al., 2021), similar to the cow dung and canola results. The accumulation of different types of acidic compounds after ginseng monocropping is a major challenge in ginseng production (Li et al., 2018). The improvement in pH after cow dung shows its neutralizing potential, as the applied cow dung was alkaline. Similarly, a previous study reported the acid-neutralizing potential of manure and its potential to prevent nitrate leaching (Sun et al., 2015). Chloroflexi is often highly correlated with several soil-borne diseases (Liang et al., 2018; Ren et al., 2018) and is described as disease-inducing bacteria (Niu et al., 2016). This may be due to the fact that the majority of Chloroflexi members are not able to fix nitrogen but instead compete with beneficial soil microbes and host plants for nitrogen resources (Niu et al., 2016; Ren et al., 2018). In contrast, members of Bacillota, including *Bacillus* and *Clostridium* were differentially abundant in cow dung treatment. Bacillota, known for their crop growth promotion and high antifungal activity, are often strongly associated with soil suppressiveness (Lee et al., 2021) and subsequently protect ginseng plant health. Microbial biomarkers, such as *Bacillus* and *Streptomyces*, have an inverse relationship with GRP, and they are significantly enriched in healthy ginseng soil (Li et al., 2019; Ji et al., 2021a). This was partly due to their ability to hydrolyze ginsenosides, one of the main components of GRP, *via* β-glucosidase and β-glucuronidase (Li et al., 2019). *Clostridium* and *Rhodanobacter* often increase with substrate soil amendment and improve soil suppressiveness (Liang et al., 2018; Poret-Peterson et al., 2019) *via* their toxic organic acids (Huang et al., 2015). In addition, *Rhodanobacter* degrades diisobutyl phthalate, a toxic allelopathic chemical that causes GRP (Dong et al., 2018). This suggests that the enrichment of such biomarkers in cow dung may have reduced obstacles to ginseng replanting (Ji et al., 2021a). In the fungal community, Leotiomycetes, which include diverse groups of plant pathogens and are often enriched in continuous ginseng cultivation (Bao et al., 2020), were found to be remarkably reduced by cow dung compared to control and canola. However, *Chaetomium*, a biomarker in healthy ginseng soil (Dong et al., 2022), was abundant in cow dung. *Chaetomium* is a beneficial fungus for controlling soil-borne diseases, including ginseng diseases (Grunewaldt-Stöcker and von Alten, 2003; Zhou et al., 2019; Li et al., 2020), and it also increases crop tolerance to abiotic stresses (Liu et al., 2021b). In canola treatment, the decline in the abundance of Gemmatimonadota, Armatimonadota, Desulfobacterota, Myxococcota, and Planctometota could be attributed to their sensitivity to ITCs released from soil biofumigants (Tagele et al., 2021).

Co-occurrence network analysis is a novel method that helps us to understand the complex association among microbial communities in soil ecosystems and highlights how such complex interaction is impacted by agricultural activities (Goberna and Verdú, 2022). The more clustered network and firmly connected microbial community in cow dung could potentially make the community highly stable (Sun et al., 2015) to soil sickness owing to continuous ginseng

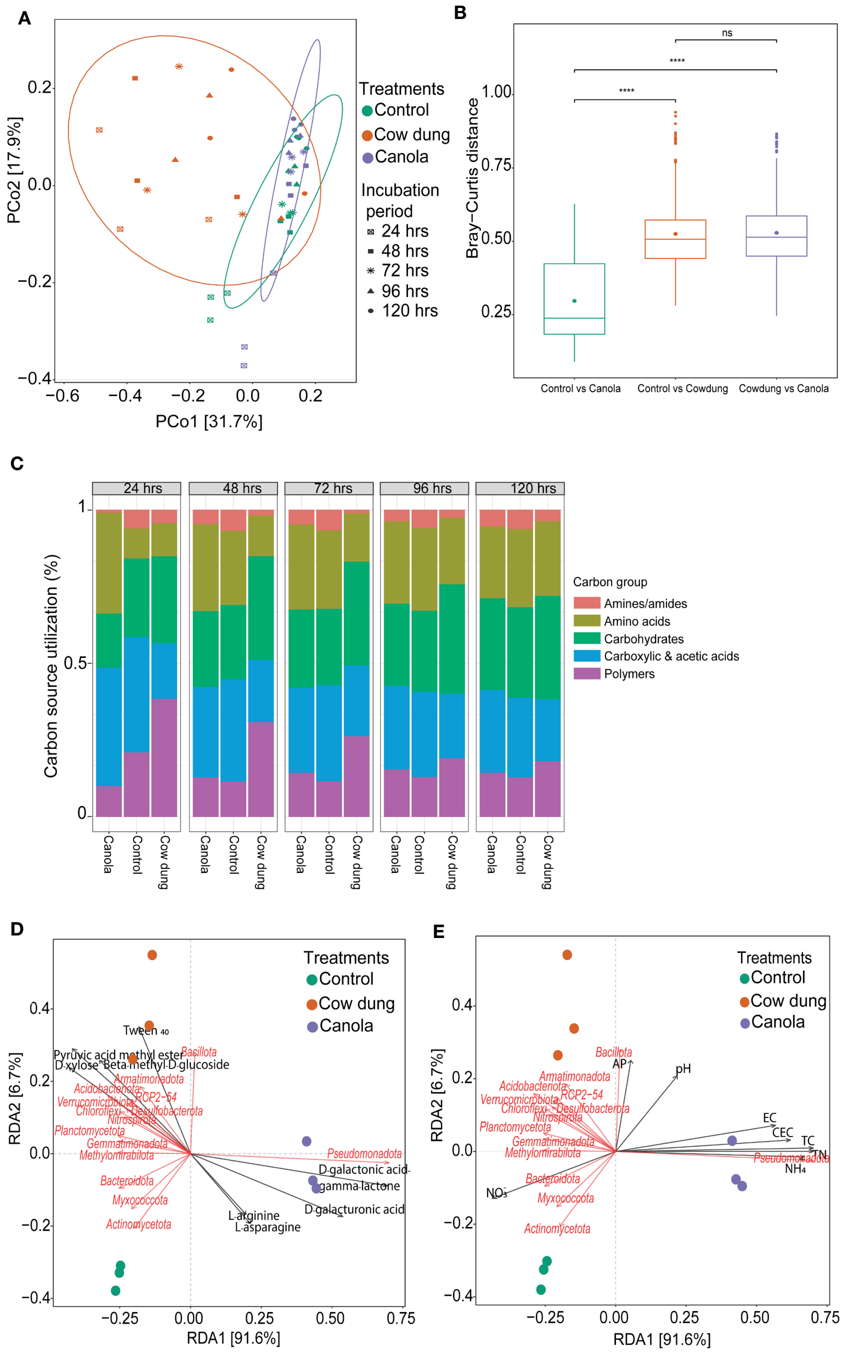

FIGURE 5
Effects of soil amendments on soil chemical properties, microbial communities, and their metabolic activities. PCOA plot showing the community-level physiological profiling using Biolog EcoPlates with 31 different carbon sources at different incubation periods **(A, B)**. Relative carbon source utilization (%) **(C)**. Distance-based redundancy analysis (dbRDA) based on Bray-Curtis distance displaying the relationship of the soil bacterial communities with metabolic activities **(D)** and soil chemical properties **(E)** as indicated by the angles and projection of arrows. The length of the arrows represents the contribution of each soil chemical parameter to the variation in the bacterial community structure. Refer to Table 1 for soil chemical property abbreviations.

monocropping (He et al., 2021), pathogen colonization (Rybakova et al., 2017), and environmental stresses (He et al., 2021), thereby maintaining soil health (Liu et al., 2021a). In contrast, scattered niches in control and canola would harm the prompt defense against foreign pathogen invasion (Tao et al., 2018). Similar to our results, previous reports have documented larger modularity and a higher percentage of negative links in disease-conducive soil than in disease-suppressive soils, in which the latter has dense, high degree, and low modularity (Gao et al., 2021; Ji et al., 2021b). Furthermore, structural shifts in the microbiota are mostly associated with functional changes that drive the agricultural ecosystem (Dubey et al., 2015). Alterations in soil carbon pools can affect the metabolic activity of the soil bacterial and fungal communities. The high utilization of carbohydrate and polymer carbon sources and the predicted function of high fermentation, as seen in cow dung, increase the conversion of carbohydrates to organic acids (Yu et al., 2021), which can potentially reduce soil-borne pathogens, including those causing GRP (Poret-Peterson et al., 2019), although this requires further investigation. Furthermore, such high microbial metabolic activity coupled with plastic cover during BSD process can potentially enhance the soil temperature that may, in turn, contribute to a high decomposition rate of residual antibiotics (Cycon et al., 2019). The saprotroph trophic mode was the most dominant functional group in control, which agrees with previous reports that continuous ginseng cultivation leads to significantly enriched saprotrophs (Bao et al., 2020; Ji et al., 2021b). In addition, the reduced enrichment of predicted functions related to plant pathogens and fungal parasites in cow dung suggests that its application may have resulted in the enrichment of various ecological functions that contribute to reducing GRP.

5 Conclusions

Amending soil with cow dung improved soil nutritional content, increased ginseng survival, and showed a remarkable positive effect on ginseng shoot length and shoot. Microbial profiling by sequencing showed that cow dung modified the soil microbial composition, in which Acidobacteriota and Leotiomycetes were highly depleted, whereas Bacillota and Actinomycetota were enriched. Further microbial biomarker analysis revealed that *Bacillus*, *Turicibacter*, *Streptomyces*, *Rhodanobacter*, *Paeniclostridium*, and *Chaetomium* were the most highly stimulated genera in cow dung. The microbial communities in the cow dung soil had higher utilization rates of carbohydrates and polymer carbon sources, which were most highly associated with Bacillota. In contrast, in Pseudomonadota-dominated canola soil, there was a higher metabolic activity of carboxylic and acetic acids, mainly D-galactonic acid and D-galacturonic acid. After soil substrate amendment, soil nutritional changes, such as soil TN, total carbon, and CEC, were found to be determinant factors in microbial community composition. Furthermore, RMT analysis revealed that cow dung transformed the microbial co-occurrence network into a highly connected and complex network. In contrast, canola harmed the complexity of the microbial co-occurrence network. The predicted functional profiles of ginseng soil, based on FUNGuild trophic mode, showed that cow dung was less enriched with functions related to plant pathogens and fungal parasites compared to canola and control, signifying its potential to enhance soil suppressiveness.

Data availability statement

The original contributions presented in the study are publicly available. This data can be found here: NCBI, PRJNA846516 (BioSample accessions: SRR19568260-SRR19568295, SRR21733898–SRR21733899).

Author contributions

ST and J-HS planned and designed the research study. ST, R-HK, MJ, D-RJ, KL, DL, and WK performed the research. ST and J-HS analyzed the data. ST prepared the figures and tables. ST and J-HS wrote the manuscript. All authors contributed to the article and approved the submitted version.

Funding

This research was supported by the Basic Science Research Program through the National Research Foundation (NRF) of Korea (NRF-2020R1I1A3074522 and NRF-2022R1I1A3071893) and the Korea Basic Science Institute (National Research Facilities and Equipment Center), funded by the Ministry of Education (NRF-2021R1A6C101A416), Republic of Korea. This research was also supported by the Ministry of Environment, Republic of Korea, for training professional personnel in biological materials.

Acknowledgments

The authors are grateful to the NRF for financial support. We also thank Editage (www.editage.co.kr) for English language editing.

Conflict of interest

The authors declare that the research was conducted in the absence of any commercial or financial relationships that could be construed as a potential conflict of interest.

Publisher's note

Supplementary material

The Supplementary Material for this article can be found online at: https://www.frontiersin.org/articles/10.3389/fpls.2023.1072216/full#supplementary-material

SUPPLEMENTARY MATERIAL 2
Bacterial and fungal biomarkers detected using Aldex2, metastat, and metagenomeSeq.

References

Anderson, M. J., Crist, T. O., Chase, J. M., Vellend, M., Inouye, B. D., Freestone, A. L., et al. (2011). Navigating the multiple meanings of β diversity: A roadmap for the practicing ecologist. *Ecol. Lett.* 14, 19–28. doi: 10.1111/j.1461-0248.2010.01552.x

Bao, Y., Qi, B., Huang, W., Liu, B., and Li, Y. (2020). The fungal community in non-rhizosphere soil of *Panax ginseng* are driven by different cultivation modes and increased cultivation periods. *PeerJ* 8, 1–15. doi: 10.7717/peerj.9930

Bastian, M., Heymann, S., and Jacomy, M. (2009). "Gephi: An open source software for exploring and manipulating networks," in *Proceedings of the International AAAI conference on weblogs and social media*. 3 (1), 361–362. doi: 10.1609/icwsm.v3i1.13937

Beck, D., and Foster, J. A. (2014). Machine learning techniques accurately classify microbial communities by bacterial vaginosis characteristics. *PloS One* 9 (2), e87830. doi: 10.1371/journal.pone.0087830

Browne, G. T., Ott, N., Poret-Peterson, A., Gouran, H., and Lampinen, B. (2018). Efficacy of anaerobic soil disinfestation for control of *Prunus* replant disease. *Plant Dis.* 102, 209–219. doi: 10.1094/PDIS-09-16-1392-RE

Bziuk, N., MacCario, L., Douchkov, D., Lueck, S., Babin, D., Sørensen, S. J., et al. (2021). Tillage shapes the soil and rhizosphere microbiome of barley-but not its susceptibility towards blumeria graminis f. sp. hordei. *FEMS Microbiol. Ecol.* 97, 1–14. doi: 10.1093/femsec/fiab018

Callahan, B. J., McMurdie, P. J., Rosen, M. J., Han, A. W., Johnson, A. J. A., and Holmes, S. P. (2016). DADA2: High-resolution sample inference from illumina amplicon data. *Nat. Methods* 13, 581–583. doi: 10.1038/nmeth.3869

Cycoń, M., Mrozik, A., and Piotrowska-Seget, Z. (2019). Antibiotics in the soil environment–degradation and their impact on microbial activity and diversity. *Front. Microbiol.* 10. doi: 10.3389/fmicb.2019.00338

De Corato, U. (2020). Soil microbiota manipulation and its role in suppressing soil-borne plant pathogens in organic farming systems under the light of microbiome-assisted strategies. *Chem. Biol. Technol. Agric.* 7, 1–26. doi: 10.1186/s40538-020-00183-7

Dixon, P. (2003). Computer program review VEGAN , a package of r functions for community ecology. *J. Veg. Sci.* 14, 927–930. doi: 10.1111/j.1654-1103.2002.tb02049.x

Dong, L., Bian, X., Zhao, Y., Yang, H., Xu, Y., Han, Y., et al. (2022). Rhizosphere analysis of field-grown *Panax ginseng* with different degrees of red skin provides the basis for preventing red skin syndrome. *BMC Microbiol.* 22, 1–15. doi: 10.1186/s12866-021-02430-9

Dong, L., Xu, J., Li, Y., Fang, H., Niu, W., Li, X., et al. (2018). Manipulation of microbial community in the rhizosphere alleviates the replanting issues in *Panax ginseng*. *Soil Biol. Biochem.* 125, 64–74. doi: 10.1016/j.soilbio.2018.06.028

Dubey, R. K., Tripathi, V., and Abhilash, P. C. (2015). Book review: Principles of plant-microbe interactions: Microbes for sustainable agriculture. *Front. Plant Sci.* 6. doi: 10.3389/fpls.2015.00986

DuPont, S. T., Hewavitharana, S. S., and Mazzola, M. (2021). Field scale application of *Brassica* seed meal and anaerobic soil disinfestation for the control of apple replant disease. *Appl. Soil Ecol.* 166, 104076. doi: 10.1016/j.apsoil.2021.104076

Eo, J., and Park, K. C. (2016). Long-term effects of imbalanced fertilization on the composition and diversity of soil bacterial community. *Agric. Ecosyst. Environ.* 231, 176–182. doi: 10.1016/j.agee.2016.06.039

Fernandes, A. D., Macklaim, J. M., Linn, T. G., Reid, G., and Gloor, G. B. (2013). ANOVA-like differential expression (ALDEx) analysis for mixed population RNA-seq. *PloS One* 8 (7), e67019. doi: 10.1371/journal.pone.0067019

Gao, M., Xiong, C., Gao, C., Tsui, C. K. M., Wang, M. M., Zhou, X., et al. (2021). Disease-induced changes in plant microbiome assembly and functional adaptation. *Microbiome* 9, 1–18. doi: 10.1186/s40168-021-01138-2

Giovannini, D., Brandi, F., Lanteri, A. P., Lazzeri, L., Maltoni, M. L., Matteo, R., et al. (2021). Non-chemical soil fumigation for sustainable strawberry production in southern italy. *Agronomy* 11, 1–15. doi: 10.3390/agronomy11081678

Goberna, M., and Verdú, M. (2022). Cautionary notes on the use of co-occurrence networks in soil ecology. *Soil Biol. Biochem.* 166, 108534. doi: 10.1016/j.soilbio.2021.108534

Grunewaldt-Stöcker, G., and von Alten, H. (2003). Plant health effects of acremonium root endophytes compared to those of arbuscular mycorrhiza. *Roots Dyn. Interface Between Plants Earth* (Dordrecht: Springer) 445–454. doi: 10.1007/978-94-017-2923-9_44

Gu, Z., Eils, R., and Schlesner, M. (2016). Complex heatmaps reveal patterns and correlations in multidimensional genomic data. *Bioinformatics* 32, 2847–2849. doi: 10.1093/bioinformatics/btw313

Gupta, K. K., Aneja, K. R., and Rana, D. (2016). Current status of cow dung as a bioresource for sustainable development. *Bioresour. Bioprocess.* 3, 1-11. doi: 10.1186/s40643-016-0105-9

He, Q., Wang, S., Hou, W., Feng, K., Li, F., Hai, W., et al. (2021). Temperature and microbial interactions drive the deterministic assembly processes in sediments of hot springs. *Sci. Total Environ.* 772, 145465. doi: 10.1016/j.scitotenv.2021.145465

Huang, X., Wen, T., Zhang, J., Meng, L., Zhu, T., and Cai, Z. (2015). Toxic organic acids produced in biological soil disinfestation mainly caused the suppression of *Fusarium oxysporum* f. sp. cubense. *BioControl* 60, 113–124. doi: 10.1007/s10526-014-9623-6

Hu, X., Liu, J., Zhu, P., Wei, D., Jin, J., Liu, X., et al. (2018). Long-term manure addition reduces diversity and changes community structure of diazotrophs in a neutral black soil of northeast China. *J. Soils Sediments* 18, 2053–2062. doi: 10.1007/s11368-018-1975-6

Jayaraman, S., Naorem, A. K., Lal, R., Dalal, R. C., Sinha1, N. K., Patra1, A. K., et al. (2021). Disease-suppressive soils — beyond food Production: a critical review. *Soil Sci. Plant Nutr.* 21 (2), 1437–1465. doi: 10.1007/s42729-021-00451-x

Ji, L., Nasir, F., Tian, L., Chang, J., Sun, Y., Zhang, J., et al. (2021a). Outbreaks of root rot disease in different aged american ginseng plants are associated with field microbial dynamics. *Front. Microbiol.* 12. doi: 10.3389/fmicb.2021.676880

Ji, L., Tian, L., Nasir, F., Chang, J., Chang, C., Zhang, J., et al. (2021b). Impacts of replanting American ginseng on fungal assembly and abundance in response to disease outbreaks. *Arch. Microbiol.* 203, 2157–2170. doi: 10.1007/s00203-021-02196-8

Lee, B. D., Dutta, S., Ryu, H., Yoo, S. J., Suh, D. S., and Park, K. (2015). Induction of systemic resistance in *Panax ginseng* against phytophthora cactorum by native *Bacillus amyloliquefaciens* HK34. *J. Ginseng Res.* 39, 213–220. doi: 10.1016/j.jgr.2014.12.002

Lee, S. M., Kong, H. G., Song, G. C., and Ryu, C. M. (2021). Disruption of firmicutes and actinobacteria abundance in tomato rhizosphere causes the incidence of bacterial wilt disease. *ISME J.* 15, 330–347. doi: 10.1038/s41396-020-00785-x

Liang, B., Ma, C., Fan, L., Wang, Y., and Yuan, Y. (2018). Soil amendment alters soil physicochemical properties and bacterial community structure of a replanted apple orchard. *Microbiol. Res.* 216, 1–11. doi: 10.1016/j.micres.2018.07.010

Li, Y., Dai, S., Wang, B., Jiang, Y., Ma, Y., Pan, L., et al. (2020). Autotoxic ginsenoside disrupts soil fungal microbiomes by stimulating potentially pathogenic microbes. *Appl. Env. Microbiol.* 86 (9), 1–14. doi: 10.1128/AEM.00130-20

Li, Z., Fu, J., Zhou, R., and Wang, D. (2018). Effects of phenolic acids from ginseng rhizosphere on soil fungi structure, richness and diversity in consecutive monoculturing of ginseng. *Saudi J. Biol. Sci.* 25, 1788–1794. doi: 10.1016/j.sjbs.2018.07.007

Liu, X., Fang, W., Yan, D., Wang, Q., Li, Y., Jin, X., et al. (2022). Evaluation of the efficacy of fumigants allyl isothiocyanate and dimethyl disulfide against *Panax notoginseng* root rot caused by *Fusarium solani*. *Eur. J. Plant Pathol* 162 (4), 897-905. doi: 10.1007/s10658-021-02445-y

Liu, S., Khan, M. H., Yuan, Z., Hussain, S., Cao, H., and Liu, Y. (2021a). Response of soil microbiome structure and its network profiles to four soil amendments in monocropping strawberry greenhouse. *PloS One* 16, 1–20. doi: 10.1371/journal.pone.0245180

Liu, S., Wang, Z., Niu, J., Dang, K., Zhang, S., Wang, S., et al. (2021b). Changes in physicochemical properties, enzymatic activities, and the microbial community of soil significantly influence the continuous cropping of *Panax quinquefolius* l. (American ginseng). *Plant Soil* 463, 427–446. doi: 10.1007/s11104-021-04911-2

Li, Y., Wang, B., Chang, Y., Yang, Y., Yao, C., Huang, X., et al. (2019). Reductive soil disinfestation effectively alleviates the replant failure of sanqi ginseng through allelochemical degradation and pathogen suppression. *Appl. Microbiol. Biotechnol.* 103, 3581–3595. doi: 10.1007/s00253-019-09676-4

Lopes, E. A., Canedo, E. J., Gomes, V. A., Vieira, B. S., Parreira, D. F., and Neves, W (2022). Anaerobic soil disinfestation for the management of soilborne pathogens: A review. *S. Appl. Soil Ecol.* 174, 104408. doi: 10.1016/j.apsoil.2022.104408

Louca, S., Parfrey, L. W., and Doebeli, M. (2016). Decoupling function and taxonomy in the global ocean microbiome. *Sci. (80-)* 353, 1272–1277. doi: 10.1126/science.aaf4507

Momma, N., Yamamoto, K., Simandi, P., and Shishido, M. (2006). Role of organic acids in the mechanisms of biological soil disinfestation (BSD). *J. Gen. Plant Pathol.* 72, 247–252. doi: 10.1007/s10327-006-0274-z

Nguyen, N. H., Song, Z., Bates, S. T., Branco, S., Tedersoo, L., Menke, J., et al. (2016). FUNGuild: An open annotation tool for parsing fungal community datasets by ecological guild. *Fungal Ecol.* 20, 241–248. doi: 10.1016/j.funeco.2015.06.006

Nilsson, R. H., Larsson, K. H., Taylor, A. F. S., Bengtsson-Palme, J., Jeppesen, T. S., Schigel, D., et al. (2019). The UNITE database for molecular identification of fungi: Handling dark taxa and parallel taxonomic classifications. *Nucleic Acids Res.* 47, D259–D264. doi: 10.1093/nar/gky1022

Niu, J., Rang, Z., Zhang, C., Chen, W., Tian, F., Yin, H., et al. (2016). The succession pattern of soil microbial communities and its relationship with tobacco bacterial wilt. *BMC Microbiol.* 16, 1–10. doi: 10.1186/s12866-016-0845-x

Oksanen, J., Blanchet, F. G., Friendly, M., Kindt, R., Legendre, P., McGlinn, D., et al. (2020). Community Ecology.

Paulson, J. N., Stine, O. C., Bravo, H. C., and Pop, M. (2013). Differential abundance analysis for microbial marker-gene surveys. *Nat. Methods* 10, 1200–1202. doi: 10.1038/nmeth.2658

Picazo, A., Villaescusa, J. A., Rochera, C., Miralles-Lorenzo, J., Quesada, A., and Camacho, A. (2021). Functional metabolic diversity of bacterioplankton in maritime antarctic lakes. *Microorganisms* 9, 1–22. doi: 10.3390/microorganisms9102077

Poret-Peterson, A. T., Albu, S., McClean, A. E., and Kluepfel, D. A. (2019). Shifts in soil bacterial communities as a function of carbon source used during anaerobic soil disinfestation. *Front. Environ. Sci.* 6. doi: 10.3389/fenvs.2018.00160

Qi, G., Chen, S., Ke, L., Ma, G., and Zhao, X. (2020). Cover crops restore declining soil properties and suppress bacterial wilt by regulating rhizosphere bacterial communities and improving soil nutrient contents. *Microbiol. Res.* 238, 126505. doi: 10.1016/j.micres.2020.126505

Quast, C., Pruesse, E., Yilmaz, P., Gerken, J., Schweer, T., Yarza, P., et al. (2013). The SILVA ribosomal RNA gene database project: Improved data processing and web-based tools. *Nucleic Acids Res* 41 (D1), D590-D596. doi: 10.1093/nar/gks1219

R Core Team (2022). *R: A language and environment for statistical computing* (Vienna, Austria: R Foundation for Statistical Computing). Available at: https://www.r-project.org/.

Ren, G., Ma, Y., Guo, D., Gentry, T. J., Hu, P., Pierson, E. A., et al. (2018). Soil bacterial community was changed after brassicaceous seed meal application for suppression of *Fusarium* wilt on pepper. *Front. Microbiol.* 9. doi: 10.3389/fmicb.2018.00185

Romdhane, S., Spor, A., Banerjee, S., Breuil, M. C., Bru, D., Chabbi, A., et al. (2022). Land-use intensification differentially affects bacterial, fungal and protist communities and decreases microbiome network complexity. *Environ. Microbiomes* 17, 1–15. doi: 10.1186/s40793-021-00396-9

Rybakova, D., Mancinelli, R., Wikström, M., Birch-Jensen, A. S., Postma, J., Ehlers, R. U., et al. (2017). The structure of the *Brassica napus* seed microbiome is cultivar-dependent and affects the interactions of symbionts and pathogens. *Microbiome* 5, 104. doi: 10.1186/s40168-017-0310-6

Segata, N., Izard, J., Waldron, L., Gevers, D., Miropolsky, L., Garrett, W. S., et al. (2011). Metagenomic biomarker discovery and explanation. *Genome Biol.* 12, R60. doi: 10.1186/gb-2011-12-6-r60

Seo, M. W., Han, Y. K., Bae, Y. S., and Lee, S. H. (2019). The disease severity and related pathogens caused by root rot on 6 years old ginseng cultivation fields. *Korean J. Plant Res,* 32, 144–152. doi: 10.7732/kjpr.2019.32.2.144

Srivastava, A. K., Das, A. K., Jagannadham, P. T. K., Bora, P., Ansari, F. A., and Bhate, R. (2022). Bioprospecting microbiome for soil and plant health management amidst huanglongbing threat in citrus: A review. *Front. Plant Sci.* 13. doi: 10.3389/fpls.2022.858842

Suleiman, A. K. A., Gonzatto, R., Aita, C., Lupatini, M., Jacques, R. J. S., Kuramae, E. E., et al. (2016). Temporal variability of soil microbial communities after application of dicyandiamide-treated swine slurry and mineral fertilizers. *Soil Biol. Biochem.* 97, 71–82. doi: 10.1016/j.soilbio.2016.03.002

Sun, R., Zhang, X. X., Guo, X., Wang, D., and Chu, H. (2015). Bacterial diversity in soils subjected to long-term chemical fertilization can be more stably maintained with the addition of livestock manure than wheat straw. *Soil Biol. Biochem.* 88, 9–18. doi: 10.1016/j.soilbio.2015.05.007

Tagele, S. B., Kim, R. H., and Shin, J. H. (2021). Interactions between *Brassica* biofumigants and soil microbiota: Causes and impacts. *J. Agric. Food Chem.* 69, 11538–11553. doi: 10.1021/acs.jafc.1c03776

Tao, J., Meng, D., Qin, C., Liu, X., Liang, Y., Xiao, Y., et al. (2018). Integrated network analysis reveals the importance of microbial interactions for maize growth. *Appl. Microbiol. Biotechnol.* 102, 3805–3818. doi: 10.1007/s00253-018-8837-4

Tong, A. Z., Liu, W., Liu, Q., Xia, G. Q., and Zhu, J. Y. (2021). Diversity and composition of the panax ginseng rhizosphere microbiome in various cultivation modesand ages. *BMC Microbiol.* 21, 1–13. doi: 10.1186/s12866-020-02081-2

Wang, L., and Mazzola, M. (2019). Field evaluation of reduced rate brassicaceae seed meal amendment and rootstock genotype on the microbiome and control of apple replant disease. *Phytopathology* 109, 1378–1391. doi: 10.1094/PHYTO-02-19-0045-R

White, J. R., Nagarajan, N., and Pop, M. (2009). Statistical methods for detecting differentially abundant features in clinical metagenomic samples. *PloS Comput. Biol.* 5 (4), e1000352. doi: 10.1371/journal.pcbi.1000352

Wickham, H. (2016). *ggplot2: Elegant graphics for data analysis* (New York: Springer-Verlag). Available at: https://ggplot2.tidyverse.org/, ISBN: .

Yang, M., Yuan, Y., Huang, H., Ye, C., Guo, C., Xu, Y., et al. (2019). Steaming combined with biochar application eliminates negative plant-soil feedback for sanqi cultivation. *Soil Tillage Res.* 189, 189–198. doi: 10.1016/j.still.2019.02.006

Yang, M., Zhang, X., Xu, Y., Mei, X., Jiang, B., Liao, J., et al. (2015). Autotoxic ginsenosides in the rhizosphere contribute to the replant failure of panax *notoginseng*. *PloS One* 10, 1–17. doi: 10.1371/journal.pone.0118555

Ye, G., Banerjee, S., He, J. Z., Fan, J., Wang, Z., Wei, X., et al. (2021). Manure application increases microbiome complexity in soil aggregate fractions: Results of an 18-year field experiment. *Agric. Ecosyst. Environ.* 307, 107249. doi: 10.1016/j.agee.2020.107249

Yu, Y., Zheng, L., Zhou, Y., Sang, W., Zhao, J., Liu, L., et al. (2021). Changes in soil microbial community structure and function following degradation in a temperate grassland. *J. Plant Ecol.* 14, 384–397. doi: 10.1093/jpe/rtaa102

Zhang, J., Fan, S., Qin, J., Dai, J., Zhao, F., Gao, L., et al. (2020). Changes in the microbiome in the soil of an American ginseng continuous plantation. *Front. Plant Sci.* 11. doi: 10.3389/fpls.2020.572199

Zhao, J., Liu, S., Zhou, X., Xia, Q., Liu, X., Zhang, S., et al. (2020). Reductive soil disinfestation incorporated with organic residue combination significantly improves soil microbial activity and functional diversity than sole residue incorporation. *Appl. Microbiol. Biotechnol.* 104, 7573–7588. doi: 10.1007/s00253-020-10778-7

Zhao, J., Li, Y., Wang, B., Huang, X., Yang, L., Lan, T., et al. (2017). Comparative soil microbial communities and activities in adjacent sanqi ginseng monoculture and maize-sanqi ginseng systems. *Appl. Soil Ecol.* 120, 89–96. doi: 10.1016/j.apsoil.2017.08.002

Zhou, X., Li, C., Liu, L., Zhao, J., Zhang, J., Cai, Z., et al. (2019). Control of *Fusarium* wilt of *Lisianthus* by reassembling the microbial community in infested soil through reductive soil disinfestation. *Microbiol. Res.* 220, 1–11. doi: 10.1016/j.micres.2018.12.001

frontiers | Frontiers in Plant Science

TYPE Original Research
PUBLISHED 14 March 2023
DOI 10.3389/fpls.2023.1057133

Check for updates

OPEN ACCESS

EDITED BY
Amanullah,
University of Agriculture, Peshawar, Pakistan

REVIEWED BY
Behnam Asgari Lajayer,
University of Tabriz, Iran
Fadime Karabulut,
Firat University, Türkiye
Sajid Ali,
Yeungnam University, Republic of Korea

*CORRESPONDENCE
Martin Brtnicky
martin.brtnicky@seznam.cz
Adnan Mustafa
adnanmustafa780@gmail.com

SPECIALTY SECTION
This article was submitted to Plant Nutrition, a section of the journal Frontiers in Plant Science

RECEIVED 29 September 2022
ACCEPTED 02 February 2023
PUBLISHED 14 March 2023

CITATION
Hammerschmiedt T, Holatko J, Zelinka R, Kintl A, Skarpa P, Bytesnikova Z, Richtera L, Mustafa A, Malicek O and Brtnicky M (2023) The combined effect of graphene oxide and elemental nano-sulfur on soil biological properties and lettuce plant biomass. *Front. Plant Sci.* 14:1057133. doi: 10.3389/fpls.2023.1057133

The combined effect of graphene oxide and elemental nano-sulfur on soil biological properties and lettuce plant biomass

Tereza Hammerschmiedt[1], Jiri Holatko[1,2], Radim Zelinka[3], Antonin Kintl[1,4], Petr Skarpa[1], Zuzana Bytesnikova[3], Lukas Richtera[3], Adnan Mustafa[1,5,6]*, Ondrej Malicek[1] and Martin Brtnicky[1,5]*

[1]Department of Agrochemistry, Soil Science, Microbiology and Plant Nutrition, Faculty of AgriSciences, Mendel University in Brno, Brno, Czechia, [2]Agrovyzkum Rapotin, Ltd., Rapotin, Czechia, [3]Department of Chemistry and Biochemistry, Mendel University in Brno, Brno, Czechia, [4]Agricultural Research, Ltd., Troubsko, Czechia, [5]Institute of Chemistry and Technology of Environmental Protection, Faculty of Chemistry, Brno University of Technology, Brno, Czechia, [6]Institute for Environmental Studies, Faculty of Science, Charles University in Prague, Praha, Czechia

The impact of graphene oxide (GO) nanocarbon on soil properties is mixed, with both negative and positive effects. Although it decreases the viability of some microbes, there are few studies on how its single amendment to soil or in combination with nanosized sulfur benefits soil microorganisms and nutrient transformation. Therefore, an eight-week pot experiment was carried out under controlled conditions (growth chamber with artificial light) in soil seeded with lettuce (*Lactuca sativa*) and amended with GO or nano-sulfur on their own or their several combinations. The following variants were tested: (I) Control, (II) GO, (III) Low nano-S + GO, (IV) High nano-S + GO, (V) Low nano-S, (VI) High nano-S. Results revealed no significant differences in soil pH, dry plant aboveground, and root biomass among all five amended variants and the control group. The greatest positive effect on soil respiration was observed when GO was used alone, and this effect remained significant even when it was combined with high nano-S. Low nano-S plus a GO dose negatively affected some of the soil respiration types: NAG_SIR, Tre_SIR, Ala_SIR, and Arg_SIR. Single GO application was found to enhance arylsulfatase activity, while the combination of high nano-S and GO not only enhanced arylsulfatase but also urease and phosphatase activity in the soil. The elemental nano-S probably counteracted the GO-mediated effect on organic carbon oxidation. We partially proved the hypothesis that GO-enhanced nano-S oxidation increases phosphatase activity.

KEYWORDS

soil amendments, agricultural production, microbial activity, nutrient cycling, sulfur nutrition

1 Introduction

In the last decade, 2D carbon-based nanomaterials, such as graphene, graphene oxide, and reduced graphene oxide have been widely applied in various experimental and technological fields, primarily to purify aquatic and soil environments from pollutants. (Teng et al., 2019). GO (42-62% wt carbon, 24-36% wt oxygen) can be prepared from graphite in the laboratory using the Hummers and Offemans method (Marcano et al., 2010; Yu et al., 2016), and further modified by reduction of C=O groups or their derivatization e.g., with metal atoms (Zn, Cu, Ag), which enables environmental adsorptive detoxication from metalloids (Zhang et al., 2020; Sengupta et al., 2022). GO is quite mobile in soil (Sangani et al., 2019; Xia et al., 2021); however, its leaching can be reduced by aggregation mediated by Ca^{2+} in concentration ≥ 0.5 mM (Qi et al., 2014). Amendment of GO to soil alters its hygroscopic and adsorptive capabilities and water content, and reduces the impact of drought stress (Zhao et al., 2020; Zhao et al., 2022); as a carrier, it increases the uptake of mineral micronutrients to plants *via* controlled release (Kabiri et al., 2017; Li et al., 2019; Carneiro et al., 2022; Mohammadi Alagoz et al., 2022). These effects on soil nutritional traits are positive for plant growth and physiology (Lahiani et al., 2015; Juarez-Maldonado et al., 2019) and GO may also benefit by protecting against other plant-harming factors (Arikan et al., 2022). However, the impact of GO on plants is dose-dependent, and high levels of application (up to 2000 mg/L) have been found to lead to increased reactive oxygen species in cabbage, necrotic lesions in tomatoes, and decreased photosystem II activity in peas. (Samadi et al., 2021).

GO has also been found to exhibit varying levels of toxicity towards bacteria, fungi, and algae, negatively impacting their growth and altering the structure of microbial communities in soil (Gurunathan et al., 2012; Chung et al., 2015; Du et al., 2015; Forstner et al., 2019). GOs are generally more toxic to gram-positive bacteria (Kulshrestha et al., 2017) but showed neutral to positive effects on other soil microbes (Wang et al., 2003; Ge et al., 2016). It was also reported that GOs contain soil biological properties (Ren et al., 2015). In some cases, GO has been found to increase bacterial community richness in a concentration-dependent manner (Luo et al., 2022). It has been acknowledged that the integration of GO and other nanomaterials may improve GO properties (Yap et al., 2019; Hammerschmiedt et al., 2022) and provide new specifically-featured materials (Gupta et al., 2015; Liu et al., 2017), which may ameliorate salinity stress on crops (Zahedi et al., 2023). In this context, one of the promising types of nanomaterials is nanosized elemental sulfur. It is highly beneficial in agriculture (Teng et al., 2019) because it is insoluble and thus, does not leach after being added to soil (Riley et al., 2002; Lee et al., 2011; Lucheta and Lambais, 2012; Samadi et al., 2021), and it promotes tolerance to abiotic and biotic stresses in plants (Fuentes-Lara et al., 2019). It should be noted that elemental sulfur needs to be oxidized by bacteria into sulfates (SO_4^{2-}) in order to serve as a nutrient for soil organisms and plants (Degryse et al., 2021). Bacterial oxidation is carried out by several specific soil taxa, i.e., the genus *Thiobacillus* (Germida and Janzen, 1993) and *Betaproteobacteria* (Tourna et al., 2014). On the other hand, some other soil microorganisms, mainly fungi, are adversely affected by elemental sulfur (Williams and Cooper, 2004; Massalimov et al., 2012). Elemental sulfur oxidation is dependent on soil water potential, temperature, aeration (Germida and Janzen, 1993), hydrophobicity of its particles, and their size (Steudel, 2003). Oxidation rate depends indirectly on elemental sulfur particle size (Watkinson and Blair, 1993), therefore, fine-formulated (micronized, nanosized) elemental sulfur is used for accelerated conversion to sulfates and nutrient availability (Chapman 1989; Soltanaeva et al., 2018), improved plant nutrition efficiency (Matamwa et al., 2018; Soltanaeva et al., 2018), enhanced alleviation of metalloid toxicity (Dixit et al., 2015), soil pH modulation (Hu et al., 2007; Almutairi et al., 2017), and plant pests control (Gadino et al., 2011). Crushing, ball milling (Hegedüs et al., 2018; Lonkar et al., 2018), or sonication (Raghavan et al., 2018) are methods used to manufacture micro-/nanosized elemental sulfur, which is sometimes further combined with other types of nanomaterials.

Elemental sulfur combined with carbon nanomaterials (e.g. activated carbon, GO) brings benefits i.e., in environmental and forestry applications (Yang et al., 2019; Jeon et al., 2020; Huang et al., 2021). The stimulatory effect of GO and elemental sulfur on the specific elemental sulfur-oxidizing microbiome in amended soil and successive enhanced transformation to sulfates could be ascribed from the referred supportive impact of graphite plate on the biofilm development of *Acidithiobacillus thiooxidans* (Méndez Tovar et al., 2019). Studies describing similar effects of co-application of nano- or microsized elemental sulfur and GO on soil quality biological indicators, such as respiration (basal as well as substrate-induced) and soil extracellular enzymes activity, have remained largely overlooked. This work aims to better understand this issue and bridge the knowledge gap in order to evaluate the actual benefits of currently developing usage of nanotechnologies in agriculture (Behl et al., 2022). Furthermore, the novelty of this work lies in the original and previously untested combination of GO and elemental nano-sulfur in a composite product, which was designed as a carrier of sulfur for improved accessibility and liability to oxidation and accelerated transformation into plant available form. It is expected that the composite could provide a more quickly transformable form of elemental sulfur and concurrently would not disadvantageously increase its solubility and risk of losses from excessive solubilization and leaching.

Therefore, keeping in view the above background, a pot experiment was carried out to evaluate the combined effect of GO and elemental nano-sulfur (nano-S) on soil pH, biological properties, and dry plant biomass under controlled conditions (growth chamber with artificial light). We hypothesized that:

Abbreviations: ANOVA, one-way analysis of variance; AGB_dry, dry aboveground plant biomass; Ala_SIR, soil respiration induced by L-alanine; Arg_SIR, soil respiration induced by L-arginine; ARS, arylsulfatase; BR, soil basal respiration; DHA, dehydrogenase activity; Glc_SIR, soil respiration induced by D-glucose; GN, graphene; GO, graphene oxide; GLU, β-glucosidase; Man_SIR, soil respiration induced by D-mannose; NAG, N-acetyl-β-D-glucosaminidase; NAG_SIR, soil respiration induced by N-acetyl-β-D-glucosaminidase; nano-S, nanosized elemental sulfur; OM, organic matter; SOM, soil organic matter; p, p-value of statistical significance; PCA, Principal component analysis; Phos, phosphatase; Pro_SIR, soil respiration induced by protocatechuic acid; r, correlation coefficient; rGO, reduced graphene oxide; Root_dry, dry root plant biomass; S, sulfur; SIR, substrate-induced soil respiration; Tre_SIR, soil respiration induced by D-trehalose; Ure, urease.

i. GO application would enhance soil respiration due to its function as an oxidative agent.
ii. Nano-S as an oxidizable substrate would suppress soil respiration, moreover, it could counteract and mitigate the GO-derived effect on organic carbon oxidation.
iii. However, the effect of both amendments on plant biomass yield may depend on the dose and combination of GO and S.

2 Material and methods

2.1 Sources and preparation of materials

Nanoparticles of elemental sulfur in water dispersion were purchased from US Research Nanomaterials, Inc (Houston, TX, USA). The method of GO synthesis has been previously described by (Đurović et al., 2022). The nanocomposite of GO with nano-S was synthesized by the following procedure: 25 mL of GO (2 g·L^{-1}) was mixed with 25 mL of nano-S (100 g·L^{-1}) for high dose and 2.5 mL of nano-S (100 g·L^{-1}) for low dose as described in (Hammerschmiedt et al., 2022).

2.2 Pot experiment settings

The present pot experiment was carried out under controlled conditions in a growth chamber Climacell EVO (BMT, Czech Republic). The experimental soil consisted of topsoil from a rural area near the town of Troubsko, Czech Republic (49°10'28" N, 16° 29'32" E). The collected soil was sieved through a 2.0 mm sieve, and mixed with fine quartz sand (0.1-1.0 mm) in a ratio of 1:1, w/w. The properties of the used silty clay loam (Haplic Luvisol) are stated in (Table 1).

Pots of 1 L volume (three replicates per variant) were filled with 1 kg of experimental soil. The control soil variant was not amended, the soil of other variants was mixed in the whole volume with GO and nano-S at various doses and combinations displayed in (Table 2). The doses of graphene oxide were estimated as a compromise between the dosing reported by Anjum et al. (2014) and Forstner et al. (2019).

The pot experiment with lettuce (*Lactuca sativa* L. var. *capitata* L.) cv. Smaragd was conducted over a period of 8 weeks, during which the following conditions were ensured: full-spectrum LED lighting, intensity 370 μmol·m^{-2}·s^{-1}; photoperiod 12 h; temperature 18/22°C night/day; and relative air humidity 70%, soil moisture 60% of water holding capacity. Lettuce seeds were germinated for two days on filter paper, then four seeds were sown in each pot to a depth of approximately 2 mm. After sowing, each pot was watered with 100 ml of demineralized water. The 10-day-old seedling was reduced to only one per pot. At the end of the experiment (56 days after sowing), the plants were harvested at ground level, and the roots were removed from the soil and washed with demineralized water. Aboveground biomass (AGB) and roots were air-dried at 60°C to constant weight in a laboratory oven to determine the dry biomass of AGB and roots (AGB_dry and Root_dry) by weighing on laboratory scales (n = 3). A mixed soil sample was also taken from each pot.

TABLE 1 The properties of topsoil used for the pot substrate preparation.

Parameter	Value	Unit	Parameter	Value	Unit
pH($CaCl_2$)	7.29	–	C/N	8.77	–
TC	14.00	g·kg^{-1}	S	145	mg·kg^{-1}
TN	1.60	g·kg^{-1}	P	97	mg·kg^{-1}
$N_{mineral}$	62.84	mg·kg^{-1}	K	231	mg·kg^{-1}
N-NO_3	56.80	mg·kg^{-1}	Ca	3259	mg·kg^{-1}
N-NH_4	6.04	mg·kg^{-1}	Mg	236	mg·kg^{-1}

pH($CaCl_2$) was determined according to ISO 10390:2005; TC and TN were determined using the Vario Macro Cube (Elementar Analysensysteme GmbH, Langenselbold, Germany); N-NO_3, N-NH_4 were determined according to ISO 15476:2009; $N_{mineral}$ is a sum of N-NO_3 and N-NH_4 content; C/N was calculated from TC and TN; S, P, K, Ca, Mg were determined according to ISO 15178:2000, ISO 14869-3:2017, and ISO 13196:2013.

TABLE 2 The experimental variants used in this study.

Abbreviation	Name	Amendment and dose	Replicates
–	Control	–	4
GO	GO	GO 10 mg·kg^{-1} of soil	4
S1GO	Low nano-S + GO	nano-S 0.05 g·kg^{-1} + GO 10 mg·kg^{-1} of soil	4
S2GO	High nano-S + GO	nano-S 0.5 g·kg^{-1} + GO 10 mg·kg^{-1} of soil	4
S1	Low nano-S	nano-S 0.05 g·kg^{-1} of soil	4
S2	High nano-S	nano-S 0.5 g·kg^{-1} of soil	4

2.3 Methods for soil properties determination

The following soil properties were evaluated following standard methods, such as pH in $CaCl_2$ (ISO_10390 2005), n = 6; dehydrogenase activity (DHA) (Casida et al., 1964), n = 24; soil basal respiration (BR) and substrate-induced respiration (Campbell et al., 2003): Glc_SIR, Pro_SIR, Tre_SIR, NAG_SIR, Ala_SIR, Man_SIR, n = 12; enzyme activities (ISO_20130 2018): arylsulfatase, urease, phosphatase, N-acetyl-β-D-glucosaminidase, β-glucosidase, n = 18.

2.4 Statistical analyses

Statistical analyses were carried out using program R, version 3.6.1. (R Core Team 2020). PCA was performed to characterize the relationship between soil properties and dependence on the selected treatments. ANOVA type I (sequential) sum of squares was used to test the statistical effect of the selected treatment on the soil properties. For detecting the statistically significant difference after ANOVA, the Tukey's honest significant difference (HSD) test at a significance level of 0.05 was employed. Factor level means were determined by using treatment contrast. Besides, the Shapiro-Wilk test for the verification of normality and Levene's test for the verification of homogeneity of variances were also performed at a significance level of 0.05. Pearson correlation coefficient was used to determine the linear correlation among soil properties.

3 Results

3.1 Effect of graphene oxide, nano-sulfur, and their combination on soil respiration and enzymes

Determination of basal respiration (BR) and different types of substrate-induced soil respiration (SIR) provided the greatest variability among the tested experimental variants: inducing substrates D-glucose, protocatechuic acid, D-trehalose, N-acetyl-β-D-glucosamine, D-mannose, L-alanine, and L-arginine. Only the variant GO showed a significant increase in BR, Tre_SIR, and NAG_SIR, compared to the Control (Figures 1A, D, E). Glc_SIR, Man_SIR, Ala_SIR, and Arg_SIR (Figures 1B, F, G, H) were significantly increased in variants GO and S2GO compared to Control, whereas a single amended high dose of nano-S (variant S2) decreased Pro_SIR (Figure 1C).

Apparent soil respiration types by added GO were found to be mitigated by the low dose of nano-S, albeit not by the high dose. Therefore, values of BR, Glc_SIR, Tre_SIR, Ala_SIR, and Arg_SIR were comparable between the Control and the variant S1GO (Figures 1A, B, D, G, H), whereas Man_SIR, Ala_SIR, and Arg_SIR were significantly increased in S2GO compared to both the Control and S1GO (Figures 1F, G, H). Further, a single application of a high dose of nano-S had a negative impact on sugar-induced respirations (Glc_SIR, Tre_SIR, and Man_SIR) as compared to the variants with a low nano-S dose. In general, a single application of GO was beneficial for all types of soil respiration, whereas amendment of GO combined with nano-S enhanced only Man_SIR, Ala_SIR, and Arg_SIR respiration at high nano-S dose. Nano-S amendment did not significantly affect respiration (except for increased Arg_SIR – both variants S1, S2 – and Man_SIR, variant S1), nor did it have a significant negative effect (Pro_SIR) and the benefit of the high nano-S dose was less beneficial.

Beneficial to partially (significantly) positive effect of single GO application was also detected *via* determination of soil enzyme activities; DHA, NAG, Ure, GLU, and Phos activities of variant GO were comparable to the Control and ARS was significantly increased (Figures 2A–F). Similarly, significant positive effects of High nano-S + GO on Phos and ARS (compared to Control) were revealed (Figure 2E, F), albeit DHA and N-acetyl-β-D-glucosaminidase NAG were affected significantly negatively by nano-S + GO at both doses (Figures 2A, B2). The benefit of low nano-S + GO was again weaker than high nano-S + GO, showing values of Ure, GLU, and ARS, comparable to the Control, the only significant increment (compared to the Control) was found for Phos (Figure 2C, F). Whereas a single amendment of the high nano-S

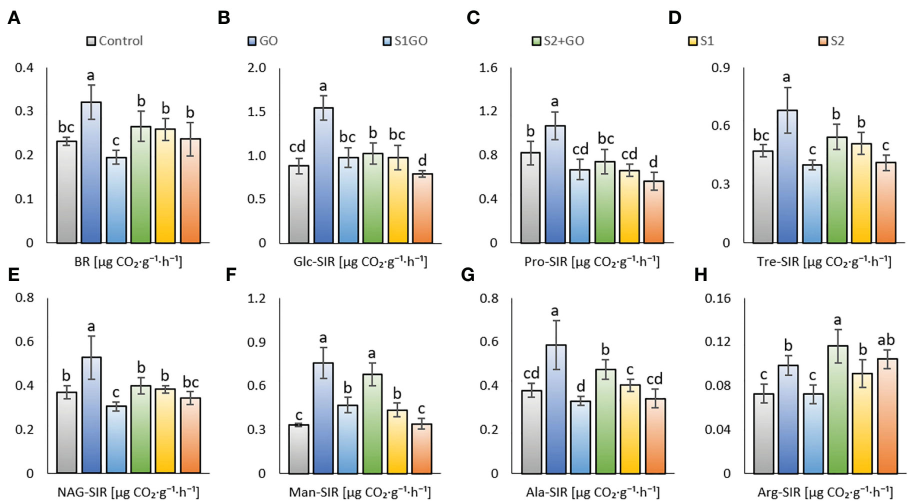

FIGURE 1
Basal respiration **(A)** and respiration induced by D-glucose **(B)**, protocatechuic acid **(C)**, D-trehalose **(D)**, N-acetyl- β -D-glucosamine **(E)**, D-mannose **(F)**, L-alanine **(G)**, and L-arginine **(H)** in the soil amended with GO, nano-S, and their combination. Mean values (n = 12) are displayed with error bars (standard deviation). Different letters indicate statistically significant differences between variants at $p \leq 0.05$.

dose was less beneficial to soil respiration (Glc_SIR, Tre_SIR, and Man_SIR), activities of NAG, GLU, Phos, and ARS, of this variant (S2) showed (compared to variant S1) significant increment, Figures 2B, D–F. In general, any variant amended with nano-S showed an adverse effect on DHA; moreover, single-applied nano-S at both doses mitigated Ure activity. While nano-S + GO (both S1GO and S2GO) enhanced the activity of Phos.

3.2 Effect of graphene oxide, nano-sulfur, and their combination on soil pH and plant biomass

The described values of soil respiration and enzyme activities in all experimental variants were likely negligibly influenced (Figure 2G). The response of soil parameters to the application of GO and Nano-S was not significantly related to the final values of aboveground dry matter (AGB) and root biomass of lettuce, which were comparable for all variants including the Control variant (Figures 3A, B). Some markable results of the determined biomass properties were the relatively highest average dry AGB value of variant S1 and the relatively lowest average root biomass weight in the Control. The outcome of these findings was the highest AGB_Root biomass ratio in the variant S1 (and in the Control as well – this indicates improved shoot growth), compared to the other variants, i.e., the variant S1GO, which in contrast stimulated the growth and biomass of roots, instead of shoots (Figure 3C).

4 Discussion

4.1 Effect of graphene oxide, nano-sulfur, and their combination on soil respiration and enzymes

It was referred that GO in soil may harm microorganisms by penetrating cell walls and extracting phospholipids (Tu et al., 2013), as well as by degreasing abundances of different functional microbial groups associated with the processes of nutrient transformation and respiration (Du et al., 2020). The most influenced soil properties in the experiment were basal and substrate-induced respiration, which (with the exception of Man_SIR and Ala_ SIR) were significantly higher in the soil enriched with GO compared to all other variants. These findings did not prove an adverse effect of GO but corroborated our hypothesis (i). GO can be reversibly reduced and oxidized because it enhances electron transfer (Pan et al., 2017). Apart from several studies which referred to the adverse effect of GO on soil microbiome (Gurunathan et al., 2012; Du et al., 2015; Xie et al., 2016), the positive effect on microbial growth and activity is assumed due to reported improved delivery of macro- and micronutrients *via* adsorption (Kabiri et al., 2017; Navarro et al., 2020). Nevertheless, few studies described the GO effect on microbial respiration, e.g. addition of GO (up to 60 $mg{\cdot}L^{-1}$) increased the oxygen uptake rate coefficient of municipal landfill leachate bacterial cultures (Jamialahmadi et al., 2018) and aerobic bacteria isolated from various environments, including soil, were able to increase GO reduction under respiration (Salas et al., 2010; Chouhan et al., 2016). However, our previous study (Hammerschmiedt et al., 2022) showed contrasting results of various types of microbial respiration in lettuce-planted soil under illumination with color (blue+red) light (20 klx), where the GO amended variant showed comparable or lower (Glc_SIR) values than the Control. Due to the relation between illumination (intensity and quality) and plant physiology (Gouinguene and Turlings, 2002; Hee-Sun Kook, 2013), both stimulation, and composition, as well as activity of the microbial community in the rhizosphere, were reported in several studies e.g., blue color light stimulation of multiplication of moldy fungi (Bonomi et al., 2012; Borowiak et al., 2019).

High nano-S + GO (variant S2GO) had a positive effect on these particular types of soil respiration (Glc_SIR, Man_SIR, Ala_SIR, and Arg_SIR) in comparison to the Control, whereas single soil application of high nano-S led only to the comparable values (as the Control) of the respective properties (except significantly

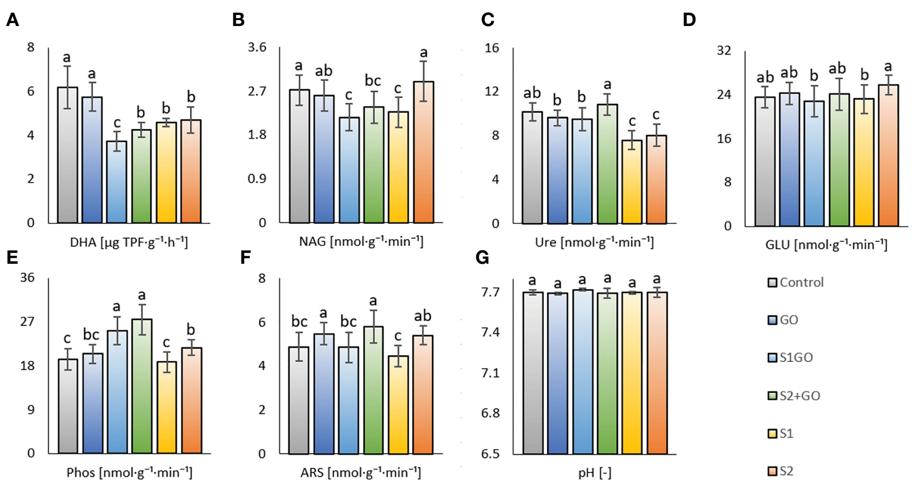

FIGURE 2
Dehydrogenase **(A)** (n=24), N-acetyl- β -D-glucosaminidase **(B)**, urease **(C)**, β -glucosidase **(D)**, phosphatase **(E)** arylsulfatase **(F)**, and activities (n=18) and pH **(G)** (n=6) in the soil amended with GO, nano-S, and their combination. Mean values are displayed with error bars = standard deviation. Different letters indicate statistically significant differences between variants at $p \leq 0.05$.

increased Arg_SIR, Figures 1B, F–H). These findings partially corroborated our hypothesis (ii), confirming a negative impact of sole nano-S addition on respiration but a positive effect of a combination of both amendments. As compared to the GO variant or even the Control, it was ascribed that the impact of a low dose of nano-S (variant S1) on the soil respiration was neutral or negative, which was in line with the results of our previous study (Hammerschmiedt et al., 2022). Thus, elemental (nano)sulfur has been reported to attenuate soil aerobic microbial activity and the respiratory capacity of the soil microbiome, as described in a few studies (Kelleher et al., 2017; Zakari et al., 2020). Nevertheless, this study showed a less significant negative effect of nano-S on the GO-associated aerobic carbon mineralization benefits than in the previously conducted pot experiment (Hammerschmiedt et al., 2022), which showed a very strong negative effect of the nano-S + GO. In line with these results, Kelleher et al. (2017) referred to an initial surge in the production of CO_2 through microbial respiration, which was followed by increased capture of carbon dioxide as elemental sulfur was oxidized to sulfate (Kelleher et al., 2017). The conditions set up in this experiment did not promote complete nano-S-mediated attenuation of GO stimulation. However, significant mitigation of most types of respiration in the variant S2GO and even more in the S1GO variant, compared to the values of variant GO, was evident. We corroborated our hypotheses (ii) and (iii) that nano-S would counteract the GO-mediated beneficial effect of organic carbon oxidation and weaken the stimulation of soil respiration, and that these effects would be dose-dependent. An even higher negative effect of nano-S + GO co-application (compared to both sole amended GO and sole low nano-S) was observed in the variant S1GO for the properties NAG_SIR, Tre_SIR, Ala_SIR, and Arg_SIR (Figures 1D, E, G, H), which values were significantly lowered compared to the single-treated variants (GO, S1). We presumed that this feature was caused by a generally decreased degradation activity of soil microbiome in this (S1GO) variant, which was ascribed the lowest value of dehydrogenase (DHA) in comparison to all other variants (Figure 2A). Even at the lower nano-S dose in this variant (S1GO), the highly oxygen-dependent aerobic catabolism of particular substrates (e.g., protocatechuic acid) putatively competed with the oxygen-demanding elemental sulfur utilization. These presumptions were supported by the results of the PCA analysis (synergy between dehydrogenase and respirations) and Pearson correlation analysis (Supplementary Figures 1, 2), showing a significant ($p < 0.001$) positive correlation of DHA and Pro_SIR (r = 0.62); further, BR and Tre_SIR, NAG_SIR, and Ala_SIR (r were 0.69, 0.7, 0.72) were also correlated.

As we mentioned in the previous paragraph, dehydrogenase activity (DHA), which indicates the ability of soil microbiome to degrade soil organic matter (SOM), was decreased by the application of nano-S at both doses as compared to the Control and GO variant, Figure 2A. N-acetyl-β-D-glucosaminidase (NAG), an enzyme involved in the degradation of main fungal cell wall polymer chitin, also exerted a decrease in most nano-S-treated variants (S1GO, S2GO, and S1 - except for S2) compared to Control (Figure 2B). These results again contrast with a previous study (Hammerschmiedt et al., 2022), in which the addition of a very high dose of Nano-S (1 g S. kg^{-1}) stimulated both dehydrogenase and NAG activities (compared with the Control). The positive effect of high dose nano-S on the preservation of NAG activity (of variant S2, comparable to the Control) in this current experiment allowed us to presume that the efficient elemental sulfur stimulation of fungal biomass multiplication (due to the fungal involvement in elemental sulfur oxidation (Germida and Janzen, 1993)) occurs at higher application levels. This proved hypothesis (iii). The results of the respective previous study corresponded to the referred beneficial effect of waste elemental sulfur application on soil DHA in unsown arable soil (Tabak et al., 2020). On the other hand, a dose of 50 $mg.kg^{-1}$ of elemental sulfur added to alkaline S-deficient soil did not affect DHA (Malik et al., 2021), similarly observed in this study. We further assumed that the activity of NAG could be enhanced in the first experiment due to the putative blue color light stimulation of moldy fungi growth (Borowiak et al., 2019), and subsequent higher access of residual fungal biomass in soil. Contrary to the effect of nano-S, GO amendment to soil helped to preserve values of DHA and NAG (as well as other enzymes – urease, β-glucosidase, phosphatase) comparable with the Control, which was in contrast with the referred detrimental effect of GO (Chung et al., 2015), but close to the opposite reports of a beneficial effect of graphene-based nanomaterials on soil enzymatic activities (Ren et al., 2015). The other study (Rong et al., 2017) showed that the positive or negative effect of either graphene or GO on microbial enzymes was vastly dependent on the composition of the soil microbial community. Arylsulfatase activity was enhanced by the single soil application of GO (compared to the Control) Arylsulfatase, as the only one from determined enzymes. had enhanced activity by the single soil application of GO (compared to the Control). We attributed this result to the reported positive role of GO in sulfur oxidation and mineralization, as it was referred (Rong et al., 2017),

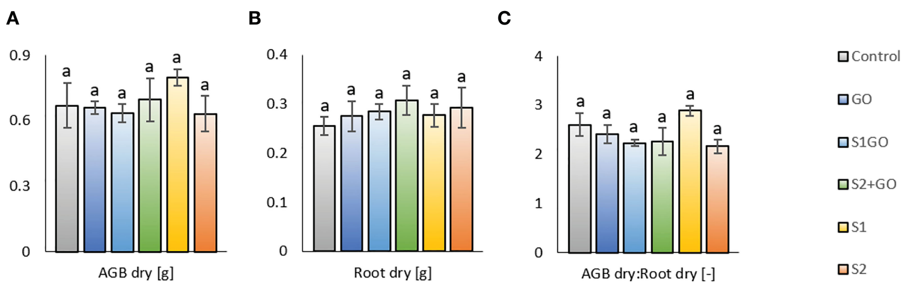

FIGURE 3
Dry aboveground **(A)**, root **(B)** biomass, and their ratio AGB_Root **(C)** for lettuce grown in the soil amended with GO, nano-S, and their combination. Mean values (n = 3) are displayed with error bars = standard deviation. Different letters indicate statistically significant differences between variants at $p \leq 0.05$.

and to the beneficial general effect of GO on distinct soil microbiota and their activity (Rong et al., 2017). Nevertheless, GO-promoted ARS activity was again discordant to the previous study (Hammerschmiedt et al., 2022) and the role of different illumination in the soil microbial community composition (as reported by (Carvalho and Castillo, 2018)) and their related enzyme activities could be considered. As well as variant GO, high nano-S + GO increased the activity of ARS in comparison to the Control (Figure 2F); therefore, we deduced that GO mitigation of enzyme activity (Chung et al., 2015) did not overwhelm the positive effect of elemental sulfur on ARS (Malik et al., 2021).

The only variant with significantly increased Ure activity (compared to the Control) was high nano-S + GO (S2GO), while both doses of nano-S applied alone (S1, S2) to the soil showed significantly decrease Ure activity (as compared to the Control). We assumed that next to the oxidative mineralization of nano-S, the reductive transformation to sulfides and hydrogen sulfide could also occur in the soil. Considering the referred inhibition of nitrification activity by elevated sulfide levels (Joye and Hollibaugh, 1995) we ascribed that higher access of nano-S in soil (S1, S2) might have decreased the Ure activity.

No significant change in β-glucosidase activity was observed in any of the altered variants compared to the Control (Figure 2D). A significant decline in GLU activity was detected for the low-dose nano-S-amended variants (S1GO and S1) as compared to the sole high nano-S amended variant (S2). This feature was consistent with reports of increased GLU in soils receiving higher levels of elemental sulfur (Ye et al., 2011). The most significant enzyme response to the amendment of GO (in combination with a low or high dose of nano-S) showed Phos, both GO variants with nano-S (irrespective of dose) increased Phos as compared to the Control. We related these results to the effect of elemental sulfur – there was reported higher Phos activity promoted by sulfur fertilization at the background of NPK (Godlewska, 2018) – and to the putatively higher retention of soil phosphate content due to interaction with added GO. Absorption properties of GO were reported to be beneficial for phosphate loading on the surfaces of the nanoparticles (Kabiri et al., 2020), and we ascribed from this decreased leaching and losses of phosphorus (P) and thus, its higher P accessibility to transformation (enzyme-catalyzed). A general positive effect of GO on the increased availability of various nutrients to transformation processes may be ascribed from synergy (PCA biplot, Supplementary Figure 1) and significant ($p < 0.001$) positive correlation of Phos and Ure, ARS (r were 0.42 and 0.52, respectively), while enhanced SOM degradation could increase P losses as assumable from the negative correlation of Phos and DHA ($r = -0.47$) and antagonism (PCA biplot), Figures A1, A2. Further, we hypothesized (i.): if the sulfur transformation (locally in the rhizosphere) takes place under oxidative conditions, the soil would tend to slightly lower pH and improve phosphate dissolution, which would further increase its availability and, subsequently, Phos activity. A significant antagonism (PCA biplot, Supplementary Figure 1) and negative correlation between pH and Phos was detected ($r = -0.53$, $p < 0.001$) (Supplementary Figure 2).

4.2 Effect of graphene oxide, nano-sulfur, and their combination on soil pH and plant biomass

However, no significant differences in soil pH values were observed between the variants (Figure 2G). Neither the final values of lettuce dry aboveground and root biomass, which were comparable between all variants including the Control (Figures 3A, B), displayed any significant effect of presumed and detected differences in the soil biological properties, determined by the differing diversity of soil microbial community. Nevertheless, the relatively highest average dry AGB value of variant S1 and the relatively lowest average root biomass in the Control were coupled with the highest AGB_Root biomass ratio in variant S1 (and in the Control), compared to the other variants. These results indicated that the sulfur uptake preferentially contributed to the growth of aboveground parts of lettuce. It agreed with the research findings based on a greenhouse experiment, in which the application of elemental sulfur (570 $mg.kg^{-1}$) significantly increased stem diameter, plant height, shoot weight, and sulfate uptake by maize plants (Pourbabaee et al., 2020). Another study reported that elemental sulfur amended to the soil at a rate of up to 50 $mmol.kg^{-1}$ elemental sulfur also led to a higher concentration of sulfur in the shoots than in the roots (Cui and Wang, 2005).

On the contrary, the variant S1GO (low nano-S + GO) stimulated the growth and biomass of roots, instead of shoots (Figure 3C). It was referred that very high (> 400 $mg.L^{-1}$ GO) amendment of GO to soil significantly increased root biomass and length (Anjum et al., 2014). However, our result seemed closer to the study of (Xiao et al., 2022), which reported little effect of GO exposure at doses 10 and 100 $mg.L^{-1}$ on plant growth. Increased nutrient availability to lettuce plants, derived by GO and its physicochemical properties as reported (Lahiani et al., 2015; Kabiri et al., 2017; Juarez-Maldonado et al., 2019; Carneiro et al., 2022), could have been one of the possible reasons. Another mechanism of beneficial interaction of GO and elemental sulfur could have been a positive effect on soil water retention as referred to by (Zhao et al., 2020; Zhao et al., 2022). In the previously published study by (Hammerschmiedt et al., 2022), in which the lettuce plants were illuminated by color (blue+red) light instead of artificial white light, the plant biomass yield responded to GO and co-applied S^0 + GO differently, showing the significantly higher AGB values than other amended soil variants. These significant differences could be ascribed to the presumed contrasting plant physiology and qualitative properties of plant biomass, which were not determined, and coupled with the significantly weaker positive impact of GO (applied solely or with S^0) on soil microbial properties, namely basal and other types of soil respiration. Thus, concerning the findings of this research, as well as the previous one (Hammerschmiedt et al., 2022), it can be concluded that the different types of supplements exerted contradictory effects on soil biological properties and plant growth in a similar way, as found, for example, for GO in recent studies (Fattahi et al., 2022).

5 Conclusions

GO applied on its own exerted the most positive effect on soil respiration, which was still significant in the combination of high nano-S + GO. While low nano-S + GO negatively affected some types of soil respiration (NAG_SIR, Tre_SIR, Ala_SIR, and Arg_SIR). We verified our hypothesis that elemental nano-S would probably counteract the GO-mediated effect of organic carbon oxidation. The benefit of GO was detectable *via* the determination of soil enzyme activities: GO on its own enhanced ARS, and GO + high nano-S dose enhanced ARS, Ure, and Phos. Several contrasts were found between the results of this experiment and the previously carried-out pot trial, performed with nanosized (microsized) elemental sulfur and GO in soil sown with lettuce and illuminated by color (blue+red) light instead of artificial white light. This difference in the experimental conditions was the most noticeable in the contrasting effect of GO (applied on its own or with S^0) on plant biomass quantity (and presumably also quality) and concurrently on plant growth-associated soil biological properties, namely respiration indicators.

Data availability statement

The original contributions presented in the study are included in the article/Supplementary Material. Further inquiries can be directed to the corresponding authors.

Author contributions.

TH was involved in conceptualization, data curation, and writing the original draft. JH was involved in data curation, investigation, and writing, namely review and editing. RZ was involved in software and methodology. AK was involved in formal analysis, investigation, and software. PS was involved in conceptualization, methodology, and writing, namely review and editing. ZB was involved in software and writing, namely review and editing. LR was involved in formal analysis, supervision, and writing, namely review and editing. AM was involved in formal analysis and writing, namely review and editing. OM was involved in data curation and validation. MB was involved in conceptualization, formal analysis, funding acquisition, supervision, and writing, namely review and editing. All authors contributed to the article and approved the submitted version

Funding

The work was supported by the projects of the Technology Agency of the Czech Republic TJ04000519 and TH04030142, by the Ministry of Agriculture of the Czech Republic, institutional support MZE-RO1218, MZE-RO1722, and by the Ministry of Education, Youth and Sports of the Czech Republic, grant number FCH-S-22-8001 and by ERDF “Multidisciplinary research to increase application potential of nanomaterials in agricultural practice” (No. CZ.02.1.01/0.0/0.0/16_025/0007314).

Conflict of interest

The author JH is employed by Agrovyzkum Rapotin, Ltd., Vyzkumniku 267, 788 13 Rapotin, Czech Republic and AK is employed by Agricultural Research, Ltd., Troubsko, Czech Republic.

The remaining authors declare that the research was conducted in the absence of any commercial or financial relationships that could be construed as a potential conflict of interest.

Publisher’s note

Supplementary material

The Supplementary Material for this article can be found online at: https://www.frontiersin.org/articles/10.3389/fpls.2023.1057133/full#supplementary-material

References

Almutairi, K. F., Machado, R. M. A., Bryla, D. R., and Strik, B. C. (2017). "Chemigation with micronized sulfur rapidly reduces soil pH in a new planting of northern highbush blueberry.". *HortScience* 52 (10), 1413–1418. doi: 10.21273/hortsci12313-17

Anjum, N. A., Singh, N., Singh, M. K., Sayeed, I., Duarte, A. C., Pereira, E., et al. (2014). Single-bilayer graphene oxide sheet impacts and underlying potential mechanism assessment in germinating faba bean (*Vicia faba* l.). *Sci. Total Environ.* 472, 834–841. doi: 10.1016/j.scitotenv.2013.11.018

Arikan, B., Alp, F. N., Ozfidan-Konakci, C., Balci, M., Elbasan, F., Yildiztugay, E., et al. (2022). Fe2o3-modified graphene oxide mitigates nanoplastic toxicity *via* regulating gas exchange, photosynthesis, and antioxidant system in *Triticum aestivum*. *Chemosphere* 307, 16. doi: 10.1016/j.chemosphere.2022.136048

Behl, T., Kaur, I., Sehgal, A., Singh, S., Sharma, N., Bhatia, S., et al. (2022). The dichotomy of nanotechnology as the cutting edge of agriculture: Nano-farming as an asset versus nanotoxicity. *Chemosphere* 288, 27. doi: 10.1016/j.chemosphere.2021.132533

Bonomi, H. R., Posadas, D. M., Paris, G., Carrica Mdel, C., Frederickson, M., Pietrasanta, L. I., et al. (2012). Light regulates attachment, exopolysaccharide production, and nodulation in *Rhizobium leguminosarum* through a LOV-histidine kinase photoreceptor. *Proc. Natl. Acad. Sci. U.S.A.* 109 (30), 12135–12140. doi: 10.1073/pnas.1121292109

Borowiak, K., Wolna-Maruwka, A., and Schroeter-Zakrzewska, A. (2019). Influence of the light color and microbiological inoculums on the zonal pelargonium quality and microbiological and enzymatic state of the substrate. *Acta Scientiarum Polonorum Hortorum Cultus* 18 (4), 169–180. doi: 10.24326/asphc.2019.4.16

Campbell, C. D., Chapman, S. J., Cameron, C. M., Davidson, M. S., and Potts, J. M. (2003). A rapid microtiter plate method to measure carbon dioxide evolved from carbon substrate amendments so as to determine the physiological profiles of soil microbial communities by using whole soil. *Appl. Environ. Microbiol.* 69 (6), 3593–3599. doi: 10.1128/AEM.69.6.3593-3599.2003

Carneiro, J. S. D., Leite, D. A. D., de Castro, G. M., Franca, J. R., Botelho, L., Soares, J. R., et al. (2022). Biochar-graphene oxide composite is efficient to adsorb and deliver copper and zinc in tropical soil. *J. Cleaner Production* 360, 13. doi: 10.1016/j.jclepro.2022.132170

Carvalho, S. D., and Castillo, J. A. (2018). Influence of light on plant-phyllosphere interaction. *Front. Plant Sci.* 9. doi: 10.3389/fpls.2018.01482

Casida, L. E., Klein, D. A., and Santoro, T. (1964). Soil dehydrogenase activity. *Soil Sci.* 98 (6), 371–376. doi: 10.1097/00010694-196412000-00004

Chapman, S. J. (1089). Oxidation of micronized elemental sulphur in soil. *Plant Soil* 116 (1), 69–76. doi: 10.1007/bf02327258

Chouhan, R. S., Pandey, A., Qureshi, A., Ozguz, V., and Niazi, J. H. (2016). Nanomaterial resistant microorganism mediated reduction of graphene oxide. *Colloids Surf B Biointerfaces* 146, 39–46. doi: 10.1016/j.colsurfb.2016.05.053

Chung, H., Kim, M. J., Ko, K., Kim, J. H., Kwon, H. A., Hong, I., et al. (2015). Effects of graphene oxides on soil enzyme activity and microbial biomass. *Sci. Total Environ.* 514, 307–313. doi: 10.1016/j.scitotenv.2015.01.077

Cui, Y., and Wang, Q. (2005). Interaction effect of zinc and elemental sulfur on their uptake by spring wheat. *J. Plant Nutr.* 28 (4), 639–649. doi: 10.1081/pln-200052637

Degryse, F., Baird, R., Andelkovic, I., and McLaughlin, M. J. (2021). Long-term fate of fertilizer sulfate- and elemental s in co-granulated fertilizers. *Nutrient Cycling Agroecosystems* 120 (1), 31–48. doi: 10.1007/s10705-021-10137-6

Dixit, G., Singh, A. P., Kumar, A., Dwivedi, S., Deeba, F., Kumar, S., et al. (2015). Sulfur alleviates arsenic toxicity by reducing its accumulation and modulating proteome, amino acids and thiol metabolism in rice leaves. *Sci. Rep.* 5, 16205. doi: 10.1038/srep16205

Du, J., Hu, X., and Zhou, Q. (2015). Graphene oxide regulates the bacterial community and exhibits property changes in soil. *RSC Adv.* 5 (34), 27009–27017. doi: 10.1039/c5ra01045d

Du, J., Zhou, Q., Wu, J., Li, G., Li, G., and Wu, Y. (2020). Soil bacterial communities respond differently to graphene oxide and reduced graphene oxide after 90 days of exposure. *Soil Ecol. Lett.* 2, 176–179. doi: 10.1007/s42832-020-0043-5

Đurović, A., Stojanović, Z., Bytešníková, Z., Kravić, S., Švec, P., Přibyl, J., et al. (2022). Reduced graphene oxide/zno nanocomposite modified electrode for the detection of tetracycline. *J. Materials Sci.* 57 (9), 5533–5551. doi: 10.1007/s10853-022-06926-1

Fattahi, N., Hekmatdoust Tabrizi, B., Rani, S., Sadeghi, Z., Dehghanian, Z., Asgari Lajayer, B., et al. (2022). Chapter 4 - toxicity of nanoparticles onto plants: Overview of the biochemical and molecular mechanisms. *Toxicity Nanoparticles Plants* 5, 69–94.

Forstner, C., Orton, T. G., Skarshewski, A., Wang, P., Kopittke, P. M., and Dennis, P. G. (2019). Effects of graphene oxide and graphite on soil bacterial and fungal diversity. *Sci. Total Environ.* 671, 140–148. doi: 10.1016/j.scitotenv.2019.03.360

Fuentes-Lara, L. O., Medrano-Macias, J., Perez-Labrada, F., Rivas-Martinez, E. N., Garcia-Enciso, E. L., Gonzalez-Morales, S., et al. (2019). From elemental sulfur to hydrogen sulfide in agricultural soils and plants. *Molecules* 24 (12), 2282. doi: 10.3390/molecules24122282

Gadino, A. N., Walton, V. M., and Dreves, A. J. (2011). Impact of vineyard pesticides on a beneficial arthropod, *Typhlodromus pyri* (*Acari: Phytoseiidae*), in laboratory bioassays. *J. Econ Entomol* 104 (3), 970–977. doi: 10.1603/ec10330

Ge, Y., Priester, J. H., Mortimer, M., Chang, C. H., Ji, Z., Schimel, J. P., et al. (2016). Long-term effects of multiwalled carbon nanotubes and graphene on microbial communities in dry soil. *Environ. Sci. Technol.* 50 (7), 3965–3974. doi: 10.1021/acs.est.5b05620

Germida, J. J., and Janzen, H. H. (1993). Factors affecting the oxidation of elemental sulfur in soils. *Fertilizer Res.* 35 (1-2), 101–114. doi: 10.1007/bf00750224

Godlewska, A. (2018). Assessment of the effect of lstialalationsation and elemental sulphur on soil enzyme activity. *Fresenius Environ. Bull.* 27 (1), 180–186.

Gouinguene, S. P., and Turlings, T. C. (2002). The effects of abiotic factors on induced volatile emissions in corn plants. *Plant Physiol.* 129 (3), 1296–1307. doi: 10.1104/pp.001941

Gupta, V. K., Eren, T., Atar, N., Yola, M. L., Parlak, C., and Karimi-Maleh, H. (2015). $CoFe_2O_4$@TiO_2 decorated reduced graphene oxide nanocomposite for photocatalytic degradation of chlorpyrifos. *J. Mol. Liquids* 208, 122–129. doi: 10.1016/j.molliq.2015.04.032

Gurunathan, S., Han, J. W., Dayem, A. A., Eppakayala, V., and Kim, J. H. (2012). Oxidative stress-mediated antibacterial activity of graphene oxide and reduced graphene oxide in *Pseudomonas aeruginosa*. *Int. J. Nanomedicine* 7, 5901–5914. doi: 10.2147/IJN.S37397

Hammerschmiedt, T., Holatko, J., Huska, D., Kintl, A., Skarpa, P., Bytesnikova, Z., et al. (2022). Impact of smart combinations of graphene oxide and micro/nanosized sulfur particles on soil health and plant biomass accumulation. *Chem. Biol. Technol. Agric.* 9 (1), 53. doi: 10.1186/s40538-022-00323-1

Hee-Sun Kook, K. K. (2013). The effect of blue-light-emitting diodes on antioxidant properties and resistance to *Botrytis cinerea* in tomato. *J. Plant Pathol. Microbiol.* 04 (09), 9. doi: 10.4172/2157-7471.1000203

Hegedüs, M., Baláž, P., Baláž, M., Siffalovic, P., Daneu, N., Kaňuchová, M., et al. (2018). Mechanochemical approach to a Cu_2ZnSnS_4 solar cell absorber *via* a "micro-nano" route. *J. Materials Sci.* 53 (19), 13617–13630. doi: 10.1007/s10853-018-2228-1

Hu, Z. Y., Beaton, J. D., Cao, Z. H., and Henderson, A. (2007). Sulfate formation and extraction from red soil treated with micronized elemental sulfur fertilizer and incubated in closed and open systems. *Commun. Soil Sci. Plant Anal.* 33 (11-12), 1779–1797. doi: 10.1081/css-120004822

Huang, M., Wang, X. L., Liu, C., Fang, G. D., Gao, J., Wang, Y. J., et al. (2021). Facile ball milling preparation of sulfur-doped carbon as peroxymonosulfate activator for efficient removal of organic pollutants. *J. Environ. Chem. Eng.* 9 (6), 9. doi: 10.1016/j.jece.2021.106536

ISO 10390 (2005). *Soil qu–lity - determination of pH* (Geneva, Switzerland: International Organization for Standardization).

ISO 20130 (2018). *Soil quality — measurement of enzyme activity patterns in soil samples using colorimetric substrates in micro-well plates* (Geneva, Switzerland: International Organization for Standardization).

Jamialahmadi, N., Safari, E., and Baghdadi, M. (2018). Interaction of graphene oxide nano-sheets and landfill leachate bacterial culture. *Environ. Technol.* 39 (19), 2457–2466. doi: 10.1080/09593330.2017.1356875

Jeon, C., Solis, K. L., An, H. R., Hong, Y., Igalavithana, A. D., and Ok, Y. S. (2020). Sustainable removal of Hg(II) by sulfur-modified pine-needle biochar. *J. Hazard Mater* 388, 122048. doi: 10.1016/j.jhazmat.2020.122048

Joye, S. B., and Hollibaugh, J. T. (1995). Influence of sulfide inhibition of nitrification on nitrogen regeneration in sediments. *Science* 270 (5236), 623–625. doi: 10.1126/science.270.5236.623

Juarez-Maldonado, A., Ortega-Ortiz, H., Morales-Diaz, A. B., Gonzalez-Morales, S., Morelos-Moreno, A., Cabrera-De la Fuente, M., et al. (2019). Nanoparticles and nanomaterials as plant biostimulants. *Int. J. Mol. Sci.* 20 (1), 162. doi: 10.3390/ijms20010162

Kabiri, S., Andelkovic, I. B., da Silva, R. C., Degryse, F., Baird, R., Tavakkoli, E., et al. (2020). Engineered phosphate fertilizers with dual-release properties. *Ind. Eng. Chem. Res.* 59 (13), 5512–5524. doi: 10.1021/acs.iecr.0c00403

Kabiri, S., Degryse, F., Tran, D. N. H., da Silva, R. C., McLaughlin, M. J., and Losic, D. (2017). Graphene oxide: A new carrier for slow release of plant micronutrients. *ACS Appl. Mater Interfaces* 9 (49), 43325–43335. doi: 10.1021/acsami.7b07890

Kelleher, B. P., Flanagan, P. V., Hart, K. M., Simpson, A. J., Oppenheimer, S. F., Murphy, B. T., et al. (2017). Large Perturbations in co2 flux and subsequent chemosynthesis are induced in agricultural soil by the addition of elemental sulfur. *Sci. Rep.* 7 (1), 4732. doi: 10.1038/s41598-017-04934-9

Kulshrestha, S., Qayyurn, S., and Khan, A. U. (2017). Antibiofilm efficacy of green synthesized graphene oxide-silver nanocomposite using lagerstroemia speciosa floral extract: A comparative study on inhibition of gram-positive and gram-negative biofilms. *Microbial Pathogenesis* 103, 167–177. doi: 10.1016/j.micpath.2016.12.022

Lahiani, M. H., Chen, J., Irin, F., Puretzky, A. A., Green, M. J., and Khodakovskaya, M. V. (2015). Interaction of carbon nanohorns with plants: Uptake and biological effects. *Carbon* 81, 607–619. doi: 10.1016/j.carbon.2014.09.095

Lee, A., Boswell, C. C., and Watkinson, J. H. (2011). Effect of particle size on the oxidation of elemental sulphur, thiobacilli numbers, soil sulphate, and its availability to pasture. *New Z. J. Agric. Res.* 31 (2), 179–186. doi: 10.1080/00288233.1988.10417943

Li, T., Gao, B., Tong, Z., Yang, Y., and Li, Y. (2019). Chitosan and graphene oxide nanocomposites as coatings for controlled-release fertilizer. *Water Air Soil pollut.* 230 (7), 146. doi: 10.1007/s11270-019-4173-2

Liu, G., Li, L., Xu, D., Huang, X., Xu, X., Zheng, S., et al. (2017). Metal-organic framework preparation using magnetic graphene oxide-beta-cyclodextrin for neonicotinoid pesticide adsorption and removal. *Carbohydr Polym* 175, 584–591. doi: 10.1016/j.carbpol.2017.06.074

Lonkar, S. P., Pillai, V. V., and Alhassan, S. M. (2018). Facile and scalable production of heterostructured ZnS-ZnO/graphene nano-photocatalysts for environmental remediation. *Sci. Rep.* 8 (1), 13401. doi: 10.1038/s41598-018-31539-7

Lucheta, A. R., and Lambais, M. R. (2012). Sulfur in agriculture. *Bras. Ciênc. Solo* 36, 5, 1369–1379. doi: 10.1590/S0100-06832012000500001Rev

Luo, N., Zhang, X. J., Zhang, H. G., Liu, D., Wang, H. X., and Song, J. F. (2022). Graphene oxide influences on bacterial community diversity of *Larix olgensis* rhizosphere of haplic cambisols in northeast China. *Eurasian Soil Sci.* 55 (10), 1470–1481. doi: 10.1134/s1064229322100106

Malik, K. M., Khan, K. S., Billah, M., Akhtar, M. S., Rukh, S., Alam, S., et al. (2021). Organic amendments and elemental sulfur stimulate microbial biomass and sulfur oxidation in alkaline subtropical soils. *Agronomy* 11 (12), 2514. doi: 10.3390/agronomy11122514

Marcano, D. C., Kosynkin, D. V., Berlin, J. M., Sinitskii, A., Sun, Z., Slesarev, A., et al. (2010). Improved synthesis of graphene oxide. *ACS Nano* 4 (8), 4806–4814. doi: 10.1021/nn1006368

Massalimov, I., Medvedev, U. A., Zaynitdinova, R. M., Mufazalova, N. A., and Mustafin, A. G. (2012). Assessment of antifungal activity of micronized and nanosized elemental sulfur. *Nanotechnol Nanosci* 3 (1), 55–58.

Matamwa, W., Blair, G., Guppy, C., and Yunusa, I. (2018). Plant availability of sulfur added to finished fertilizers. *Commun. Soil Sci. Plant Anal.* 49 (4), 433–443. doi: 10.1080/00103624.2018.1430236

Méndez Tovar, M., García Meza, J. V., and Gonzalez, I. (2019). Electrochemical monitoring of *Acidithiobacillus thiooxidans* biofilm formation on graphite surface with elemental sulfur. *Bioelectrochemistry* 128, 30-38. doi: 10.1016/j.bioelechem.2019.03.004

Mohammadi Alagoz, S., Ramezanzadeh Arvanaghi, H., Dolatabadi, N., Khalaki, M., Moameri, M., Asgari Lajayer, B., et al. (2022). "Chapter 15 - impact on nutritional status of plants treated with nanoparticles," in *Toxicity of nanoparticles in plants*, vol. 5 . Eds. V. D. Rajput, T. Minkina, S. Sushkova, S. S. Mandzhieva and C. Rensing (Cambridge, Massachusetts: Academic Press), 333–358. doi: 10.1016/B978-0-323-90774-3.00005-2

Navarro, D. A., Kah, M., Losic, D., Kookana, R. S., and McLaughlin, M. J. (2020). Mineralisation and release of 14C-graphene oxide (GO) in soils. *Chemosphere* 238, 124558. doi: 10.1016/j.chemosphere.2019.124558

Pan, M., Zhang, Y., Shan, C., Zhang, X., Gao, G., and Pan, B. (2017). Flat graphene-enhanced electron transfer involved in redox reactions. *Environ. Sci. Technol.* 51 (15), 8597–8605. doi: 10.1021/acs.est.7b01762

Pourbabaee, A. A., Koohbori Dinekaboodi, S., Seyed Hosseini, H. M., Alikhani, H. A., and Emami, S. (2020). Potential application of selected sulfur-oxidizing bacteria and different sources of sulfur in plant growth promotion under different moisture conditions. *Commun. Soil Sci. Plant Anal.* 51 (6), 735–745. doi: 10.1080/00103624.2020.1729377

Qi, Z., Zhang, L., and Chen, W. (2014). Transport of graphene oxide nanoparticles in saturated sandy soil. *Environ. Science-Processes Impacts* 16 (10), 2268–2277. doi: 10.1039/C4EM00063C

Raghavan, N., Thangavel, S., Sivalingam, Y., and Venugopal, G. (2018). Investigation of photocatalytic performances of sulfur based reduced graphene oxide-TiO_2 nanohybrids. *Appl. Surface Sci.* 449, 712–718. doi: 10.1016/j.apsusc.2018.01.043

Ren, W., Ren, G., Teng, Y., Li, Z., and Li, L. (2015). Time-dependent effect of graphene on the structure, abundance, and function of the soil bacterial community. *J. Hazard Mater* 297, 286–294. doi: 10.1016/j.jhazmat.2015.05.017

Riley, N. G., Zhao, F. J., and McGrath, S. P. (2002). Leaching losses of sulphur from different forms of sulphur fertilizers: A field lysimeter study. *Soil Use Manage.* 18 (2), 120–126. doi: 10.1079/sum2002115

Rong, Y., Wang, Y., Guan, Y., Ma, J., Cai, Z., Yang, G., et al. (2017). Pyrosequencing reveals soil enzyme activities and bacterial communities impacted by graphene and its oxides. *J. Agric. Food Chem.* 65 (42), 9191–9199. doi: 10.1021/acs.jafc.7b03646

R Core Team (2020). *R: A language and environment for statistical computing* (Vienna, Austria: R Foundation for Statistical Computing).

Salas, E. C., Sun, Z., Luttge, A., and Tour, J. M. (2010). Reduction of graphene oxide *via* bacterial respiration. *ACS Nano* 4 (8), 4852–4856. doi: 10.1021/nn101081t

Samadi, S., Asgari Lajayer, B., Moghiseh, E., and Rodríguez-Couto, S. (2021). Effect of carbon nanomaterials on cell toxicity, biomass production, nutritional and active compound accumulation in plants. *Environ. Technol. Innovation* 21, 101323. doi: 10.1016/j.eti.2020.101323

Sangani, M. F., Owens, G., and Fotovat, A. (2019). Transport of engineered nanoparticles in soils and aquifers. *Environ. Rev.* 27 (1), 43–70. doi: 10.1139/er-2018-0022

Sengupta, S., Pari, A., Biswas, L., Shit, P., Bhattacharyya, K., and Chattopadhyay, A. P. (2022). Adsorption of arsenic on graphene oxide, reduced graphene oxide, and their Fe_3O_4 doped nanocomposites. *Biointerface Res. Appl. Chem.* 12 (5), 6196–6210. doi: 10.33263/briac125.61966210

Soltanaeva, A., Suleimenov, B., Saparov, G., and Vassilina, H. (2018). Effect of sulfur-containing fertilizers on the chemical properties of soil and winter wheat field. *Bulgarian J. Agric. Sci.* 24 (4), 586–591.

Steudel, R. (2003). Aqueous sulfur sols. *Elemental Sulfur Sulfur-Rich Compounds I* 230, 153–166. doi: 10.1007/b12113

Tabak, M., Lisowska, A., and Filipek-Mazur, B. (2020). Bioavailability of sulfur from waste obtained during biogas desulfurization and the effect of sulfur on soil acidity and biological activity. *Processes* 8 (7), 863. doi: 10.3390/pr8070863

Teng, Y., Zhou, Q., and Gao, P. (2019). Applications and challenges of elemental sulfur, nanosulfur, polymeric sulfur, sulfur composites, and plasmonic nanostructures. *Crit. Rev. Environ. Sci. Technol.* 49 (24), 2314–2358. doi: 10.1080/10643389.2019.1609856

Tourna, M., Maclean, P., Condron, 'L., O'Callaghan, M., and Wakelin, S. A. (2014). "Links between sulphur oxidation and sulphur-oxidising bacteria abundance and diversity in soil microcosms based on soxb functional gene analysis.". *FEMS Microbiol. Ecol.* 88 (3), 538–549. doi: 10.1111/1574-6941.12323

Tu, Y., Lv, M., Xiu, P., Huynh, T., Zhang, M., Castelli, M., et al. (2013). Destructive extraction of phospholipids from escherichia coli membranes by graphene nanosheets. *Nat. Nanotechnol.* 8, 594–601. doi: 10.1038/nnano.2013.125

Wang, D., Wang, G., Zhang, G., Xu, X., and Yang, F. (2003). Using graphene oxide to enhance the activity of anammox bacteria for nitrogen removal. *Bioresour Technol.* 131, 527–530. doi: 10.1016/j.biortech.2013.01.099

Watkinson, J. H., and Blair, G. J. (1993). Modelling the oxidation of elemental sulfur in soils. *Fertilizer Res.* 35, 115–126. doi: 10.1007/BF00750225

Williams, J. S., and Cooper, R. M. (2004). The oldest fungicide and newest phytoalexin - a reappraisal of the fungitoxicity of elemental sulphur. *Plant Pathol.* 53 (3), 263–279. doi: 10.1111/j.0032-0862.2004.01010.x

Xia, T. J., Lin, Y. X., Li, S. L., Yan, N., Xie, Y., He, M. R., et al. (2021). Co-Transport of negatively charged nanoparticles in saturated porous media: Impacts of hydrophobicity and surface O-functional groups. *J. Hazardous Materials* 409, 9. doi: 10.1016/j.jhazmat.2020.124477

Xiao, X., Wang, X., Liu, L., Chen, C., Sha, A., and Li, J. (2022). Effects of three graphene-based materials on the growth and photosynthesis of *Brassica nanus* l. *Ecotoxicol Environ. Saf.* 234, 113383. doi: 10.1016/j.ecoenv.2022.113383

Xie, J., Ming, Z., Li, H., Yang, H., Yu, B., Wu, R., et al. (2016). Toxicity of graphene oxide to white rot fungus *Phanerochaete chrysosporium*. *Chemosphere* 151, 324–331. doi: 10.1016/j.chemosphere.2016.02.097

Yang, X., Wan, Y., Zheng, Y., He, F., Yu, Z., Huang, J., et al. (2019). Surface functional groups of carbon-based adsorbents and their roles in the removal of heavy metals from aqueous solutions: A critical review. *Chem. Eng. J.* 366, 608–621. doi: 10.1016/j.cej.2019.02.119

Yap, P. L., Kabiri, S., Auyoong, Y. L., Tran, D. N. H., and Losic, D. (2019). Tuning the multifunctional surface chemistry of reduced graphene oxide *via* combined elemental doping and chemical modifications. *ACS Omega* 4 (22), 19787–19798. doi: 10.1021/acsomega.9b02642

Ye, R., McCray, J. M., and Wright, A. L. (2011). Microbial response of a calcareous histosol to sulfur amendment. *Soil Sci.* 176 (9), 479–486. doi: 10.1097/SS.0b013e31822769e7

Yu, H. T., Zhang, B. W., Bulin, C. K., Li, R. H., and Xing, R. G. (2016). High-efficient synthesis of graphene oxide based on improved hummers method. *Sci. Rep.* 6, 7. doi: 10.1038/srep36143

Zahedi, S. M., Abolhassani, M., Hadian-Deljou, M., Feyzi, H., Akbari, A., Rasouli, F., et al. (2023). Proline-functionalized graphene oxide nanoparticles (GO-pro NPs): A new engineered nanoparticle to ameliorate salinity stress on grape (*Vitis vinifera* l. cv sultana). *Plant Stress* 7, 10. doi: 10.1016/j.stress.2022.100128

Zakari, S., Liu, W., Wu, J., Singh, A. K., Jiang, X., Yang, B., et al. (2020). Decay and erosion-related transport of sulfur compounds in soils of rubber based agroforestry. *J. Environ. Manage* 274, 111200. doi: 10.1016/j.jenvman.2020.111200

Zhang, Q., Hou, Q. X., Huang, G. X., and Fan, Q. (2020). Removal of heavy metals in aquatic environment by graphene oxide composites: A review. *Environ. Sci. pollut. Res.* 27 (1), 190–209. doi: 10.1007/s11356-019-06683-w

Zhao, D. Q., Fang, Z. W., Tang, Y. H., and Tao, J. (2020). Graphene oxide as an effective soil water retention agent can confer drought stress tolerance to *Paeonia ostii* without toxicity. *Environ. Sci. Technol.* 54 (13), 8269–8279. doi: 10.1021/acs.est.0c02040

Zhao, L., Wang, W., Fu, X. H., Liu, A., Cao, J. F., and Liu, J. F. (2022). Graphene oxide, a novel nanomaterial as soil water retention agent, dramatically enhances drought stress tolerance in soybean plants. *Front. Plant Sci.* 13. doi: 10.3389/fpls.2022.810905

frontiers | Frontiers in Plant Science

TYPE Original Research
PUBLISHED 21 March 2023
DOI 10.3389/fpls.2023.1135947

Check for updates

Effects of Hanwoo (Korean cattle) manure as organic fertilizer on plant growth, feed quality, and soil bacterial community

Junkyung Lee[1], Na-Yeon Jo[1], Su-Yeon Shim[1], Le Tran Yen Linh[2], Soo-Ryang Kim[3], Myung-Gyu Lee[3] and Sun-Goo Hwang[1*]

[1]College of Life and Environment Science, Sangji University, Wonju-si, Republic of Korea, [2]Department of Smart-Farm, Sangji University, Wonju-si, Republic of Korea, [3]Department of Earth Environment Engineering, Sangji University, Wonju-si, Republic of Korea

OPEN ACCESS

EDITED BY
Amanullah,
University of Agriculture, Peshawar, Pakistan

REVIEWED BY
Modupe Stella Ayilara,
North-West University, South Africa
Everlon Cid Rigobelo,
São Paulo State University, Brazil

*CORRESPONDENCE
Sun-Goo Hwang
sghwang9@sangji.ac.kr

SPECIALTY SECTION
This article was submitted to Plant Nutrition, a section of the journal Frontiers in Plant Science

RECEIVED 02 January 2023
ACCEPTED 06 March 2023
PUBLISHED 21 March 2023

CITATION
Lee J, Jo N-Y, Shim S-Y, Linh LTY, Kim S-R, Lee M-G and Hwang S-G (2023) Effects of Hanwoo (Korean cattle) manure as organic fertilizer on plant growth, feed quality, and soil bacterial community.
Front. Plant Sci. 14:1135947.
doi: 10.3389/fpls.2023.1135947

Introduction: The development of organic manure from livestock excreta is a useful source for sustainable crop production in environment-friendly agriculture. Organic manure increases soil microbial activity and organic matter (OM) supply. The excessive use of chemical fertilizers (CFs) leads to air and water pollution caused by toxic chemicals and gases, and soil quality degradation via nutrient imbalance due to supplying specific chemical components. Thus, the use of organic manure will serve as a long-term supply of various nutrients in soil *via* OM decomposition reaction as well as the maintenance of environment.

Methods: In this study, we aimed to analyze the diverse effects of Hanwoo manure (HM) on plant growth, feed quality, and soil bacterial communities in comparison with CFs, commercial poultry manure (CM), and the combined use of chemical fertilizer and Hanwoo manure (HM+CF). We analyzed the contents of crude matter (protein, fat, fiber, and ash), P, acid detergent fiber (ADF), and neutral detergent fiber (NDF) through feed quality analysis, and the contents or activities of total phenol, total flavonoid, ABTS, nitrite scavenging, and reducing power *via* the antioxidant assay. Furthermore, the soil microbial communities were determined using 16S rRNA sequencing. We compared the soil bacteria among different soil samples by using amplicon sequence variant (ASV) analysis.

Results and discussion: We observed increased OM in the soil of the HM group compared to that of the CF and non-treated groups over a period of two years. Moreover, HM+CF treatment enormously improved plant growth. Organic manure, especially HM, caused an increase in the content of crude ash and phosphorus in plants. There were no significant differences in total polyphenol, total flavonoid, ABTS, nitrite scavenging, and reducing power in plants between

HM and CF groups. Finally, we detected 13 soil bacteria (*Acidibacter*, *Algisphaera*, *Cystobacter*, *Microvirga*, *Ohtaekwangia*, *Panacagrimonas*, *Pseudarthrobacter*, *Reryanella*, *Rhodoligotrophos*, *Solirubrobacter*, *Stenotrophobacter*, *Tellurimicrobium*, and *Thermomarinilinea*) that were considerably correlated with OM and available phosphorus, and three considerably correlated bacteria were specifically distributed in CF or organic manure. The results suggest that HM is a valuable source of organic manure that can replace CF for sustainable crop production.

KEYWORDS

organic fertilizer, bacterial community, amplicon sequence variant, Hanwoo manure, maize

1 Introduction

Chemical fertilizers (CFs) are mainly used to improve crop production and plant growth because they are easily absorbed by plants (Savci, 2012; Han et al., 2016). Using these CFs leads to nutritional imbalances and acidification in the soil because of the high accumulation of several chemical components (Simpson et al., 2011; Bisht and Chauhan, 2020). Although organic manure has low nutrient contents and decomposes nutrients slowly, it has various benefits in the soil, such as a good balance of multiple nutrients and an improvement in microbial activity and physical soil structure (Han et al., 2016). In previous studies, long-term use of organic fertilizers increased crop yield and nutrient uptake rate compared to that of CFs (Lu et al., 2021; Nie et al., 2007). Furthermore, Ji et al. (2017) reported that liquid fertilizer from organic matter (OM) improved root development and soil microbial diversity in *Chrysanthemum morifolium*. Thus, organic liquid fertilizer can suitably decrease the use of CFs in agriculture owing to their positive effects on plant growth and soil improvement.

Many microorganisms exist in the soil, including fungi, viruses, and bacteria. Microbial communities in the soil are influenced by the growth of different plant species (Fierer, 2017). The microbial communities affected water and nutrient uptake from the environment, leading to plant growth promotion (Kim et al., 2012). The plant growth-promoting bacteria (PGPB) play a role in the nutrient fixation of nitrogen, iron, and phosphorus depending on soil composition; plant growth is influenced by providing the fixed nutrients (Kim et al., 2012). Moreover, these beneficial bacteria positively affected organic matter decomposition and soil structure maintenance (Mumtaz et al., 2017; Suman et al., 2022). The proper use of PGPB can reduce the application of chemical fertilizers in agriculture (Adesemoye et al., 2009). The physical and chemical properties and soil microbiome were improved by providing organic manure (Adekambi and Drancourt, 2004; Naik et al., 2019). In a multi-generation experiment, the soil microbial community influenced the flowering time of *Arabidopsis thaliana* (Panke-Buisse et al., 2015). Furthermore, the plant pathogens are suppressed by soil microbiomes, such as *Pseudomonas* and *Bacillus* bacteria, which can be subsequently transferred by soil transplantation (Wei et al., 2019). In a previous study, organic biofertilizer inoculated with *Trichoderma* improved the production and quality of tomatoes compared with CF (Ye et al., 2020). Thus, the proper use of organic manure may reduce CF usage for environmental conservation in agriculture.

Maize (*Zea mays* L.) is an important crop worldwide, with an abundance of nutritional benefits and fibrous matter as an edible crop for humans and livestock (Duvick, 2005; Zhang et al., 2022). Corn has high digestibility in livestock diets because of the different types and associations with corn starch (Loy and Lundy, 2019). The livestock's rumen can digest corn with a soft texture. Corn is relatively high in sulfur-containing amino acids, such as methionine and cysteine, while it is low in essential amino acids, such as lysine and tryptophan (Loy and Lundy, 2019). However, corn has been shown to improve protein quality and oil and amylose contents, depending on human requirements (Darrah et al., 2019). Unlike white corn, the kernels of yellow corn have carotenoid pigments; thus, yellow corn silage can be a useful source of provitamin A (Watson, 1962). The high oil content of corn results in a high level of energy supply in poultry (Lee et al., 2001) and swine livestock (Adeola and Bajjalieh, 1997). Corn contains diverse types of B vitamins, such as niacin, biotin, thiamin, and pyridoxine, but not cobalamin and vitamin E (Ball and Ratcliff, 1978; Cort et al., 1983; Lynch et al., 1996; Loy and Lundy, 2019). Thus, corn provides high amounts of energy and nutrients to livestock. Therefore, the demand for maize has rapidly increased worldwide, especially in developing countries (Shiferaw et al., 2011).

Cattle manure contains relatively lower nitrogen (N) and phosphorus pentoxide than poultry, swine, and sheep (Cravotta, 1995). In particular, the N content is most deficient in cattle manure, whereas it is highest in poultry manure based on unit weight. However, manures from dairy cows and beef cattle have higher contents of dry materials as OM sources than those from hog and poultry. As the economy grows, human demand for meat increases and excessive supply has increased environmental and social problems (Tilman et al., 2011). The amount of livestock excretions in Hanwoo cattle in Korea is higher than that in swine and poultry (Choi, 2007). Although Hanwoo manure (HM) has a low N content, the use of HM must be encouraged in crop production, which will contribute to environmental conservation and environment-friendly agricultural development. In this study, we attempted to observe the diverse effects of HM on plant growth, antioxidants, and microbial communities in the cultivation of forage maize and compare its impact with CF and commercial poultry manure. Furthermore, the availability of HM was evaluated to reduce the use of chemical fertilizer in the forage maize production.

2 Materials and methods

2.1 Plant growth condition and survey

Maize (*Z. mays* L., Kwangpyeongok) was obtained from the Agricultural Technology Center (Hoengseong-gun, Gangwon-do, Republic of Korea), and its seeds were grown in a greenhouse for two weeks. The seedlings were transplanted into an experimental field (37° 22' 16.2″ N, 127° 55' 30.1″ E) at Sangji University (Wonju-si, Gangwon-do, Republic of Korea). The experiment for non-treatment (NT), CF, commercial manure (CM), HM, and a mixture of HM and CF was performed in the field using randomized complete block design. Thus, all treatments were randomly assigned to the experimental units within the blocks in the experimental field. Fertilizers were applied following the cultivation method used in a previous experiment by Byeon et al. (2022). Plant growth was observed with respect to plant length, leaf width, and leaf length in the different fertilizer-treated plant groups. The chlorophyll concentration of the leaves was measured using a SPAD-502plus chlorophyll meter (Konica Minolta Inc., Teban Gardens Crescent, Singapore). Fresh and dry weights were measured in the aboveground parts of the plants before and after dehydration, respectively. The plant tissues were dried at 60°C for 24 h.

2.2 Total nitrogen

A soil sample of 10 g was mixed with 50 mL of distilled water; then, the electrical conductivity (EC) and pH were detected using multiparameter analysis (Edge HI2020, HANNA instruments, Woonsocket, USA). The total nitrogen was measured using the Kjeldahl method (Barbano et al., 1990; Aoac, 1995), where a 5 g sample was mixed with a solution of 50 g potassium sulfate and 50 g copper (II) sulfate (9:1). The samples were heated for 4 h. Subsequently, 500 µL of phenolphthalein solution was added (0.04 g phenolphthalein, 50 mL 95% ethyl alcohol, and 50 mL distilled water). Sodium hydroxide (NaOH; 0.01 N) was added to the prepared sample until it turned red. To collect the distillate from the sample, 2% bromocresol green solution (0.5 g bromocresol green, 0.1 g methyl red, and 100 mL 95% ethyl alcohol) was used. Finally, the end-effect points of 0.01 N sulfuric acid (H_2SO_4) for changing color from blue to red were measured. The total nitrogen content was calculated for each treatment as follows:

$$factor\ of\ 0.01N\ \mathrm{H2SO4} = \frac{amounts\ of\ 0.1N\ NaOH\ for\ the\ end-effect\ point \times f\ of\ 0.1N\ NaOH}{amounts\ of\ 0.1N\ \mathrm{H2SO4}}$$

$$Total\ nitrogen\ (\%) = \frac{(T-B)\times f \times Normality \times 14 \times 100}{sample\ weight\ (mg)} \times diluted\ ratio\ of\ sample$$

where T represents the amounts of 0.01N H_2SO_4 for the end-effect point, B represents the blank, f represents the factor of 0.01N H_2SO_4, and Normality represents the concentration (N) of H_2SO_4.

2.3 Total phosphorus

Total phosphorus (P) and available phosphorus pentoxide (P_2O_5) were detected using the Lancaster soil testing method (Lancaster, 1980). A soil sample of 5 g was added into the 20 mL extracting solutions that comprised 400 mL acetic acid (CH_3COOH), 300 mL 10N lactic acid ($CH_3CH[OH]COOH$), 22.2 g ammonium bifluoride (NH_4F), 133.3 g diazanium sulfate ($[NH_4]2SO_4$), and 170 g NaOH, and the mixture was boiled for 10 min. Standard P solutions (10, 100, and 1000 ppm) were used to evaluate the available P_2O_5 in the samples. A 6 mL ammonium paramolybdate solution (200 mL ammonium paramolybdate and 100 mL 0.8M boric acid [H_3BO_3]) was added for absorbance determination using an Ultraviolet-visible (UV-Vis) spectrophotometer (NEO–S2117, NEOGEN). The total P and available P_2O_5 were calculated for each treatment as follows:

$$Available\ phosphorus\ pentoxide = \frac{detected\ ppm \times extracted\ liquid\ (ml)}{sample\ weight\ (g)} \times 2.2914$$

$$Total\ P = Available\ phosphorus\ pentoxide \times 0.4364$$

2.4 Exchangeable cations

Exchangeable cations were detected using the ammonium acetate method. The four exchangeable cations (potassium [K], calcium [Ca], magnesium [Mg], and natrium [Na]) were determined in the 5 g samples and 50 mL of 1N-NH_4OAc at pH 7 by inductively coupled plasma atomic emission spectrometry (ICP-OES; SPECTROBLUE, SPECTRO). The four exchangeable cations were calculated for each treatment as follows:

$$Ex-cations = ICP-AES\ value \times \frac{extracted\ liquid\ (mL)}{sample\ weight\ (g) \times 10} \div electrochemical\ equivalent$$

The electrochemical equivalent was 39.1 for K, 20.04 for Ca, 12.15 for Mg, and 22.99 for Na.

2.5 Organic matter

OM was determined using the Tyurin method (Schollenberger, 1927). The 5-g sample was added to 10 mL of 0.4 N potassium dichromate solution (40 g potassium dichromate [K_2Cr2O_7] per 1 L H_2SO_4). The solution was then boiled for 5 min on a hot plate (C-HP, CHANGSHIN SCIENCE), and 150 mL of distilled water was added. Five milliliters of 85% H_3PO_4 and 500 µL diphenylamine were added to the sample. To determine the end-effect point, 0.2N ammonium iron (II) sulfate hexahydrate solution (78.44 g [NH_4] $2SO_4FeSO_4$ $6H_2O$ per 1 L $H2_SO_4$) was added to the reactants until it turned from orange to green. The OM was calculated for each treatment as follows:

$$OM\ (\%) = (B - T) \times 0.2 \times 3 \times 0.001 \times \frac{100}{sample\ weight\ (g)} \times 1.724$$

where T represents the amounts of 0.2N ammonium iron (II) sulfate hexahydrate solution for the end-effect point, B represents the blank, 0.2 represents the normal concentration of ammonium iron (II) sulfate hexahydrate solution, 3 represents the chemical equivalent of 1 mg carbon, and 1.724 represents the carbon ratio for soil erosion.

2.6 Cation exchange capacity of fertilizers

The cation exchange capacity (CEC) of the fertilizer was determined using the ammonium acetate method (Thomas, 1982) with 5 g of sample and 100 mL of 1N NH_4OAc. After 4 h of incubation, 100 mL of 80% ethyl alcohol (pH 7.0) was added. Then, 500 µL phenolphthalein solution (0.04 g Phenolphthalein, 50 mL ethyl alcohol, and 50 mL distilled water) and MgO were added until they turned red. Finally, 20 g of H_3BO_3 and 5 mL of 2% bromocresol green solution per liter (L) were added to the reactants, and the endpoint of 0.01N H_2SO_4 for changing color from blue to red was measured. The CEC was calculated for each treatment as follows:

$$CEC\ (me/100g) = \frac{T - B}{sample\ weight\ (g)} \times f \times Normality \times 100$$

where T represents the amounts of 0.01N $H2_SO_4$ at the end-effect point, B represents the blank, f represents the f of 0.01N H_2SO_4, and Normality represents the concentration (N) of H_2SO_4.

2.7 Crude protein content

The content of crude protein was extracted following the Kjeldahl method (Barbano et al., 1990; Aoac, 1995). Briefly, 0.5 g of a dried sample was mixed with 7 g of potassium sulfate solution (9 g potassium sulfate and 1 g copper sulfate) and 10 mL of H_2SO_4. Then, 100 µL liquid indicator was added to the prepared mix. The solution was then distilled after adding zinc and sodium hydroxide solution (sodium hydroxide 500 g, sodium thiosulfate 100 g, distilled water 1 L). The amount of 0.1 N hydrochloric acid was observed until the desired color (reddish brown) was obtained. The percentage of crude oil content was calculated using the following formula:

$$Crude\ protein\ (\%) = \frac{0.00140067\ (0.1N\ HCl) \times T \times F \times 6.25 \times 100}{W}$$

where T represents the amount of 0.01 N H_2SO_4 for the end effect point, F represents the amount of 0.1 N HCl for the blank, and W represents the weight of the sample.

2.8 Crude fat content

The crude fat content was extracted using the ether extract method (Padmore, 1990). In this method, after drying 2 g of the sample on a filter paper for 2 h at 100°C, ether was mixed and placed in the Soxhlet extractor (ANKOM XT15 Extractor, ANKOM Technology, USA) for boiling at 80°C for 8 h to extract the fat. The ether was extracted and dried in the solvent flask for 3 h at 100°C. Afterward, the sample was cooled in a desiccator for 40 min, and using the following formula, the crude fat content was calculated:

$$Crude\ fat\ (\%) = \frac{a - b}{c} \times 100$$

where a and b are the total mass of the solvent flask after and before extraction, respectively, and c is the total mass of the sample.

2.9 Crude fiber content

The content of crude fiber was extracted by following Henneberg and Stohmann's method (Henneberg and Stohmann, 1859). In this method, a mix of 1 g of sample, 50 mL of 5% sulfuric acid solution (27 mL H_2SO_4, and 1 L distilled water), and 150 mL distilled water were placed in a 500 mL beaker, followed by the addition of 2 drops of an anti-foaming agent. After boiling the mix for 30 min, it was filtered, and the residue was washed with hot distilled water until the alkaline was eliminated with quantitative filter paper (2.5 µM). Then, 130 mL of the washed residue was added to 50 mL of 5% sodium hydroxide solution (50 g NaOH and 1 L distilled water) in a beaker, and distilled water was added until the total volume reached 200 mL. After boiling the mix again for 30 min and washing the residue with hot distilled water, the resultant residue was washed thrice with 95% ethyl alcohol and twice with ethyl-ether, followed by drying the residue for 2 h at 100°C and 2 h at 135°C. The dried mass was then cooled in a desiccator for 40 min, burned in a porcelain crucible, and cooled again. The crude fiber content was then calculated as follows;

$$Crude\ fiber\ (\%) = \frac{d-a}{s} \times 100$$

where d represents the dry weight of the residue filtered after decomposition, a represents the residue after the last burning in the porcelain crucible, and s represents the weight of the sample.

2.10 Crude ash content

The crude ash content was determined following Liu's method (Liu, 2019). In this method, the porcelain crucible was burnt in an electric furnace (Lindberg/Blue M, Thermo Fisher Scientific, USA) at 600°C for 1 h and cooled in a desiccator for 40 min. Then, 2 g of the sample was placed in an electric furnace at 600°C for 2 h, cooled in a desiccator for 40 min, and measured. The crude ash content was calculated for each treatment as follows:

$$Crude\ ash\ (\%) = \frac{a-b}{c} \times 100$$

where a represents the weight of the burnt sample and the porcelain crucible, b represents the weight of the porcelain crucible, and c represents the raw sample weight.

2.11 Phosphorus content

The P content was measured following Cavell's method (Cavell, 1955). In this method, the P content of corn was determined by measuring its absorbance after adding a coloring agent. First, 1 mL of sample solution (filtrate of 2 g burned sample mixed with 10 mL of hydrochloric acid [1:1]) was taken in a 25 mL mass flask and mixed with 2.5 mL of ammonium molybdite solution (25 g ammonium molybdite with 400 mL distilled water). The absorbance was then measured at 470 nm wavelength. The P content was calculated for each treatment as follows:

$$Phosphorus\ (\%) = \frac{a/b \times c}{d \times 106} \times 100$$

where a is the absorbance of the sample, b is the standard absorbance (1 ppm), c is the dilution factor, and d is the sample weight.

2.12 Neutral detergent fiber

Neutral detergent fiber (NDF) was measured using 1 g of sample and 100 mL of neutral detergent solution (150 g of sodium lauryl sulfate, 93.05 g of EDTA disodium salt, 34.05 g of sodium borate, 22.8 g of sodium phosphate, 22.8 g of dibasic dodecahydrate, and 50 mL of ethylene glycol monoethyl ether). Then, 5 L of distilled water was added to 2 mL of decahydronaphthalene and 0.5 g sodium sulfite. The mix was boiled for 1 h in an automated fiber analyzer (ANKOM A2000, ANKOM Technology, USA) and then filtered through a glass filter. The residue was then washed with acetone and dried at 105°C for 4 h. NDF was calculated for each treatment as follows:

$$NDF\ (\%) = \frac{a-b}{c} \times 100$$

where a represents the sample weight after drying, b represents the residual weight, and c represents the sample weight.

2.13 Acid detergent fiber

For measurement of acid detergent fiber (ADF), 2 g of the sample was added to a 500 mL beaker along with 100 mL of acid detergent solution (melted mix of 20 g of cetyltrimethylammonium bromide [CTAB] and 1 N 1 L of H_2SO_4), and 2 mL of decalin. The mixture was then boiled for 1 h in an automated fiber analyzer and filtered using a glass filter. The residue was washed with acetone and dried at 105°C for 4 h. The ADF was calculated for each treatment as follows:

$$ADF\ (\%) = \frac{a-c}{c} \times 100$$

where a represents the sample weight after drying, b represents the residual weight, and c represents the sample weight.

2.14 Antioxidant analysis

The top part of forage maize was used to evaluate the antioxidant activities of plants in the different fertilizer-treated groups. The total phenol and flavonoid contents, nitrate-scavenging activities, reducing power, and ABTS were determined as described previously (Jo et al., 2022). All measurements were performed in triplicate. The plant extracts were collected using methanol, and standard curves were generated for quantitative analysis using standard materials (quercetin for total flavonoid and gallic acid for total phenol) (Figure S1). A high R-squared value ($R^2 > 99$) was obtained in the regression line. The absorbance was measured using a spectrometer at 760, 510, 520, 734, and 700 nm for total phenol, total flavonoid, nitrate-scavenging activity, ABTS assay, and reducing power assay, respectively.

2.15 Soil microbiome 16s rRNA sequencing analysis

To compare the microbial diversity in the fertilizer-treated soils, an Illumina MiSeq microbiome analysis was conducted. The soil microbial DNA was isolated using DNeasy Power Soil Kit (Qiagen, Hilden, Germany) followed the manufacturer's protocol, and a DNA library was generated using the Illumina 16S Metagenomic Sequencing Library (Amplicon et al., 2013). According to the manufacturer's instructions, polymerase chain reaction (PCR) was performed using Herculase II Fusion DNA Polymerase (Agilent Technologies, Santa Clara, CA, USA). The first PCR process involved heat activation for 30 min at 95°C, followed by 25 cycles of denaturation for 30 s at 95°C, annealing for 30 s at 55°C,

10.3389/fpls.2023.1135947

extension for 30 s at 72°C, and a final extension for 10 min at 72°C. The sequences of the primer pairs used for the first amplification are as follows:

V3-F: 5′-TCGTCGGCAGCGTCAGATGTGTATAAGAGA CAGCCTACGGGNGGCWGCAG-3′,

V4-R: 5′-GTCTCGTGGGCTCGGAGATGTGTATAA GAGACAGGACTACHVGGGTATCTAATCC-3′.

AMPure XP beads (Agencourt Bioscience, Beverly, MA, USA) were used to purify the first PCR products. The purified first PCR product was used for library construction using the NexteraXT Indexed Primer (Illumina Inc., CA, USA). The second PCR and purification were performed using the same method as the first PCR. Sequencing was performed using the MiSeq™ platform (Illumina, San Diego, CA, USA) with a paired-end method (2 × 300 bp).

2.16 Amplicon sequence variant and statistical analysis

Raw sequencing data (fastq) were used to remove adapter sequences using the Cutadapt program (Martin, 2011). We performed an error correction of filtered paired-end sequencing data using the R package DADA2 (Callahan et al., 2016) and identified the amplicon sequence variant (ASV). The ASVs obtained from different samples were normalized using QIME (Caporaso et al., 2010). The taxonomy of each ASV was identified from the NCBI 16S microbial database using BLAST+ with a query coverage of 85% (Camacho et al., 2009). Statistical analysis of bacterial diversity was performed using the R packages dplyr (Wickham et al., 2015), taxa (Foster et al., 2018), apes (Paradis et al., 2004), ggrepel (http://cran.nexr.com/web/packages/ggrepel/index.html), pyloseq (McmurdieHolmes, 2013), DESeq2 (Love et al., 2014), vegan (https://cran.r-project.org/web/packages/vegan/index.html), ggsignif (https://cran.r-project.org/web/packages/ggsignif/index.html), and ggplot2 (Wickham and Chang, 2016). Significant differences were evaluated using the R package Agricolae (https://cran.r-project.org/web/packages/agricolae/index.html) with Duncan's test for comparisons between different treatment groups ($p \leq 0.05$). To determine the significant correlation between soil chemical components and bacterial communities, the Mantel test was performed using the R package vegan (https://cran.r-project.org/web/packages/vegan/index.html) with 9,999 permutations, and canonical correspondence analysis (CCA) was performed using the R package CCA (https://cran.r-project.org/web/packages/CCA/index.html).

3 Results

3.1 Soil chemical components

We analyzed the chemical components of soil in each experimental field [NT, CF, CM, HM, and combined treatments of Hanwoo manure and chemical fertilizer (hereinafter named HM+CF)] after harvesting maize (Table 1). The pH was considerably lower in the CF group (5.51) than in the other groups (5.57 for NT, 6.21 for CM, 5.93 for HM, and 5.79 for HM+CF). The highest CEC was observed in CM (10.93 cmol+/kg). Total Nitrogen content was markedly higher in the CM (0.139%) and HM+CF (0.139%) groups; however, the HM group (0.131%) was not significantly different from the CM and HM+CF groups. The available P was increased in CM (301.70 mg/kg), CF (297.85 mg/kg), and HM+CF (285.86 mg/kg). Ca and Mg exchangeable cations were high in the CM (7.72 cmol+/kg for Ca, 1.37 cmol+/kg for Mg) and HM+CF (7.98 cmol+/kg for Ca, 1.38 cmol+/kg for Mg) groups, while exchangeable K and Na showed no considerable difference. Finally, a high OM was observed in HM (2.58%) and HM+CF (2.49%) groups. The EC and

TABLE 1 Chemical components of fertilizers remaining in the soil.

	NT	CM	HM	CF	HM + CF
pH[1:5]	5.57 (± 0.17) ab	6.21 (± 0.18) a	5.93 (± 0.13) ab	5.51 (± 0.14) b	5.79 (± 0.22) ab
EC[1:5] (dS/m)	0.10 (± 0.006) a	0.11 (± 0.008) a	0.10 (± 0.05) a	0.10 (± 0.008) a	0.12 (± 0.006) a
C.E.C. (cmol+/kg)	9.02 (± 0.17) b	10.63 (± 0.17) a	9.45 (± 0.15) b	9.24 (± 0.17) b	9.58 (± 0.13) b
Total N (%)	0.105 (± 0.004) c	0.139 (± 0.002) a	0.131 (± 0.003) ab	0.126 (± 0.004) b	0.139 (± 0.003) a
Available P (mg/kg)	201.63 (± 7.72) c	301.70 (± 4.54) a	245.32 (± 6.61) b	297.85 (± 5.56) a	285.86 (± 3.52) a
Exchangeable K (cmol+/kg)	0.07 (± 0.01) a	0.09 (± 0.01) a	0.11 (± 0.013) a	0.08 (± 0.01) a	0.09 (± 0.015) a
Exchangeable Ca (cmol+/kg)	7.32 (± 0.092) b	7.72 (± 0.093) a	7.07 (± 0.099) b	7.24 (± 0.085) b	7.98 (± 0.104) a
Exchangeable Mg (cmol+/kg)	1.20 (± 0.02) b	1.37 (± 0.03) a	1.26 (± 0.02) b	1.20 (± 0.02) b	1.38 (± 0.02) a
Exchangeable Na (cmol+/kg)	0.08 (± 0.01) a	0.07 (± 0.01) a	0.09 (± 0.01) a	0.08 (± 0.005) a	0.09 (± 0.01) a
Salinity (%)	0.005 (± 0.0008) a	0.004 (± 0.0005) a	0.005 (± 0.0005) a	0.005 (± 0.0005) a	0.005 (± 0.0005) a
OM (%)	1.48 (± 0.05) d	2.32 (± 0.03) b	2.58 (± 0.04) a	1.95 (± 0.03) c	2.49 (± 0.03) a

NT, non-treatment; CM, commercial manure; HM, Hanwoo manure; CF, chemical fertilizer; HM + CF, combined use of Hanwoo manure and chemical fertilizer.
Lowercase letters represent significant differences ($p < 0.05$) between groups as determined using Duncan's test.

salinity showed no considerable differences among the different experimental soils. Overall, livestock manure showed high total nitrogen, available P, and OM contents in the soil, suggesting that the nitrogen and available P contents increased in the soil owing to increased OM.

3.2 Effect of different liquid fertilizers on plant growth

To analyze the effects of HM application on maize cultivation, the effects of different fertilizers on plant growth were observed (Figure 1). The length of maize plants was considerably higher in the HM+CF group (285.34 cm) after 93 days than in the other groups (Figure 1A). However, there were no considerable differences in plant length between the CF (79.54 cm) and HM+CF (79.61 cm) groups after 51 days. The highest measured stem diameter and leaf length were in the HM+CF and CF groups in 51–93 days. On day 51, the leaf widths in different groups were in the order of HM+CF (6.76 cm), CF (6.51 cm), and HM (6.37 cm), while the HM+CF group had the largest leaf width (7.78 cm) at 93 days. In particular, plant length and leaf width increased in the HM+CF group compared to those in the CF group as the day progressed, suggesting a positive effect of HM in the late stages of plant growth. A high SPAD unit was observed in the HM+CF and CF groups after 51 days. The SPAD units of HM+CF and CF increased until 65 days and then decreased until 93 days, suggesting that the phase changed from vegetative to reproductive (Figure 1B). The highest SPAD units of the HM+CF group were observed after 65 and 79 days; no marked difference was observed between the SPAD units of HM+CF and CF groups after 93 days. The corn emergence rate after 79 and 93 days was highest in the HM+CF group and insignificantly different among the different experimental groups, except NT. The HM+CF and CF groups, which showed a relatively significant decrease in SPAD units, showed a higher emergence rate of corn after 79 days. Furthermore, the fresh and dry weights of corn were highly increased by HM+CF treatment. HM +CF and CF treatments improved plant growth compared to other treatments; in particular, HM+CF treatment demonstrated strong effects on plant length, leaf width, initial emergence rate, and corn weight. Although HM had a lower impact on the promotion of plant growth than the HM+CF and CF groups, the possible utilization of HM in agriculture needs to be considered.

3.3 Feed quality analysis and antioxidant activities

To analyze the feed value of maize after supplying different fertilizers, we analyzed the contents of crude matter (protein, fat, fiber, and ash), P, ADF, and NDF in the plants (Figure 2). The crude contents of protein, fat, fiber, ADF, and NDF were not considerably different between the HM and CF groups. The crude ash and P contents were relatively high in the HM and CM groups, indicating that inorganic matter, including crude ash and P, increased in plants treated with organic manure. However, crude ash and P contents were low in the CF and HM+CF groups, indicating that inorganic matter in plants with CF supply was low. The contents and activities of antioxidants were analyzed in maize plants in terms of total polyphenols and flavonoids, 2,2'-Azino-bis (3-ethylbenzothiazoline-6-sulfonic acid) (ABTS), nitrite, and reducing power (Figure 3). The CM group had a relatively high total flavonoid content, and the HM+CF group had a relatively weak ABTS activity. No considerable difference was observed in the antioxidant levels of the HM and CF groups. In summary, the feed qualities, except for crude ash, P, and antioxidants, had a similar effect between the HM and CF groups.

3.4 Soil microbial composition

To analyze the effects of different fertilizers on soil microbial communities, a 16s rRNA sequencing analysis was conducted

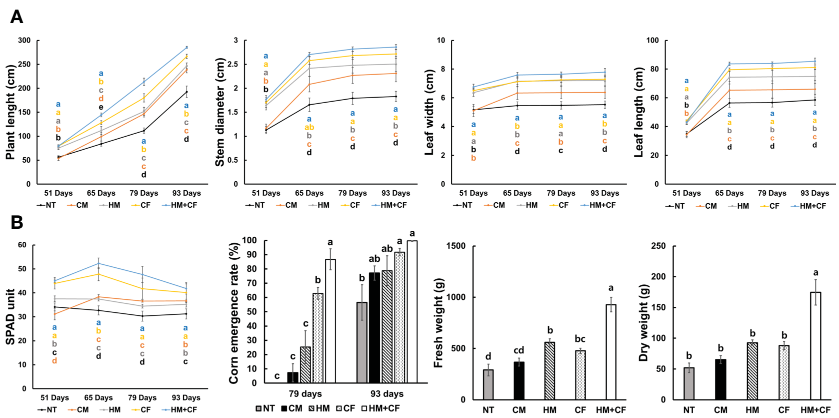

FIGURE 1
Difference in the growth of corn (NT, non-treatment; CM, commercial manure; HM, Hanwoo manure; CF, chemical fertilizer; HM+CF, combined use of Hanwoo manure and chemical fertilizer). **(A)** Plant length, stem diameter, and the width and length of leaves 93 days after planting. **(B)** SPAD unit, corn emergence rate, and fresh and dry weight of plant 93 days after planting. The line colors represent the different fertilizer treatments. The values are the mean ± standard deviation (n = 18). The lowercase letters represent the significant differences ($p < 0.05$) between groups using the Duncan test.

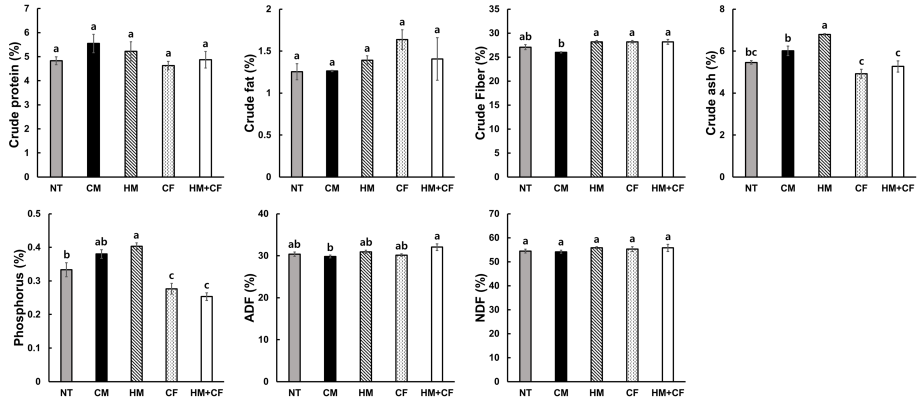

FIGURE 2
Feed values differ after applying different fertilizers (NT, non-treatment; CM, commercial manure; HM, Hanwoo manure; CF, chemical fertilizer; HM+CF, combined use of Hanwoo manure and chemical fertilizer). The values are the mean ± standard deviation (n = 3). The lowercase letters represent the significant differences ($p < 0.05$) between groups using the Duncan test.

(Figure 4). The HM group had a high alpha diversity (360 α-diversity) in the bacterial community. In comparison, the CF (327 α-diversity) and CM (312 α-diversity) groups had decreased alpha diversity compared to the NT (353 α-diversity) group (Figure 4A). However, there was no marked difference in the alpha diversity among the different soil samples. Soil microbial ASVs were clustered into 21 bacterial phyla (Figure 4B). Nine phyla (*Acidobacteria*, *Actinobacteria*, *Bacteroidetes*, *Chloroflexi*, *Firmicutes*, *Gemmatimonadetes*, *Planctomycetes*, *Proteobacteria*, and *Verrucomicrobia*) comprising over 1,000 ASVs were detected from soil bacteria in each sample. Notably, the ASVs of *Actidobacteria* and *Proteobacteria* constituted a large percentage of soil bacterial DNA (Figure 4B). The ASVs of *Acidobacteria*, *Actinobacteria*, and *Chloroflexi* were higher in the NT group than in the CM group (Figure S2). In contrast, ASVs of *Bacteroidetes* were high in the CM group and low in the NT group. Similarly, *Proteobacteria* and *Verrucomicrobia* were distinctly distributed between the HM and CF groups. High correlations of ASVs between soil samples were observed in two groups (CM and HM, and CF and HM+CF); in particular, HM+CF was closely correlated with CF (Figure 4C). This result suggests that the microbial community of the HM group was similar to that of the CF group, resulting in a change in the form of bacteria by supplying CF.

3.5 Associations between soil microbiome and fertilizer factors

To analyze differentially distributed bacteria, the ASVs of each soil sample were compared to those of the NT group at the phylum level (Figure 4D). In both soil samples, we obtained 158 considerable ASVs (65 increased and 93 decreased ASVs) divided into 21 phyla. The increased ASVs were 32 for the CM group, 36 for the HM group, 26 for the CF group, and 30 for the HM+CF group, whereas the decreased ASVs were 41, 35, 42, and 26 in the CM, HM, CF, and HM+CF groups, respectively. The highest number of significantly distributed bacteria was observed in the HM group for increased ASVs and in the CF group for decreased ASVs. This result suggests a positive effect of HM and a negative effect of CF on the bacterial community. Furthermore, many soil bacteria were commonly observed in CM, HM, CF, and HM+CF groups.

We attempted to determine significantly correlated factors between the 158 ASVs and 7 soil chemical compositions, which had a significant difference in chemical quantities in at least one experimental soil across all samples (Figure 5). We found a significant positive correlation between available P ($R = 0.43$; $p < 0.01$) and OM ($R = 0.32$; $p < 0.05$) and bacterial communities (Figure 5A). Furthermore, we determined the significantly

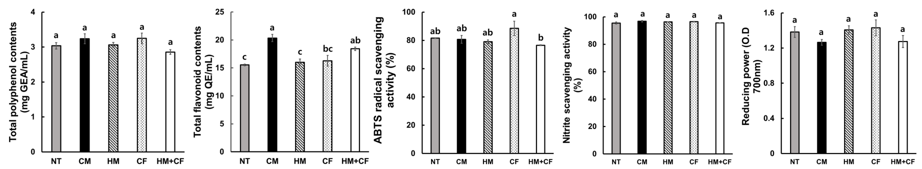

FIGURE 3
Total polyphenol and flavonoid contents, ABTS radical and nitrite scavenging activities, and reducing power activities after different fertilizer supplies (NT, non-treatment; CM, commercial manure; HM, Hanwoo manure; CF, chemical fertilizer; HM+CF, combined use of Hanwoo manure and chemical fertilizer). The values are the mean ± standard deviation (n = 3). The lowercase letters represent the significant differences ($p < 0.05$) between groups using the Duncan test.

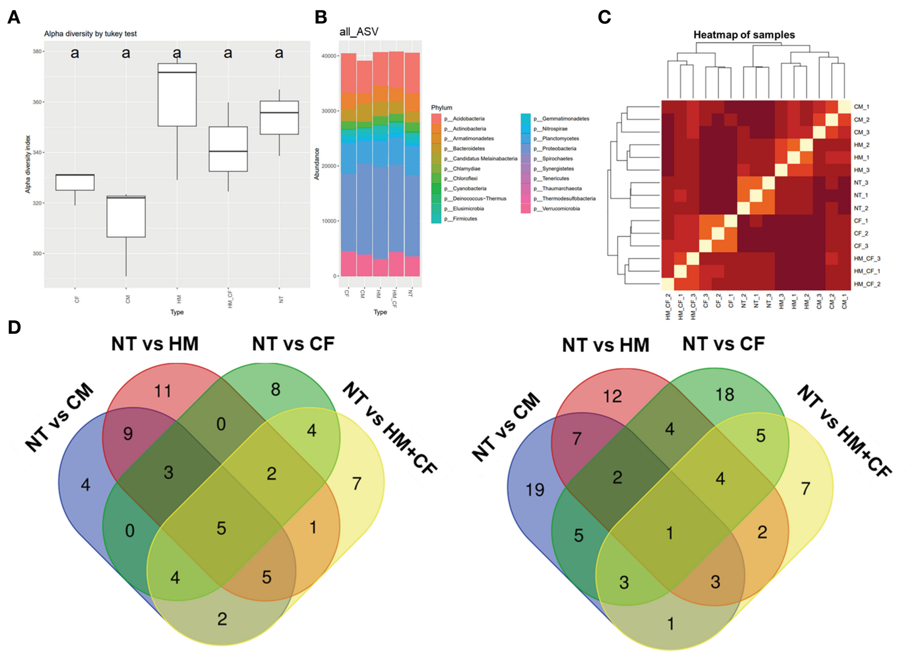

FIGURE 4
Amplicon sequence variant (ASV) approach of bacteria in the soils after different fertilizer supplies (NT, non-treatment; CM, commercial manure; HM, Hanwoo manure; CF, chemical fertilizer; HM+CF, combined use of Hanwoo manure and chemical fertilizer). **(A)** Alpha diversity of the bacterial population in each sample using the inverse Simpson (InvSimpson) method. The lowercase letters represent the significant differences ($p < 0.05$) between groups by using Tukey's HSD test. **(B)** Bacterial communities of each sample in the phylum level. The box colors represent the phylum of bacteria. **(C)** Hierarchical clustering of samples. The line colors represent the different levels of beta diversity using the Bray–Curtis dissimilarity. **(D)** The comparison of differentially distributed bacteria in the soils after different fertilizer supplies.

correlated bacteria ($p < 0.05$) for available P and OM within the bacterial phylum of 158 ASVs and found 13 significant bacterial genera (Figure 5B). *Algisphaera* (R = 0.8) and *Thermomarinilinea* (R = 0.76) were significantly positively correlated with available P content among the soil samples. In contrast, 9 bacterial genera (*Cystobacter*, *Microbirga*, *Panacagrimonas*, *Pseudarthrobacter*, *Reyranella*, *Rhodoligotrophos*, *Solirubrobacter*, *Stenotrophobacter*, and *Tellurimicrobium*) were negatively correlated with available P. OM was positively correlated with *Acidibacter* and *Ohtaekwangia* and negatively correlated with *Panacagrimonas*, *Reyranella*, and *Tellurimicrobium*. Three bacterial genera (*Panacagrimonas*, *Reyranella*, and *Tellurimicrobium*), which had negative correlations, were commonly exhibited in both P and OM. In the CCA analysis between chemical components and significantly

A

Soil Composition	R
pH	0.07 ns
C.E.C	0.09 ns
T-N	0.16 ns
Available P	0.43**
Exchangeable Ca	-0.06 ns
Exchangeable Mg	-0.04 ns
O.M.	0.32*

B

Genus	Available P	O.M.
Acidibacter	0.04	0.71*
Algisphaera	0.8*	0.32
Cystobacter	-0.91***	-0.53
Microvirga	-0.82**	-0.38
Ohtaekwangia	0.21	0.7*
Panacagrimonas	-0.8**	-0.72*
Pseudarthrobacter	-0.83**	-0.67
Reyranella	-0.73*	-0.68*
Rhodoligotrophos	-0.69*	-0.29
Solirubrobacter	-0.79*	-0.34
Stenotrophobacter	-0.83**	-0.3
Tellurimicrobium	-0.84**	-0.82**
Thermomarinilinea	0.76*	0.52

C

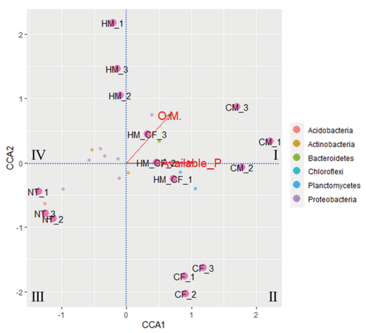

FIGURE 5
Correlation analysis between soil properties and bacterial community structures in the soils after different fertilizer supplies (NT, non-treatment; CM, commercial manure; HM, Hanwoo manure; CF, chemical fertilizer; HM+CF, combined use of Hanwoo manure and chemical fertilizer). **(A)** Mantel test between soil properties on bacterial community composition. Significant results are indicated by *$P < 0.05$ and **$P < 0.01$ (NS = no significance). **(B)** Significant correlation between two chemical components and soil bacteria. The significance was measured by using the n-2 degrees of freedom (*$P < 0.05$, **$P < 0.01$, and ***$P < 0.001$). **(C)** Canonical correspondence analysis of bacterial community composition and soil properties in soils after different fertilizer supplies.

correlated bacteria, OM and available P were closely correlated with livestock manures, except for NT and CF (Figure 5C). Although all bacterial ASVs were correlated between CF and HM+CF groups, the HM+CF group, along with livestock manure (HM and CM), was located close to OM and available P, as well as the significant bacterial genus (Figure 5C). This result suggests a distinct form of 13 significant bacterial genera in the HM+CF group due to increased OM and available P contents compared to those in the NT and CF groups. We identified a high correlation of 13 significant bacterial genera between the HM and HM+CF groups in the heatmap analysis, indicating a high distribution of specific bacteria in HM (Figure 6A) and specifically distributed bacteria in each experimental soil compared to NT (Figure 6B). *Ohtaekwangia* was found to be decreased in the CF group, while *Acidibacter* was increased in the other groups (CM, HM, and HM+CF groups), except in the CF group. *Algisphaera* increased in the CM, CF, and HM+CF groups, except for the HM group. The HM+CF group showed a distinct form of 13 significant bacteria between the HM and CF groups.

4 Discussion

In this study, we observed distinct phenotypic changes in plant growth for two years compared with the previous experiment by Byeon et al. (2022). There were no significant differences between the CF and HM+CF groups regarding OM content or plant growth. Notably, maize showed enhanced plant growth in the HM+CF group and increased OM content in the second year of the experiment, similar to the previous experiment. The combined supply of chemical and organic fertilizers positively improved crop production for long-term fertilization. The long-term use of organic fertilizers led to increased soil organic carbon (SOC) content compared to CFs (Wang et al., 2019). The combined supply of chicken manure and N increased the grain yield and dry matter content of spring maize compared with CF, suggesting that the appropriate proportion of organic substitution led to improved crop production (Geng et al., 2019). In a long-term fertilization experiment, Chand et al. (2006) demonstrated the beneficial effects of farmyard manure and CF in increasing dry matter and nutrient uptake for mint and mustard. In soil, nitrogen accumulation is stimulated in strongly acidic soils by organic manure application, along with swine manure and mushroom waste (Chen et al., 2001). Furthermore, Adekiya et al. (2020) reported that different sources of organic manure lead to increased amounts of OM, N, P, Ca, and Mg in the soil by enhancing the mineralization and steady supply of available nutrients. We identified relatively increased amounts of total N, exchangeable cations of Ca and Mg, and OM in the HM+CF group compared to the CF group, indicating soil nutrient changes caused by HM application. Thus, we suggest that the increased use of HM has additional effects on plant growth and soil nutrient changes.

Crude ash is related to the content of inorganic substances such as Ca, P, and Mg. In a previous study, the ash content in whole millet plants was increased by cattle manure and decreased by CF compared to NT; however, there were no significant differences in ash content among the different treatments (Raimundo et al., 2022). The crude ash content of onions was higher in the organic fertilizer-treated groups than in the control group without fertilization (Olle and Williams, 2014). Makinde et al. (2010) reported that organic material and its combination with CF caused a significant increase in crude ash content. Similarly, we identified increased contents of crude ash and P in the HM and CM groups, suggesting the positive effect of organic manures on the increase of inorganic matter in forage maize. Furthermore, there were no significant differences in antioxidant levels between the HM and CF groups. Thus, HM can replace CFs in the production of forage maize for livestock production.

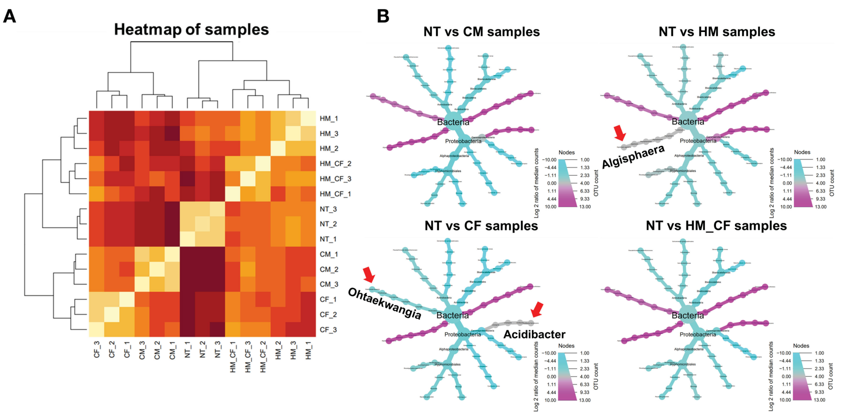

FIGURE 6
Taxonomic composition of significant bacteria analysis in the soils after different fertilizer supplies (NT, non-treatment; CM, commercial manure; HM, Hanwoo manure; CF, chemical fertilizer; HM+CF, combined use of Hanwoo manure and chemical fertilizer). **(A)** Hierarchical clustering of samples with significant bacteria. The line colors represent the different levels of beta diversity by using Bray–Curtis dissimilarity. **(B)** The relative abundances of significantly correlated bacteria in NT, CM, HM, CF, and HM+CF groups compared to the NT group. Circle size represents the number of bacteria for ASV. The color indicates the log 2-fold change of ASV with p-adjust < 0.05. Arrow represents the specific bacteria in each treatment.

We confirmed that 13 soil bacterial genera were significantly correlated with the OM and available P in the soil. The positively correlated bacteria were *Algisphaera* and *Thermomarinilinea* for available P and *Acidibacter* and *Ohtaekwangia* for OM. *Acidibacter* was a gram-negative bacterium isolated from a lake around a mine (Falagán and Johnson, 2014). The presence of *Acidibacter* is decreased by forest conversion because it prefers an acidic soil environment (Ezeokoli et al., 2020). In particular, *Ohtaekwangia* increased during the fermentation of sheep manure, and the presence of *Ohtaekwangia* and *Planomicrobium* could explain the suitability of sheep manure for using organic fertilizer (Yoon et al., 2011; Tortosa et al., 2017). We confirmed that *Ohtaekwangia* was significantly increased by organic manures, except for CF. *Algisphaera* had no significant differences in the HM group compared to the NT group, but it increased dramatically in the CM, CF, and HM+CF groups. *Algisphaera* is a gram-negative aerobic bacterium whose effects on plant growth remain unknown (Yoon et al., 2014). Furthermore, we found no significant difference in the presence of *Acidibacter* spp. in the CF group. *Acidibacter* was increased by organic manure application and correlated with SOC content (Guo et al., 2017; Jimenez-Castaneda et al., 2020; Zhang et al., 2021). Additionally, *Acidibacter* plays a role in the microbial reduction of Fe (III), and Fe (III) reduction by manure addition leads to an increase in pH (Falagán and Johnson, 2014; Jimenez-Castaneda et al., 2020). Thus, the enhanced microbial formation of *Acidibacter* by CM, HM, and HM+CF affected the pH of the soil.

5 Conclusions

The organic manure caused changes in soil nutrient compositions; in particular, the HM group showed increased amounts of total nitrogen, several exchangeable cations, and OMs compared to the CF group. The combined use of CF and HM led to improved plant growth compared with CF and organic manure. Although the HM+CF supply had substantial effects on plant growth, HM increased the inorganic matter content of crude ash, and P. ASV analysis revealed that increases in available P and OM drove 13 bacterial genera. We found specific bacteria, such as *Ohtaekwangia* and *Acidibacter*, in both organic manures, except for CF, and *Algisphaera* in others, except for HM. In particular, *Ohtaekwangia* and *Acidibacter* were considerably higher in organic manure. However, the beneficial interactions between significantly correlated bacteria and plants remain unknown. Further studies are needed to identify the functional roles of these soil bacteria in agriculture using organic manure. According to the results of this study, the use of HM as a useful organic source is suggested for environment-friendly agricultural practices, promoting sustainable crop production by replacing CFs.

Data availability statement

The datasets presented in this study can be found in online repositories. The names of the repository/repositories and accession number(s) can be found below: BioProject, PRJNA923140.

Author contributions

JL and S-GH conceived and designed the study. S-RK and M-GL provided the Hanwoo manure. JL, N-YJ, S-YS, LL, and S-GH led the field experiment. JL and S-GH performed ASV analysis. JL, N-YJ, S-YS, LL, and S-GH led the measurements of feed quality and antioxidant. All authors contributed to the article and critically to the drafts and revisions, and gave final approval for publication.

Funding

This work was supported by the Korea Institute of Planning and Evaluation for Technology in Food, Agriculture and Forestry (IPET) and the Korea Smart Farm R&D Foundation (KosFarm) through the Smart Farm Innovation Technology Development Program, funded by the Ministry of Agriculture, Food and Rural Affairs (MAFRA), Ministry of Science and ICT (MSIT), Rural Development Administration (RDA) (421046-03).

Conflict of interest

The authors declare that the research was conducted in the absence of any commercial or financial relationships that could be construed as a potential conflict of interest.

Publisher's note

Supplementary material

The Supplementary Material for this article can be found online at: https://www.frontiersin.org/articles/10.3389/fpls.2023.1135947/full#supplementary-material

References

Adekambi, T., and Drancourt, M. (2004). Dissection of phylogenetic relationships among 19 rapidly growing mycobacterium species by 16S rRNA, hsp65, sodA, recA and rpoB gene sequencing. *Int. J. Syst. Evolut. Microbiol.* 54, 2095–2105. doi: 10.1099/ijs.0.63094-0

Adekiya, A. O., Ejue, W. S., Olayanju, A., Dunsin, O., Aboyeji, C. M., Aremu, C., et al. (2020). Different organic manure sources and NPK fertilizer on soil chemical properties, growth, yield and quality of okra. *Sci. Rep.* 10, 16083. doi: 10.1038/s41598-020-73291-x

Adeola, O., and Bajjalieh, N. L. (1997). Energy concentration of high-oil corn varieties for pigs. *J. Anim. Sci.* 75, 430–436. doi: 10.2527/1997.752430x

Adesemoye, A. O., Torbert, H. A., and Kloepper, J. W. (2009). Plant growth-promoting rhizobacteria allow reduced application rates of chemical fertilizers. *Microb. Ecol.* 58, 921929. doi: 10.1007/s00248-009-9531-y

Amplicon, P., Clean-up, P., and Index, P. (2013). *16s metagenomic sequencing library preparation* (San Diego, CA, USA: Illumina).

Aoac, A. (1995). *Official methods of analysis. 16th ed* (Washington DC: Association of Official Analytical Chemists). Sci. Educ. doi: 10.12691/afjn-3-6-1

Ball, G. F. M., and Ratcliff, P. W. (1978). The analysis of tocopherols in corn oil and bacon fat by thin-layer chromatography and spot density measurement. *Int. J. Food Sci. Technol.* 13, 433–443. doi: 10.1111/j.1365-2621.1978.tb00823.x

Barbano, D. M., Clark, J. L., Dunham, C. E., and Flemin, R. J. (1990). Kjeldahl method for determination of total nitrogen content of milk: collaborative study. *J. Assoc. Off. Anal. Chem.* 73, 849–859. doi: 10.1093/jaoac/73.6.849

Bisht, N., and Chauhan, P. S. (2020). "Excessive and disproportionate use of chemicals cause soil contamination and nutritional stress", in *Soil Contamination-Threats and Sustainable Solutions*, ed. M. L. Larramendy and S. Soloneski (London, UK: IntechOpen). doi: 10.5772/intechopen.94593

Byeon, J.-E., Lee, J. K., Park, M.-S., Jo, N. Y., Kim, S.-R., Hong, S.-H., et al. (2022). Influence of hanwoo (Korean native cattle) manure compost application in soil on the growth of maize (Zea mays l.). *Korean J. Crop Sci.* 67, 164–171. doi: 10.7740/kjcs.2022.67.3.164

Callahan, B. J., Mcmurdie, P. J., Rosen, M. J., Han, A. W., Johnson, A. J. A., and Holmes, S. P. (2016). DADA2: high-resolution sample inference from illumina amplicon data. *Nat. Methods* 13, 581–583. doi: 10.1038/nmeth.3869

Camacho, C., Coulouris, G., Avagyan, V., Ma, N., Papadopoulos, J., Bealer, K., et al. (2009). Blast+: architecture and applications. *BMC Bioinf.* 10, 421. doi: 10.1186/1471-2105-10-421

Caporaso, J. G., Kuczynski, J., Stombaugh, J., Bittinger, K., Bushman, F. D., Costello, E. K., et al. (2010). QIIME allows analysis of high-throughput community sequencing data. *Nat. Methods* 7, 335–336. doi: 10.1038/nmeth.f.303

Cavell, A. J. (1955). The colorimetric determination of phosphorus in plant materials. *J. Sci. Food Agric.* 6, 479–480. doi: 10.1002/jsfa.2740060814

Chand, S., Anwar, M., and Patra, D. D. (2006). Influence of long-term application of organic and inorganic fertilizer to build up soil fertility and nutrient uptake in mint-mustard cropping sequence. *Commun. Soil Sci. Plant Anal.* 37, 63–76. doi: 10.1080/00103620500408704

Chen, J.-H., Wu, J.-T., and Huang, W.-T. (2001). *Effects of compost on the availability of nitrogen and phosphorus in strongly acidic soils* Vol. 155 (Taipei, Taiwan: Food and Fertilizer Technology Center), 1–10.

Choi, S.-H. (2007). Treatment and management of the livestock manure. *KCID J.* 14, 110–120.

Cort, W. M., Vicente, T. S., Waysek, E. H., and Williams, B. D. (1983). Vitamin e content of feedstuffs determined by high-performance liquid chromatographic fluorescence. *J. Agric. Food Chem.* 31, 1330–1333. doi: 10.1021/jf00120a045

Cravotta, C. A. (1995). *Use of stable isotopes of carbon, nitrogen, and sulfur to identify sources of nitrogen in surface waters in the lower Susquehanna river basin. open-file report* Vol. 2497 (Reston, Virginia: United States Geological Survey), 94–510. doi: 10.3133/ofr94510

Darrah, L., Mcmullen, M., and Zuber, M. (2019). *Breeding, genetics and seed corn production* (Washington, DC: AACC International Press), 19–41. Corn. doi: 10.1016/B978-0-12-811971-6.00002-4

Duvick, D. N. (2005). The contribution of breeding to yield advances in maize (Zea mays l.). *Adv. Agron.* 86, 83–145. doi: 10.1016/S0065-2113(05)86002-X

Ezeokoli, O. T., Bezuidenhout, C. C., Maboeta, M. S., Khasa, D. P., and Adeleke, R. A. (2020). Structural and functional differentiation of bacterial communities in post-coal mining reclamation soils of south Africa: bioindicators of soil ecosystem restoration. *Sci. Rep.* 10, 1759. doi: 10.1038/s41598-020-58576-5

Falagán, C., and Johnson, D. B. (2014). Acidibacter ferrireducens gen. nov., sp. nov.: an acidophilic ferric iron-reducing gammaproteobacterium. *Extremophiles* 18, 1067–1073. doi: 10.1007/s00792-014-0684-3

Fierer, N. (2017). Embracing the unknown: disentangling the complexities of the soil microbiome. *Nat. Rev. Microbiol.* 15, 579–590. doi: 10.1038/nrmicro.2017.87

Foster, Z. S., Chamberlain, S., and Grünwald, N. J. (2018). Taxa: an r package implementing data standards and methods for taxonomic data. *F1000 Res.* 7, 272. doi: 10.5281/zenodo.1183667

Geng, Y., Cao, G., Wang, L., and Wang, S. (2019). Effects of equal chemical fertilizer substitutions with organic manure on yield, dry matter, and nitrogen uptake of spring maize and soil nitrogen distribution. *PloS One* 14, e0219512. doi: 10.1371/journal.pone.0219512

Guo, H., Nasir, M., Lv, J., Dai, Y., and Gao, J. (2017). Understanding the variation of microbial community in heavy metals contaminated soil using high throughput sequencing. *Ecotoxicol. Environ. Saf.* 144, 300–306. doi: 10.1016/j.ecoenv.2017.06.048

Han, S. H., An, J. Y., Hwang, J., Kim, S. B., and Park, B. B. (2016). The effects of organic manure and chemical fertilizer on the growth and nutrient concentrations of yellow poplar (Liriodendron tulipifera lin.) in a nursery system. *For. Sci. Technol.* 12, 137–143. doi: 10.1080/21580103.2015.1135827

Henneberg, W., and Stohmann, F. (1859). Uber das erhaltungsfutter volljahrigen rindviehs. *J. Landwirtsch.* 3, 485–551.

Ji, R., Dong, G., Shi, W., and Min, J. (2017). Effects of liquid organic fertilizers on plant growth and rhizosphere soil characteristics of chrysanthemum. *Sustainability* 9, 841. doi: 10.3390/su9050841

Jimenez-Castaneda, M. E., Scarinci, C., Burke, A., Boothman, C., Vaughan, D. J., Lloyd, J. R., et al. (2020). Generation of alkalinity by stimulation of microbial iron reduction in acid rock drainage systems: impact of natural organic matter types. *Water Air Soil pollut.* 231, 1–13. doi: 10.1007/s11270-020-04820-7

Jo, N. Y., Lee, J. K., Byeon, J. E., Park, H. J., Ryoo, J. W., and Hwang, S. G. (2022). Elevated CO2 concentration induces changes in plant growth, transcriptome, and antioxidant activity in fennel (Foeniculum vulgare mill.). *Front. Plant Sci.* 13. doi: 10.3389/fpls.2022.1067713

Kim, Y. C., Glick, B. R., Bashan, Y., and Ryu, C. M. (2012). ""Enhancement of plant drought tolerance by microbes,"," in *Plant responses to drought stress: From morphological to molecular features*. Ed. R. Aroca (Berlin, Heidelberg: Springer Berlin Heidelberg), 383–413. doi: 10.1007/978-3-642-32653-0_15

Lancaster, J. (1980). *Mississippi Soil test method and interpretation* (Beaumont, MS: Agricultural Experiment Station). Mimeograph.

Lee, B. D., Kim, D. J., and Leet, S. J. (2001). Nutritive and economic values of high oil corn in layer diet. *Poult. Sci.* 80, 1527–1534. doi: 10.1093/ps/80.11.1527

Liu, K. (2019). Effects of sample size, dry ashing temperature and duration on determination of ash content in algae and other biomass. *Algal Res.* 40, 101486. doi: 10.1016/j.algal.2019.101486

Love, M. I., Huber, W., and Anders, S. (2014). Moderated estimation of fold change and dispersion for RNA-seq data with DESeq2. *Genome Biol.* 15, 550. doi: 10.1186/s13059-014-0550-8

Loy, D., and Lundy, E. (2019). *Nutritional properties and feeding value of corn and its coproducts* (Washington, DC: AACC International Press), 633–659. doi: 10.1016/B978-0-12-811971-6.00023-1

Lu, Y., Gao, Y., Nie, J., Liao, Y., and Zhu, Q. (2021). Substituting chemical p fertilizer with organic manure: effects on double-rice yield, phosphorus use efficiency and balance in subtropical China. *Sci. Rep.* 11, 8629. doi: 10.1038/s41598-021-87851-2

Lynch, S. M., Gaziano, J. M., and Frei, B. (1996). Ascorbic acid and atherosclerotic cardiovascular disease. subcell. *Biochem* 25, 331–367. doi: 10.1007/978-1-4613-0325-1_17

Makinde, E., Ayeni, L., Ojeniyi, S., and Odedina, J. (2010). Effect of organic, organomineral and NPK fertilizer on nutritional quality of amaranthus in Lagos, Nigeria. *Researcher* 2, 91–96.

Martin, M. (2011). Cutadapt removes adapter sequences from high-throughput sequencing reads. *EMBnet J.* 17, 10–12. doi: 10.14806/ej.17.1.200

Mcmurdie, P. J., and Holmes, S. (2013). Phyloseq: an r package for reproducible interactive analysis and graphics of microbiome census data. *PloS One* 8, e61217. doi: 10.1371/journal.pone.0061217

Mumtaz, M., Ahmad, M., Jamil, M., and Hussain, T. (2017). Zinc solubilizing bacillus spp. potential candidates for biofortification in maize. *Microbiol. Res.* 202, 51–60. doi: 10.1016/j.micres.2017.06.001

Naik, K., Mishra, S., Srichandan, H., Singh, P. K., and Sarangi, P. K. (2019). Plant growth promoting microbes: Potential link to sustainable agriculture and environment. *Biocatalysis Agric. Biotechnol.* 21, 101326. doi: 10.1016/j.bcab.2019.101326

Nie, J., Zhou, J. M., Wang, H. Y., Chen, X. Q., and Du, C. W. (2007). Effect of long-term rice straw return on soil glomalin, carbon and nitrogen. *Pedosphere* 17, 295–302. doi: 10.1016/S1002-0160(07)60036-8

Olle, M., and Williams, I. H. (2014). The effect of organic fertilizers on the chemical quality of onions. acta hortic. *Int. Conf. Agric. Eng.: New Technol. Sustain. Agric. Production Food Security* 1054), 319–324. doi: 10.17660/ActaHortic.2014.1054.38

Padmore, J. (1990). "Fat (crude) or ether extract in animal feed. AOAC Official Method 920.39," in *Official methods of analysis of association of official analytical chemists, 15th ed* (Arlington, VA: Oxford University Press).

Panke-Buisse, K., Poole, A. C., Goodrich, J. K., Ley, R. E., and Kao-Kniffin, J. (2015). Selection on soil microbiomes reveals reproducible impacts on plant function. *ISME J.* 9, 980–989. doi: 10.1038/ismej.2014.196

Paradis, E., Claude, J., and Strimmer, K. (2004). APE: analyses of phylogenetics and evolution in r language. *Bioinformatics* 20, 289–290. doi: 10.1093/bioinformatics/btg412

Raimundo, E. K. M., Zacharias, M. B., Borges, M. T. M. R., Da Silva, J. D. T., and Forti, V. A. (2022). The potential of organic fertilizer application on the production and bromatological composition of millet (Cenchrus americanu). *Research Square*. doi: doi: 10.21203/rs.3.rs-1486898/v1

Savci, S. (2012). An agricultural pollutant: chemical fertilizer. *Int. J. Environ. Sci. Dev.* 3, 73–80. doi: 10.7763/IJESD.2012.V3.191

Schollenberger, C. J. (1927). A rapid approximate method for determining soil organic matter. *Soil Sci.* 24, 65–68. doi: 10.1097/00010694-192707000-00008

Shiferaw, B., Prasanna, B. M., Hellin, J., and Bänziger, M. (2011). Crops that feed the world 6. past successes and future challenges to the role played by maize in global food security. *Food Sec.* 3, 307–327. doi: 10.1007/s12571-011-0140-5

Simpson, R. J., Oberson, A., Culvenor, R. A., Ryan, M. H., Veneklaas, E. J., Lambers, H., et al. (2011). Strategies and agronomic interventions to improve the phosphorus-use efficiency of farming systems. *Plant Soil.* 349, 89–120. doi: 10.1007/s11104-011-0880-1

Suman, J., Rakshit, A., Ogireddy, S. D., Singh, S., Gupta, C., and Chandrakala, J. (2022). Microbiome as a key player in sustainable agriculture and human health. *Front. Soil Sci.* 2. doi: 10.3389/fsoil.2022.821589

Thomas, G. W. (1982). “Exchangeable cations, in methods soil anal,” in *Agronomy*, vol. 9 . Ed. A. L. Page (Madison, WI: Madison Book Company), 154–157.

Tilman, D., Balzer, C., Hill, J., and Befort, B. L. (2011). Global food demand and the sustainable intensification of agriculture. *Proc. Natl. Acad. Sci. U. S. A.* 108, 20260–20264. doi: 10.1073/pnas.1116437108

Tortosa, G., Castellano-Hinojosa, A., Correa-Galeote, D., and Bedmar, E. J. (2017). Evolution of bacterial diversity during two-phase olive mill waste (“alperujo”) composting by 16S rRNA gene pyrosequencing. *Bioresour. Technol.* 224, 101–111. doi: 10.1016/j.biortech.2016.11.098

Wang, H., Xu, J., Liu, X., Zhang, D., Li, L., Li, W., et al. (2019). Effects of long-term application of organic fertilizer on improving organic matter content and retarding acidity in red soil from China. *Soil Till. Res.* 195, 104382. doi: 10.1016/j.still.2019.104382

Watson, S. (1962). *The yellow carotenoid pigments of corn. 17th hybrid corn industry res conf* (Chicago, IL: American Seed Trade Association), 92–100.

Wei, Z., Gu, Y., Friman, V. P., Kowalchuk, G. A., Xu, Y., Shen, Q., et al. (2019). Initial soil microbiome composition and functioning predetermine future plant health. *Sci. Adv.* 5, eaaw0759. doi: 10.1126/sciadv.aaw0759

Wickham, H., and Chang, W. (2016). Package ‘ggplot2’: create elegant data visualisations using the grammar of graphics description. *CRAN Repos.* 2, 1–189.

Wickham, H., Fran Ois, R., Henry, L., and Miller, K. (2015). *Dplyr: A grammar of data manipulation. r package version 0.4*, Vol. 3. p156.

Ye, L., Zhao, X., Bao, E., Li, J., Zou, Z., and Cao, K. (2020). Bio-organic fertilizer with reduced rates of chemical fertilization improves soil fertility and enhances tomato yield and quality. *Sci. Rep.* 10, 177. doi: 10.1038/s41598-019-56954-2

Yoon, J., Jang, J. H., and Kasai, H. (2014). Algisphaera agarilytica gen. nov., sp. nov., a novel representative of the class phycisphaerae within the phylum planctomycetes isolated from a marine alga. *Antonie Leeuwenhoek.* 105, 317–324. doi: 10.1007/s10482-013-0076-1

Yoon, J. H., Kang, S. J., Lee, S. Y., Lee, J. S., and Park, S. (2011). Ohtaekwangia koreensis gen. nov., sp. nov. and ohtaekwangia kribbensis sp. nov., isolated from marine sand, deep-branching members of the phylum bacteroidetes. *Int. J. Syst. Evol. Microbiol.* 61, 1066–1072. doi: 10.1099/ijs.0.025874-0

Zhang, Z., Yan, J., Han, X., Zou, W., Chen, X., Lu, X., et al. (2021). Labile organic carbon fractions drive soil microbial communities after long-term fertilization. *Glob. Ecol. Conserv.* 32, e01867. doi: 10.1016/j.gecco.2021.e01867

Zhang, H., Zhang, L., Xue, X., Zhang, X., Wang, H., Gao, T., et al. (2022). Effect of feeding a diet comprised of various corn silages inclusion with peanut vine or wheat straw on performance, digestion, serum parameters and meat nutrients in finishing beef cattle. *Anim. Biosci.* 35, 29–38. doi: 10.5713/ab.21.0088

frontiers | Frontiers in Plant Science

TYPE Original Research
PUBLISHED 14 April 2023
DOI 10.3389/fpls.2023.1162572

OPEN ACCESS

EDITED BY
Amanullah,
University of Agriculture, Peshawar, Pakistan

REVIEWED BY
Roxana Vidican,
University of Agricultural Sciences and Veterinary Medicine of Cluj-Napoca, Romania
Sanjay Singh Rathore,
Indian Agricultural Research Institute (ICAR), India

*CORRESPONDENCE
Waqar Islam
Ddoapsial@yahoo.com
Zhihao Zhang
zhangzh@ms.xjb.ac.cn
Fanjiang Zeng
zengfj@ms.xjb.ac.cn

†These authors have contributed equally to this work

SPECIALTY SECTION
This article was submitted to Plant Nutrition, a section of the journal Frontiers in Plant Science

RECEIVED 09 February 2023
ACCEPTED 23 March 2023
PUBLISHED 14 April 2023

CITATION
Du Y, Zhang Y, Chai X, Li X, Ullah A, Islam W, Zhang Z and Zeng F (2023) Effects of different tillage systems and mowing time on nutrient accumulation and forage nutritive value of *Cyperus esculentus*. *Front. Plant Sci.* 14:1162572.
doi: 10.3389/fpls.2023.1162572

Effects of different tillage systems and mowing time on nutrient accumulation and forage nutritive value of *Cyperus esculentus*

Yi Du[1,2,3,4†], Yulin Zhang[1,2,3,5†], Xutian Chai[1,2,3,4], Xiangyi Li[1,2,3], Abd Ullah[1,2,3,4], Waqar Islam[1,2,3*], Zhihao Zhang[1,2,3*] and Fanjiang Zeng[1,2,3,4,5*]

[1]State Key Laboratory of Desert and Oasis Ecology, Xinjiang Institute of Ecology and Geography, Chinese Academy of Sciences, Urumqi, China, [2]Xinjiang Key Laboratory of Desert Plant Roots Ecology and Vegetation Restoration, Xinjiang Institute of Ecology and Geography, Chinese Academy of Sciences, Urumqi, China, [3]Cele National Station of Observation and Research for Desert-Grassland Ecosystems, Cele, China, [4]University of Chinese Academy of Sciences, Beijing, China, [5]College of Ecology and Environmental, Xinjiang University, Urumqi, China

Revealing the complex relationships between management practices, crop growth, forage nutritive value and soil quality will facilitate the development of more sustainable agricultural and livestock production systems. *Cyperus esculentus* is known as the king of oil crops and high-quality forage. However, there is little information about the effects of different planting modes {continuous cropping (CC)/rotation cropping (RC)} and initial mowing time on the plant nutrient accumulation and forage nutritive value. Here, in a field experiment, we designed two planting patterns, *C. esculentus* CC and *C. esculentus* - wheat RC. The leaves, tubers, roots, and soil samples were collected at three mowing time (on the 78th, 101th, and 124th days after seed sowing). Results revealed that RC significantly increased the total nitrogen (TN) and potassium (TK) content of the tuber (p<0.05), while significantly decreased the TN, total phosphorus (TP), crude protein (CP), and acid detergent fiber (ADF) contents of the leaves. Under the CC pattern, the TN, TP, and TK content of roots increased significantly on the 78th days after seed sowing, and the TK content of tubers increased significantly. Under the RC pattern, the ether extract (EE) content of tubers increased significantly on the 124th days after seed sowing, while the CP and TN content of leaves decreased significantly. Correlation analysis showed that soil pH was negatively correlated with TN content in leaves, tubers, and roots. The structural equation model showed that the soil pH directly affected the plant nutrient accumulation and forage nutritive value (β=0.68) *via* regulating these properties by changing soil available nutrients, anions, cations, and total nutrients. Overall, we propose that RC for *C. esculentus*-wheat is should not be recommended to maximize tubers and forage yield.

KEYWORDS

continuous/rotation cropping, mowing time, relative abundance, nutrient content, structural equation model

1 Introduction

Continuous cropping (CC) is the practice of growing the same crop on the same land for several years. This practice usually leads to the loss of soil nutrients and aggravation of pests and diseases, ultimately causing the decline in crop yield and quality (Xiong et al., 2015; Delang, 2018). In contrast, rotation cropping (RC), the scientific and orderly planting of different crops in the same field can improve the water use efficiency of crops (Zhou et al., 2011; Li et al., 2014; Peterson et al., 2020), balance soil nutrients, enhance soil functions, and increase crop yield (Larkin, 2003; Zhou et al., 2011; Moulin et al., 2015). However, the advantages of crop rotation are influenced by crop type, soil moisture and nutrient availability (Giacometti et al., 2021). For example, compared with non-leguminous crops, rotation with leguminous crops can effectively improve soil nitrogen (N) availability and system productivity (Ilyas et al., 2022). However, since different crops have different soil requirements (e.g. nutrient requirements), long-term rotation can accelerate soil nutrient loss and can intensify nutrient competition between crops and microorganisms, which adversely affects the yield of the two crops in rotation (Brankatschk and Finkbeiner, 2015). Therefore, accurate assessment of the response of specific crops to CC and RC is crucial for farmers to choose suitable cropping strategies in terms of soil fertility and nutrients of different organs.

Crude protein (CP), ether extract (EE), acid detergent fiber (ADF), and neutral detergent fiber (NDF) are important indexes for evaluating forage nutritive value (Richman et al., 2015). Some studies have shown that the soluble sugar (SS) content in the rotation was significantly higher than in CC (Yang et al., 2010; Hou et al., 2013). Meanwhile, the research found that the RC significantly increased the contents of CP and EE, reduced the content of SS, and improved the quality of tubers (Ma and Han, 2000; Wang et al., 2017). Mowing is a common practice to increase forage efficiency and yield for livestock (Zhao et al., 2021). The effects of initial mowing time on grassland productivity have been extensively studied under different climatic and soil conditions (Donaghy et al., 2008; Binnie et al., 2010). For example, medium initial mowing (15 July to 15 August) increased total dry matter yield and nutritional value of *Leymus chinensis* (Trin.) Tzvel. in Songnen grassland, China (Zhao et al., 2021). On the contrary, the early (April) and late (May) mowing reduced the total yield of the forage sugarcane in the Amami Region of Kagoshima Prefecture, Japan (Sakaigaichi et al., 2010). These inconsistencies in forage yield and forage nutritive value were mainly due to the interaction of initial mowing time, grass species and geographical location.

Animal husbandry is a mainstay of economic development in arid and semi-arid regions, however it is suffering from inadequate forage production and supply due to water constraints (Blum, 2009; Jia et al., 2022). Therefore, it is of great significance to select crops that are more suitable for both forage yield, grain and oil supply under water shortage conditions to improve livestock production and may alleviate food crisis in arid and semi-arid areas. Meanwhile, the *Cyperus esculentus* is a grass like plant widely distributed in many northern temperate regions and is gaining popularity in China, India, Egypt and the United States as an energy crop (Arafat et al., 2009; Bamishaiye et al., 2010; De Castro et al., 2015; Ayeni, 2022). Its aboveground parts (leaves) are used as forage, and its belowground parts are edible tubers with sweet taste with high levels of protein, fatty acids and starch, that make it a potential alternative to wheat and soybeans in many countries (Sánchez-Zapata et al., 2012; Ahmed and Hussein, 2014; Codina-Torrella et al., 2015; Ayeni, 2022). However, to our best knowledge, there is a little information on the nutritive value of the above- and under-ground parts of *C. esculentus* in respond to different planting modes (CC vs RC) and initial mowing time, even though it has been cultivated for many years in the desert oasis transition zone (Tan et al., 2022; Zhang et al., 2022).

Therefore, to research the understanding of response mechanisms to planting modes in *C. esculentus* is timely. Herein, we designed a field study containing two dependent treatments, two planting modes (CC vs RC) and three initial mowing time (on the 78th, 101th, and 124th days after seed sowing). Total nitrogen (TN), total phosphorus (TP), and total potassium (TK) contents in leaves, tubers, and roots were used to evaluate the nutrients of *C. esculentus*, CP, EE, and NDF contents in leaves, and EE, CP, and ADF in tubers were determined to characterize the above- and belowground nutritive value of *C. esculentus*, respectively. Our objectives were to (i) elucidate the influences of planting modes and initial mowing time on nutrient content and forage nutritive value of *C. esculentus*, and (ii) identify the factors affecting the nutrient content and forage nutritive value of *C. esculentus*. These attempts will provide a reference for the management of *C. esculentus* in the desert oasis transition zone.

2 Material and methods

2.1 Site description and experiment design

This experiment was carried out at Shache farm in Xinjiang (38.41° N, 77.24° E). The region has a warm temperate continental climate. The mean annual temperature, precipitation, and evaporation are 11.6°C, 53.3 mm, and 2246 mm, respectively. The frost-free period is 225 days and average temperature is above 10°C for the whole year (Arzigul and Xianmixinuer, 2017).

Our experiment was established on May 2018. The background of soil physicochemical properties in both CC and RC plots was similar, pH 8.87, soil organic matter (SOM) 2.527 g·kg^{-1}, TN 0.093 g·kg^{-1}, TP 0.325 g·kg^{-1}, TK 16.133 g·kg^{-1}, available nitrogen (AN) 18.677 mg·kg^{-1}, the available phosphorus (AP) 4.260 mg·kg^{-1}, the available potassium (AK) 50.867 mg·kg^{-1}. After wheat harvest in May, the seeds of "fengchan No. 2", a variety of *C. esculentus*, were sown simultaneously in the CC and RC treatments at the end of May by using a drop planter using 75 kg (seed)·hm^{-2} with the density of 20 × 35 cm (plant spacing × row spacing). The planting density was 142,860 plants·hm^{-2}. The N, P, K fertilizer were dissolved in water and dripped to the root during the whole growth period every year. In each year, the first time of drip irrigation was carried out on the 30th day after the emergence of seedlings, and then six times at 15-day intervals. Before the final harvest (end of September) every year, the dosage of water and fertilizer was 6500 $m^3 \cdot hm^{-2}$ water, 335 $kg \cdot hm^{-2}$ N-fertilizer (urea, 46% N), 218 $kg \cdot hm^{-2}$ P-fertilizer (monoammonium phosphate, 10% N; 50% P_2O_5), and 68 $kg \cdot hm^{-2}$ K- fertilizer (potassium sulphate, 50% K_2O).

Our sampling work was conducted on the 78th day after seed sowing. In each planting mode, three 10 × 5 m plots, 5 m apart, were set at each mowing time (on the 78th, 101th, and 124th days after seed sowing). In each plots, three 50 × 50 cm quadrats along the diagonal were set to collect plant (leaves, roots, and tubers) samples. Five topsoil (0~30 cm) samples along the diagonal in each plots were collected and mixed to prepare one sample to determine the soil physicochemical properties.

2.2 Measurement of plant nutrient content

The leaves, tubers, and roots were washed with running water and dried in an oven (65°C) until the constant weight was used to obtain biomass. These dry matters were powdered in a vibratory disc mill (RS200, Retsch GmbH Inc., Haan, Germany). To subsequent determination of nutrient content and quality of different organs after passing through a 0.42 mm sieve. The TN was measured using an elemental analyzer (2400 II CHN elemental analyzer; Perkin-Elmer, USA), TP was determined using the molybdenum-antimony anti-spectrophotometric method, and TK was determined by flame photometry (Bao, 2000). The EE was extracted by the Soxhlet extractor method, 2~5 g sample was weighed, adding anhydrous ether or petroleum ether was to 2/3 of the bottle content volume, heated in a water bath, so that ether or petroleum ether was continuously refluxed and extracted for 6~12 h. The CP content was determined by the Kjeldahl nitrogen determination method, 2~5g samples were weighed, and 0.5 g copper sulfate and 10 mL sulfuric acid were added. The content of ADF and NDF was determined by Fan's detergent fiber analysis method (Li, 2000). 2g samples were accurately weighed and divided into two parts, one of which was added with 100 mL neutral detergent. Another 1 g sample was added with 100 mL acid detergent. Boil in 5~10 min, and keep boiling for 60 min. After boiling, remove the straight beaker, pour the solution in the beaker into the known weight glass heap installed on the filter bottle for filtration, remove all the residue in the beaker, and rinse the glass heap and residue with boiling water until the filtrate is neutral. Rinse twice with 20 mL acetone, and suction filtration. The glass pile was placed in a 105°C oven for 2 h and then cooled in a dryer for 30 min.

2.3 Measurement of soil physicochemical properties

Soil samples were air-dried after the removal of roots. TN, TP, TK, AN, AP, AK, and pH were determined after passing through a 2 mm sieve. The value of pH was evaluated by a PHS-3C digital pH meter in a 1:5 soil-water ratio suspension (IQ 150, IQ Scientific Instruments, CA, USA). The TN content was determined by using the $CuSO_4$–Se powder diffusion method (Hooper and Vitousek, 1998). The Mo-Sb and Van-Mo-yellow colorimetry methods were applied to detect TP content (Lu et al., 2015). The TK content was determined by using molybdenum-antimony colorimetry (Lu et al., 2015). Additionally, soil available N was tested using 2-M KCl extracts by AA3-automated flow injection analysis (Bran + Luebbe GmbH, Norderstedt, Germany); available P was extracted using 0.5 M $NaHCO_3$, and available K was measured by the NH4OAc method (Neff et al., 2005; Warra et al., 2015). Soil organic matter (SOM) was determined by the wetoxidation technique. Total salt (TS) content and salt ion content were extracted with soil extract (soil and water ratio 5:1). The TS content was determined by using the conductivity method. The HCO^{3-}, Cl^-, SO_4^{2-}, Ca^{2+}, Mg^{2+}, K^+, and Na^+ contents were measured according to the mothed of Bao (2000) and Lu (1999). Ca^{2+}, Mg^{2+}, K^+, and Na^+ were determined by plasma spectrometer with the test solution prepared by three acid mixture (1 mL 60% $HClO_4$, 6 mL HNO_3) digestion method (IRIS-ICP, TJA Ltd, USA). HCO^{3-}, Cl^-, and SO_4^{2-} were determined by chemical titration.

2.4 Statistical analyses

All statistical analyses were conducted in the R v4.1.0 (R Core Team, 2018). Most of the results were visualized using the 'ggplot2 package'. Two-way ANOVA was used to analyze the independent and interaction effects of CC/RC and mowing time on soil properties and nutrient content and forage nutritive value of *C. esculentus*. Duncan's method was used for multiple comparisons (α=0.05), and the significance level was 0.05, expressed as mean ± standard error (SE, n = 3). T-test was used to analyze and compare the differences between different tillage patterns (CC and RC) at the same mowing time. Correlation analysis of soil properties, nutrient content, and forage nutritive value was computed and visualized by using the 'psych package' and 'corrplot package'. The causal relationships between soil properties, nutrient content and forage nutritive value of *C. esculentus* were explored by the structural equation model using Amos-24 software.

3 Results

3.1 Soil physicochemical properties

The pH value, SOM, TK, and AP contents in soil were independently influenced by both planting pattern (CC/RC) and mowing time, while the AN and AK contents were independently influenced by mowing time and planting pattern, respectively (p<0.05, Table 1). The interaction of these factors significantly changed TK content (p<0.05). However, soil TN and TP contents were not significantly affected by planting mode and mowing time (p>0.05). The RC mode significantly increased soil pH, while significantly reduced SOM, TK, AP, and AK contents (p<0.05, Table 2). With the postponement of mowing time, soil pH gradually increased, while SOM and AP gradually decreased. The AN content showed a significant decline at the end of mowing time (Table 2). Except for Cl^- and SO2-4 that reduced in RC mode

TABLE 1 Two-way ANOVA analysis of effects of the planting mode and mowing time on soil physicochemical properties.

Factor	pH	SOM ($g\cdot kg^{-1}$)	TN ($g\cdot kg^{-1}$)	TP ($g\cdot kg^{-1}$)	TK ($g\cdot kg^{-1}$)	AN ($mg\cdot g^{-1}$)	AP ($mg\cdot g^{-1}$)	AK ($mg\cdot g^{-1}$)
planting mode (CC/RC)	6.09*	5.13*	2.74	0.45	13.79**	0.05	5.83*	10.81**
Mowing time (M)	4.86*	4.04*	0.93	3.50	68.61***	4.62*	4.20*	0.33
CC/RC×M	0.84	1.51	2.71	1.06	5.70*	0.98	0.77	0.16

Here: CC, continuous cropping; RC, rotation cropping. M, Mowing time (T1, on the 78th day after seed sowing; T2, on the 101th day after seed sowing; T3, on the 124th day after seed sowing). SOM, soil organic matter; TN, total nitrogen; TP, total phosphorus; TK, total potassium; AN, available nitrogen; AP, the available phosphorus; AK, the available potassium. Values indicate results of F value *p < 0.05; **p < 0.01; ***p < 0.001. The same as below.

(Table 3), the other parameters of soil salinity did not respond significantly to planting pattern and mowing time (Table 4).

3.2 The nutrient content and allocation of the leaves, tubers, and roots

Planting mode and mowing time independently and interactively impacted the TN and TP contents in leaves and tubers, that is, the response of these two elements in the specific organ to mowing times varied from CC and RC systems (p<0.05, Table 5). For example, RC significantly decreased foliar N and P content, while these two elements in tubers were improve in CC systems (p<0.05, Figure 1). No interaction between planting mode and mowing time on nutrient was observed in roots (Table 5; Figure 1).

3.3 The forage nutritive value of the leaves, tubers, and roots

Planting mode interacted with mowing time significantly altered the foliar CP and NDF contents and the CP contents in tubers (p<0.05, Table 6). Foliar ADF content was significantly influenced by planting modes. Planting modes and mowing time independently affected EE content in tubers, while they did not exert significant effects on foliar EE content (p>0.05). Compared with CC system, RC had a significantly adverse effect on the accumulation of CP and ADF in leaves, and CP in tubers (Figures 2A, B, E). On the 124th day after seed sowing, more ADF and NDF accumulated in leaves, while the CP contents in leaves and tubers showed a lower level than those at other periods (Figure 2).

3.4 The relationships between the nutrient content and forage nutritive value of leaves, tubers, roots, and soil factors

The Pearson's correlation analysis showed that foliar forage nutritive value (i.e., CP, EE, ADF, and NDF) had a significant correlation with some soil factors, such as SOM, AN, AP, AK, and Ca^{2+} (p<0.05, Figure 3). The EE content of tubers was negatively influenced by AN, while positively affected by TK (p<0.05). Compared with other elements, plant TP was slightly affected by soil factors, only having a significant positive correlation with TN in the tuber and a significant negative correlation with AK in the root (p<0.05).

The structural equation model revealed an important role of soil pH in regulating the accumulation of nutrients and forage nutritive value of the leaves and tubers. Soil pH, base ions, cations, and available and total nutrients exhibited 26% of the variation in nutrient and nutritive value of the leaves and tubers (X^2 = 2.403,

TABLE 2 Soil physical and nutrient content.

Planting mode	Mowing time	pH	SOM ($g\cdot kg^{-1}$)	TN ($g\cdot kg^{-1}$)	TP ($g\cdot kg^{-1}$)	TK ($g\cdot kg^{-1}$)	AN ($mg\cdot g^{-1}$)	AP ($mg\cdot g^{-1}$)	AK ($mg\cdot g^{-1}$)
CC	T1	8.56 ± 0.09 a	2.24 ± 0.14 a	0.10 ± 0.11 a	0.35 ± 0.006 a	15.93 ± 0.15 b	61.07 ± 24.86 a	9.72 ± 0.81 a	94.70 ± 23.05 a
	T2	8.83 ± 0.04 a	1.84 ± 0.15 a	0.08 ± 0.01a	0.29 ± 0.008 a	15.20 ± 0.10 c	51.90 ± 14.37 a	5.65 ± 2.58 a	94.43 ± 3.66 a
	T3	8.83 ± 0.09 a	1.85 ± 0.04 a	0.08 ± 0.002 a	0.33 ± 0.04 a	16.43 ± 0.09 a	18.53 ± 7.60 a	5.04 ± 0.96 a	89.40 ± 6.79 a
RC	T1	8.81 ± 0.11 a	1.86 ± 0.04 a	0.07 ± 0.004 a	0.36 ± 0.01 a	15.37 ± 0.29 b	45.17 ± 12.64 ab	5.54 ± 0.59 a	65.03 ± 5.45 a
	T2	8.88 ± 0.02 a	1.71 ± 0.09 a	0.07 ± 0.006 a	0.33 ± 0.02 a	14.33 ± 0.07 c	82.57 ± 27.83a	4.01 ± 0.23 ab	60.33 ± 1.92 a
	T3	8.98 ± 0.06 a	1.81 ± 0.09 a	0.09 ± 0.01 a	0.31 ± 0.01 a	16.53 ± 0.03 a	13.23 ± 3.51 b	3.59 ± 0.68 b	67.10 ± 7.81 a

Here: CC, continuous cropping; RC, rotation cropping. M, Mowing time (T1, on the 78th day after seed sowing; T2, on the 101th day after seed sowing; T3, on the 124th day after seed sowing). Different lowercase letters (a, b, and c) indicate that the same farming mode and different mowing time have significant differences (Duncan's test, p<0.05). The same as below.

TABLE 3 saltiness of soil.

Planting mode	Mowing time	Cl^- ($mg \cdot g^{-1}$)	SO_4^{2-} ($mg \cdot g^{-1}$)	Ca^{2+} ($mg \cdot g^{-1}$)	K^+ ($mg \cdot g^{-1}$)	Mg^{2+} ($mg \cdot g^{-1}$)	Na^+ ($mg \cdot g^{-1}$)	HCO_3^- ($mg \cdot g^{-1}$)	TS ($g \cdot kg^{-1}$)
	T1	0.08 ± 0.02 a	0.33 ± 0.07 a	0.64 ± 0.41 a	0.12 ± 0.10 a	0.11 ± 0.07 a	0.14 ± 0.08 a	0.09 ± 0.01 a	1.94 ± 0.80 a
CC	T2	0.08 ± 0.03 a	0.23 ± 0.03 a	0.12 ± 0.01 a	0.03 ± 0.001 a	0.02 ± 0.003 a	0.07 ± 0.02 a	0.10 ± 0.002 a	0.76 ± 0.14 a
	T3	0.11 ± 0.04 a	0.39 ± 0.14 a	0.20 ± 0.05 a	0.03 ± 0.005 a	0.04 ± 0.01 a	0.10 ± 0.03 a	0.09 ± 0.008 a	1.11 ± 0.33 a
	T1	0.04 ± 0.01 a	0.16 ± 0.04 a	0.46 ± 0.27a	0.16 ± 0.14 a	0.08 ± 0.07 a	0.36 ± 0.32 a	0.09 ± 0.01 a	1.71 ± 1.00 a
RC	T2	0.03 ± 0.01 a	0.13 ± 0.01 a	0.11 ± 0.01 a	0.01 ± 0.0005 a	0.02 ± 0.001 a	0.05 ± 0.005a	0.10 ± 0.003 a	0.52 ± 0.06 a
	T3	0.06 ± 0.02 a	0.22 ± 0.07 a	0.13 ± 0.03 a	0.02 ± 0.003 a	0.02 ± 0.003 a	0.06 ± 0.02 a	0.09 ± 0.003 a	1.00 ± 0.07 a

Here: CC, continuous cropping; RC, rotation cropping. M, Mowing time (T1, on the 78th day after seed sowing; T2, on the 101th day after seed sowing; T3, on the 124th day after seed sowing).

p=0.301, Figure 4). Among them, the nutrient and nutritive value of leaves and tubers were dominantly and directly affected by soil pH, with a standardized direct effect of 0.68 (Figure 4). Additionally, soil pH indirectly affected the nutrients and nutritive value of the leaves and tubers by changing the available nutrients, anions, cations, and total nutrients in soil.

4 Discussion

In this study, the nutrient and nutritional value of leaves and tubers, as well as the nutrient content of soil were determined and analyzed by selecting different planting patterns (RC and CC) and setting three mowing time. Finally, it was found that RC was not conducive to the growth and development of *C. esculentus*. On the 124th day after seed sowing, the EE content of tubers was increased, which indirectly increased its oil yield.

4.1 The effects of RC on plant nutrient accumulation and forage nutritive value

Crop rotation in present study exerted a negative effect of on foliar nutrient (e.g., TN, and TP) accumulation and forage nutritive value of *C. esculentus* (Figure 1A, B), inconsistent with the promoting effect of rotation found by previous studies (Sun et al., 2018; Ding et al., 2019; Lenssen et al., 2020). Two possible factors explain this inconsistency. On the one hand, the root distribution of *C. esculentus* and wheat highly overlapped in topsoil (~30 cm depth), which intensifies competition for soil nutrients (e.g., SOM, TK, AP, and AK contents, Table 2), although these two crops did not exist at the same time (Duan et al., 2019). On the other hand, the root exudates of the two species are inconsistent, and the microbial communities absorbed and enriched are also different, resulting in changes in soil physical and chemical properties and soil structure (Li et al., 2014). Therefore, it affects the seed germination and plant growth of the same or heterogeneous plants, especially for heterogeneous plants (Lendzemo et al., 2009).

N is a key element in the formation of nutrient value of forage. With mowing time, AN in soil decreased continuously, which hindered the formation of CP in leaves and reduced the forage quality (Table 2; Figure 1). First, wheat is an important allelopathic crop and some substances (such as benzoxazinoids and polyphenols) in its root exudates can inhibit the growth of its neighboring heterologous species (Lendzemo et al., 2009; Hussain et al., 2022). The accumulation of these allelopathic substances in the soil may inhibit the growth of *C. esculentus*. Second, during the growth and development of plants, root exudates can not only affect the absorption and transport of nutrient availability in the soil, but also adsorb some heavy metal elements around the root system to affect the crop rotation next year (Sun et al., 2018).

Indeed, *C. esculentus* has been treated as a weed in many countries (Devries, 1991; Werle et al., 2022). Conversely, the rotation showed a positive effect on *C. esculentus* by enhancing

TABLE 4 Two-way ANOVA analysis of effects of the planting mode and mowing time on soil physicochemical properties.

Factor	Cl^- ($mg \cdot g^{-1}$)	SO_4^{2-}($mg \cdot g^{-1}$)	Ca^{2+} ($mg \cdot g^{-1}$)	K^+ ($mg \cdot g^{-1}$)	Mg^{2+} ($mg \cdot g^{-1}$)	Na^+ ($mg \cdot g^{-1}$)	HCO_3^-($mg \cdot g^{-1}$)	TS ($g \cdot kg^{-1}$)
planting mode (CC/RC)	6.16*	6.17*	0.29	0.00	0.29	0.22	0.01	0.21
Mowing time (M)	0.93	1.57	2.78	1.93	2.15	1.21	0.69	2.46
CC/RC×M	0.01	0.17	0.10	0.07	0.03	0.53	0.09	0.11

Here: CC, continuous cropping; RC, rotation cropping. M, Mowing time (T1, on the 78th day after seed sowing; T2, on the 101th day after seed sowing; T3, on the 124th day after seed sowing). TS. Total salt; Values indicate results of F value *$p < 0.05$.

TABLE 5 Two-way ANOVA analysis of effects of the planting mode and mowing time on the physicochemical property of the leaves, tubers, and roots of *C. esculentus*.

Factor	Leaves			Tubers			Roots		
	TN (g•kg^{-1})	TP (g•kg^{-1})	TK (g•kg^{-1})	TN (g•kg^{-1})	TP (g•kg^{-1})	TK (g•kg^{-1})	TN (g•kg^{-1})	TP (g•kg^{-1})	TK (g•kg^{-1})
planting mode (CC/RC)	100.93***	1.75	64.52***	6.91*	6.06*	147.99***	0.79	8.79*	21.49**
Mowing time (M)	68.89***	6.83**	47.18***	54.07***	2.74	166.20***	43.27***	10.33**	188.38***
CC/RC×M	25.22***	0.01	97.49***	10.90**	2.03	31.99***	0.59	3.74	2.64

Here: CC, continuous cropping; RC, rotation cropping. M, Mowing times (T1, on the 78th day after seed sowing; T2, on the 101th day after seed sowing; T3, on the 124th day after seed sowing). Values indicate results of F value.
*p < 0.05; **p < 0.01; ***p < 0.001.

nutrient (e.g., TN and TK) accumulation in tubers (Figure 1D, F). Tubers are a key reproductive organ of *C. esculentus* and its nutrient content determines the initial conditions of germination (Ozcan et al., 2021). Nutrient allocation to reproductive organs is an important stress adaptation strategy to increase the survival of offspring (Coello and Martinez-Barajas, 2016). Based on the above discussion, on the one hand, wheat should be carefully introduced into the rotation system of *C. esculentus*, while leguminous crops (e.g., Alfalfa and soybeans) may be preferred due to better nitrogen fixation and soil improvement ability. On the other hand, the application of organic manure is also a more effective way to overcome the obstacles caused by RC in this study by improving soil quality (Alburquerque et al., 2012).

4.2 Relationship between plant nutrient content and forage nutritive value and soil properties

Our study uncovered that soil pH is the vital factor influencing plant nutrient content and forage nutritive value (Figure 4). Previous studies have proved that pH can not only change the decomposition

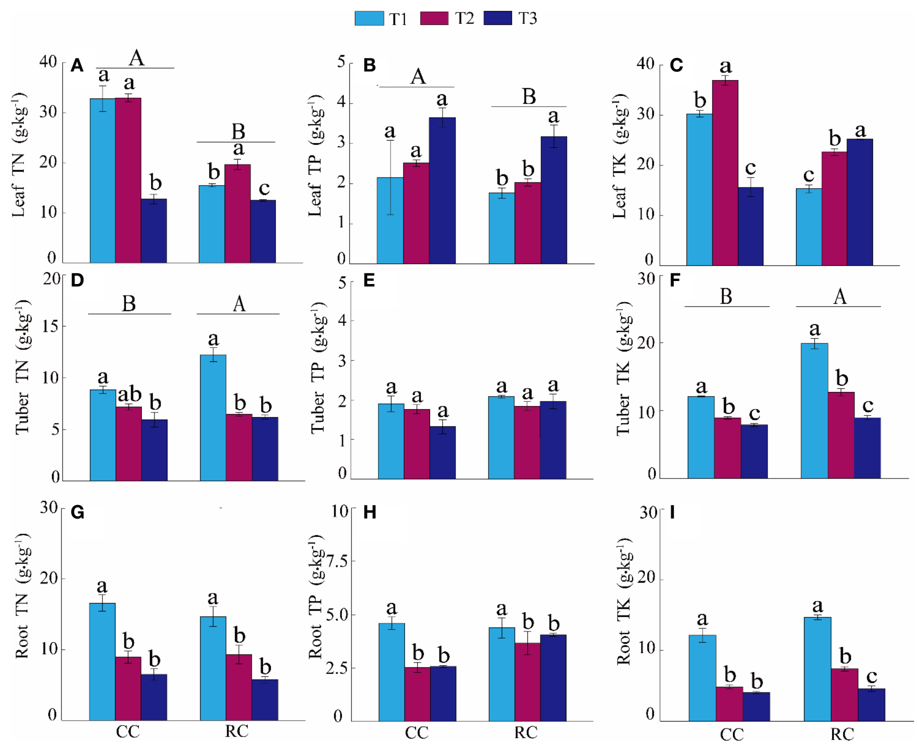

FIGURE 1
Effects of the continuous cropping (CC)/rotation cropping (RC) and mowing time on [**A** (total nitrogen (TN)], **B** [total phosphorus (TP)], and **C** [total potassium (TK)] of the leaves, [**D** (total nitrogen (TN)], **E** [total phosphorus (TP)], and **F** [total potassium (TK)] of the tubers, and [**G** (total nitrogen (TN)], **H** [total phosphorus (TP)], and **I** [total potassium (TK)] of the roots.

TABLE 6 Two-way ANOVA analysis of effects of the planting mode and mowing time on the forage nutritive value of the leaves of *C. esculentus*.

Factor	Leaves				Tubers	
	CP (mg•g^{-1})	EE (mg•g^{-1})	NDF (mg•g^{-1})	ADF (mg•g^{-1})	CP (mg•g^{-1})	EE (mg•g^{-1})
planting mode (CC/RC)	101.34***	3.79	137.91***	4.84*	41.02***	20.08**
Mowing time (M)	69.13***	3.01	19.11***	2.26	26.34***	132.80***
CC/RC×M	25.57***	0.49	10.65**	3.63	22.70***	2.29

Here: CC, continuous cropping; RC, rotation cropping. M, Mowing times (T1, on the 78th day after seed sowing; T2, on the 101th day after seed sowing; T3, on the 124th day after seed sowing). Values indicate results of F value.
*$p < 0.05$; **$p < 0.01$; ***$p < 0.001$.

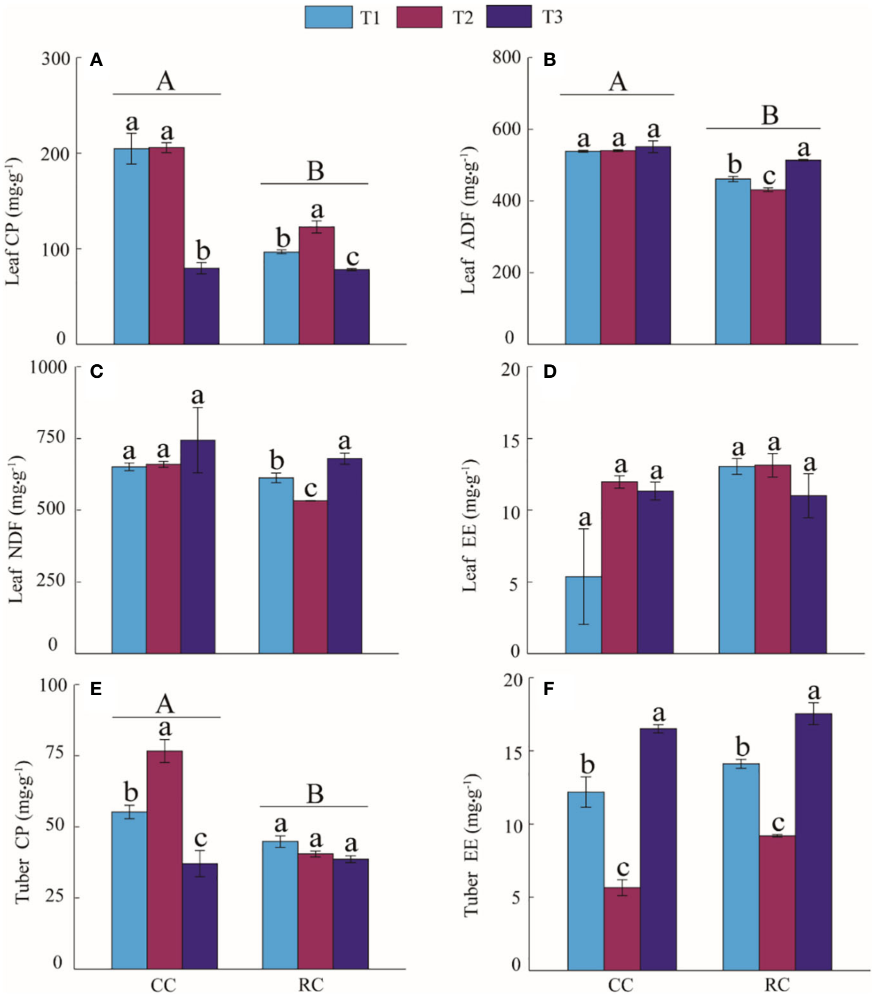

FIGURE 2
Effects of the continuous cropping (CC)/rotation cropping (RC) and mowing time on [**A** (crude protein (CP)], **B** [acid detergent fiber (ADF)], **C** [neutral detergent fiber (NDF)], and **D** [ether extract (EE)], contents of the leaves and **E** [crude protein (CP)] and **F** [ether extract (EE)], contents of the tubers.

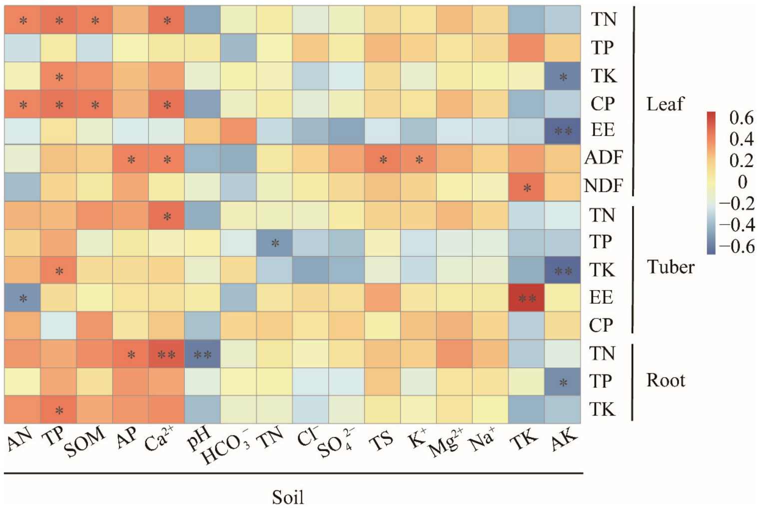

FIGURE 3
Correlation analysis of leaves, tubers, roots, and soil factors. Here: SOM, soil organic matter; TN, total nitrogen; TP, total phosphorus; TK, total potassium; AN, available nitrogen; AP, the available phosphorus; AK, the available potassium; TS, Total salt; EE, ether extract; CP, Crude protein; ADF, acid detergent fiber; NDF, neutral detergent fiber. *p < 0.05; **p < 0.01.

process of SOM and nutrient availability, but also directly affect the reaction rates of enzymes associated with biochemical reactions and soil microbial activities, thus it can regulate crop growth by affecting soil properties (Dick et al., 2000; Guo et al., 2010). The soil AK and sodium ion content are less, resulting in a relative excess of soil H^+, leading to soil acidification (Dick et al., 2000; Ozcan et al., 2021). However, RC changed the soil pH value, making the soil TN, soil TP, soil TK, and soil available nutrients variation significantly, which affected the accumulation of nutrients and nutritional quality of the leaf and tuber (Guo et al., 2010). Higher soil pH was observed in RC systems than in CC (Table 3), that may be due to much higher uptake of nitrate (NO- 3) and compensatory secretion of OH^- by crops in the rotation system (Alvey et al., 2001). Higher level of Mg^{2+} may also contribute to the higher pH in RC system (Table 3). In our study, soil pH exerted a direct and indirect impact on plant nutrient accumulation and forage nutritive value by regulating the available nutrients, anions, cations, and total nutrients in soil (Figure 4). Therefore, a range of physical, chemical, and biological processes may be involved in the negative effects of rotations on nutrient accumulation and forage nutritive value. These processes will be explored by introducing key indicators such as plant physiology, microbial activity and soil enzyme activity in our future studies.

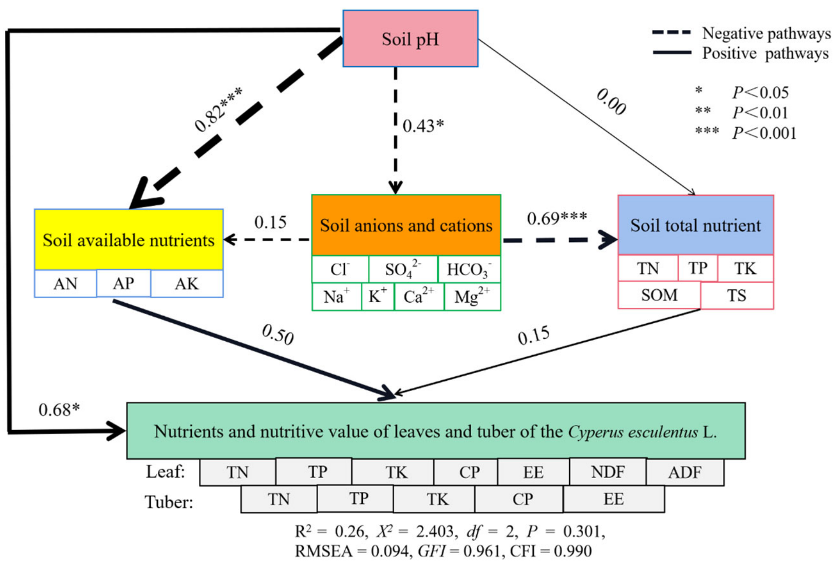

FIGURE 4
The structural equation model of effects of the continuous cropping (CC)/rotation cropping (RC) on nutrient content and forage nutritive value of leaves and tubers. Here: The principal component (soil available nutrients, soil anions and cations, soil total nutrients, and nutrient and forage nutritive value of the leaves and tubers) first axis data are reported in Table 7.

TABLE 7 The principal component first axis data (soil available nutrients, soil anions and cations, soil total nutrients, and nutrient and forage nutritive value of the leaves and tubers).

Soil available nutrients	pH	Soil anions and cations	Soil total nutrient	Nutrients and nutritive value (leaves and tubers)
-0.59267	0.32803	1.54209	-0.98532	-0.54155
-0.64265	0.72498	-0.46442	0.08915	-0.53676
-0.35805	-0.26739	-0.32869	-0.21075	-0.53915
-0.59267	0.32803	1.54209	-0.98532	-0.54155
-0.64265	0.72498	-0.46442	0.08915	-0.53676
-0.35805	-0.26739	-0.32869	-0.21075	-0.53915
0.65725	-1.85517	-0.02982	-0.44283	-0.40714
2.05449	-2.78137	1.5454	-0.81002	-0.82544
0.14463	-0.66433	-0.35341	0.01456	-0.47403
-0.12847	1.25424	-0.54395	0.20505	-0.92046
0.20114	-1.06128	-0.28644	0.28048	-0.7682
-0.1228	-0.59817	1.68642	0.09066	-1.00025
0.82174	-0.46586	-0.1924	0.61666	0.3564
0.33515	0.39419	-0.43289	0.21451	0.49894
0.18698	0.0634	-0.25048	0.20955	0.56515
-0.2876	0.12956	-0.40453	0.48568	0.28125
0.28809	0.26187	-0.48191	0.72617	0.01618
0.02923	0.65882	-0.46377	0.66031	0.20052
0.16063	-0.66433	0.20819	0.04184	0.69623
0.0785	-0.46586	-0.02156	0.09273	0.84186
0.01452	1.18808	-0.46037	-0.11046	1.02772
-0.73504	1.51887	-0.44572	0.15485	0.46659
-0.05167	0.26187	-0.15553	-0.26716	0.53505
-0.46004	1.25424	-0.4152	0.05126	0.5271

5 Conclusions

In conclusion, RC, irrespective of mowing time, exerted a positive effect on nutrient accumulation (e.g., total nitrogen, and potassium) in tubers, but a negative influence on nutrient accumulation (total nitrogen, phosphorus, and potassium) in leaves and roots, and their nutritive value (evaluated by CP, EE, ADF, and NDF). Soil properties, especially pH, may explain the variation of the performance of *C. esculentus* growing in CC and RC. The plant nutrient accumulation and forage nutritive value were directly affected by soil pH and were indirectly regulated by the variations in soil available nutrients, anions, cations, and total nutrients induced by soil pH. Therefore, RC for *C. esculentus* is not a good planting mode at any mowing time in terms of plant nutrient accumulation and forage nutritive value, likely due to degraded soil quality induced by nutrient competition between crops. For the intensive cultivation of *C. esculentus*, organic manure supplementation and rotation with legumes may overcome these adverse effects caused by rotation with wheat that will be explored in our future research.

Data availability statement

The original contributions presented in the study are included in the article/supplementary material. Further inquiries can be directed to the corresponding authors.

Author contributions

Conceptualization: YD, YZ, FZ. Data curation: YD, YZ and XC. Formal analysis: YD, YZ, and ZZ. Funding acquisition: FZ. Investigation: YD, YZ, XC, FZ. Methodology: YD, YZ and AU. Project administration: FZ. Resources: FZ. Software: YD, YZ and ZZ. Supervision: FZ. Validation: FZ, YD, YZ, WI and ZZ. Writing -original draft: YD, YZ. Writing - review and editing: YD, YZ, XL, FZ, WI, ZZ. All authors contributed to the article and approved the submitted version.

Funding

Key Research and Development Project of Xinjiang Uygur Autonomous Region (No. 2022B02040-1) and National Key Research and Development Project of China (No. 2019YFC0507603).

Conflict of interest

The authors declare that the research was conducted in the absence of any commercial or financial relationships that could be construed as a potential conflict of interest.

Publisher's note

All claims expressed in this article are solely those of the authors and do not necessarily represent those of their affiliated organizations, or those of the publisher, the editors and the reviewers. Any product that may be evaluated in this article, or claim that may be made by its manufacturer, is not guaranteed or endorsed by the publisher.

References

Ahmed, Z. S., and Hussein, A. M. S. (2014). Exploring the suitability of incorporating tiger nut flour as novel ingredients in gluten free biscuit. *Polish J. Food Nutr. Sci.* 64 (1), 27–33. doi: 10.2478/v10222–012–0087–z

Alburquerque, J. A., de la Fuente, C., Campoy, M., Carrasco, L., Najera, I., Baixauli, C., et al. (2012). Agricultural use of digestate for horticultural crop production and improvement of soil properties. *Eur. J. Agron.* 43, 119–128. doi: 10.1016/j.eja.2012.06.001

Alvey, S., Bagayoko, M., Neumann, G., and Buerkert, A. (2001). Cereal/legume rotations affect chemical properties and biological activities in two West African soils. *Plant Soil* 231, 45–54. doi: 10.1023/A:1010386800937

Arafat, S. M., Gaafar, A. M., Basuny, A. M., and Nassef, S. L. (2009). Chufa tubers (*Cyperus esculentus* l.): As a new source of food. *World Appl. Sci. J.* 7 (2), 151–156.

Arzigul, Y. S., and Xianmixinuer, K. L. M. (2017). Characteristics of agricultural climate resources and analysis of main meteorological disasters in shache county. *Modern Agric. Sci. Technol.* 20, 200.

Ayeni, A. O. (2022). Hoop house and field evaluation of tigernut (*Cyperus esculentus* l. var. sativus boeck) selections in new Jersey, USA. *Plants* 11 (7), 897. doi: 10.3390/plants11070897

Bamishaiye, E. I., Muhammad, N. O., and Bamishaiye, O. M. (2010). Assessment of biological value of tiger nut (*Cyperus esculentus*) tuber oil meal-based diet in rats. *Ann. Biol. Res.* 1, 274–280. doi: 10.1007/978-3-030-12473-1_11

Bao, S. D. (2000). *Analysis of soil and agrochemistry. 3 ed* (Beijing: China Agriculture Press), 25–200.

Binnie, R. C., Chestnutt, D. M. B., and Murdoch, J. C. (2010). The effect of time of initial defoliation and height of defoliation on the productivity of perennial ryegrass swards. *Grass Forage Sci.* 35 (4), 267–273. doi: 10.1111/j.1365-2494.1980.tb01522.x

Blum, A. (2009). Effective use of water (EUW) and not water-use efficiency (WUE) is the target of crop yield improvement under drought stress. *Field Crops Res.* 112 (2-3), 119–123. doi: 10.1016/j.fcr.2009.03.009

Brankatschk, G., and Finkbeiner, M. (2015). Modeling crop rotation in agricultural LCAs — challenges and potential solutions. *Agric. Syst.* 138, 66–76. doi: 10.1016/j.agsy.2015.05.008

Codina-Torrella, I., Guamis, B., and Trujillo, A. J. (2015). Characterization and comparison of tiger nuts (*Cyperus esculentus* l.) from different geographical origin: Physico-chemical characteristics and protein fractionation. *Ind. Crops Products* 65, 406–414. doi: 10.1016/j.indcrop.2014.11.007

Coello, P., and Martinez-Barajas, E. (2016). Changes in nutrient distribution are part of the mechanism that promotes seed development under severe nutrient restriction. *Plant Physiol. Biochem.* 99, 21–26. doi: 10.1016/j.plaphy.2015.11.022

De Castro, O., Gargiulo, R., Del Guacchio, E., Caputo, P., and De Luca, P. (2015). A molecular survey concerning the origin of *Cyperus esculentus* (Cyperaceae, poales): two sides of the same coin (weed vs. crop). *Ann. Bot.* 115, 733–745. doi: 10.1093/aob/mcv001

Delang, C. O. (2018). The consenquences of soil degradation in China: A review. *Geoscape* 12, 92–103. doi: 10.2478/geosc-2018-0010

Devries, F. T. (1991). Chufa (*Cyperus esculentus*, cyperaceae) - a weedy cultivar or a cultivated weed. *Econ. Bot.* 45 (1), 27–37. doi: 10.1007/bf02860047

Dick, W. A., Cheng, L., and Wang, P. (2000). Soil acid and alkaline phosphatase activity as pH adjustment indicators. *Soil Biol. Biochem.* 32 (13), 1915–1919. doi: 10.1016/s0038-0717(00)00166-8

Ding, D. Y., Feng, H., Zhao, Y., Hill, R. L., Yan, H., Chen, H. X., et al. (2019). Effects of continuous plastic mulching on crop growth in a winter wheat-summer maize rotation system on the loess plateau of China. *Agric. For. Meteorol.* 271, 385–397. doi: 10.1016/j.agrformet.2019.03.013

Donaghy, D. J., Turner, L. R., and Adamczewski, K. A. (2008). Effect of defoliation management on water-soluble carbohydrate energy reserves, dry matter yields, and herbage quality of tall fescue. *Agron. J.* 100 (1), 122–127. doi: 10.2134/agronj2007.0016

Duan, Z. P., Gan, Y. W., Wang, B. J., Hao, X. D., Xu, W. L., Zhang, W., et al. (2019). Interspecific interaction alters root morphology in young walnut/wheat agroforestry systems in northwest China. *Agroforestry Syst.* 93, 419–434. doi: 10.1007/s10457-017-0133-2

Giacometti, C., Mazzon, M., Cavani, L., Triberti, L., Baldoni, G., Ciavatta, C., et al. (2021). Rotation and fertilization effects on soil quality and yields in a long term field experiment. *Agronomy* 11, 636. doi: 10.3390/agronomy11040636

Guo, J. H., Liu, X. J., Zhang, Y., Shen, J. L., Han, W. X., Zhang, W. F., et al. (2010). Significant acidification in major chinese croplands. *Science* 327 (5968), 1008–1010. doi: 10.1126/science.1182570

Hooper, D. U., and Vitousek, P. M. (1998). Effects of plant composition and diversity on nutrient cycling. *Ecol. Monogr.* 68 (1), 121–149. doi: 10.2307/2657146

Hou, J. J., Zhao, G. Q., Jiao, T., Chai, J. K., and Wang, H. X. (2013). Evaluation on adaptability of six avena varieties in xiahe county, gansu province. *Grassland Turf* 33 (2), 26–32. doi: 10.13817/j.cnki.cyycp.2013.02.006

Hussain, M. I., Vieites-Álvarez, Y., Otero, P., Prieto, M. A., Simal-Gandara, J., Reigosa, M. J., et al. (2022). Weed pressure determines the chemical profile of wheat (*Triticum aestivum* l.) and its allelochemicals potential. *Pest Manage. Sci.* 78, 1605–1619. doi: 10.1002/ps.6779

Ilyas, N., Yang, Y., Zhang, C., Singh, R. P., Yu, Q., Yuan, Y., et al. (2022). Temporal dynamics and variation in the alfalfa root nodule and rhizosphere microbial communities of coastal sand and lawn soil. *J. Plant Interact.* 17, 173–182. doi: 10.1080/17429145.2021.2024899

Jia, X., Zhang, Z., and Wang, Y. (2022). Forage yield, canopy characteristics, and radiation interception of ten alfalfa varieties in an arid environment. *Plants* 11 (9), 1112. doi: 10.3390/plants11091112

Larkin, R. P. (2003). Characterization of soil microbial communities under different potato cropping systems by microbial population dynamics, substrate utilization, and fatty acid profiles. *Soil Biol. Biochem.* 35 (11), 1451–1466. doi: 10.1016/s0038-0717(03)00240-2

Lendzemo, V., Kuyper, T. W., Urban, A., Vegvari, G., Puschenreiter, M., Schickmann, S., et al. (2009). The arbuscular mycorrhizal host status of plants can not be linked with the *Striga* seed-germination-activity of plant root exudates. *J. Plant Dis. Prot.* 116 (2), 86–89. doi: 10.1007/BF03356291

Lenssen, A. W., Sainju, U. M., Allen, B. L., Stevens, W. B., and Jabro, J. D. (2020). Diversified crop rotation and management system influence durum yield and quality. *Agron. J.* 112 (5), 4407–4419. doi: 10.1002/agj2.20311

Li, H. S. (2000). *Experimental principles and techniques of plant physiology and biochemistry* (Beijing: Higher Education Press).

Li, X., Ding, C., Hua, K., Zhang, T. L., Zhang, Y. N., Zhao, L., et al. (2014). Soil sickness of peanuts is attributable to modifications in soil microbes induced by peanut root exudates rather than to direct allelopathy. *Soil Biol. Biochem.* 78, 149–159. doi: 10.1016/j.soilbio.2014.07.019

Lu, R. K. (1999). *Soil agrochemical analysis* (Beijing: China Agricultural Science Technology Press), 80–89.

Lu, X., Yan, Y., Sun, J., Zhang, X., Chen, Y., Wang, X., et al. (2015). Carbon, nitrogen, and phosphorus storage in alpine grassland ecosystems of Tibet: Effects of grazing exclusion. *Ecol. Evol.* 19)5, 4492–4504. doi: 10.1002/ece3.1732

Ma, C. H., and Han, J. G. (2000). The research of the best on mowing time of unicast and oats and vetch mixed grassland. *Grass Feeding Livestock* 3, 42–45. doi: 10.16863/j.cnki.1003-6377.2000.03.015

Moulin, A. P., Buckley, K. E., and Volkmar, K. (2015). Soil quality as affected by amendments in bean-potato rotations. *Can. J. Soil Sci.* 91 (4), 533–542. doi: 10.4141/cjss10011

Neff, J. C., Reynolds, R. L., Belnap, J., and Lamothe, P. (2005). Multi-decadal impacts of grazing on soil physical and biogeochemical properties in southeast Utah. *Ecol. Appl.* 15 (1), 87–95. doi: 10.1890/04-0268

Ozcan, M. M., Ghafoor, K., AlJuhaimi, F., Uslu, N., Babiker, E. E., and Ahmed, I. A. M. (2021). Influence of germination on bioactive properties, phytochemicals and mineral contents of tigernut (*Cyperus esculentus* l.) tuber and oils. *J. Food Measurement Characterization* 15, 3580–3589. doi: 10.1007/s11694-021-00929-3

Peterson, G. A., Westfall, D. G., Schipanski, M. E., and Fonte, S. J. (2020). Soil and crop management systems that ameliorate damage caused by decades of dryland agroecosystem mismanagement. *Agron. J.* 112 (5), 3227–3238. doi: 10.1002/agj2.20257

R Core Team. (2018). R: A Language and Environment for Statistical Computing. Publisher Foundation for Statistical Computing, Vienna, Austria URL: https://www.r-project.org/.

Richman, S. E., Leafloor, J. O., Karasov, W. H., and Mcwilliams, S. R. (2015). Ecological implications of reduced forage quality on growth and survival of sympatric geese. *J. Anim. Ecol.* 84 (1), 284–298. doi: 10.1111/1365-2656.12270

Sakaigaichi, T., Tarumoto, Y., Hattori, I., Kamiya, M., and Yoshida, H. (2010). Effect of dense planting on the growth and yield of forage sugarcane variety, KRFo93-1, in planting cane. *Japanese J. Crop Sci.* 79 (1), 1–9. doi: 10.1626/jcs.83.356

Sánchez-Zapata, E., Fernández-López, J., and Angel Pérez-Alvarez, J. (2012). Tiger nut (*Cyperus esculentus*) commercialization: health aspects, composition, properties, and food applications. *Compr. Rev. Food Sci. Food Saf.* 11 (4), 366–377. doi: 10.1111/j.1541-4337.2012.00190.x

Sun, L., Wang, S. L., Zhang, Y. J., Li, J., Wang, X. L., Wang, R., et al. (2018). Conservation agriculture based on crop rotation and tillage in the semi-arid loess plateau, China: Effects on crop yield and soil water use. *Agric. Ecosyst. Environ.* 251, 67–77. doi: 10.1016/j.agee.2017.09.011

Tan, J., Wu, X., Zeng, F., Li, X., Feng, M., Liao, G., et al. (2022). Effects of crop residue on wind erosion due to dust storms in hotan prefecture, xinjiang, China. *Soil Tillage Res.* 221, 105387. doi: 10.1016/j.still.2022.105387

Wang, Y. M., Lei, Y. F., and Wei, Z. W. (2017). Effects of different rotation modes on yield, quality of silage corn, and soil fertility. *J. Nucl. Agric. Sci.* 31 (9), 1803–1810. doi: 10.11869/j.issn.100-8551.2017.09.1803

Warra, H. H., Ahmed, M. A., and Nicolau, M. D. (2015). Impact of land cover changes and topography on soil quality in the kasso catchment, bale mountains of southeastern Ethiopia. *Singapore J. Trop. Geogr.* 36 (3), 357–375. doi: 10.1111/sjtg.12124

Werle, I. S., Castro, E., Pucci, C., Soni Chakraborty, B., Broderick, S., and Tseng, T. M. (2022). Identification of weed-suppressive tomato cultivars for weed management. *Plants* 11 (3), 411. doi: 10.3390/plants11030411

Xiong, W., Li, Z., Liu, H., Xue, C., Zhang, R. F., Wu, H. S., et al. (2015). The effect of long-term continuous cropping of black pepper on soil bacterial communities as determined by 454 pyrosequencing. *PloS One* 10 (8), e0136946. doi: 10.1371/journal.pone.0136946

Yang, J., Shen, Y. Y., Nan, Z. B., Gao, C. Y., Niu, Y. N., Wang, X. Z., et al. (2010). Effects of conservation tillage on crop yield and carbon pool management index on top soil within a maize-wheat-soy rotation system in the loess plateau. *Acta Prataculturae Sin.* 19 (1), 75–82.

Zhang, S., Li, P., Wei, Z., Cheng, Y., Liu, J., Yang, Y., et al. (2022). Cyperus (*Cyperus esculentus* l.): A review of its compositions, medical efficacy, antibacterial activity and allelopathic potentials. *Plants* 11 (9), 1127. doi: 10.3390/plants11091127

Zhao, C. Z., Li, Q., Cheng, L., and Zhong, R. Z. (2021). Effects of mowing regimes on forage yield and crude protein of *Leymus chinensis* (Trin.) tzvel in songnen grassland. *Grassland Sci.* 67, 275–284. doi: 10.1111/grs.12314

Zhou, X., Yu, G., and Wu, F. (2011). Effects of intercropping cucumber with onion or garlic on soil enzyme activities, microbial communities and cucumber yield. *Eur. J. Soil Biol.* 47 (5), 279–287. doi: 10.1016/j.ejsobi.2011.07.001

Frontiers in
Plant Science

Cultivates the science of plant biology and its applications

The most cited plant science journal, which advances our understanding of plant biology for sustainable food security, functional ecosystems and human health.

Discover the latest Research Topics

See more →

Frontiers

Avenue du Tribunal-Fédéral 34
1005 Lausanne, Switzerland
frontiersin.org

Contact us

+41 (0)21 510 17 00
frontiersin.org/about/contact